Queen Mary
University of London

# Assessment and development of adenovirus type 11 for cancer therapy

Wong, Han Hsi

The copyright of this thesis rests with the author and no quotation from it or information derived from it may be published without the prior written consent of the author

For additional information about this publication click this link.
https://qmro.qmul.ac.uk/jspui/handle/123456789/375

Information about this research object was correct at the time of download; we occasionally make corrections to records, please therefore check the published record when citing. For more information contact scholarlycommunications@qmul.ac.uk

# ASSESSMENT AND DEVELOPMENT OF ADENOVIRUS TYPE 11 FOR CANCER THERAPY

---

Han Hsi Wong

MRC Clinical Research Training Fellow

A thesis submitted for the degree of Doctor of Philosophy

Institute of Cancer
Barts and The London School of Medicine and Dentistry
Queen Mary, University of London

March 2010

Barts and The London
School of Medicine and Dentistry

# ATTESTATION OF AUTHORSHIP

I hereby declare that the work presented in this thesis is my own and was performed between February 2007 and February 2010. To the best of my knowledge and belief it contains no material previously published or written by another person (except where otherwise indicated), nor material which to a substantial extent has been submitted for the award of any other degree or diploma of a university or other institution of higher learning.

The copyright of this thesis rests with the author and no quotation from it nor information derived from it may be published without the prior written consent of the author.

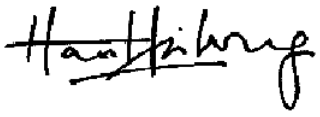

Han Hsi Wong

# ABSTRACT

The efficacy of oncolytic virotherapy is influenced by the interactions between the tumour, virus and host immunity. The first generation of oncolytic adenoviruses, based on serotype 5 (Ad5), has achieved limited success in clinical trials. Its shortcomings include the downregulation and inaccessibility of its receptor, the Coxsackie and adenovirus receptor (CAR) in cancer cells, high prevalence of neutralising antibodies and hepatotoxicity. In contrast, Ad11 binds to CD46 and other receptor(s) but its potential as an oncolytic virus remains to be explored.

A panel of human cancer cell lines were found to express higher levels of CD46 than CAR. However, not all cell lines were more sensitive to Ad11-mediated cytotoxicity *in vitro* compared to Ad5. Treatment of Ad5-insensitive PC-3 human prostate cancer xenografts with Ad11 resulted in significant reduction in tumour growth, but not Ad11-insensitive MIA PaCa-2 human pancreatic cancer xenografts. Virus attachment and nuclear entry of Ad11 were significantly better than Ad5 even in cells that were insensitive to Ad11 killing. In these cells, however, Ad11 *E1A* mRNA levels were much lower than those of Ad5, producing a negative effect on viral DNA amplification, structural protein synthesis, progeny production and cell killing. Cells that were sensitive to Ad11 cytotoxicity showed higher levels of *E1A* mRNA.

The region upstream of Ad5 *E1A* demonstrated higher transcription-enhancing activity than the corresponding region of Ad11. Two Ad11 mutants were constructed in which *E1A* was under the control of the Ad5 *E1A* promoter and enhancer-promoter, respectively. With the latter virus, improved oncolytic potency was observed. It was superior to Ad11 and also to Ad5 in many cancer cell lines, and was as effective as Ad5 in the MIA PaCa-2 xenograft model. Therefore, Ad11 with the Ad5 *E1A* enhancer-promoter should be used as a backbone for the future development of potent and tumour-specific oncolytic Ad11 mutants.

# ACKNOWLEDGEMENTS

I wish to express my deepest gratitude to Yaohe Wang for being such an exceptional supervisor. His brilliance, enthusiasm, guidance and motivation have not only made this research possible but also a wholly enjoyable experience. I am extremely grateful to Nick Lemoine for his support and for giving me the opportunity to work at and contribute to the Institute.

I would like to acknowledge the help of the following Viral and Gene Therapy Group members: Guozhong Jiang for his help in recombinant virus construction; Rathi Gangeswaran for her help with confocal microscopy; Ming Yuan for his numerous tips and technical advice; Vipul Bhakta, Heike Muller and Jennelle Francis for virus production; Hexiao Wang for her assistance in some of the MTS assays; Daniel Öberg for his pSS plasmid. I am also thankful to Emma Spurrell, Jonathan Hughes, Natasha Choudhury, Crispin Hiley, Chikkanna Gowda Puttaswamaiah and Louisa Chard for being such good company in the laboratory.

My sincere gratitude also goes to Iain McNeish for his help and advice both in my PhD and my clinical career. I would also like to thank John Marshall, Helen Hurst and Ian Hart for their suggestions that led to the improvement of this project. I am grateful to the Medical Research Council and Cancer Research UK for funding my PhD. I would also like to thank Daniel Stone and André Lieber in the USA for providing the Ad11 virus and plasmid.

I am forever indebted to my parents Peng Lam Wong and Yoke Chee Tan, and my brother Han Min Wong. I would not have gone so far without their understanding, encouragement and patience.

None of this would ever be possible without my wife Pik Kun Liew. I am eternally grateful to her for the sacrifices that she has made, her endless support and her undying faith in me at times when I even doubted myself. Finally, I would like to dedicate this thesis to my beautiful daughters Emily Sixuan and Lauren Tingjing for making everything worthwhile. Thanks for the laughter and joy (and sleepless nights) that both of you have brought into my life.

# TABLE OF CONTENTS

# LIST OF TABLES

# LIST OF FIGURES

**Chapter 8**

**Chapter 9**

# ABBREVIATIONS

| | |
|---|---|
| A | Alanine (amino acid) / Adenine (nucleic acid) |
| Ad | Adenovirus |
| ADAR | Adenosine deaminase acting on RNA |
| ADP | Adenovirus death protein |
| $Amp^r$ | Ampicillin resistance |
| ARF | Alternate reading frame |
| ATCC | American Type Culture Collection |
| BALB | Bagg albino |
| Bax | Bcl-2-associated X protein |
| BEGM | Bronchial epithelial cell growth medium |
| BID | Bcl-2 homology 3 interacting domain death agonist |
| Bp | Base pair(s) |
| BSA | Bovine serum albumin |
| C | Cytosine |
| °C | Degree(s) Celsius |
| $CaCl_2$ | Calcium chloride |
| CAR | Coxsackie and adenovirus receptor |
| CBP | Cyclic adenosine monophosphate response element-binding-binding protein |
| CD | Cluster of differentiation |
| CDK | Cyclin-dependent kinase |
| cDNA | Complementary DNA |
| CDP | CCAAT displacement protein |
| C/EBP | CCAAT-enhancer-binding protein |
| $Chlr^r$ | Chloramphenicol resistance |
| CIP1/WAF1 | CDK-interacting protein-1/wild-type p53-activated fragment-1 |
| CMV | Cytomegalovirus |
| $CO_2$ | Carbon dioxide |
| COUP-TF | Chicken ovalbumin upstream promoter-transcription factor |
| CPE | Cytopathic effect |
| CpG | Cytosine-phosphate-guanine |
| CR | Conserved region |
| CR-UK | Cancer Research UK |
| CsCl | Caesium chloride |
| Ct | Threshold cycle |
| CT | Computed tomography |
| CTF | CCAAT-binding transcription factor |

| | |
|---|---|
| CTL | Cytotoxic T lymphocyte |
| D | Aspartic acid |
| DAPI | 4',6-diamidino-2-phenylindole |
| DBP | DNA-binding protein |
| DC | Dendritic cell |
| dCMP | Deoxycytidine monophosphate |
| DEPC | Diethylpyrocarbonate |
| DMEM | Dulbecco's modified Eagle's medium |
| DMSO | Dimethyl sulfoxide |
| DNA | Deoxyribonucleic acid |
| dNTP | Deoxynucleotide triphosphate |
| DSMZ | Deutsche Sammlung von Mikroorganismen und Zellkulturen |
| dsRNA | Double-stranded RNA |
| E | Glutamic acid |
| *E. coli* | *Escherichia coli* |
| E2F | *E2* promoter-binding factor |
| EBER | EBV-encoded RNA |
| EBV | Epstein-Barr virus |
| $EC_{50}$ | Half maximal effective concentration(s) |
| ECL | Enhanced chemiluminescence |
| EDTA | Ethylenediaminetetraacetic acid |
| EF-1A | Enhancer-binding factor to the *E1A* core motif |
| EGFR | Epidermal growth factor receptor |
| eIF-2 | Eukaryotic initiation factor-2 |
| EMT | Epithelial-mesenchymal transition |
| ER | Endoplasmic reticulum |
| F | Phenylalanine (amino acid) / Farad(s) (capacitance) |
| FBS | Foetal bovine serum |
| Fc | Crystallisable fragment (of immunoglobulin molecule) |
| FITC | Fluorescein isothiocyanate |
| g | Gram(s) |
| G | Glycine (amino acid) / Guanine (nucleic acid) |
| GABP | Guanine-adenine-binding protein |
| GAPDH | Glyceraldehyde 3-phosphate dehydrogenase |
| GDP | Guanosine diphosphate |
| GFP | Green fluorescent protein |
| GTP | Guanosine triphosphate |
| GTPase | Guanosine triphosphatase |
| H | Histidine |
| HCl | Hydrochloric acid |

| | |
|---|---|
| HEK | Human embryonic kidney |
| HRP | Horseradish peroxidase |
| HSPG | Heparan sulfate proteoglycan |
| HSV | Herpes simplex virus |
| hTERT | Human telomerase reverse transcriptase |
| HVR | Hypervariable region |
| ICP | Infected cell protein |
| IFN | Interferon |
| Ig | Immunoglobulin |
| IL | Interleukin |
| INK4A | Inhibitor of CDK4A |
| ITR | Inverted terminal repeat |
| K | Lysine |
| Kb | Kilobase pair(s) |
| KCl | Potassium chloride |
| kDa | Kilodalton(s) |
| L (l) | Litre(s) |
| LB | Lysogeny broth |
| LRRC | Leucine-rich repeat containing |
| *luc*+ | Firefly luciferase reporter gene |
| LXCXE | Leucine-X-cysteine-X-glutamate |
| m | Metre(s) |
| M | Molar |
| MAPK | Mitogen-activated protein kinase |
| Mdm2 | Murine double minute |
| MEM EBSS | Minimum essential medium with Earle's balanced salts |
| MGB | Minor groove binder |
| $MgCl_2$ | Magnesium chloride |
| MHC | Major histocompatibility complex |
| miRNA | MicroRNA |
| MLP | Major late promoter |
| mRNA | Messenger RNA |
| MTS | 3-(4,5-dimethylthiazol-2-yl)-5-(3-carboxymethoxyphenyl)-2-(4-sulfophenyl)-2H-tetrazolium, inner salt |
| M.u. | Map unit(s) |
| MV | Measles virus |
| MWCO | Molecular weight cutoff |
| *n* | Number in group |
| N | Asparagine |
| $Na_2HPO_4$ | Dibasic sodium orthophosphate |

| | |
|---|---|
| NaCl | Sodium chloride |
| NDV | Newcastle disease virus |
| NEB | New England Biolabs |
| NF | Nuclear factor |
| NF-κB | Nuclear factor κ-light-chain-enhancer of activated B cells |
| NK | Natural killer |
| NRF | Nuclear respiratory factor |
| N.s | Not significant |
| Oct | Octamer-binding protein |
| OD | Optical density |
| ORF | Open reading frame |
| Ori | Origin of replication |
| P | Proline |
| *P* | Probability |
| PAGE | Polyacrylamide gel electrophoresis |
| PBS | Phosphate-buffered saline |
| PCNA | Proliferating cell nuclear antigen |
| PCR | Polymerase chain reaction |
| PFU | Plaque-forming unit |
| pH | Potentiometric hydrogen ion concentration |
| PI | Propidium iodide |
| PI3K | Phosphatidylinositol-3-kinase |
| PKR | dsRNA-activated protein kinase |
| PMS | Phenazine methosulfate |
| Pol | Polymerase |
| Poly(A) | Polyadenylation |
| pRb | Retinoblastoma protein |
| PS | Packaging signal |
| pTP | Pre-terminal protein |
| PVDF | Polyvinylidene difluoride |
| Q | Glutamine |
| qPCR | Quantitative real-time PCR |
| R | Residue |
| RecA | Recombinase A |
| RGD | Arginine-glycine-aspartate |
| RID | Receptor internalisation and degradation |
| RISC | RNA-induced silencing complex |
| RNA | Ribonucleic acid |
| Rpm | Revolution(s) per minute |
| RPMI | Roswell Park Memorial Institute |

| | |
|---|---|
| rRNA | Ribosomal RNA |
| S | Serine |
| SDS | Sodium dodecyl sulfate |
| SEM | Standard errors of the mean |
| siRNA | Small interfering RNA |
| SV40 | Simian vacuolating virus 40 |
| T | Threonine (amino acid) / Thymine (nucleic acid) |
| TBE | Tris-borate-EDTA |
| TBST | Tris-buffered saline with Tween 20 |
| $TCID_{50}$ | 50% tissue culture infective dose(s) |
| TEMED | Tetramethylethylenediamine |
| TESS | Transcription Element Search System |
| TLR | Toll-like receptor |
| TNF | Tumour necrosis factor |
| TP | Terminal protein |
| TPL | Tripartite leader |
| TRAIL | TNF-related apoptosis-inducing ligand |
| Tris | Trishydroxymethylaminomethane |
| tRNA | Transfer RNA |
| U | Unit(s) |
| UK | United Kingdom |
| USA | United States of America |
| UV | Ultraviolet |
| UV/Vis | Ultraviolet-visible |
| V | Valine (amino acid) / Volt(s) (voltage) |
| VA RNA | Virus-associated RNA |
| VEGF | Vascular endothelial growth factor |
| VGF | Vaccinia growth factor |
| VSV | Vesicular stomatitis virus |
| w/v | Weight/volume |

# CHAPTER 1

# Introduction

## 1.1 Oncolytic virus

Cancer is a major cause of death globally. Conventional chemotherapy and radiotherapy still have limited effects against many forms of cancer, not to mention a plethora of treatment-related side effects. Cancer is a complex disease, characterised by a combination of multiple genetic aberrations, epigenetic changes and post-transcriptional modifications. Multimodality treatment, therefore, is still far more effective than monotherapy. Indeed there has been a move towards combination chemotherapy and the use of targeted agents with standard chemotherapy. Although the use of targeted agents has led to significant improvements in the outcome of patients with malignancies such as breast cancer and gastrointestinal stromal tumour, little progress has been made for pancreatic cancer, widely considered as one of the deadliest of malignant diseases. Only about 10% of patients present with potentially curable, resectable disease at diagnosis[1]. Outcome has not improved substantially over the past 30 years, with overall five-year survival remaining dismally poor at 5%[2]. Patients with locally advanced disease have a median survival of six to ten months, whilst for those with metastatic disease it is only three to six months[3]. So far only erlotinib, an epidermal growth factor receptor (EGFR) tyrosine kinase inhibitor, has shown a statistically significant but small survival benefit in combination with gemcitabine for patients with advanced disease (median survival of 6.24 versus 5.91 months with gemcitabine alone)[4]. Nine other phase III clinical trials with various targeted agents, ranging from matrix metalloproteinase inhibitors to anti-vascular endothelial growth factor (VEGF) antibody, have failed to make any measureable impact (see Appendix for a more thorough review)[5]. Clearly there is a need for the development of novel therapies to treat this devastating disease. One such approach is the use of oncolytic viruses.

The ability of viruses to kill cancer cells has been recognised for more than a century, when tumour regression was reported to coincide with natural virus infection[6]. They achieve this by a number of mechanisms, including direct lysis, apoptosis, expression of toxic proteins, autophagy and shutdown of protein synthesis, as well as the induction of anti-tumoural immunity[7, 8]. In 1912, a patient with cervical carcinoma reportedly responded after rabies vaccination[9]. In 1949, in one of the first trials of

virotherapy for cancer, Hoster *et al*.[10] injected serum or tissue extract from patients with viral hepatitis into 22 patients suffering from Hodgkin's lymphoma. Seven patients showed improvement lasting at least one month in one or more aspects of their disease, but 14 of them developed hepatitis. Since the 1950s, clinical trials of several other viruses were initiated, including the use of adenoviruses (Ads)[11-13]. Although tumour regression was reported in some cases, this mode of therapy was later abandoned due to its side effects, absence of significant anti-tumoural efficacy and failure to prolong survival.

Improvements in our understanding of virus and tumour biology, together with advancements in recombinant DNA technology and molecular techniques, have led to the revival of oncolytic virotherapy. In 1991, a herpes simplex virus-1 (HSV-1) with deletion of its thymidine kinase *UL23* gene was tested in the laboratory[14], starting an era of genetically-engineered, replication-selective oncolytic virus. In 2005, an Ad with *E1B 55K* gene deletion (H101 or Oncorine; Shanghai Sunway Biotech, Shanghai, China) was approved in China as the world's first oncolytic virus for head and neck cancer in combination with chemotherapy[15].

Selective intratumoural replication of virus leads to improved efficacy over non-replicating agents due to the self-perpetuating nature of the treatment with virus multiplication, lysis of the infected tumour and spread to adjacent cells. The term 'oncolytic viruses' applies to viruses that are able to replicate specifically in and destroy tumour cells, and this property is either inherent or genetically-engineered. Inherently tumour-selective viruses can specifically target cancer by exploiting the very same cellular aberrations that occur in these cells, such as surface attachment receptors, activated Ras and Akt, and the defective interferon (IFN) pathway (**Figure 1.1**). Some viruses have been engineered with specific gene deletion – these genes are crucial for the survival of viruses in normal cells but expendable in cancer cells (**Figure 1.2**). Deletion of the gene that encodes thymidine kinase, an enzyme needed for nucleic acid metabolism, results in dependence of viruses such as HSV and vaccinia virus on cellular thymidine kinase expression, which is high in proliferating cancer cells but not in normal cells. Vaccinia virus also produces the vaccinia growth factor (VGF) that binds to and activates EGFR, creating an environment that supports its replication. It follows that deletion of genes encoding for both thymidine kinase and VGF leads to further selectivity of vaccinia virus in cancers with an activated EGFR-Ras pathway[16]. Another

approach to conferring tumour selectivity is to restrict virus replication by its dependence on transcriptional activities that are constitutively activated in tumour cells (transcriptional targeting). This can be achieved by the insertion of a tumour-specific promoter driving the expression of a critical viral gene[17-22]. Other viruses either possess naturally (*e.g.* Coxsackievirus A21[23] and measles virus (MV)[24]) or have been designed to have specific tropism based on the expression of cell surface receptors unique to cancer cells (transductional targeting)[25-31].

More recently, gene silencing by RNA interference technology has been utilised to confer tumour selectivity. MicroRNAs (miRNAs) or small interfering RNAs (siRNAs) regulate gene expression post-transcriptionally by translation block or cleavage of specific, complementary messenger RNA (mRNA) via the RNA-induced silencing complex (RISC). By inserting a complementary sequence next to a critical viral gene, it is possible to confine virus replication to tumour but not normal cells that express high levels of the corresponding miRNA. This has been demonstrated by several groups[32-36]. Gürlevik *et al*.[37] developed a recombinant Ad that encodes multiple RNA-interfering transcripts under the control of a p53-responsive promoter. The transcripts can effectively silent a set of critical viral genes. As p53 is a transcription factor often lost or mutated in human malignancy, this virus can therefore replicate in cancer but not normal cells where functional p53 would lead to an anti-viral RNA interference.

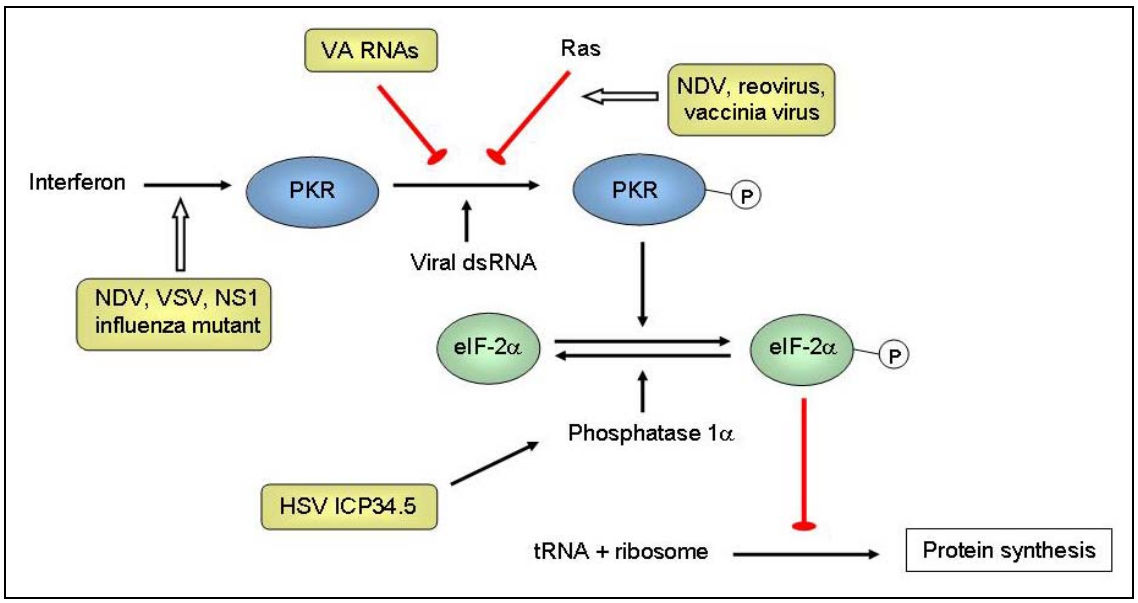


**Figure 1.1: Mechanisms of tumour selectivity of several oncolytic viruses.** The IFN/double-stranded RNA (dsRNA)-activated protein kinase (PKR) pathway is a natural anti-viral defense system. IFNs produced by infected cells result in the upregulation of PKR. On binding to viral dsRNA, PKR autophosphorylates, which in turn phosphorylates the α subunit of eukaryotic initiation factor-2 (eIF-2). Phosphorylated eIF-2α sequesters eIF-2B, a guanine nucleotide exchange factor. Without eIF-2B, the guanosine diphosphate (GDP) bound to eIF-2 cannot be exchanged for guanosine triphosphate (GTP). As a result eIF-2 is unable to bring the initiator transfer RNA (tRNA) to the 40S ribosomal subunit, and the synthesis of viral proteins is inhibited. Inactivated IFN and activated Ras pathways are frequently found in cancer (the latter can inhibit PKR), and some naturally-found viruses can replicate selectively in cancer but not normal cells, including the Newcastle disease virus (NDV)[38], reovirus[39], vaccinia virus[40] and vesicular stomatitis virus (VSV)[41]. The HSV infected cell protein (ICP)34.5 interacts with cellular phosphatase 1α to dephosphorylate eIF-2α, leading to synthesis of proteins needed for virus replication. Deletion of gene that encodes for ICP34.5 (*RL1*) results in selective replication in tumours with a defective IFN/PKR pathway[42]. The influenza virus *NS1*-deleted mutant is also dependent on this defective pathway[43]. Ads normally produce virus-associated (VA) RNAs to inhibit PKR. As such, engineered *VAI*-deleted Ad5 (*dl*331) can replicate selectively in tumours with an activated Ras pathway[44]. Epstein-Barr virus (EBV) also expresses RNAs similar to VA RNAs and these can complement *dl*331, resulting in selectivity in EBV-associated tumours[45].

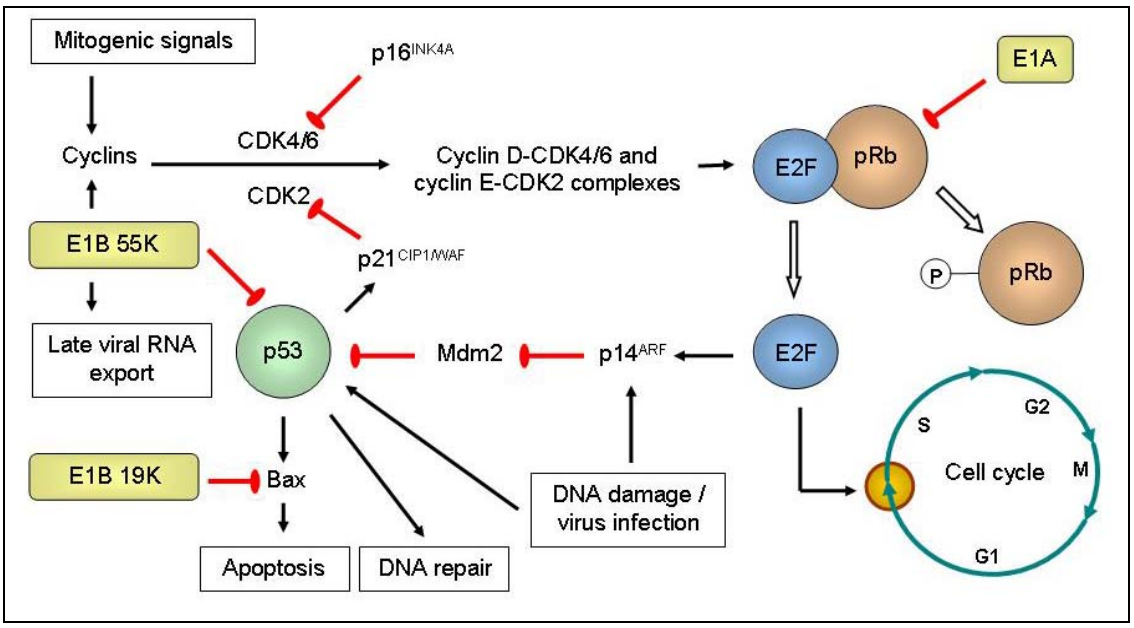


**Figure 1.2: Engineered replication selectivity of oncolytic adenoviruses by gene deletion.** Retinoblastoma protein (pRb) is normally hypophosphorylated and binds to the *E2* promoter-binding factor (E2F) transcription factor family to regulate the G1-to-S cell cycle checkpoint. Upon stimulation by mitogenic signals, upregulation of cyclins enables cyclin-dependent kinases (CDKs) to phosphorylate pRb, releasing E2F that leads to the expression of proteins needed for DNA synthesis and thus cell cycle progression. E2F upregulates $p14^{ARF}$, which inhibits Mdm2. Mdm2 normally results in p53 degradation. p53 is a transcription factor that is upregulated and activated by stress signals. It results in the expression of proteins that induce apoptosis (Bcl-2-associated X protein – Bax), cell cycle arrest ($p21^{CIP1/WAF}$ that inhibits CDK2) or DNA repair. $p16^{INK4A}$ is a tumour suppressor that inactivates CDK4/6. The adenoviral E1A proteins bind to pRb to release E2F, so that viral DNA can be replicated. E1A also promotes the acetylation of pRb by p300/CBP, causing pRb to associate with Mdm2 to inhibit p53. Because cancer cells are often in the S phase, *E1A CR2*-deleted Ad5 mutant (*dl*922-947) can selectively replicate in cancer but not normal resting cells[46]. E1B 19K binds to and inhibits Bax. The tumour selectivity of *E1B 19K*-deleted Ad2 (*dl*250) is due to multiple defects in the apoptotic pathways, where survival of the virus in normal cells would be limited owing to rapid apoptosis induction in the presence of tumour necrosis factor-α (TNF-α)[47]. E1B 55K interacts with the adenoviral *E4* open reading frame 6 (E4 ORF6) protein to form an E3 ubiquitin ligase complex that targets p53 for degradation. It also induces the expression of cyclin E and simultaneously inhibits cellular mRNA export and promotes the export of late viral mRNAs. *E1B 55K*-deleted Ad can replicate in tumour selectively because of non-functioning p53[48], cyclin E overexpression[49], and E1B 55K-independent late viral RNA export in cancer but not normal cells[50].

## 1.2 Human adenovirus

Human Ads belong to the family *Adenoviridae* and were first isolated from human adenoid tissue, from which the name was derived. They are non-enveloped, icosahedral, double-stranded DNA viruses, about 70-90 nm in diameter, with a linear DNA of approximately 34-48 kb in size[51]. The capsid is composed of three major proteins – 240 hexons (protein II) making up the 20 equilateral triangular faces and the edges of the icosahedron, as well as 12 pentons (protein III) at the vertices with protruding fibres and terminal knobs (protein IV) (**Figure 1.3**). 54 serotypes have been identified so far, which are divided into species (also termed subgenera or subgroups) A to G, based on DNA homology, agglutination properties and serological profiles (**Table 1.1**). The group B Ads have been further divided into two subgroups.

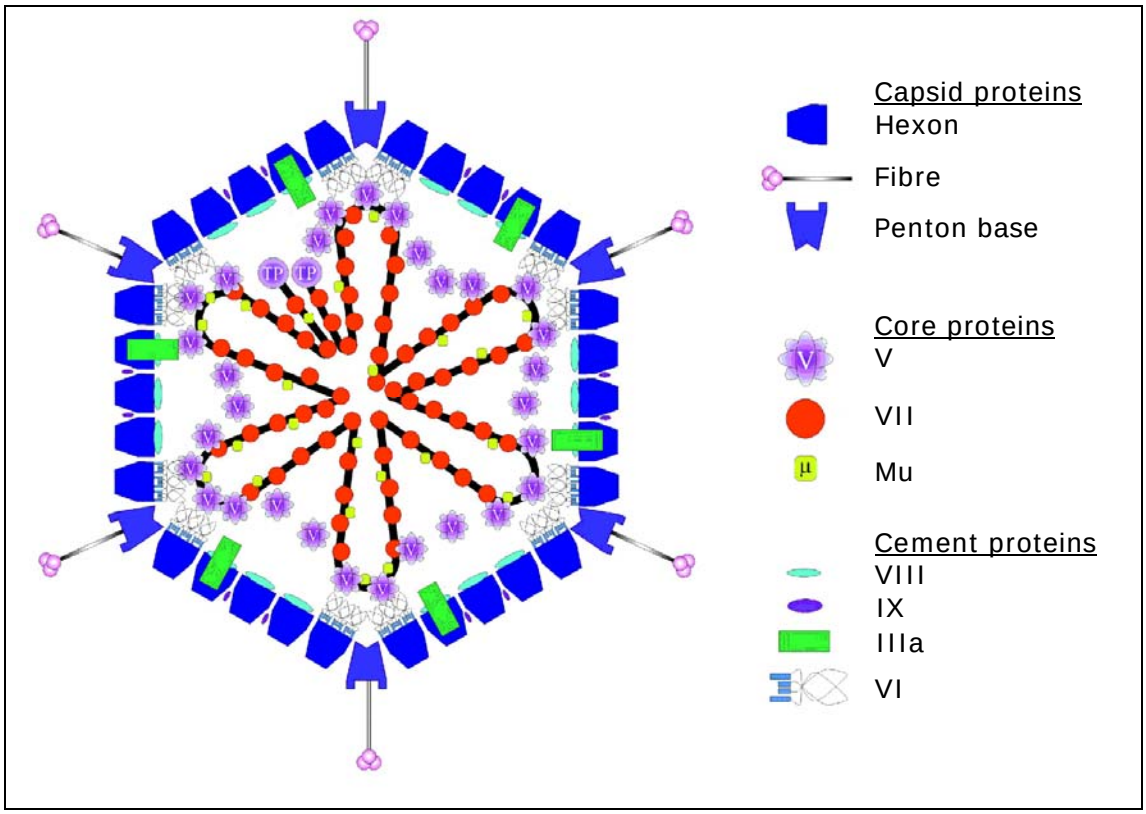


**Figure 1.3: Structure of adenovirus** (adapted from Russell WC, 2000[52]). Proteins II (hexon), III (penton base) and IV (knobbed fibre) are major capsid proteins. Proteins IIIa, VI, VIII and IX are minor capsid proteins. The viral DNA is associated with the highly basic protein VII and small arginine-rich peptide μ. Protein V wraps this DNA-protein complex to structurally link it to the capsid via protein VI. Terminal proteins (TPs) are covalently attached to the 5' ends of the DNA and facilitate its replication.

**Table 1.1: Human adenovirus serotypes**

| Subgroup | Serotype |
|---|---|
| A | 12, 18, 31 |
| B1 | 3, 7, 16, 21, 50 |
| B2 | 11, 14, 34, 35 |
| C | 1, 2, 5, 6 |
| D | 8-10, 13, 15, 17, 19, 20, 22-30, 32, 33, 36-39, 42-49, 51, 53, 54 |
| E | 4 |
| F | 40, 41 |
| G | 52 |

Ad2 and Ad5 belong to the subgroup C. They normally cause mild diseases of the respiratory tract, tonsils and adenoids. They are genetically stable, non-integrating to the host cell genome, amenable to high-titre production and purification, as well as highly efficient in entering the cell and nucleus with resulting expression of gene of interest[7]. These characteristics have made them the most studied and characterised viruses used both as oncolytic agents and gene transfer vectors.

### 1.2.1 Adenovirus genomic organisation and functions

The adenoviral genome is conventionally represented as 100 map units (m.u.) (1 m.u. = 360 bp) (**Figure 1.4**). In the nucleus the transcription of viral DNA occurs, and this can be divided into early and late events, occurring before and after DNA replication, respectively. Initially the immediate-early *E1A* gene is expressed, controlled by a constitutively active promoter. A transcriptional enhancer of adenoviral early genes, which binds to the transcription factors E2F and EF-1A (enhancer-binding factor to the *E1A* core motif; also known as E4TF1, guanine-adenine-binding protein (GABP), and nuclear respiratory factor-2 (NRF-2)), is located upstream of *E1A*[53-56] and overlaps with the packaging (or encapsidation) sequence[57, 58] (see below). *E1A* encodes three alternatively-spliced mRNAs, named 9S, 12S and 13S[59]. These are translated into proteins of 55, 243 and 289 residues, respectively. The latter two are identical except for an extra 46 amino acids in the larger product. 289R contains four conserved regions (CR1-4) whilst 243R lacks CR3[60]. They are expressed throughout infection, whereas the expression of 55R only occurs in the late phase. The properties and functions of the

E1A proteins are diverse and complex[61]. Essentially they force quiescent cells into S phase so that viral DNA can be replicated, and induce the expression of delayed-early proteins encoded by *E1B*, *E2*, *E3* and *E4* transcriptional units[62]. They do not bind to DNA directly, but bind to key cellular proteins that control gene expression and cell growth. Of particular importance is the binding of E1A CR2 (through its leucine-X-cysteine-X-glutamate (LXCXE) motif), and to a lesser extent CR1, to pRb. This interaction releases the transcription factor E2F, leading to cell cycle progression from G1 to S phase (**Figure 1.2**). This formed the basis of the *E1A CR2*-deleted Ad5 mutant, *dl*922-947, which has shown significant selectivity and potency in replicating cancer cells but not normal resting cells[46].

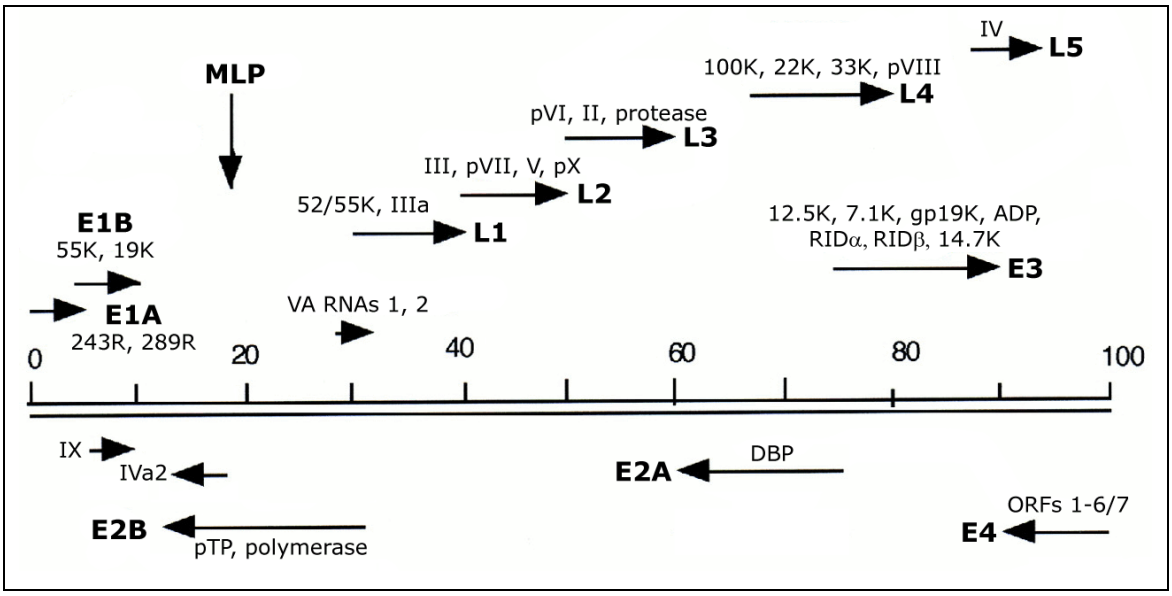


**Figure 1.4: Genomic organisation of Ad5.** Transcriptional units are shown with arrows indicating the directions of transcription. *E1-4* and *L1-L5* represent early and late genes, respectively. *IX* and *IVa2* are intermediate genes. Proteins produced as precursors for cleavage by viral protease are prefaced by a 'p'. See main text for further explanations. Abbreviations: ADP, adenovirus death protein; DBP, DNA-binding protein; MLP, major late promoter; pTP, pre-terminal protein; RID, receptor internalisation and degradation.

The E1B 55K protein is able to bind and inactivate p53, an essential step for effective virus replication (**Figure 1.2**). It was thought that as most tumours have lost the functions of the p53 pathway, deletion of *E1B 55K* would enable the virus to selectively replicate in cancer but not normal cells[48]. However, the interaction between E1B 55K and p53 is more complex than originally thought, because this mutant virus

can also replicate in some tumour cells that retain the wild-type p53[63]. It was later shown that tumour selectivity is determined not by p53, but by the export of late viral RNAs, a function requiring E1B 55K in normal but not in tumour cells[50]. Recent evidence also suggested that E1B 55K can regulate the cell cycle by inducing cyclin E, whereby cyclin E overexpression in cancer cells would allow for the efficient replication of the mutant virus[49].

The E1B 19K protein is a homologue of the cellular anti-apoptotic protein Bcl-2. It prolongs cell survival by inhibition of the death-receptor (extrinsic) and the mitochondrial (intrinsic) apoptotic signalling pathways. After the initiation of apoptosis by TNF-α, caspase-8 is activated, leading to BID (Bcl-2 homology 3 interacting domain death agonist) truncation which is then translocated to the mitochondrion where it binds to Bax, resulting in the release of cytochrome *c* and caspase-9 activation[64]. E1B 19K interacts with and inhibits the p53-inducible Bax protein[65-67] (**Figure 1.2**). It can also prevent Fas-mediated apoptosis[68]. Replication of the mutant Ad2 with *E1B 19K* deletion (*dl*250) was significantly reduced in normal cells secondary to rapid apoptosis induction in the presence of TNF-α, whilst the opposite occurred in cancer cells due to multiple defects in the apoptotic pathways (*e.g.* p53 mutation, Bcl-2 overexpression)[47]. Virus replication, spread and anti-tumoural potency was significantly better than *dl*1520 (an Ad with *E1B 55K* and *E3* deletion, see below) and wild-type Ad2. *E1B 19K*-deleted Ad5-infected cancer cells also expressed lower levels of EGFR and anti-apoptotic proteins[69].

The *E3* gene is involved in immune-response evasion and virus release from cells. It is dispensable, meaning that it is not required for virus replication and survival, and is often deleted in recombinant Ads to allow for insertion of therapeutic genes (about 2 kb), although recent work has suggested that transgene expression is higher if gene was inserted at regions other than *E3*, such as *L3*[70]. This is based on the observation that Ad5 can only package foreign DNA with size not more than 5% of the wild-type adenoviral genome (*i.e.* about 1.8 kb)[71]. Adenoviral *E3* is normally divided into *E3A* and *E3B*. In Ad5, *E3A* encodes the 12.5K, 7.1K (6.7K in Ad2), gp19K and ADP (10.5K; 11.6K in Ad2) proteins, whilst *E3B* encodes for the proteins RIDα (10.4K), RIDβ (14.6K; 14.5K in Ad2) and 14.7K. E3 12.5K is a non-membrane protein localised in the nucleus and cytoplasm, whereas 7.1K is an endoplasmic reticulum (ER)-localised integral membrane glycoprotein. Their functions are still not clearly defined.

E3 gp19K is an ER membrane glycoprotein that inhibits the transport of major histocompatibility complex (MHC) class I to the cell surface and also delays its expression to avoid killing by cytotoxic T lymphocytes (CTLs)[72, 73]. CTL evasion by tumour cells is well documented[74] and therefore the function of gp19K is redundant in these cells. Deletion of this gene, however, would ensure normal cells infected with this virus will be eradicated, and this in effect confines virus replication only to tumour cells. gp19K can also inhibit natural killer (NK) cell activation[75]. Deletion of *E3 7.1K* and *gp19K* has been found to accelerate virus clearance in immunocompetent Syrian hamster model[76]. E3B proteins inhibit apoptosis mediated by Fas-ligand, TNF-related apoptosis-inducing ligand (TRAIL) and TNF[77-79]. In a murine model, deletion of *E3B* (*dl*309) was found to attenuate virus efficacy due to faster clearance at the tumour site by increased macrophage infiltration and expression of TNF and IFN-γ, whereas *gp19K* deletion (*dl*704) retains the potency of its wild-type form due to the activation of CTLs[80, 81]. Finally ADP facilitates late cytolysis of infected cells and causes efficient release of progeny viruses[82]. It is expressed at low levels in the early stages of infection but later splicing of the major late pre-mRNA occurs such that it is expressed at high levels[83]. Ads that overexpress ADP result in better cell lysis and spread[84, 85].

The *E2* region is involved in viral DNA replication[86], whilst *E4* plays an auxiliary role in addition to other regulatory activities[87]. Each end of the genome is flanked by 100-150 bp of inverted terminal repeat (ITR) sequences needed for the initiation of DNA replication. Late transcription of *L1-5*, which encode for structural viral components, is under the control of the MLP. This results in five mRNAs that share a common 5' non-translated region of 200 bp in length, spliced to the mRNA coding region[88]. This 5' region is called the tripartite leader (TPL) as it is coded in three spatially separated segments of the viral DNA that are joined by splicing. MLP is in turn regulated by the intermediate gene products IX and IVa2[89, 90]. The VA RNAs are RNA polymerase III transcripts that are obligatory for efficient translation of viral and cellular mRNAs by blocking PKR[91, 92] (**Figure 1.1**). Lei *et al*.[93] reported that VA RNAs may affect viral and cellular gene expression by modulation of RNA editing by antagonising the RNA-editing activity of ADAR (adenosine deaminase acting on RNA). VA RNA-1 can also activate 2',5'-oligoadenylate synthetase that could affect virus replication[94], as well as suppress the activity of Dicer thus inhibiting RNA interference[95]. Because EBV also expresses similar RNAs (EBV-encoded RNAs – EBER1 and EBER2), they can complement *VAI*-deleted Ad5 (*dl*331), which has shown impressive oncolytic potency

and selectivity in EBV-associated tumours such as Burkitt's lymphoma and nasopharyngeal carcinoma[45]. Interestingly, anti-tumoural efficacy *in vitro* and *in vivo* is superior to wild-type Ad5 and this might be the result of PKR-induced apoptosis, increased IFN-β production and the adenoviral *E3B* gene deletion.

### 1.2.2 Adenovirus infectious cycle

For the cellular entry of most Ads they must first bind to the Coxsackie and adenovirus receptor (CAR) on the surface membrane via the knob portions of their fibres[96] (except for subgroup B Ads – see below. Ad37 is unusual because it can bind to CAR, CD46 and sialic acid but only uses the latter two as functional receptors[97-99]). The arginine-glycine-aspartate (RGD) motif on the penton base interacts with cellular integrins ($\alpha_V\beta_{1,3,5}$), resulting in clathrin-mediated endocytosis of the virus[100, 101], a process dependent on the phosphatidylinositol-3-kinase (PI3K) signalling pathway that triggers the Rho family of GTPases and the polymerisation and reorganisation of actin[102, 103]. The penton-integrin interaction also contributes to the characteristic cytopathic effect (CPE) on infected cells[104]. The use of integrins for internalisation has been shown to occur with some Ads of species A, B, C and E[105], whilst Ad40 and Ad41 of subgroup F lack the RGD-$\alpha_V$ integrin-binding motif resulting in inefficient uptake into A549 cells[106]. Cellular heparan sulfate proteoglycans (HSPGs) have also been shown to be a co-/receptor for Ad2, -3, -5 and -35[107-109]. Once internalised, acidification of the endosomes results in cytosolic penetration of the viruses, mediated by the fibre shafts[110]. Virus particles are dismantled in a stepwise manner[111]. The fibres are released, the penton base structures are dissociated, the structural proteins VI are degraded, and finally the minor capsid proteins are eliminated. The partially disrupted virus is transported to the nuclear membrane, a process involving p32, dynein and microtubules[52]. The genome is passaged through the nuclear pore and into the nucleus, where primary transcription events are initiated.

Viral DNA replication begins at about seven hours post-infection[83]. A pre-initiation complex is assembled at the origins of replication, consisting of DNA polymerase, the protein primer pTP, DBP and the cellular transcription factors nuclear factor I/CCAAT-binding transcription factor I (NFI/CTFI) and nuclear factor III/octamer-binding protein-1 (NFIII/Oct-1)[86]. DNA replication is initiated by DNA polymerase-mediated transfer of deoxycytidine monophosphate (dCMP) onto pTP. Elongation is catalysed by DNA polymerase and DBP in a strand displacement

mechanism. Cellular NFII is a type I topoisomerase that is required for elongation beyond approximately 10% of the genome[112].

Viral mRNAs are transported preferentially over cellular mRNAs from the nucleus, mediated by the E1B 55K, E4 ORF3 and ORF6 proteins[87, 113]. After protein synthesis, assembly of new virion begins with the formation of an empty procapsid, followed by the entry of the DNA molecule, in a polar fashion from left to right, guided by its packaging signal[114]. The proteins IVa2, L1 52/55K, L4 22K, 33K and 100K are all involved in virion assembly[115]. This begins at 20-24 hours post-infection. After two to three days, cell lysis and the release of progeny viruses occur, facilitated by the ADP[82].

### 1.2.3 Obstacles facing oncolytic adenovirus

At present, the widespread use of oncolytic virotherapy for cancer is still far from reality. Promising laboratory results have not been translated to improved clinical outcomes, and this appears to be determined by the complex interactions between the tumour and its microenvironment, the virus, and the host immunity[116] (**Figure 1.5**; refer to the Appendix for a more detailed review).

*dl*1520 (ONYX-015; Onyx Pharmaceuticals, California, USA) is an oncolytic Ad2/Ad5 hybrid with deletion of its *E1B 55K* and *E3B* genes. This virus was the first engineered, replicating Ad to enter clinical trials for cancers including those of the head and neck[117-119] and pancreas. In a phase I trial, ONYX-015 was administered via computed tomography (CT)-guided (22 patients) or intraoperative injection (one patient) into pancreatic primary tumours every four weeks until tumour progression[120]. Six patients showed 25-49% tumour regression, 11 were stable, and five showed tumour progression. Another phase I/II study of 21 patients was done to evaluate the use of endoscopic ultrasound-guided intratumoural injection of advanced pancreatic carcinomas with ONYX-015 and then in combination with systemic gemcitabine[121]. Two had partial progression, two had minor response, six had stable disease, and 11 progressed or had to go off the study because of treatment toxicity. Disappointingly, virus replication was not detected on fine needle biopsy of the tumours, unlike other trials for head and neck cancer[118, 119, 122] and liver metastases of colorectal carcinoma[123]. Whilst the virus has shown good tumour selectivity and safety[122], the lack of durable objective responses with this virus as a single agent could be partly due to the loss of

other essential functions of the *E1B 55K* and *E3B* genes. Another important reason lies in the attachment receptor CAR. CAR is ubiquitously expressed in epithelial cells, but its expression is often downregulated in many cancer types due to the activation of the Raf-mitogen-activated protein kinase (MAPK) pathway[124]. The expression of the leucine-rich repeat containing 15 (LRRC15 or hLib) protein, frequently upregulated in tumour cells, can also result in the redistribution of CAR away from cell surfaces, thus impeding Ad infection[125]. As such high virus doses are required but would increase the risk of toxicity and immunogenicity. Furthermore CAR is a transmembrane component of tight junctions and may limit virus infection across epithelial surfaces[126]. Several approaches have been studied to direct Ads to tumour cells independent of CAR, including fibre modification (*e.g.* to target EGFR[29] or $\alpha_V\beta_6$[27]), the use Ad5 bearing the fibres of other adenoviral subgroups (chimeric viruses, *e.g.* Ad5/35[127] to target CD46), mosaic viruses (*e.g.* combining the fibres of Ad3 and Ad5 in the same virus[128]), and bridging molecules (*e.g.* anti-fibre knob antibody fused with folate to target folate receptors)[129].

Intravenous virus delivery could be hindered by neutralising antibodies, complement activation, non-specific uptake by other tissues such as the liver and spleen, as well as poor virus escape from the vascular compartment. Numerous experiments have been done to modify the immune response in favour of virus replication and tumour lysis. One method is by using an immunosuppressive agent, such as cyclophosphamide, that has been shown to improve virus spread and anti-tumoural efficacy[130]. Various data suggest that pre-existing antibodies decrease virus spread after intravenous delivery[131-133], but have a lesser effect on intratumoural injection[118, 134]. Although antibodies could prevent possible toxicity[135], they could also reduce efficacy. Possible ways to circumvent this include plasmapheresis to deplete antibodies, the use of other viral strains with a lower prevalence of antibodies in the human population[136-138] and cell carriers to deliver the virus[139-141].

Adhesion to blood cells could also lead to therapeutic inhibition[142-144]. After intravenous delivery the liver, part of the reticuloendothelial system, is the predominant site of Ad sequestration[145, 146]. Accumulation in the liver sinusoids is thought to be the result of Ad-platelet binding[144, 147]. These are subsequently taken up by the Kupffer cells through scavenger receptors, complement receptors and immunoglobulin (Ig) Fc-receptors[148, 149]. This causes the death of these cells[150] and the excess Ads are able to

overcome this biological filter to transduce liver hepatocytes[151]. Ad5 is known to cause liver toxicity, and its use has raised some concerns after the death of Jesse Gelsinger in 1999 from Ad5-based gene therapy injected directly into the hepatic artery[152]. It is now known that the binding of adenoviral hexon protein hypervariable regions (HVRs) to the blood coagulation factor X allows the virus to interact with HSPGs to mediate liver transduction[153, 154]. Ways to reduce liver uptake have been suggested by recent experiments performed by Barry *et al*. They studied the effect of Kupffer cell depletion (by pre-dosing mice with non-replicating Ad5) and warfarin treatment (to inhibit vitamin K-dependent coagulation factors) and found that this approach significantly increased the anti-tumoural effect of systemically delivered oncolytic Ad5 in nude mice[155]. Good results have also been demonstrated by coating Ad5 with high molecular weight polyethylene glycol[156] or by genetic modification of the hexon protein to ablate blood factor binding[157] for liver detargeting.

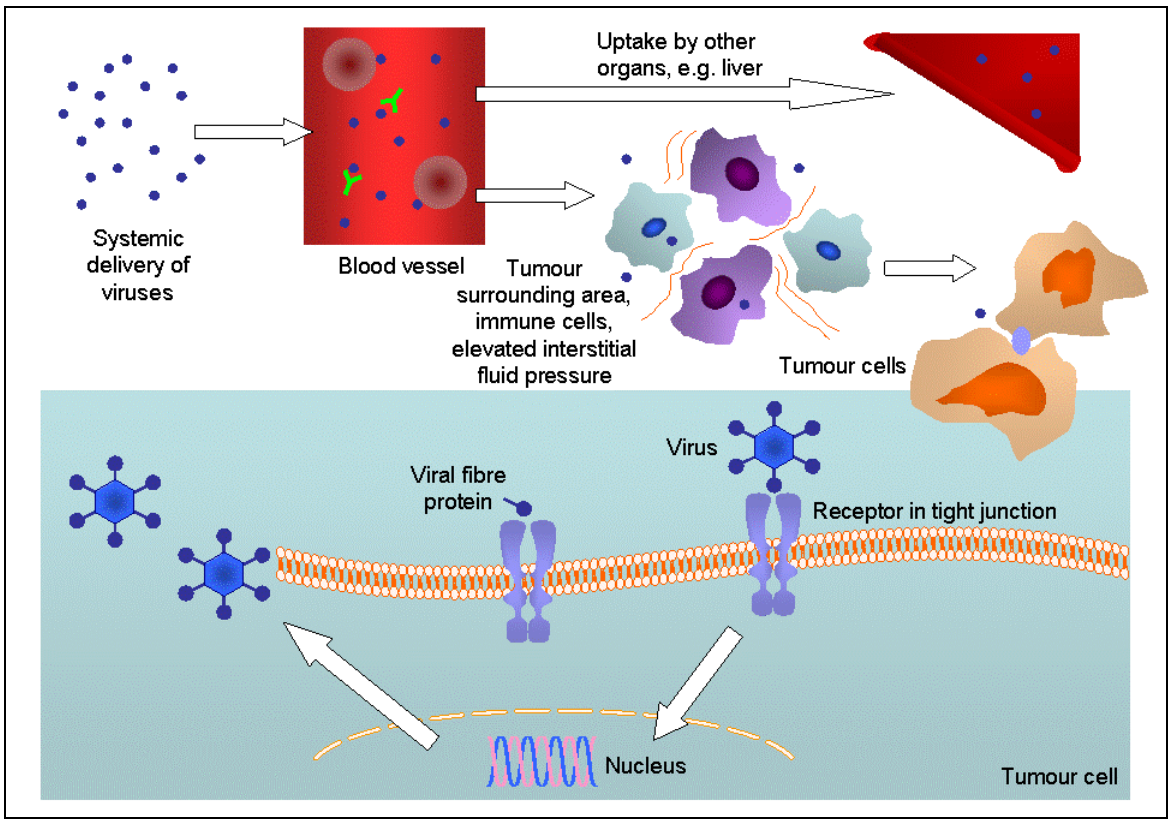


**Figure 1.5: Obstacles to successful delivery of oncolytic viruses to tumour cells[116].** After intravenous injection, viruses are neutralised by pre-existing antibodies and complement activation. Ads also interact with blood cells. It is now known that Ad5 binds to erythrocytes via CAR and complement receptor 1 in the absence and presence of anti-Ad5 antibodies, respectively[143]. Other Ad serotypes interact with these cells via different cellular receptors[158]. Sequestration into other organs and the reticuloendothelial system is a particular problem, often with resulting toxicities. From the blood stream, viruses have to pass through a mixture of extracellular matrix and cells (including normal and immune cells) and high interstitial fluid pressure before reaching the tumour. They then have to attach to the cellular receptor (often trapped in tight junction), be internalised, translocate to the nucleus, replicate, produce structural and other proteins, lyse the cell and release their progenies – some of these steps could be inhibited by factors such as the natural host immune response, hypoxic environment, soluble factors and genetic changes in the tumour cell. Fibre molecules released from infected cells could also bind to receptors of nearby cells, limiting virus spread across the tumour[159].

## 1.3 Adenovirus 11

Ad11 was first isolated from a stool sample of a patient with poliomyelitis[160]. It belongs to subgroup B2, and can be classified into at least two strains – Ad11p (Slobitski strain) and Ad11a (BC34 strain). Ad11p, the prototype strain, was originally isolated from a patient with urinary tract infection that developed into a persistent renal infection, and has been found in Europe, America and Japan[161-164]. It has much better binding affinity than Ad11a in several human cell lines[165]. The less common Ad11a was recovered from a patient with acute respiratory tract infection and has been found in China, Spain and Latin America[166-168].

### 1.3.1 Genomic differences with Ad5

The complete genome of Ad11 has been sequenced (GenBank accession numbers AF532578 and AY163756) and described separately by two groups (**Figure 1.6**)[169, 170]. Some major differences of its genome and gene products with Ad5 are shown in **Table 1.2**. The genome of Ad11 is 1,141 bp shorter than Ad5's, and they share 57% nucleotide identity. The highest and lowest amino acid identities are 85% and 24.6% for pTP and fibre, respectively. The packaging signal of Ad5 lies in the *E1A* transcriptional enhancer region[55, 57, 58]. This region of Ad11 shares only 67.4% nucleotide identity with that of Ad5, and does not contain binding sites for the EF-1A transcription factor[169]. The *E3* of Ad11 cannot be divided into *E3A* and *E3B* due to the absence of a polyadenylation signal. The *E3 20.3K* (*20.1K*) and *20.6K* (*20.8K*) genes are not present in Ad5 and could potentially be deleted to give additional space for foreign DNA insertion. The gene that encodes for ADP (*10.5K*) is absent in Ad11. Although there is a relatively high identity between the hexons of Ad5 and Ad11 (78.8%), pronounced differences were found in the seven HVRs[171]. Other major differences include the E1A proteins, the presence of only one VA RNA and *L6* in Ad11. The latter encodes an unidentified putative protein of 169 amino acids.

a)

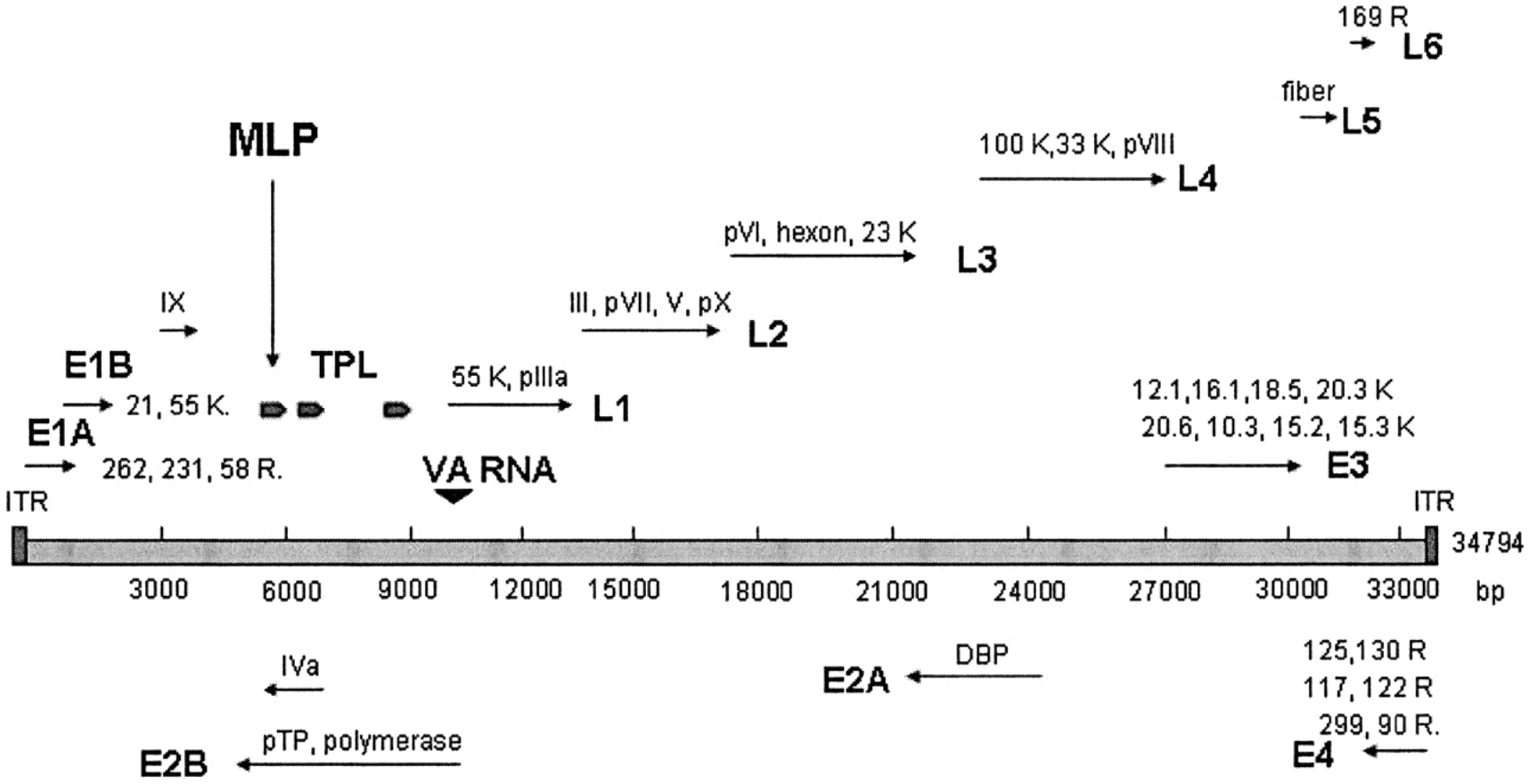
169 R
L6
fiber
L5
MLP
100 K,33 K, pVIII
L4
pVI, hexon, 23 K
L3
IX
III, pVII, V, pX
L2
E1B
TPL
55 K, pIIIa
L1
21, 55 K.
E1A
262, 231, 58 R.
VA RNA
12.1,16.1,18.5, 20.3 K
20.6, 10.3, 15.2, 15.3 K
E3
ITR
ITR
34794
3000
6000
9000
12000
15000
18000
21000
24000
27000
30000
33000
bp
IVa
DBP
E2A
125,130 R
117, 122 R
299, 90 R.
E4
pTP, polymerase
E2B

**b)**

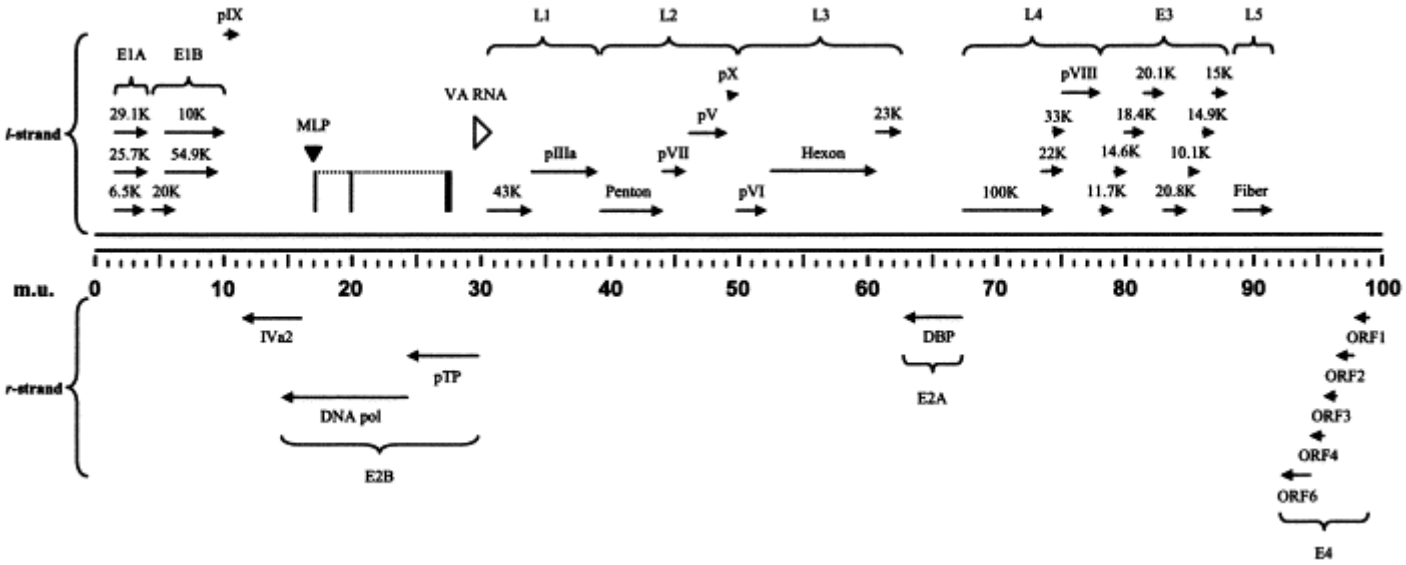


**Figure 1.6: Genomic organisation of Ad11 by (a) Mei *et al.*[169] and (b) Stone *et al*[170].** Abbreviation: pol, polymerase.

**Table 1.2: Some major genomic and gene product differences between Ad5 and Ad11**[169, 170]

| | Ad5 | | Ad11 |
|---|---|---|---|
| Whole genome | 35,935 bp | | 34,794 bp |
| | 57% nucleotide identity | | |
| GC content | 55.19% | | 48.87% |
| Packaging signal | 67.4% nucleotide identity | | |
| EF-1A binding sites | Present | | Absent |
| E1A proteins | | | |
| Number of amino acids | 289 | (35.9%) | 262 |
| (% identity) | 243 | (36.4%) | 231 |
| | 55 | (14.3%) | 58 |
| E1B 55K | 53.1% amino acid identity | | |
| *E3* | *E3A* and *E3B* | | *E3* |
| *20.3K* and *20.6K* | Absent | | Present |
| *10.5K* (ADP) | Present | | Absent |
| VA RNAs | Two | | One |
| Late regions | *L1-5* | | *L1-6* |
| *L2* (penton) | 73.5% amino acid identity | | |
| *L3* (hexon) | Pronounced differences in the HVRs | | |
| *L5* (fibre) | Long | | Short |
| | 24.6% amino acid identity | | |

### 1.3.2 Advantages over Ad5 as an oncolytic virus

Ad11 has demonstrated great potential as a gene transfer vector[172, 173]. In contrast to other human Ads that utilise CAR as primary attachment receptors, most subgroup B Ads use CD46 (Ad11, -16, -21, -35, -50)[174-176]. This allows Ad11 to infect cancer cells expressing no or low levels of CAR[172, 173, 177]. CD46 (or membrane cofactor protein) is a complement regulatory protein that acts as a cofactor for factor I-mediated degradation of C3b/C4b complement, thus protecting the host cell from autologous complement attack[178]. It is a transmembrane glycoprotein that is ubiquitously expressed in all human nucleated cells (except erythrocytes) at a low level and exists in multiple isoforms[179]. It also acts as a receptor for several pathogens, including MV (Edmonston

strain)[180], human herpesvirus 6[181], group A *Streptococci*[182] and *Neisseria*[183]. Although CAR expression is often downregulated in tumour cells[124, 184, 185], CD46 expression, however, is upregulated in a number of tumour types, including breast, cervical, liver, lung, endometrial and haematological malignancies[186-188]. Several chimeric oncolytic Ad5 have been developed (with fibres derived from subgroup B Ads but the remainder of the particle from Ad5) to target CD46 and they all have shown encouraging results[127, 189-191]. However, the use of intact subgroup B Ads as oncolytic agents is still underexplored but has great potential. They have different tropism and infectivity compared to chimeric viruses[147], and are more beneficial in terms of a reduced propensity for neutralisation by pre-existing antibodies (see below).

Several lines of evidence suggest that in contrast to other species B Ads, Ad11 also attaches to receptor(s) other than CD46. After infecting the human hepatoma cell line HuH-7 with MV, which downregulated CD46, there was suppression of transduction by chimeric Ad5/35 (where the fibres were derived from Ad35) but not Ad5/11[192]. Incubation of HeLa and A549 cells with Ad11 fibre knobs completely blocked Ad5/35 and Ad5/11 infection, but Ad35 fibres were unable to do so for Ad5/11[172]. Some have suggested that the receptors are the immunomodulatory molecules CD80 (B7-1) and CD86 (B7-2)[193, 194]. However, Tuve *et al.*[109, 176] disagreed, and have tentatively named this unidentified receptor 'receptor X'. They reported that the subgroup B members Ad3, -7 and -14 only utilise this receptor, whilst Ad16, -21, -35 and -50 exclusively use CD46. Ad11 on the other hand uses both CD46 and receptor X. They argued that CD80 and CD86 cannot be receptor X as they are mainly expressed on antigen-presenting cells and not on HeLa cells, which were permissive to Ad3, but not to Ad35 infection after siRNA knockdown of CD46. The binding of Ad11 to cancer cell lines is more efficient than to primary human fibroblasts and dendritic cells (DCs), suggesting that the expression of receptor X is lower in normal tissue. This receptor remains to be identified, but earlier studies have shown that Ad3 interacted with a 130-kDa protein in a divalent cation-dependent manner[195]. The fact that Ad11 uses two receptors has important implications – Ad11 could potentially infect a wider range of tumour cells and overcome receptor downregulation; the latter is a known problem with Ad35 and CD46[196]. A recent and significant finding by Strauss *et al.*[197] showed that Ads that utilise CAR or CD46 as primary attachment receptor failed to infect and lyse ovarian cancer cells of the epithelial phenotype, which are found in *in situ* tumours and tumour xenografts. These receptors are trapped in the tight junctions and therefore not

accessible to the virus. However, Ads that use receptor X (Ad3, -7, -11 and -14) could induce epithelial-mesenchymal transition (EMT) and result in efficient oncolysis.

Although the RGD motif is also found in its penton base, internalisation of Ad11 may occur through a RGD-independent pathway because it can efficiently infect some peripheral lymphocytes and haematopoietic cells, which contain few integrin receptors[198, 199]. $\alpha_V\beta_3$ and $\alpha_V\beta_5$ antibodies did not seem to affect Ad11 binding[200]. In fact, tropism and infectivity of Ad11 differ from those of Ad5/11 both *in vitro* and *in vivo*, suggesting a role played by hexon and penton[147, 172].

The prevalence of vector-neutralising antibodies within the human population is lower for Ad11 (10-31%) compared to Ad5 (45-90%), with no cross-reactivity between them[172, 173, 201-203]. These antibodies could reduce the efficacy of systemically-delivered virus for the treatment of metastatic diseases[131-133]. They are mainly directed against the viral hexon protein[204], suggesting that the use of intact Ad11 virion may be better than chimeric Ad5/11. Lore *et al*.[205] found that human DCs are more susceptible to Ad35 transduction than Ad5, due to the presence of CD46 receptor, resulting in more effective antigen presentation to T cells. As Ad11 also transduces DCs with higher efficiency[172, 173], this is beneficial in terms of cancer immunotherapy whereby a stronger immune response could be elicited against an Ad11-encoded tumour-specific antigen.

Because CD46 is only found in the testes of mice[206], *in vivo* biodistribution studies of Ad11 have to be performed in transgenic mice that express human CD46. The expression profile closely mimics that observed in humans, although low levels of CD46 are present on the erythrocytes[207]. In this model, more Ad11 were sequestered in the lung, kidney and spleen after intravenous injection, but they were not detectable at 72 hours[147, 172]. More importantly, there was an almost complete absence of liver transduction[172] and toxicity[137], secondary to its weak binding to factor X[153].

The advantages of Ad11 over Ad5 are summarised in **Table 1.3**.

**Table 1.3: Advantages of Ad11 over Ad5 as an oncolytic virus**

| | Ad5 | Ad11 |
|---|---|---|
| Attachment receptor | CAR – downregulated in cancer cells | CD46 and receptor X – upregulated in cancer cells |
| *In situ* epithelial cancer | CAR trapped in tight junction | Induces EMT – good infectivity and oncolysis |
| Internalisation | Integrin-dependent | ?Integrin-independent |
| Infectivity | Variable | Good across many cell types |
| Prevalence of serum neutralising antibodies | High (45-90%) | Low (10-31%) |
| DC transduction efficiency (for cancer immunotherapy) | Low | High |
| Binding to factor X and hepatotoxicity | High | Low |

## 1.4 Study aims and objectives

Given the shortcomings of Ad5 and the benefits of Ad11, this project aims to assess and develop Ad11 as an alternative oncolytic virus to Ad5. The objectives are:

1. To screen a panel of pancreatic and prostate carcinoma cell lines for CAR and CD46 expression levels.

2. To compare the oncolytic potencies of Ad5 and Ad11 in these cancer cell lines *in vitro*.

3. To confirm the oncolytic potency of Ad11 *in vivo*.

4. To dissect the mechanisms involved if a weaker oncolytic potency of Ad11 was observed in CD46-expressing tumour cells.

5. To construct a potent Ad11 and test this *in vitro* and *in vivo*.

# CHAPTER 2

# Materials and methods

## 2.1 Cell lines and cell culture

All cells were cultured at 37 °C and 5% $CO_2$, and were tested regularly for mycoplasma contamination. The human cancer cell lines used in the study are listed in **Table 2.1**.

**Table 2.1: Human cancer cell lines used**

| Cell name | Type | Culture medium | Source |
|---|---|---|---|
| Capan-1 | Exocrine pancreatic cancer | DMEM + 10% FBS | CR-UK |
| Capan-2 | Exocrine pancreatic cancer | DMEM + 10% FBS | ATCC |
| Hs766T | Exocrine pancreatic cancer | DMEM + 10% FBS | CR-UK |
| MIA PaCa-2 | Exocrine pancreatic cancer | DMEM + 10% FBS | CR-UK |
| PANC-1 | Exocrine pancreatic cancer | DMEM + 10% FBS | CR-UK |
| PaTu 8988s | Exocrine pancreatic cancer | DMEM + 10% FBS | CR-UK |
| PaTu 8988t | Exocrine pancreatic cancer | DMEM + 10% FBS | CR-UK |
| SUIT-2 | Exocrine pancreatic cancer | DMEM + 10% FBS | CR-UK |
| 22Rv1 | Prostate cancer | RPMI-1640 + 10% FBS | CR-UK |
| DU 145 | Prostate cancer | DMEM + 10% FBS | CR-UK |
| LNCaP | Prostate cancer | RPMI-1640 + 10% FBS | DSMZ |
| PC-3 | Prostate cancer | DMEM + 10% FBS | ATCC |
| MCF7 | Breast cancer | DMEM + 10% FBS | CR-UK |
| MDA-MB-231 | Breast cancer | DMEM + 10% FBS | CR-UK |
| MDA-MB-468 | Breast cancer | DMEM + 10% FBS | CR-UK |
| SK-BR-3 | Breast cancer | DMEM + 10% FBS | CR-UK |
| DLD-1 | Colon cancer | RPMI-1640 + 10% FBS | CR-UK |
| HCT 116 | Colon cancer | DMEM + 10% FBS | CR-UK |
| HT-29 | Colon cancer | DMEM + 10% FBS | CR-UK |
| SW620 | Colon cancer | DMEM + 10% FBS | CR-UK |

| | | | |
|---|---|---|---|
| A2780 | Ovarian cancer | RPMI-1640 + 10% FBS | CR-UK |
| IGROV1 | Ovarian cancer | DMEM + 10% FBS | CR-UK |
| OVCAR-3 | Ovarian cancer | DMEM + 10% FBS | CR-UK |
| A549 | Non-small cell lung cancer | DMEM + 10% FBS | CR-UK |
| Calu-1 | Non-small cell lung cancer | MEM EBSS + 10% FBS | CR-UK |
| HeLa | Cervical cancer | DMEM + 10% FBS | CR-UK |

Cells were purchased from the American Type Culture Collection (ATCC), Virginia, USA; Cancer Research UK (CR-UK) Cell Services, Hertfordshire, UK; Deutsche Sammlung von Mikroorganismen und Zellkulturen (DSMZ), Braunschweig, Germany. Culture media used are the Dulbecco's modified Eagle's medium (DMEM) and Roswell Park Memorial Institute-1640 (RPMI-1640), supplemented with foetal bovine serum (FBS) (PAA Laboratories, Pasching, Austria). Calu-1 cells were grown in minimum essential medium with Earle's balanced salts (MEM EBSS) with 10% FBS, 2 mM L-glutamine, 1 mM sodium pyruvate and 1% non-essential amino acids (CR-UK Cell Services).

The human embryonic kidney HEK-293 cell line, its subclone JH-293 (with slower growth rate), and the murine rectal carcinoma cell line CMT-93 (derived from the C57BL strain) (CR-UK Cell Services) were also used. The Syrian (golden) hamster cell lines used are: HaK (kidney; ATCC), HAP-T1 and HPD-1NR (exocrine pancreatic carcinoma; DSMZ). HPD-1NR was cultured in RPMI-1640 supplemented with 10% FBS. Other cell lines were grown in DMEM with 10% FBS. Normal human bronchial/tracheal epithelial cells and the bronchial epithelial cell growth medium (BEGM) were purchased from Lonza, Basel, Switzerland. Immortalised human pancreatic ductal epithelial cells[208] are kind gifts from Ming-Sound Tsao (University of Toronto, Ontario, Canada), and were grown in keratinocyte serum-free medium supplemented with bovine pituitary extract and human epidermal growth factor (Invitrogen, California, USA).

## 2.2 Viruses

Ad5 (Adenoid 75 strain) is regularly used in the laboratory[81]. Ad11 (Slobitski strain) is a kind gift from Daniel Stone and André Lieber (University of Washington, Washington, USA). Ad35 (Holden strain) was purchased from ATCC. Large scale virus production was performed by Vipul Bhakta, Heike Muller and Jennelle Francis (Queen

Mary, University of London, London, UK) in HEK-293 cells. Concentrations and titres of the viruses used are shown in **Table 2.2**.

**Table 2.2: Concentrations and titres of Ad5, Ad11 and Ad35 used**

| Virus | Particles/ml | PFUs/ml | Particles/PFU |
|---|---|---|---|
| Ad5 | $7.09 \times 10^{11}$ | $7.94 \times 10^{10}$ | 8.9 |
| Ad11 | $1.57 \times 10^{11}$ | $4.25 \times 10^{9}$ | 36.9 |
| Ad35 | $1.02 \times 10^{10}$ | $4.70 \times 10^{6}$ | 2170.2 |

Abbreviation: PFU, plaque-forming unit.

## 2.3 Flow cytometry for viral receptor expression

$3 \times 10^5$ cells were harvested and washed with cold buffer (phosphate-buffered saline (PBS), 2% FBS and 0.5 mM ethylenediaminetetraacetic acid (EDTA), pH 8.0). For CAR expression, cells were incubated in 100 µl of buffer with anti-CAR mouse monoclonal $IgG_1$, clone RmcB (1:200) (Millipore, Massachusetts, USA), and goat serum (1:20) (Dako, Glostrup, Denmark). Mouse $IgG_1$ (BD Biosciences, New Jersey, USA) was used in the negative controls. Incubation was performed in ice for an hour, with gentle mixing every 15 minutes. This was washed twice with buffer before incubation with fluorescein isothiocyanate (FITC)-conjugated polyclonal goat anti-mouse antibody (1:30) (Dako), in ice and away from light for an hour. For CD46 expression, cells were incubated with FITC-conjugated mouse anti-human CD46 $IgG_{2a}$, κ (1:10) (BD Biosciences) in ice for an hour and away from light, with gentle mixing every 15 minutes. FITC-conjugated mouse $IgG_{2a}$, κ isotype (BD Biosciences) was used in the negative controls. The cells were washed three times, resuspended in 300 µl of buffer with 0.5 µg/ml of propidium iodide (PI) (Sigma-Aldrich, Missouri, USA). Cells were processed through a BD FACSCalibur System flow cytometer and quantitated using BD CellQuest Pro software (BD Biosciences). 20,000 total events were recorded and gated for viability. Percentages of cells that expressed CAR and CD46 were obtained after correction for non-specific staining in the negative controls.

## 2.4 *In vitro* cell-killing assay

1,000-4,000 cells per well (cell number depended on their growth rate and the aim was for them to become confluent on day six of infection) were seeded in 96-well plates in 90 µl of medium and 5% FBS. Viruses (in 10 µl of medium and 5% FBS) were added 18 hours later at nine 1:10 serial dilutions, together with positive (no virus added) and negative (no cells, just medium alone) controls. Six days following infection cell survival was determined using the 3-(4,5-dimethylthiazol-2-yl)-5-(3-carboxymethoxyphenyl)-2-(4-sulfophenyl)-2H-tetrazolium, inner salt (MTS) assay (CellTiter 96 AQueous Non-Radioactive Cell Proliferation Assay; Promega, Wisconsin, USA). MTS was mixed with phenazine methosulfate (PMS) at a ratio of 20:1. 20 µl of the resultant mixture was added to each well and incubated for one to three hours. Absorbance was measured at 490 nm using the Opsys MR 96-well microplate reader and Revelation Quicklink 4.04 software (Dynex Technologies, Virginia, USA). The optical density (OD) for each virus dilution was compared to those of positive (no cell killing) and negative (background reading, equivalent to 100% cell death) controls to calculate the percentage of cell killing. The concentration required to kill 50% of cells (half maximal effective concentration – $EC_{50}$) was calculated by non-linear regression (sigmoidal dose-reponse curve) using GraphPad Prism (GraphPad Software, California, USA), utilising the following formula:

$$Y = \text{bottom} + \frac{(\text{top} - \text{bottom})}{1 + 10^{[(\log_{10} EC_{50} - X) \times \text{Hill slope}]}}$$

Y is the response and starts at 'bottom' and goes to the 'top' in a sigmoidal fashion.

## 2.5 Assessment of *in vivo* anti-tumoural efficacy

$1 \times 10^7$ PC-3 (in 100 µl of 50% PBS and 50% BD Matrigel Basement Membrane Matrix (BD Biosciences)) or MIA PaCa-2 cells (in 100 µl of PBS) were injected subcutaneously into the right flanks of four- to six-week-old BALB/c nude mice (Charles River Laboratories, Massachusetts, USA) and tumours were allowed to grow to approximately 6-8 mm. The mice were regrouped prior to treatment to ensure similar distribution of tumour sizes between the groups. 100 µl of PBS or Ads ($1 \times 10^{10}$ particles, diluted in PBS) were injected intratumourally on days 0, 2 and 4. Tumour volume was measured twice weekly using the standard ellipsoid formula: (length x $\text{width}^2$ x $\pi$)/6. The animals were euthanised when tumour dimension was more than

1.44 $cm^2$ (in accordance with Home Office regulations) or three months have elapsed after treatment.

To measure virus replication, tumours were grown as above and single doses of Ads were injected intratumourally. Tumours were harvested in triplicates at different time points post-injection. Each tumour was homogenised to a total volume of 2 ml in DMEM, then frozen and thawed three times in liquid nitrogen and at 37 °C, respectively. 200 µl of the resultant lysate was used for DNA extraction using the QIAamp DNA Blood Mini Kit (QIAGEN, Hilden, Germany) according to the manufacturer's instructions, and eluted in 70 µl of Buffer AE. DNA concentration was determined using the NanoDrop ND-1000 Spectrophotometer (Nanodrop Technologies, Delaware, USA) and a fixed amount of DNA was used for quantitative real-time polymerase chain reaction (qPCR) (see 2.7). DNA copies were normalised against total DNA and results are displayed as arbitrary units with the highest value of each graph set to 100. Examination of infectious particle production was performed as in 2.9 with a starting dilution of 1:1,000. Results are displayed as PFUs/ng of total DNA, using the formula:

$$\text{PFUs/ng of total DNA} = \frac{\text{PFUs/ml x 2 ml}}{\text{DNA concentration (ng/µl) x 70 µl x 2 ml / 200 µl}}$$

where 2 ml is the volume of cell lysate, 200 µl is the volume of cell lysate used for DNA extraction and 70 µl is the volume of Buffer AE used to elute DNA.

## 2.6 Immunofluorescence

100 µl of dimethyl sulfoxide (DMSO) (Thermo Fisher Scientific, Massachusetts, USA) was used to dissolve 1 mg of lyophilised Alexa Fluor 555 carboxylic acid, succinimidyl ester (Invitrogen), which was then added to 2 x $10^{10}$ virus particles in 2 ml of 0.1 M sodium bicarbonate, pH 8.4. This was foil-wrapped and mixed continuously for an hour at room temperature. The conjugated viruses were dialysed overnight at 4 °C in a Slide-A-Lyzer 10K MWCO Dialysis Cassette (Thermo Fisher Scientific), with two changes of 1 L of dialysis buffer (0.1 M Tris-HCl, pH 7.8, 0.1 M $MgCl_2$, 1.5 M NaCl and 10% glycerol). 2 x $10^4$ cells per well were seeded in 4-well Lab-Tek II Chamber Slide Systems (Thermo Fisher Scientific). 48 hours later they were incubated at 4 °C for an hour before infection with the conjugated viruses, diluted to 1:10 in 300 µl per well of serum-free medium. Viruses were allowed to attach at 4 °C for an hour,

and unbound viruses were washed away thrice with cold PBS. Virus internalisation and nuclear trafficking were achieved at 37 °C for an hour. Cells were fixed with ice-cold methanol. Cytoplasm was stained using 1:1,000 dilution of anti-α-tubulin monoclonal mouse antibody (Sigma-Aldrich) and Alexa Fluor 488 donkey anti-mouse IgG (Invitrogen). Slides were mounted with VECTASHIELD Mounting Medium with 4',6-diamidino-2-phenylindole (DAPI) (Vector Laboratories, California, USA). Images were taken using the Carl Zeiss LSM 510 laser scanning microscope (Carl Zeiss, Oberkochen, Germany).

## 2.7 qPCR of viral DNA

*E1A* primers were designed using the Primer Express Software for Real-Time PCR Version 3.0 (Applied Biosystems, California, USA):

- Ad5 *E1A* forward: 5'-TGCCAAACCTTGTACCGGA-3'
- Ad5 *E1A* reverse: 5'-CGTCGTCACTGGGTGGAAA-3'
- Ad11 *E1A* forward: 5'-GAAGGCTGCCAATGTTGGTT-3'
- Ad11 *E1A* reverse: 5'-ACAGCCATGTCCAGGAAGCT-3'

These were purchased from Sigma-Aldrich. Probes were purchased from Applied Biosystems that have the FAM reporter dye (6-carboxyfluorescein) linked to the 5' end, and the minor groove binder (MGB) and non-fluorescent quencher at the 3' end: Ad5 (5'-TTACCTGCCACGAGGCTGGC-3') and Ad11 (5'-TCAGTTGGATTGCCC-3'). qPCR was performed in MicroAmp Optical 96-Well Reaction Plates using the 7500 Real-Time PCR System and the Sequence Detection Software Version 1.3 (Applied Biosystems). The following reagents (and final concentrations) were used: TaqMan Universal PCR Master Mix (Applied Biosystems) (1x), primers (900 nM each), probe (200 nM), DNA template (fixed amount between samples needed for comparison) and diethylpyrocarbonate (DEPC)-treated water (to a total volume of 25 µl per reaction). PCR conditions were: 95 °C (10 minutes) and [95 °C (15 seconds), 60 °C (one minute)] 40 cycles. For quantitative analysis, viral genomes were purified using the QIAamp DNA Blood Mini Kit and quantified spectrophotometrically, then serially diluted to generate a standard graph that ranges from five to 5 x $10^8$ genome copy numbers (one copy is contained in *s* x 1.096 x $10^{-21}$ g of genomic DNA, where *s* is the size of the genome, *i.e.* Ad5 – 35,935 bp; Ad11 – 34,794 bp). DNA copy number of each sample was determined with reference to the

threshold cycle (Ct). Results are displayed as arbitrary units with the highest value of each graph set to 100.

### 2.7.1 Virus attachment and nuclear entry

2 x $10^5$ cells in 100 µl of cold buffer (1% bovine serum albumin (BSA) (Sigma-Aldrich) in PBS) were used for each reaction. Cells were incubated in ice for an hour before viruses (diluted in 100 µl of buffer) were added at 1,000 particles/cell and cells were left shaking for an hour at 4 °C for virus attachment. Cells were then washed twice to remove unbound viruses. For nuclear entry, cells were resuspended in 100 µl of buffer and incubated at 37 °C for 30, 60 and 120 minutes, respectively. Nuclear extracts were obtained using the NE-PER Nuclear and Cytoplasmic Extraction Reagents (Thermo Fisher Scientific) according to the manufacturer's instructions. DNA was obtained using the QIAamp DNA Blood Mini Kit for qPCR.

### 2.7.2 *In vitro* viral DNA amplification

Cells were seeded in 6-well plates in medium with 10% FBS and infected with viruses when 70-80% confluency has been reached, at 100 particles/cell in serum-free medium. After two hours of incubation, this was replaced by medium supplemented with 5% FBS. At 24, 48, 72 and 96 hours cells and media were collected by scraping. DNA was extracted using the QIAamp DNA Blood Mini Kit for qPCR.

## 2.8 Western blot

### 2.8.1 Sample preparation and protein estimation

Recipes for making up the solutions needed here are listed in the Appendix. Cells were seeded and infected as in 2.7.2, except with 200 particles/cell. Cells were washed with PBS and harvested at different time points post-infection with lysis buffer. Protein concentration was estimated based on the Bradford Protein Assay[209]. 5 µl of protein was mixed with 795 µl of water and 200 µl of Bio-Rad Protein Assay Dye Reagent Concentrate (Bio-Rad Laboratories, California, USA) in a cuvette. Following calibration with a blank sample (800 µl of water and 200 µl of reagent), the absorbance at 595 nm was determined using the DU 520 General Purpose UV/Vis Spectrophotometer (Beckman Coulter, California, USA). Protein concentration was determined by means of a standard graph, obtained by measuring the absorbance values of known quantities (1, 2, 4, 8, 16, 32 and 64 µg) of BSA.

### 2.8.2 Sodium dodecyl sulfate-polyacrylamide gel electrophoresis (SDS-PAGE)

100 µg of each sample was mixed with loading buffer and water to a total volume of 25 µl. This was heated at 95 °C for 10 minutes and then placed in ice. 10 µl of Full-Range Rainbow Molecular Weight Markers (GE Healthcare, Buckinghamshire, UK) was loaded alongside the protein samples in a 10% running gel (with 4% stacking gel).

### 2.8.3 Western blotting and immunodetection

Immobilon-P$^{SQ}$ polyvinylidene difluoride (PVDF) transfer membrane (Millipore) was pre-wet with methanol and then soaked in transfer buffer together with the gel and two Extra Thick Blot Papers (Bio-Rad Laboratories). These were moved to a Trans-Blot SD Semi-Dry Transfer Cell (Bio-Rad Laboratories) where protein transfer occurred at 20 V for 40 minutes. The membrane was soaked in methanol and subsequently air-dried. Primary antibodies used are: Ad goat polyclonal antibody (1:8,000) (Abcam, Cambridge, UK) for Ad5 hexon, Ad11 hexon rabbit polyclonal antibody (1:200) (raised against the amino acid sequence AKQKTTEQPNQKVE by GenScript, New Jersey, USA) for Ad11 hexon, and GABPA mouse monoclonal antibody (1:500) (Source BioScience AUTOGEN, Wiltshire, UK) for EF-1A. Equal loading of protein was checked using proliferating cell nuclear antigen (PCNA) mouse monoclonal antibody (1:1,000) (Santa Cruz Biotechnology, California, USA). Antibody dilution was done in 2% BSA in PBS and incubated at room temperature for an hour. Membrane was washed three times for 15 minutes each with Tris-buffered saline with Tween 20 (TBST) and then incubated with horseradish peroxidase (HRP)-conjugated secondary antibodies (Dako), diluted according to the manufacturer's instructions in TBST. After further washes chemiluminescent detection was performed using the Amersham ECL Western Blotting Detection Reagents (GE Healthcare) according to the manufacturer's instructions. Signals were visualised on Amersham Hyperfilm ECL (GE Healthcare).

## 2.9 Virus replication assay

Cells were seeded, infected and collected as in 2.7.2. The cells and media were frozen and thawed three times in liquid nitrogen and at 37 °C, respectively. 10,000 JH-293 cells were seeded in each well of 96-well plates in 200 µl of DMEM with 5% FBS. Harvested cell lysates were used to infect the JH-293 at six 1:10 serial dilutions (starting

dilution of 1:1,000) down each row of the plate (the last row was left uninfected to act as a negative control). Inspection for CPE was performed 11 days later. The 50% tissue culture infective dose ($TCID_{50}$) and number of PFUs/cell (cell count on the day of infection) were calculated using the Reed-Muench accumulative method (see Appendix).

## 2.10 Reverse transcription PCR of *E1A* mRNA

4 x $10^5$ cells per well were seeded in 6-well plates and infected as in 2.7.2. Cells were harvested at two, eight and 24 hours post-infection using 1 ml of TRIzol Reagent (Invitrogen) divided equally between three wells. The plate was rocked gently for five minutes at room temperature, and each ml was transferred to a tube and mixed with 200 µl of chloroform. The tube was shaken vigorously for 10 seconds before centrifugation for 15 minutes at 11,400 rpm and 4 °C. The upper aqueous layer was obtained and RNA was precipitated with 500 µl of cold isopropanol and incubated in ice for 30 minutes. This was then centrifuged at 11,400 rpm and 4 °C for 10 minutes. The supernatant was discarded and the RNA pellet was washed with 1 ml of 75% ethanol before centrifugation at 7,500 rpm and 4 °C for five minutes. The supernatant was removed and the RNA was allowed to air dry. 70-140 µl of DEPC-treated water (depending on pellet size) was added to dissolve the RNA and then quantified spectrophotometrically. Complementary DNA (cDNA) was produced using the TaqMan Reverse Transcription Reagents (Applied Biosystems). The following reagents (and final concentrations) were used: TaqMan reverse transcription buffer (1x), $MgCl_2$ (5.5 mM), deoxynucleotide triphosphates (dNTPs) (500 µM of each dNTP), random hexamers (2.5 µM), RNase inhibitor (0.4 U/µl), Multiscribe reverse transcriptase (1.25 U/µl), 1 µg of template RNA and DEPC-treated water (to a total volume of 50 µl per reaction). Reaction conditions were: 25 °C (10 minutes), 48 °C (30 minutes) and 95 °C (five minutes), performed in a PTC-200 Peltier Thermal Cycler (MJ Research, Massachusetts, USA). qPCR was performed as in 2.7 except that 2 µl of cDNA template was used together with 1.25 µl of 20x Eukaryotic 18S rRNA Endogenous Control (VIC/MGB Probe, Primer Limited; Applied Biosystems) for each reaction. Non-reverse transcription controls were used to rule out DNA contamination in the RNA samples. Results were normalised by subtracting the corresponding Ct value of 18S from the Ct value of each sample. RNA levels were determined with reference to the standard graph and results are displayed as arbitrary units with the highest value of each graph set to 100.

## 2.11 pGL3 vector construction

### 2.11.1 Plasmids, primers, DNA electrophoresis and restriction digestion

The wild-type Ad11 plasmid (pBGwtAd11) is a kind gift from Daniel Stone and André Lieber. The wild-type Ad5 plasmid (pTG3602) was provided by Daniel Öberg (Queen Mary, University of London). pGL3-Control Vector was purchased from Promega. To clone the adenoviral *E1A* upstream regions for insertion into pGL3, the following primers were designed (underlined are restriction enzyme recognition sites and the corresponding enzymes are stated on the right) and purchased from Sigma-Aldrich:

- Ad5-L: 5'-ATCagatctGGATCCGAATTCTTAATTAA-3' (BglII)
- Ad5-EP: 5'-ATCagatctACACAGGAAGTGACAATTTTCGCGC-3' (BglII)
- Ad5-P: 5'-ATCagatctTGGAGACTCGCCCAGGTGTTTTTCTC-3' (BglII)
- Ad5-R: 5'-ATCaagcttTTTCAGTCCCGGTGTCGGAGC-3' (HindIII)
- Ad11-L: 5'- ATCagatctAATTCGAATTCTTAATTA-3' (BglII)
- Ad11-EP: 5'-ATCagatctTTTTTCTCACGGAACTACTTAG-3' (BglII)
- Ad11-P: 5'-ATCagatctCGATTACCGTGTTTTTTACCTG-3' (BglII)
- Ad11-R: 5'- ATCaagcttTTTTTTATTATTAAACTGCCGGC-3' (HindIII)

DNA electrophoresis was performed on 1% agarose gel, prepared using Ultrapure Agarose (Invitrogen) in 1x tris-borate-EDTA (TBE) buffer with 0.5 µg/ml of ethidium bromide (Sigma-Aldrich). Samples were loaded in Blue/Orange Loading Dye (Promega). Lambda DNA/EcoRI + HindIII Markers (Promega) or 100 bp DNA Ladder (New England Biolabs (NEB), Massachusetts, USA) were used to verify band size. Restriction enzymes, buffers and BSA were purchased from NEB. Digestion was performed in a PTC-200 Peltier Thermal Cycler at 37 °C with the addition of its respective buffer and 0.1 µg/µl of BSA.

### 2.11.2 Cloning and insertion of fragments into pGL3

PCR was performed using the Phusion High-Fidelity DNA Polymerase (NEB). The following reagents (and final concentrations) were used: Phusion HF Buffer (1x), Deoxynucleotide Solution Mix (200 µM of each dNTP), primers (0.5 µM each), template DNA (300 ng), DMSO (3 µl), Phusion DNA Polymerase (0.02 U/µl) and DEPC-treated water to a total volume of 100 µl per reaction. PCR conditions were: initial denaturation (98 °C for 30 seconds), [denaturation (98 °C for 10 seconds), annealing (depended on the melting temperature of each primer, for 30 seconds),

extension (72 °C for 30 seconds/kb] 25 cycles, and final extension (72 °C for seven minutes). PCR was performed using the primers Ad5-L, Ad5-EP and Ad5-P with the reverse primer Ad5-R and pTG3602 as template, for "left end", "enhancer-promoter" and "promoter", respectively (**Figure 6.2**). pBGwtAd11 was used as a template for Ad11. DNA was extracted from gel using the QIAquick Gel Extraction Kit (QIAGEN) according to the manufacturer's instructions.

The resultant fragments and pGL3-Control Vector were digested with BglII and HindIII. Digested pGL3 was extracted using the QIAquick Gel Extraction Kit, whilst digested fragments were purified using the QIAquick Nucleotide Removal Kit (QIAGEN), according to the manufacturer's instructions. Ligation of fragments to pGL3 was performed using the LigaFast Rapid DNA Ligation System (Promega), with an insert-to-vector ratio of 2:1. The resultant plasmids were transformed into One Shot TOP10 Chemically Competent *Escherichia coli* (Invitrogen). Plasmids and bacteria were mixed and incubated in ice for 20 minutes before heat shock treatment at 42 °C for one minute. This was immediately transferred back to ice and left for two minutes. 100 µl of lysogeny broth (LB) was added and was left shaking at 37 °C for an hour. They were then spread on LB agar containing 100 µg/ml of ampicillin (Invitrogen) and cultured overnight at 37 °C. A few colonies were selected and expanded in 300 µl of ampicillin-containing LB each, left shaking at 37 °C for two hours. To confirm successful ligation, 2 µl of culture was used for PCR using the corresponding primers, in a total volume of 25 µl, and subsequently viewed by agarose gel electrophoresis. Correct cultures were then expanded and plasmids were purified using the QIAprep Spin Miniprep Kit (QIAGEN), according to the manufacturer's instructions. The resultant plasmids were sent to the Genome Centre, Queen Mary, University of London for sequencing using RVprimer3 and GLprimer2 (Promega).

## 2.12 Luciferase reporter assay

7 x $10^4$ cells per well were seeded in 24-well plates in medium supplemented with 10% FBS. Transfection was performed with 150 ng of recombinant pGL3 plasmid and 50 ng of pRL-SV40 Vector (Promega) per well, using the Effectene Transfection Reagent (QIAGEN) according to the manufacturer's instructions. To assess the effect of virus infection, cells were first infected with viruses at 100 particles/cell in serum-free

medium for two hours, before being replaced by medium with 5% FBS. The cells were transfected as above after an additional two hours.

18 hours after transfection, luciferase activity was detected using the Dual-Luciferase Reporter Assay System (Promega) according to the manufacturer's instructions. Luminescence was measured using the VICTOR$^3$ 1420-050 Multilabel Counter (PerkinElmer, Massachusetts, USA). Corrected luciferase activity was calculated using the following formula:

$$\frac{1000 \times \text{Luminescence from firefly luciferase (pGL3)}}{\text{Luminescence from } \textit{Renilla} \text{ luciferase (pRL-SV40)}}$$

## 2.13 Construction of recombinant Ad11

### 2.13.1 DNA, plasmids and primers for recombinant Ad11 construction

Ad5 and Ad11 DNA was purified from wild-type viruses using the QIAamp DNA Blood Mini Kit. pBGwtAd11 was also used. pSS was developed by Daniel Öberg. pUC18 was provided by Guozhong Jiang (Queen Mary, University of London). The following primers were purchased from Sigma-Aldrich to amplify different regions of the Ad5 and Ad11 genomes for the construction of recombinant Ad11 with Ad5 *E1A* enhancer and/or promoter (see **Figure 7.2** for details):

- pA1: 5'-ATCaagcttagatctGGAGACGGTCACAGCTTGTCTG-3' (HindIII, BglII)
- pA2: 5'-ATCtctagagcggccgcTAATTAAGAATTCGAATTAATTAATTC-3' (XbaI, NotI)
- pA3: 5'-ATCaagcttgcggccgcATCATCAATAATATACCTTATAG-3' (HindIII, NotI)
- pA4: 5'-ATCggatccgatatcAGCCTTTTTATGCGTCAC-3' (BamHI, EcoRV)
- pA5: 5'-AAAAATGAGAGATTTGCGATTTCTGC-3'
- pA6: 5'-ATCggatccctcgagCAAAGCGAACATAACAGTTC-3' (BamHI, XhoI)
- pA7: 5'-ATCaagctttacgtaACACAGGAAGTGACAATTTTCGCGC-3' (HindIII, SnaBI)
- pB1: 5'-ATCggatccgatatcAAACCTCCACGTAATGGGTCAAAGTC-3' (BamHI, EcoRV)
- pB2: 5'-ATCaagctttacgtaTGGAGACTCGCCCAGGTGTTTTTCTC-3' (HindIII, SnaBI)
- pAlinker: 5'-GCAGAAATCGCAAATCTCTCATTTTCAGTCCCGGTGTCGG

AGC-3’

### 2.13.2 Cloning of fragments from adenoviral genomes

The following fragments were cloned as in 2.11.2 (and primers used) using pBGwtAd11 as template: A1A2 (pA1 and pA2), A3A4 (pA3 and pA4), A3B1 (pA3 and pB1) and A5A6 (pA5 and pA6). The fragments B2Linker (pB2 and pAlinker) and A7Linker (pA7 and pAlinker) were cloned from Ad5 genomic DNA. DNA was extracted from gel using the QIAquick Gel Extraction Kit. To obtain the chimeric fragment B2A6, PCR was performed as above (but using an annealing temperature of 57 °C for two minutes) using B2Linker and A5A6 only. This was further amplified using the primers pB2 and pA6. A7A6 was obtained in the same way with A7Linker and A5A6, followed by amplification using pA7 and pA6.

### 2.13.3 Insertion of fragments into pUC18

pUC18, A3B1, A3A4, B2A6 and A7A6 were digested with HindIII and BamHI. pUC18 and A1A2 were digested with HindIII and XbaI. Digested pUC18 was run on agarose gel and extracted using the QIAquick Gel Extraction Kit, whilst digested fragments were purified using the QIAquick Nucleotide Removal Kit. Ligation to pUC18, transformation of bacteria, and confirmation of successful ligation by PCR and agarose gel electrophoresis were performed as in 2.11.2. The resultant plasmids (pUCA1A2, pUCA3B1, pUCA3A4, pUCB2A6 and pUCA7A6) were sent for sequencing using M13 forward and reverse primers.

### 2.13.4 Production of shuttle vectors

pUCA1A2, pUCA3B1 and pUCA3A4 were digested with NotI and BamHI. Digested pUCA1A2, A3B1 and A3A4 were extracted using the QIAquick Gel Extraction Kit. Ligation (pUCA1A2 with A3B1 or A3A4), culture, confirmation by PCR and agarose gel electrophoresis, and plasmid purification were performed as in 2.11.2, to produce the plasmids pUCA1B1 and pUCA1A4. These plasmids and pSS were digested with BglII and EcoRV.

To construct the shuttle vector for Ad11-Ad5-P (or Ad11-Ad5-EP), A1B1 (or A1A4) was ligated to pSS (selected using LB containing 50 μg/ml of chloramphenicol (Sigma-Aldrich)). The resultant pSSA1B1 (or pSSA1A4) and pUCB2A6 (or

pUCA7A6) were digested with SnaBI and XhoI. B2A6 (or A7A6) was then ligated to pSSA1B1 (or pSSA1A4) to produce pSSA1B1B2A6 (or pSSA1A4A7A6).

### 2.13.5 Homologous recombination

pSSA1B1B2A6 (or pSSA1A4A7A6) was digested with PmeI and extracted with the QIAquick Gel Extraction Kit. 1 μg of digested plasmid was mixed with 100 ng of pBGwtAd11 in 40 μl of BJ5183 Electroporation Competent Cells (Stratagene, California, USA). Transformation was done in electroporation cuvettes (Flowgen Bioscience, Nottingham, UK) using an electroporator (Gene Pulser II, Bio-Rad Laboratories) set at capacitance of 25 μF, resistance of 200 Ω and voltage of 2.5 kV. Immediately after electroporation, 600 μl of LB was added and the mixture was shaken at 37 °C for an hour. Bacteria were then grown on LB agar with ampicillin and chloramphenicol. Small- or medium-sized colonies were selected, expanded in 300 μl of ampicillin and chloramphenicol-containing LB for two hours at 37 °C. To confirm successful recombination, PCR was performed using the primer pairs pA1 and pA6, and pA1 and pALinker. Correct cultures were expanded, the plasmids were extracted and subsequently used to transform One Shot TOP10 Electrocomp *E. coli* (Invitrogen) using an electroporator. After further expansion and extraction of plasmids, they were confirmed by digestion with NotI, SwaI or EcoRV and SnaBI, and checked by electrophoresis.

### 2.13.6 Removal of antibiotic resistance gene

6 μg of homologously-recombined Ad11 plasmids were digested with SwaI at 37 °C overnight, in 100 μl of reaction volume. 300 μl of DEPC-treated water was added to the sample and 400 μl of phenol:chloroform:isoamyl alcohol 25:24:1 (saturated with 10 mM Tris, pH 8.0, 1 mM EDTA; Sigma-Aldrich) was added. This was mixed thoroughly and centrifuged at maximum speed for five minutes. The upper aqueous phase was collected and mixed with $1/10^{th}$ volume of 3 M sodium acetate, pH 5.2. Ice-cold ethanol (2.5x volume) was added and this was placed in -80 °C for 20 minutes. Centrifugation was performed at maximum speed and 4 °C for five minutes. The supernatant was removed and DNA pellet was washed with 70% ethanol. The pellet was subsequently allowed to air dry before resuspension in 12 μl of DEPC-treated water. Ligation of plasmid was done prior to transformation of One Shot TOP10 Electrocomp *E. coli*, selected by ampicillin. Correct colonies were identified by PCR using the primer pairs of pA1 and pA6, pA3 and pAlinker, and pA3 and pA6. After

expansion and plasmid extraction, further confirmation was done by digestion with NotI or EcoRV and SnaBI.

### 2.13.7 HEK-293 transfection and virus production

7 μg of plasmid was linearised with NotI at 37 °C overnight and purified as in 2.13.6. Transfection was performed using 400 ng of DNA and the Effectene Transfection Reagent per well, on 40-80% confluent HEK-293 cells in a 6-well plate. No DNA was added for mock-transfected negative controls. Transfection was performed in DMEM supplemented with 2% FBS. When CPE was noted in the plasmid-transfected cells, they were collected with the medium, frozen and thawed three times in liquid nitrogen and at 37 °C, respectively. Larger scale virus production was performed sequentially by infecting HEK-293 cells with the cell lysate in a T175 flask before stepping up to a Nunc Cell Factory 10 chamber (Sigma-Aldrich). Four T175 flasks of HEK-293 were needed to seed one chamber. When cells were > 75% confluent as indicated by a parallel culture, 8 ml of lysate from the previous T175 culture was used to infect the chamber. At full CPE, detached cells and medium were collected and centrifuged for 10 minutes at 2,000 rpm and 4 °C. The supernatant was discarded and the cells were washed with 15 ml of PBS, by centrifugation at 1,000 rpm and 4 °C for 10 minutes. The resultant pellet was resuspended with 12 ml of cold Tris-HCl, pH 8.0. This was stored at -80 °C until caesium chloride (CsCl) banding.

### 2.13.8 Virus purification

Recipes for making up the solutions needed here are listed in the Appendix. The above cell suspension was frozen and thawed as before. This was centrifuged at room temperature and 6,000 rpm for 10 minutes, and the supernatant layered onto a CsCl gradient (10 ml of 1.25 g/ml and 7.6 ml of 1.4 g/ml) in a 25 x 89 mm Ultra-Clear Centrifuge Tube (Beckman Coulter). Centrifugation was performed in an Optima LE-80K Ultracentrifuge (Beckman Coulter) for two hours at 25,000 rpm and 15 °C. Three layers were noted from top to bottom – cellular debris, empty virus particles, and successfully encapsulated infectious particles. The lowest band was extracted using a needled syringe and layered onto 3 ml of 1.35 g/ml CsCl in a 13 x 51 mm Ultra-Clear Centrifuge Tube (Beckman Coulter). This was centrifuged for > 15 hours at 40,000 rpm and 15 °C in an Optima LE-80K Ultracentrifuge. The virus band was harvested as before and the volume made up to 12 ml with TSG buffer.

The viruses were injected into a Slide-A-Lyzer 3.5K MWCO Dialysis Cassette (Thermo Fisher Scientific) and dialysed for 24 hours in 2 L of dialysis solution. The purified viruses were retrieved, aliquoted and stored at -80 °C.

### 2.13.9 Determination of virus concentration

For the determination of particle count, tubes listed in **Table 2.3** were prepared with 2x lysis buffer (2 ml of 10% SDS, 0.8 ml of 1 M Tris-HCl, pH 7.5, 17.2 ml of water) and dialysis buffer (Appendix).

**Table 2.3: Reaction mixtures for the determination of particle count**

| | #1 | #2 | #3 | #4 |
|---|---|---|---|---|
| Virus | 100 µl | 200 µl | - | - |
| Dialysis buffer | 100 µl | - | 100 µl + 100 µl | 200 µl |
| 2x lysis buffer | 200 µl | 200 µl | 200 µl | 200 µl |

These were mixed and incubated for 10 minutes at 56 °C. The volume in each tube was made up to 1 ml with water. The absorbance at 260 nm was measured thrice for each tube. Tube #3 was read first (blank reading; should be about 0.002-0.012), followed by tube #1. This was repeated for tubes #4 and #2.

The particle count formula is: $OD_{260}$ x dilution factor x 1.12 x $10^{12}$ = particles/ml, where samples #1 and #2 have dilution factors of 10 and 5 respectively. To calculate the particle count:

(Average $OD_{260}$ #1 - average $OD_{260}$ #3) x 10 x 1.12 x $10^{12}$ = A

(Average $OD_{260}$ #2 - average $OD_{260}$ #4) x 5 x 1.12 x $10^{12}$ = B

Therefore, particle count = (A+B) / 2.

For the determination of the number infectious particles, limiting dilution assay using JH-293 cells was performed as described in 2.9. The $TCID_{50}$ and number of PFUs/ml were calculated.

### 2.13.10 Sequencing of recombinant Ad11

For Ad11-Ad5-P, primers that amplify the region from approximately 150 bp upstream of Ad11 *E1A* promoter to the first 150 bp of *E1A* were designed and purchased from Sigma-Aldrich:

- forward: 5'-TGAGGTAGTTTTGACCGGAT-3'
- reverse: 5'-ATCATACAGTTCCTGAAGCG-3'

PCR was performed on the DNA of Ad11-Ad5-P and wild-type Ad11 (control). The fragments were obtained using the QIAquick Gel Extraction Kit, prior to sequencing using the forward primer.

As the region upstream of Ad11 *E1A* enhancer is very close to the virus 5'-ITR, primers that bind to this area cannot be used reliably for sequencing of Ad11-Ad5-EP. The following primers were designed (with the introduction of restriction sites) and purchased from Sigma-Aldrich to amplify the region near the start of the *E1A* enhancer (to avoid the ITR) and the first 58 bp of *E1A*, for subsequent insertion into pUC18:

- 5'-ATCaagcttGCAAGTTGTCGCGGGAAATGTG-3' (HindIII)
- 5'-ATCtctagaTTTCATTTCCAGTCTCAGCA-3' (XbaI)

PCR was performed and DNA was extracted using the QIAquick Gel Extraction Kit. Fragments were digested with HindIII and XbaI and subsequently inserted into pUC18. Confirmation of colonies was done by PCR as in 2.11.2. The resultant plasmids were sent for sequencing using M13 forward and reverse primers.

### 2.13.11 Purity check of recombinant Ad11

To rule out contamination of the recombinant Ad11 by Ad5 or wild-type Ad11, the following primers were purchased from Sigma-Aldrich for PCR:

- 5P-F: 5'-TGGAGACTCGCCCAGGTGTTTTTC-3'
- 5P-R: 5'-ATTTTCAGTCCCGGTGTCGGAGC-3'
- 11P-F: 5'-CGATTACCGTGTTTTTTACCTG-3'
- 11P-R: 5'-CTCAAAAAGCTGCACAGGTGG-3'
- 5H-F: 5'-AGTTACCTCCAATGGCATGCTTG-3'
- 5H-R: 5'-ATGCAAAGGAGCCCCGTACTTTAG-3'
- 5E-F: 5'-ATTTTCGCGCGGTTTTAGGC-3'
- 11E-F: 5'-ACGGAACTACTTAGTTTTCCCACG-3'

PCR was performed using the primer pairs 5P-F and 5P-R (Ad5 *E1A* promoter to just immediately before *E1A*), 11P-F and 11P-R (Ad11 *E1A* promoter to part of *E1A*), 5H-F and 5H-R (region within the Ad5 hexon-coding sequence), 5E-F and 5P-R (Ad5 *E1A* enhancer to just immediately before *E1A*), 11E-F and 11P-R (Ad11 *E1A* enhancer to part of *E1A*) on the purified DNA of Ad5, Ad11, Ad11-Ad5-P and Ad11-Ad5-EP.

## 2.14 Statistical analysis

Statistical analyses were performed using GraphPad Prism and data are displayed as means ± standard errors of the mean (SEM). Pair-wise comparisons were done using the unpaired, two-tailed Student's *t*-test. Progression-free percentages were analysed by the Kaplan-Meier method and the logrank test.

# CHAPTER 3

# Expression levels of receptors for Ad5 and Ad11 in human cancer cell lines and oncolytic potencies *in vitro*

Ad5's infectivity in many cancer types has been limited due to the downregulation of its attachment receptor CAR[124, 184, 185]. In contrast, Ad11 binds to CD46 and its expression has been reported to be upregulated in malignant diseases[186-188]. In this chapter, the expression levels of CAR and CD46 were analysed in a panel of human cancer cell lines by flow cytometry. This is followed by the comparison of oncolytic potencies of these two viruses *in vitro*.

## 3.1 Human pancreatic and prostate cancer cell lines express significantly higher levels of CD46 compared to CAR

CAR and CD46 expression levels in eight human pancreatic and three prostate cancer cell lines were determined by flow cytometric analysis using FITC-conjugated antibodies. Cells were analysed in triplicates and corrected for non-specific staining by means of isotype control antibodies. Dead cells were excluded by their permeability to PI. All the cell lines tested have shown significantly higher levels of CD46 compared to CAR (**Figure 3.1**). CAR was barely detectable in the pancreatic cancer cell lines Hs766T and Capan-2 but was the highest in PANC-1. CAR was nearly absent in the prostate cancer cell line PC-3 but about 90% of DU 145 cells expressed CAR. In contrast, CD46 expression was found in ≥ 90% of most cancer cells, with the exception of Hs766T where only 14% were CD46-positive.

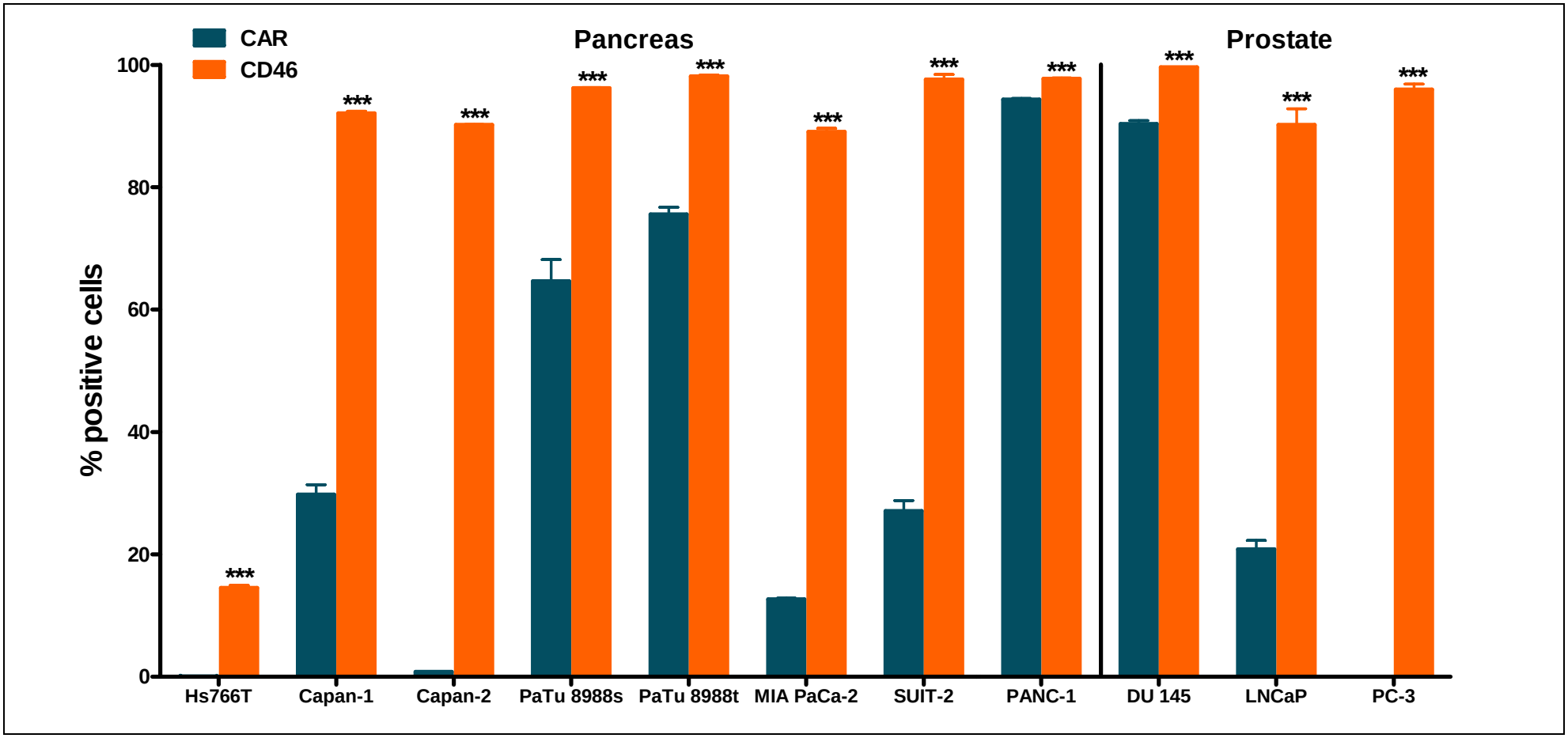


**Figure 3.1: CAR and CD46 expression levels in a panel of human pancreatic and prostate cancer cell lines.** Results represent means of triplicate readings ± SEM from flow cytometric analysis and were corrected for non-specific staining using control antibodies. Dead cells were excluded by PI staining. *** $P < 0.001$.

## 3.2 *In vitro* oncolytic potencies of Ad5 and Ad11

### 3.2.1 Oncolytic potency of Ad11 does not correlate with CD46 expression

Given that all the cancer cell lines tested have higher levels of CD46 expression compared to CAR, one might expect Ad11 to be more effective than Ad5 in killing these cells. The oncolytic potencies of Ad5 and Ad11 were compared *in vitro*. Cells were seeded in 96-well plates prior to infection. On day six after infection, MTS was first mixed with PMS, an electron coupling reagent, before it was added to the cells. MTS was bioreduced into an aqueous soluble formazan product by dehydrogenase enzymes found in metabolically active cells. The quantity of formazan product, measured by the amount of absorbance at 490 nm, is directly proportional to the number of living cells. The dose-response curves are shown in **Figure 3.2**, where 0 and 100% cell death correspond to mock infection and medium only, respectively.

The $EC_{50}$ (doses required for 50% cell killing) were calculated and are summarised in **Figure 3.3**, with lower values indicating better cell killings. In spite of the abundant expression of CD46, not all of these cells were more sensitive to Ad11 cytotoxicity. Ad11 was more effective than Ad5 in killing five of the 12 cancer cell lines tested (Hs766T, Capan-1, Capan-2, PaTu 8988s and PC-3). PaTu 8988t, MIA PaCa-2, SUIT-2, PANC-1, DU 145 and LNCaP were sensitive to Ad5 but less so with Ad11. There was no difference between Ad5 and Ad11 in 22Rv1. Although Capan-2 and PC-3, which have significantly higher levels of CD46, were more sensitive to Ad11, receptor expression alone could not explain the failure of Ad11 to effectively kill cell lines such as MIA PaCa-2 and LNCaP.

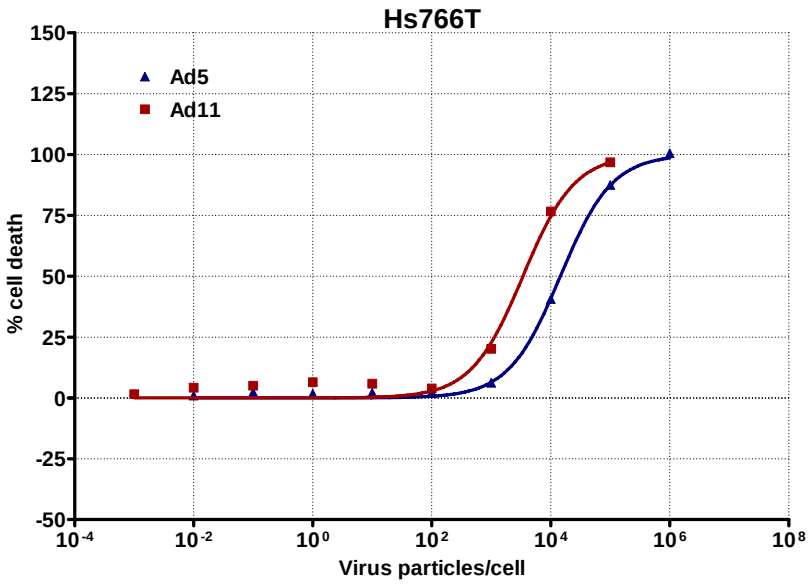
Hs766T
Ad5
Ad11
% cell death
150
125
100
75
50
25
0
-25
-50
10-4
10-2
100
102
104
106
108
Virus particles/cell

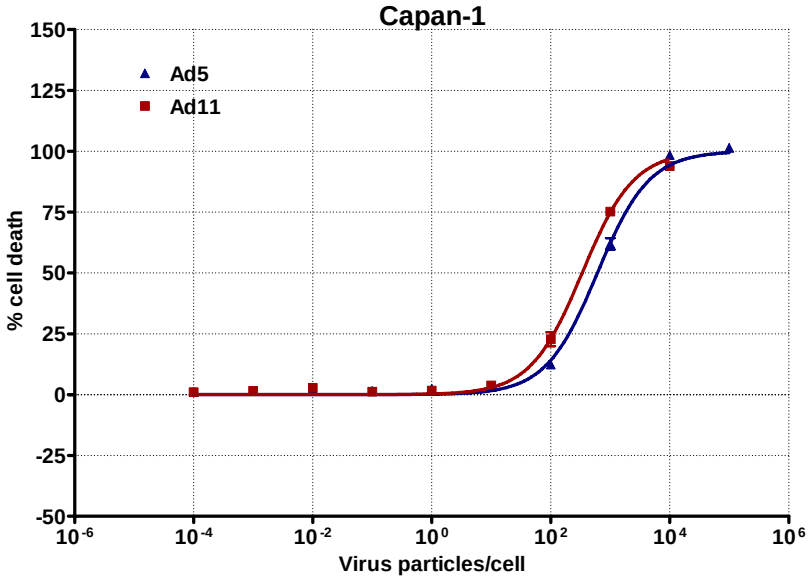
Capan-1
Ad5
Ad11
% cell death
150
125
100
75
50
25
0
-25
-50
10-6
10-4
10-2
100
102
104
106
Virus particles/cell

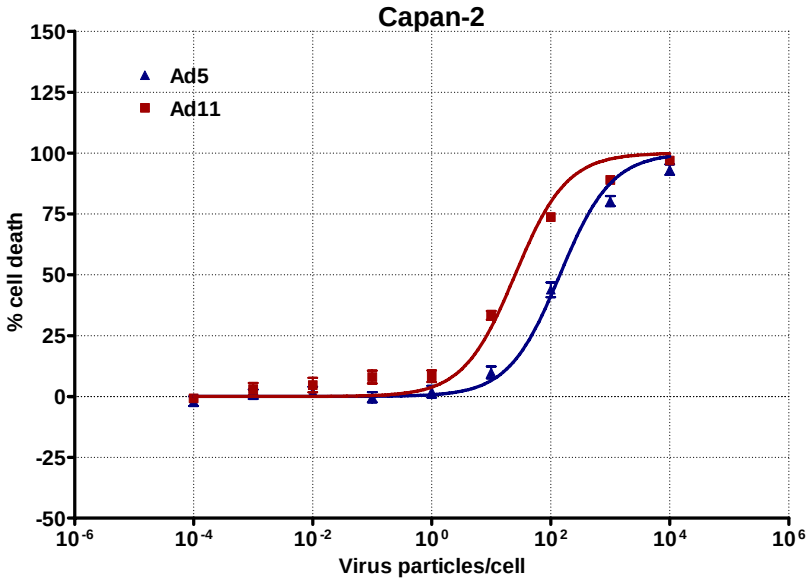
Capan-2
Ad5
Ad11
% cell death
150
125
100
75
50
25
0
-25
-50
10-6
10-4
10-2
100
102
104
106
Virus particles/cell

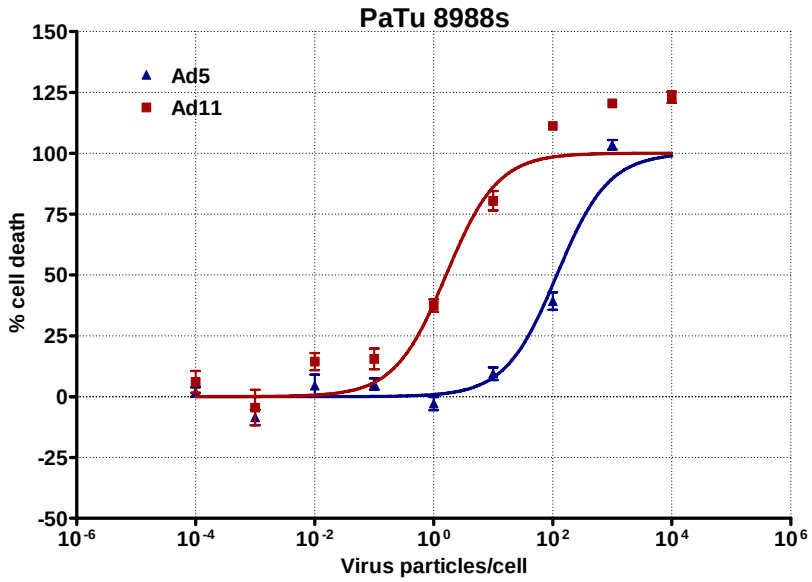
PaTu 8988s
Ad5
Ad11
% cell death
Virus particles/cell

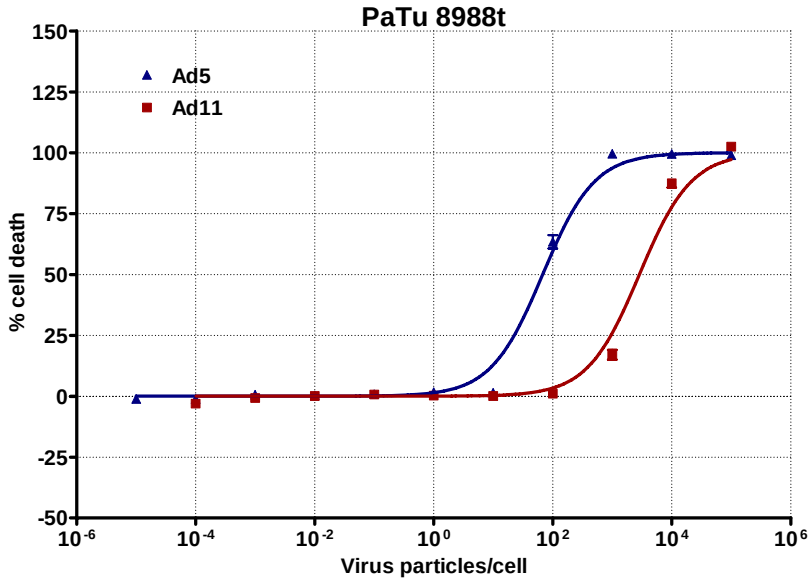
PaTu 8988t
Ad5
Ad11
% cell death
Virus particles/cell

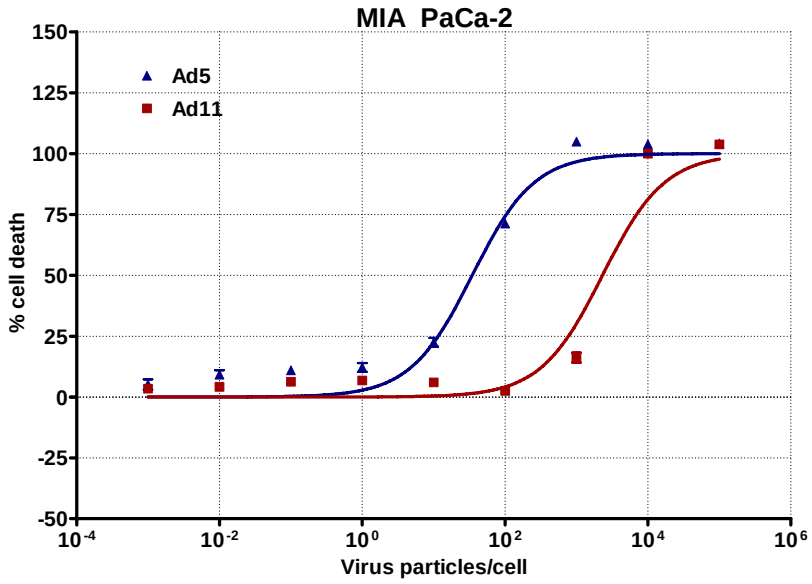
MIA PaCa-2
Ad5
Ad11
% cell death
Virus particles/cell

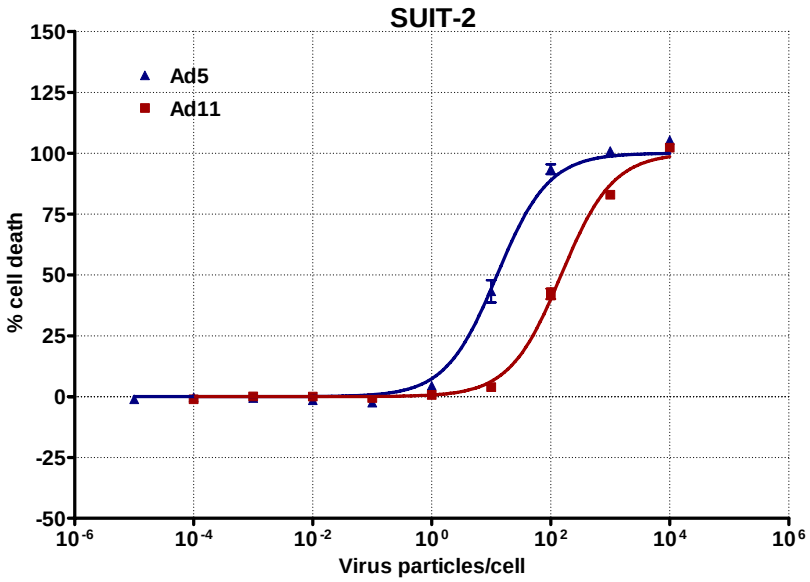
SUIT-2
Ad5
Ad11
% cell death
150
125
100
75
50
25
0
-25
-50
10-6
10-4
10-2
100
102
104
106
Virus particles/cell

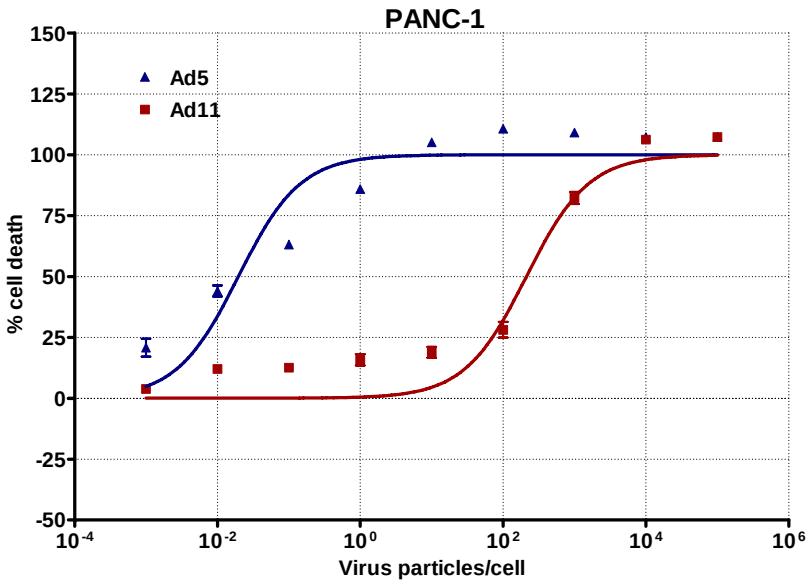
PANC-1
Ad5
Ad11
% cell death
150
125
100
75
50
25
0
-25
-50
10-4
10-2
100
102
104
106
Virus particles/cell

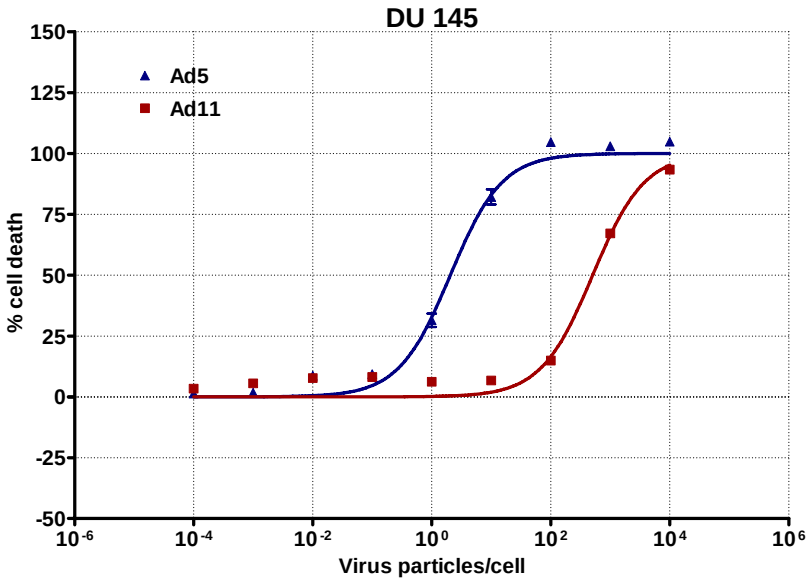
DU 145
Ad5
Ad11
% cell death
150
125
100
75
50
25
0
-25
-50
10-6
10-4
10-2
100
102
104
106
Virus particles/cell

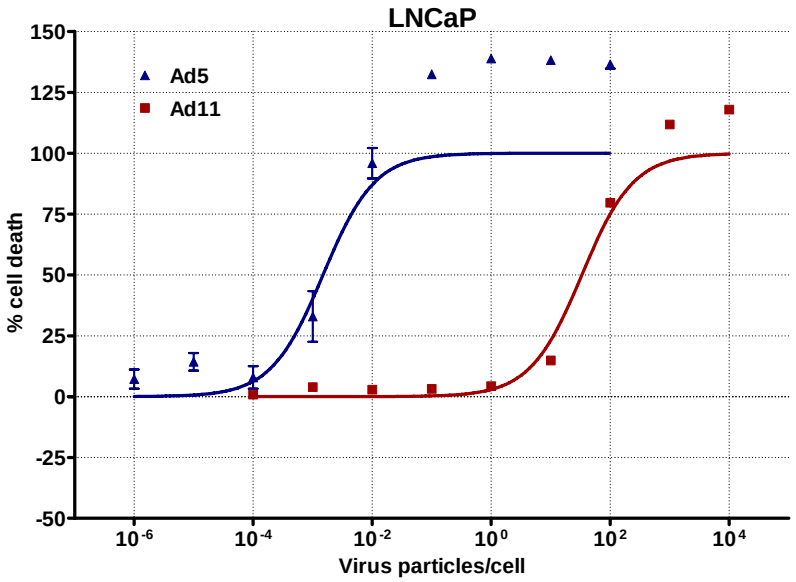
LNCaP
Ad5
Ad11
% cell death
Virus particles/cell

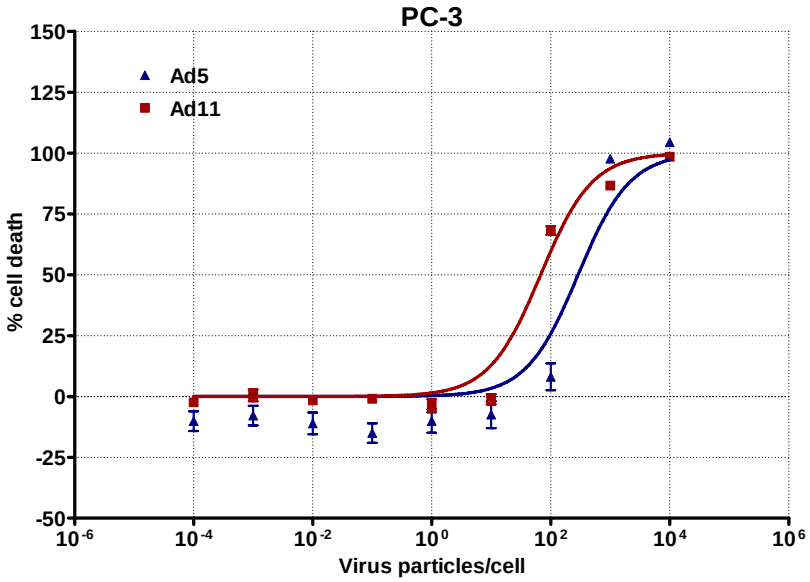
PC-3
Ad5
Ad11
% cell death
Virus particles/cell

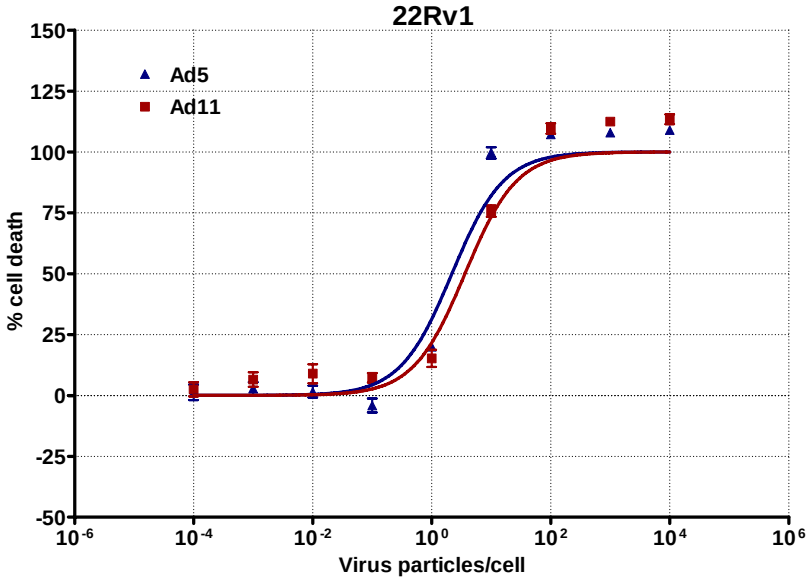
22Rv1
Ad5
Ad11
% cell death
Virus particles/cell

**Figure 3.2: Dose-response curves of Ad5 and Ad11 cytotoxicities in a panel of human pancreatic and prostate cancer cell lines.** Pancreatic (Hs766T, Capan-1, Capan-2, PaTu 8988s, PaTu 8988t, MIA PaCa-2, SUIT-2 and PANC-1) and prostate (DU 145, LNCaP, PC-3 and 22Rv1) cancer cell lines were infected in 96-well plates. Cell viability was measured on day six after infection by the MTS assay. Data represent means ± SEM from duplicate experiments (with each concentration of virus in sextuplicates).

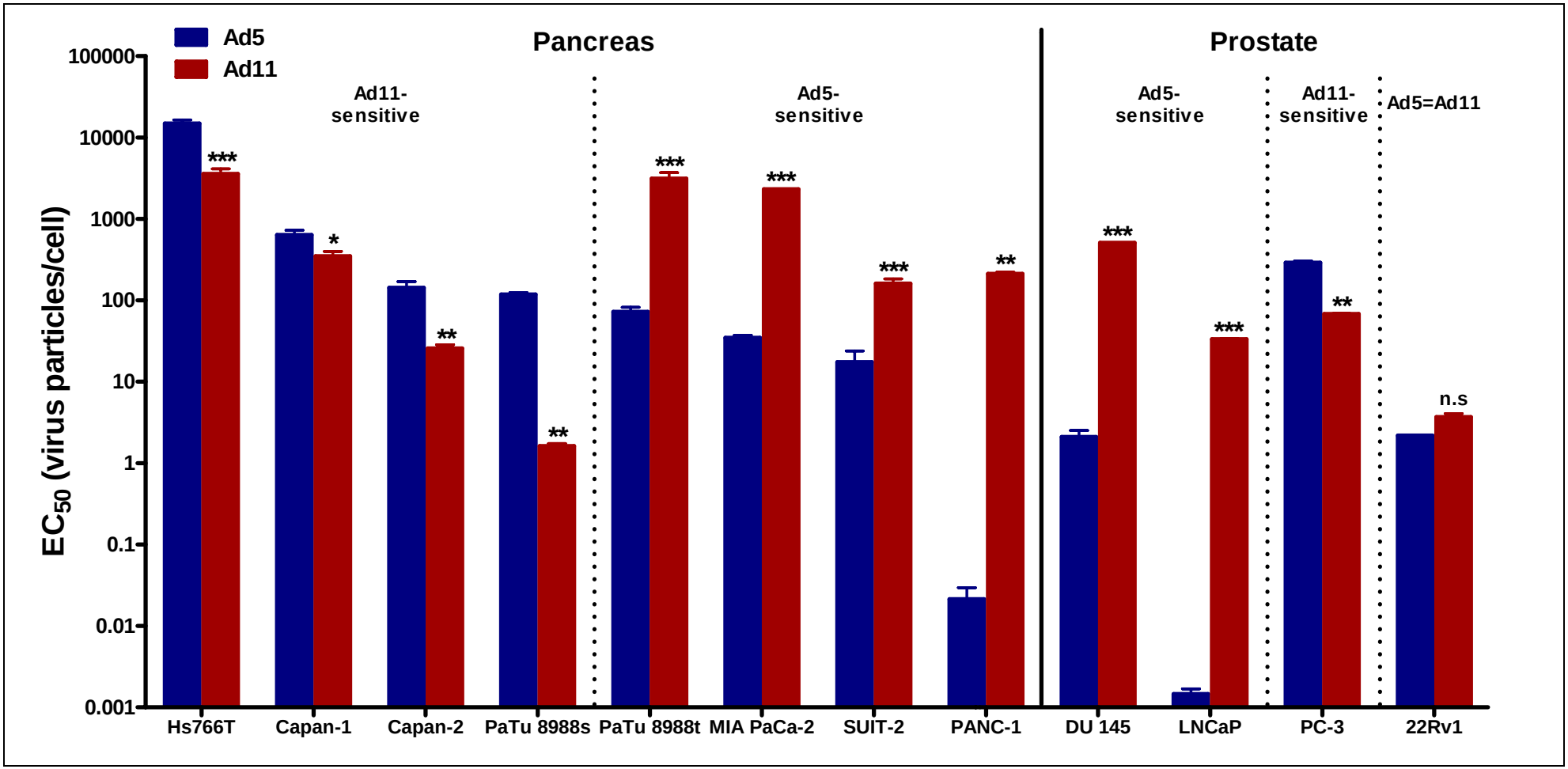


**Figure 3.3: $EC_{50}$ of Ad5 and Ad11 in a panel of human pancreatic and prostate cancer cell lines.** A lower $EC_{50}$ indicates better cell killing. Data are presented as means ± SEM. * $P < 0.05$, ** $P < 0.01$, *** $P < 0.001$, n.s – not significant.

### 3.2.2 Ad11 is less potent than Ad5 in most other cancer cell lines

The *in vitro* oncolytic potencies of Ad5 and Ad11 were further tested on a number other cancer cell lines, including cancers of the breast, colon, ovary and lung (**Figures 3.4 and 3.5**). Only four of the 13 tested were more sensitive to Ad11. Ad11 was more potent than Ad5 in killing the majority of breast cancer cell lines (MCF7, MDA-MB-468 and SK-BR-3) and the HT-29 colon cancer cell line. Ad5 was still superior to Ad11 against MDA-MB-231 (breast), SW620, HCT 116, DLD-1 (colon), A2780, OVCAR-3, IGROV1 (ovary), Calu-1 and A549 (lung).

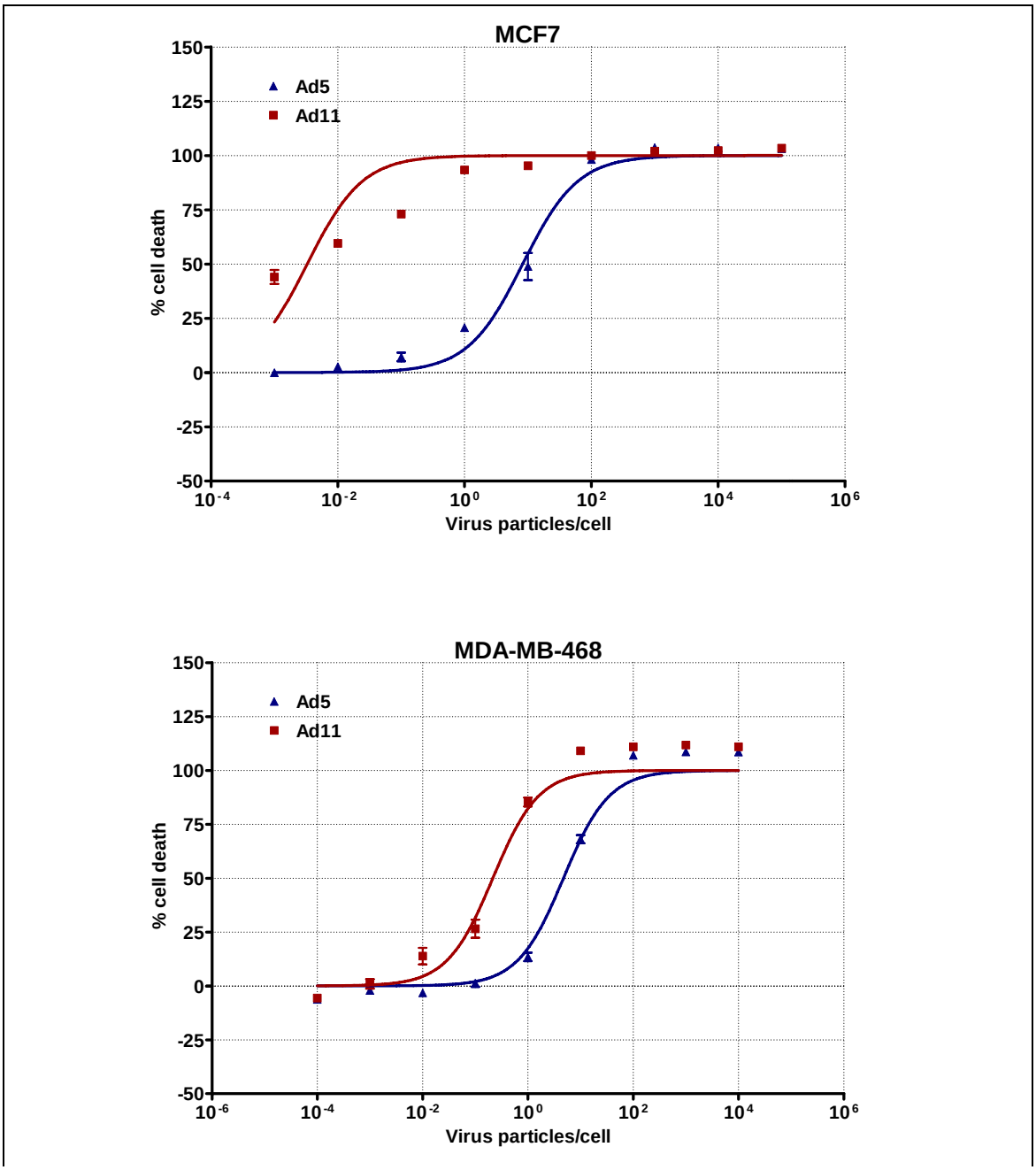

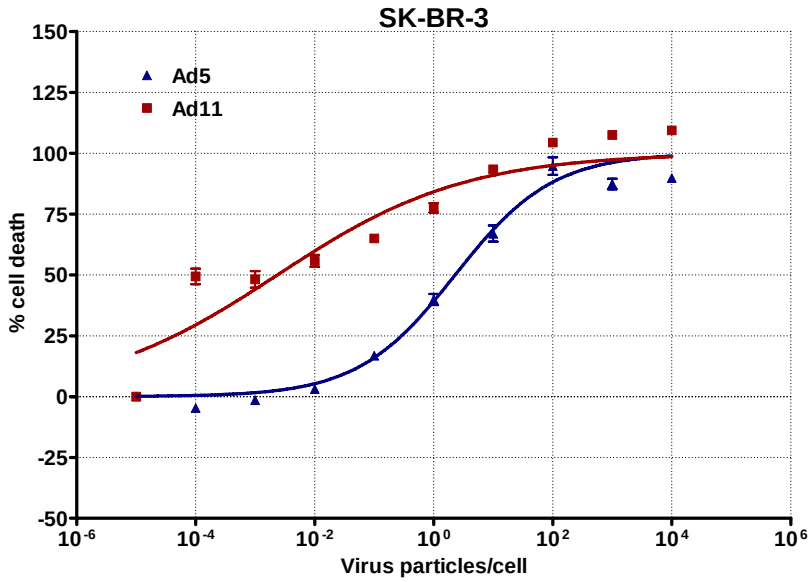
SK-BR-3
Ad5
Ad11
% cell death
Virus particles/cell

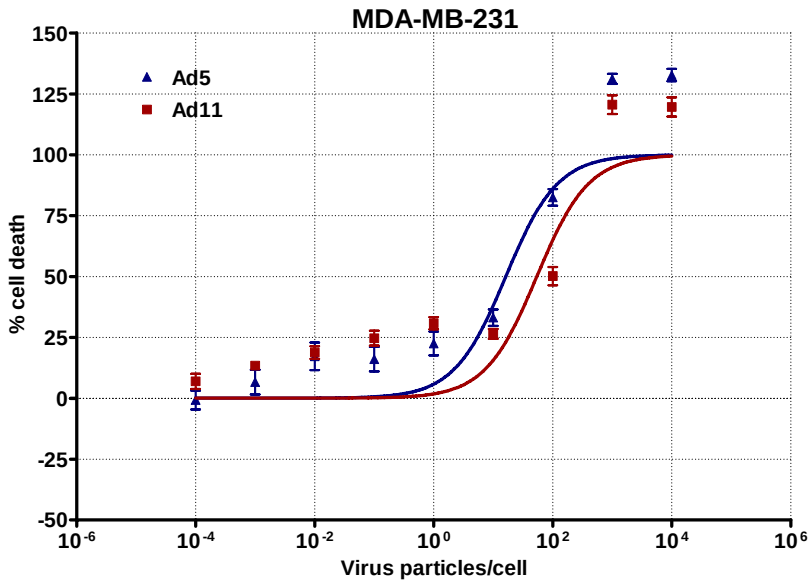
MDA-MB-231
Ad5
Ad11
% cell death
Virus particles/cell

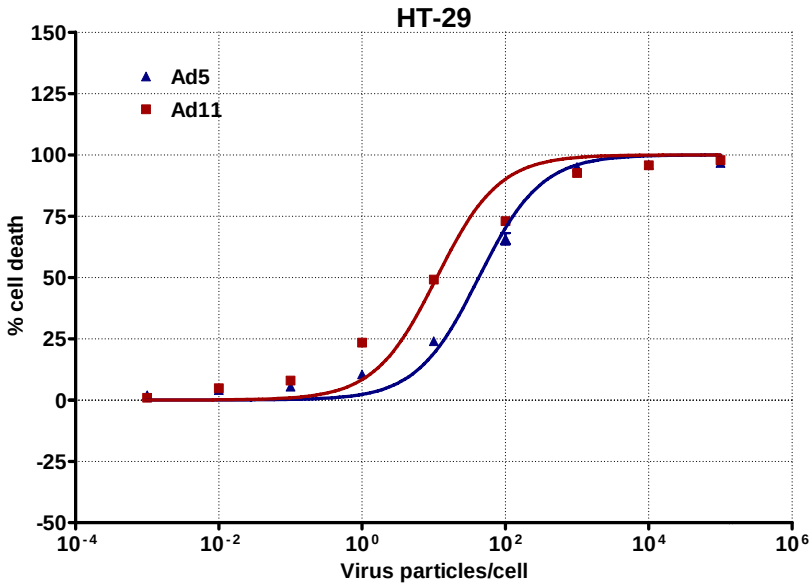
HT-29
Ad5
Ad11
% cell death
Virus particles/cell

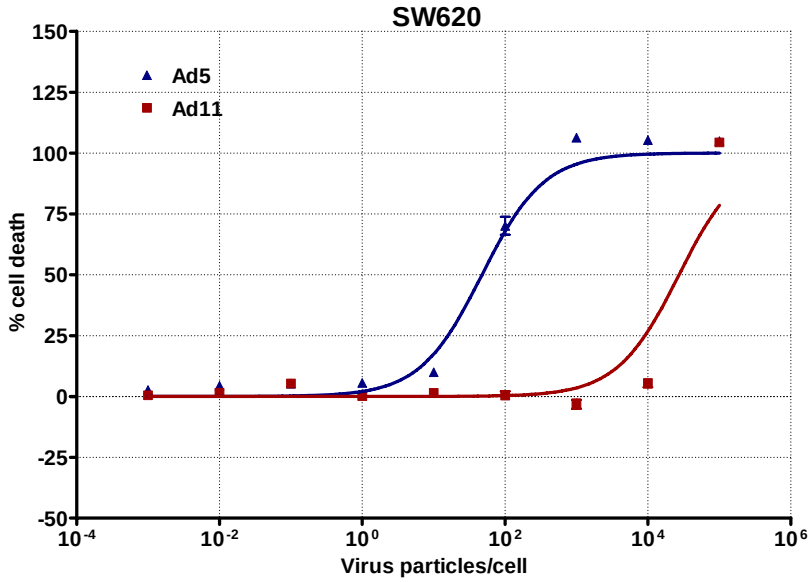
SW620
Ad5
Ad11
% cell death
150
125
100
75
50
25
0
-25
-50
10-4
10-2
100
102
104
106
Virus particles/cell

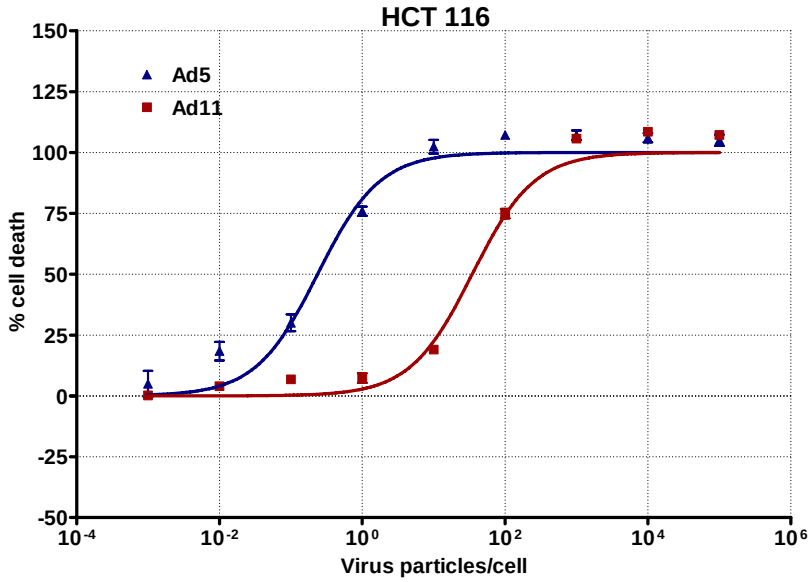
HCT 116
Ad5
Ad11
% cell death
150
125
100
75
50
25
0
-25
-50
10-4
10-2
100
102
104
106
Virus particles/cell

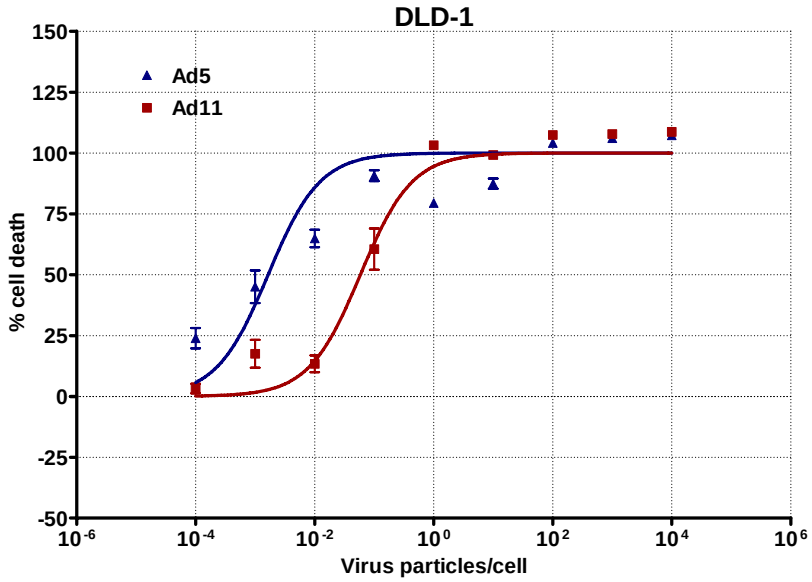
DLD-1
Ad5
Ad11
% cell death
150
125
100
75
50
25
0
-25
-50
10-6
10-4
10-2
100
102
104
106
Virus particles/cell

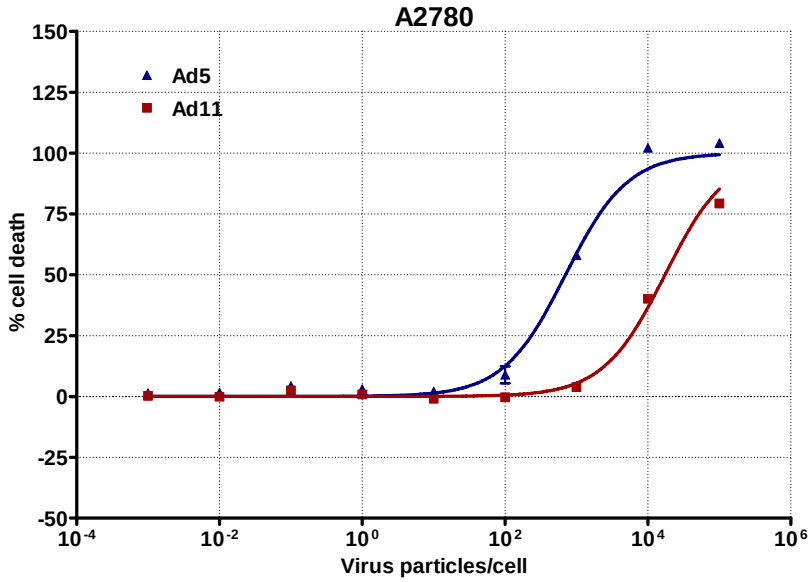
A2780
Ad5
Ad11
% cell death
150
125
100
75
50
25
0
-25
-50
10-4
10-2
100
102
104
106
Virus particles/cell

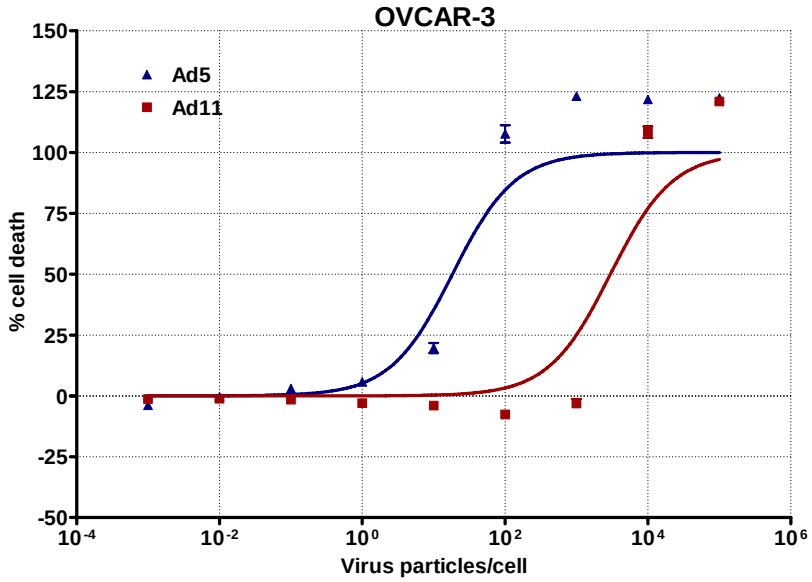
OVCAR-3
Ad5
Ad11
% cell death
150
125
100
75
50
25
0
-25
-50
10-4
10-2
100
102
104
106
Virus particles/cell

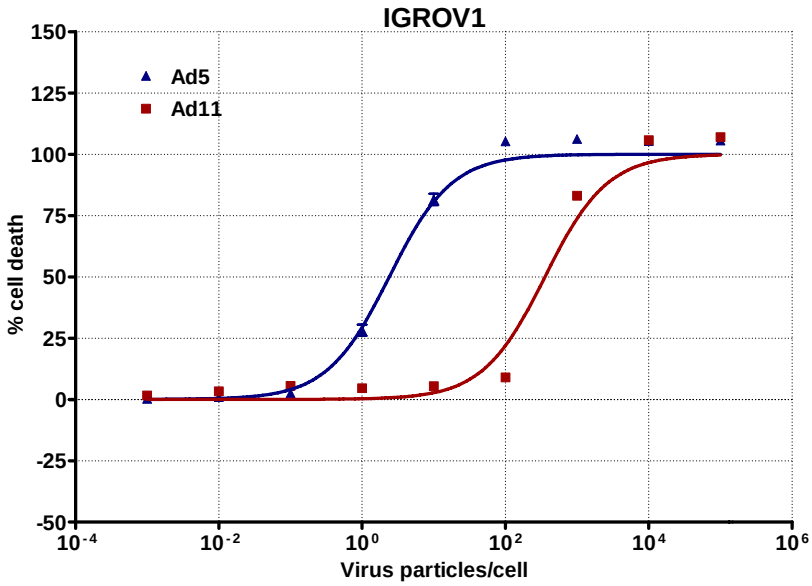
IGROV1
Ad5
Ad11
% cell death
150
125
100
75
50
25
0
-25
-50
10-4
10-2
100
102
104
106
Virus particles/cell

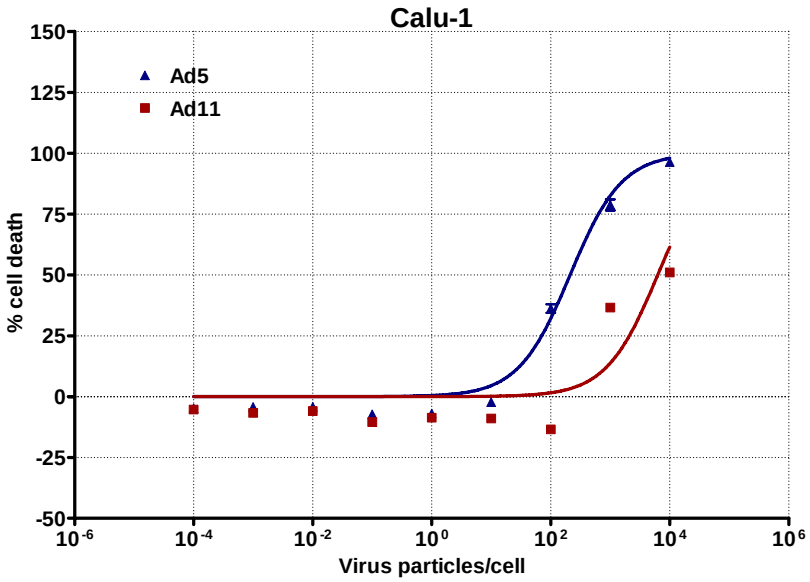


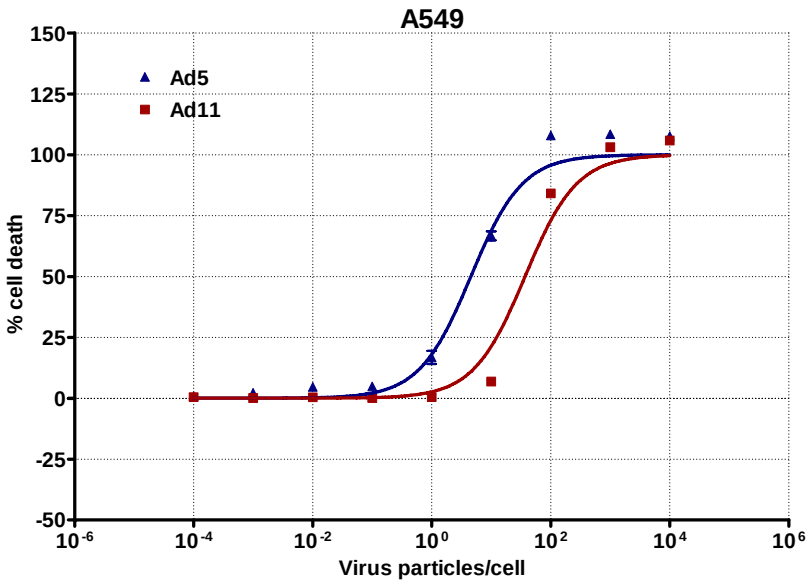


**Figure 3.4: Dose-response curves of Ad5 and Ad11 cytotoxicities in a panel of human breast, colon, ovarian and lung cancer cell lines.** MCF7, MDA-MB-468, SK-BR-3, MDA-MB-231 (breast), HT-29, SW620, HCT 116, DLD-1 (colon), A2780, OVCAR-3, IGROV1 (ovary), Calu-1 and A549 (lung) were infected in 96-well plates. Cell viability was measured on day six after infection by the MTS assay. Data represent means ± SEM from duplicate experiments (with each concentration of virus in sextuplicates).

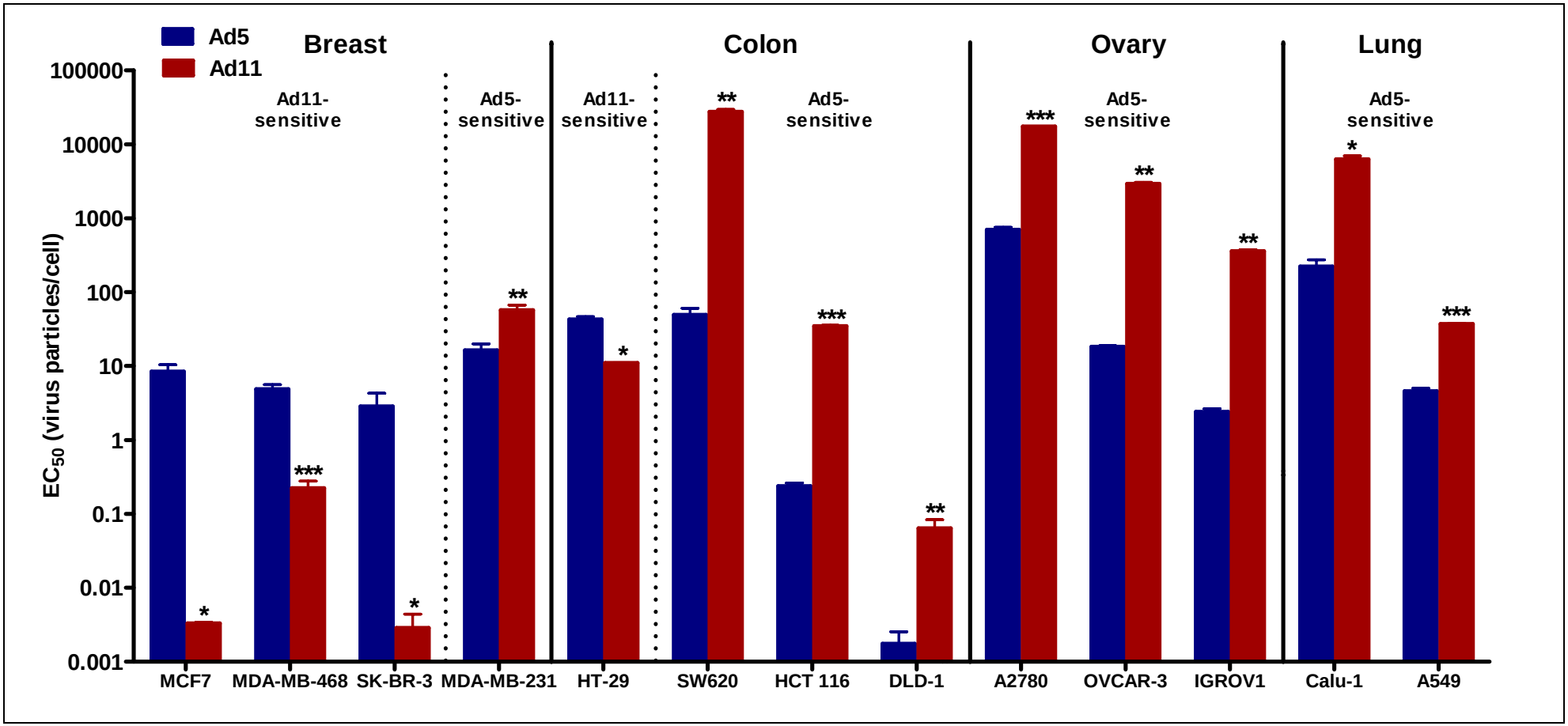


**Figure 3.5: $EC_{50}$ of Ad5 and Ad11 in a panel of human breast, colon, ovarian and lung cancer cell lines.** A lower $EC_{50}$ indicates better cell killing. Data are presented as means ± SEM. * $P < 0.05$, ** $P < 0.01$, *** $P < 0.001$.

## 3.3 Summary of Chapter 3

All the 11 human cancer cell lines tested expressed significantly higher levels of the Ad11 attachment receptor CD46 compared to CAR, the receptor for Ad5 (**Figure 3.1**). This suggests that Ad11 would have a much higher infectivity than Ad5 in these cells. However, there are some limitations to this finding. Firstly, the levels obtained here only represent the number of cells that expressed these receptors. Determination of receptor density would also be important, as is the analysis of other cell surface molecules implicated in virus attachment and internalisation, such as CD80, CD86, $\alpha_V\beta_3$ and $\alpha_V\beta_5$ integrins[100, 101, 193, 194]. Secondly, CAR and CD46 receptors are often trapped in the tight junctions in *in situ* tumours[197], whereas the flow cytometric analysis was performed on detached cells. This makes the results difficult to translate into the *in vivo* setting.

Despite the higher levels of CD46 expression, only nine out of the 25 (36%) human cancer cell lines tested were more sensitive to Ad11-mediated cytotoxicity. Ad5 and Ad11 showed similar efficacy in killing the 22Rv1 prostate cancer, but Ad5 was still superior in the other cell lines (60%) (**Figures 3.3 and 3.5**). Therefore receptor expression alone could not explain the variability in the oncolytic potencies of Ad5 and Ad11. The mechanisms involved are discussed in Chapter 5.

# CHAPTER 4

# *In vivo* oncolytic efficacies of Ad5 and Ad11

As shown in Chapter 3, some of the human cancer cell lines tested were more sensitive to Ad11-mediated cytotoxicity *in vitro* (36%), whilst the majority (60%) were more effectively killed by Ad5. To test their *in vivo* efficacies, two subcutaneous human cancer xenograft models in BALB/c nude mice were used, namely PC-3 (prostate cancer – Ad5-insensitive) and MIA PaCa-2 (pancreatic cancer – Ad5-sensitive).

## 4.1 Ad11 is more effective than Ad5 in treating Ad5-insensitive PC-3 human prostate cancer xenografts

The potent *in vitro* activity of Ad11 against the Ad5-insensitive PC-3 prostate cancer cell line prompted further evaluation of this virus *in vivo*. A subcutaneous xenograft model in BALB/c nude mice was established by the injection of 1 x $10^7$ PC-3 cells in 100 µl of 50% PBS and 50% BD Matrigel Basement Membrane Matrix into the right flanks. Established tumours were injected with three 1 x $10^{10}$ virus particles or 100 µl of PBS on alternate days. Tumours were monitored for three months and mice were euthanised when tumour dimension was more than 1.44 $cm^2$ in accordance with Home Office regulations. Significant growth suppression was observed in the Ad11-treated group compared to Ad5, together with improved number of progression-free mice (logrank $P < 0.01$) (**Figures 4.1a and b**).

To measure virus replication, tumours were injected with single doses of Ads and harvested at various time points. These were homogenised in DMEM and then frozen and thawed three times in liquid nitrogen and at 37 °C, respectively, to lyse the cells to release intracellular virus particles. After DNA extraction, qPCR was performed using Ad-specific *E1A* primers and probes. The lysates were also used to infect an indicator cell line, the Ad-sensitive JH-293, in 96-well plates at six 1:10 serial dilutions. The presence of infectious Ads would result in CPE or plaque formation of the JH-293 (**Figure 4.2**). The $TCID_{50}$ and number of PFUs were calculated using the Reed-Muench accumulative method (see Appendix). Higher levels of Ad11 DNA amplification and infectious virus production (at 96 hours) were observed (**Figures 4.1c and d**).

a)

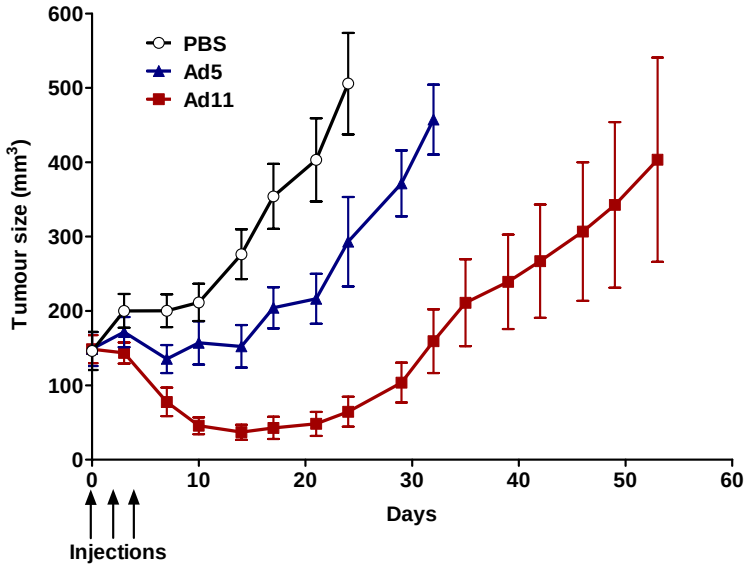
PBS
Ad5
Ad11
Tumour size (mm3)
600
500
400
300
200
100
0
0
10
20
30
40
50
60
Days
Injections

b)

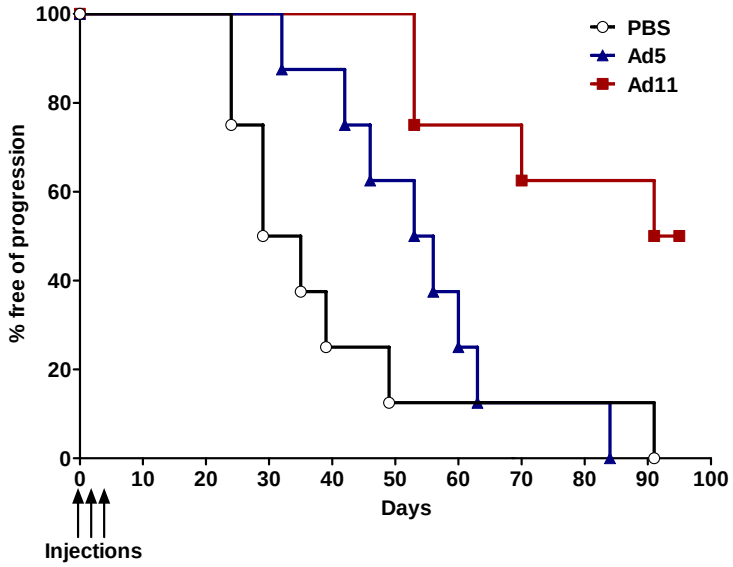
PBS
Ad5
Ad11
% free of progression
100
80
60
40
20
0
0
10
20
30
40
50
60
70
80
90
100
Days
Injections

c)

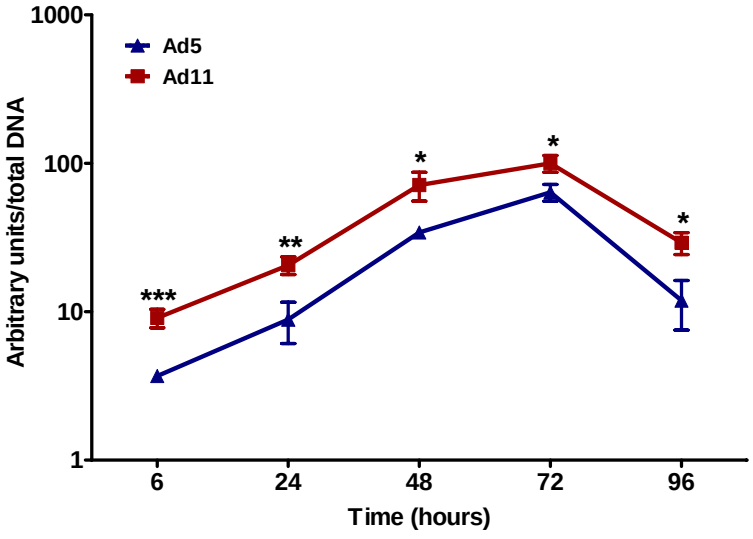
Ad5
Ad11
Arbitrary units/total DNA
1000
100
10
1
***
**
*
*
*
6
24
48
72
96
Time (hours)

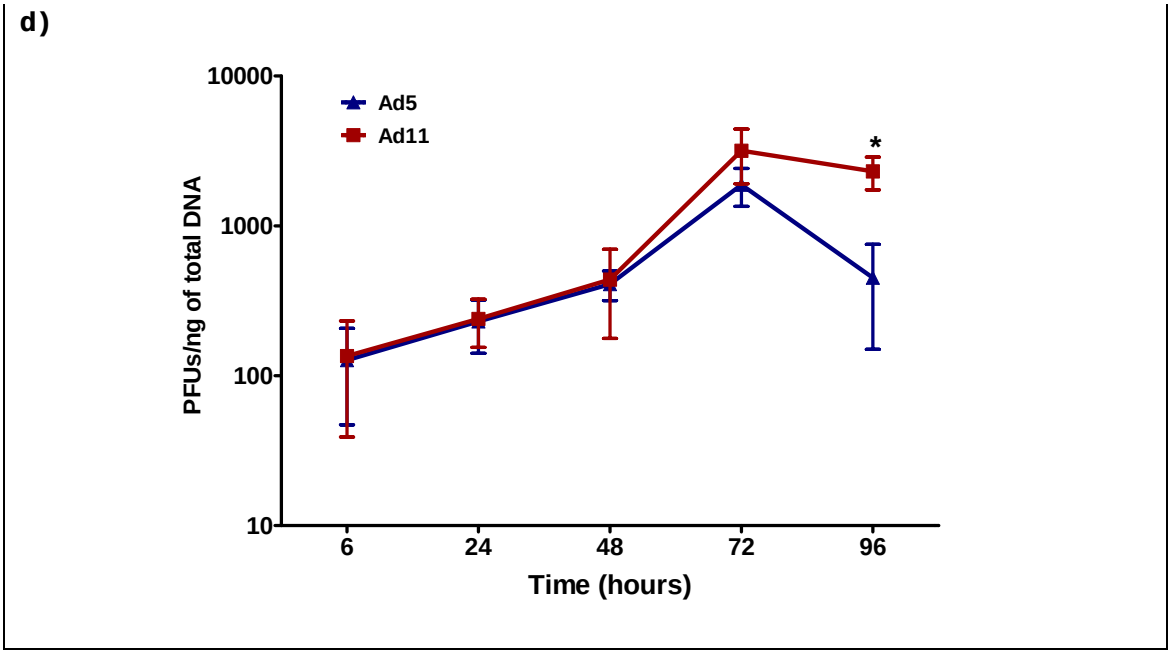


**Figure 4.1: Anti-tumoural efficacies of Ad5 and Ad11 in a PC-3 subcutaneous xenograft model.** (**a**) Established tumours in BALB/c nude mice were given three intratumoural injections of PBS (100 µl), Ad5 or Ad11 (1 x $10^{10}$ particles/injection). Tumours were measured until the first mouse in each group has a tumour dimension of > 1.44 $cm^2$. Data represent means ± SEM ($n$ = 8 per group). On day 32, significant difference was noted between the Ad-treated groups ($P < 0.001$). (**b**) Percentage of progression-free mice using the Kaplan-Meier method (logrank $P < 0.01$ between Ad5 and Ad11). (**c**) Established tumours were injected once with 1 x $10^{10}$ particles of Ad5 or Ad11. At the stated time points, tumours were harvested in triplicates, homogenised in 2 ml of DMEM, frozen and thawed three times in liquid nitrogen and at 37 °C, respectively prior to DNA extraction. qPCR was performed using *E1A* primers and probes. Results are presented as average arbitrary units ± SEM, normalised against total DNA, with the highest value arbitrarily set to 100. (**d**) The above cell lysates were used to infect an indicator cell line, JH-293, in 96-well plates at six 1:10 serial dilutions. The cells were inspected for CPE 11 days later. The $TCID_{50}$ and number of PFUs were calculated using the Reed-Muench accumulative method. Results are presented as PFUs/ng of total DNA ± SEM. * $P < 0.05$, ** $P < 0.01$, *** $P < 0.001$.

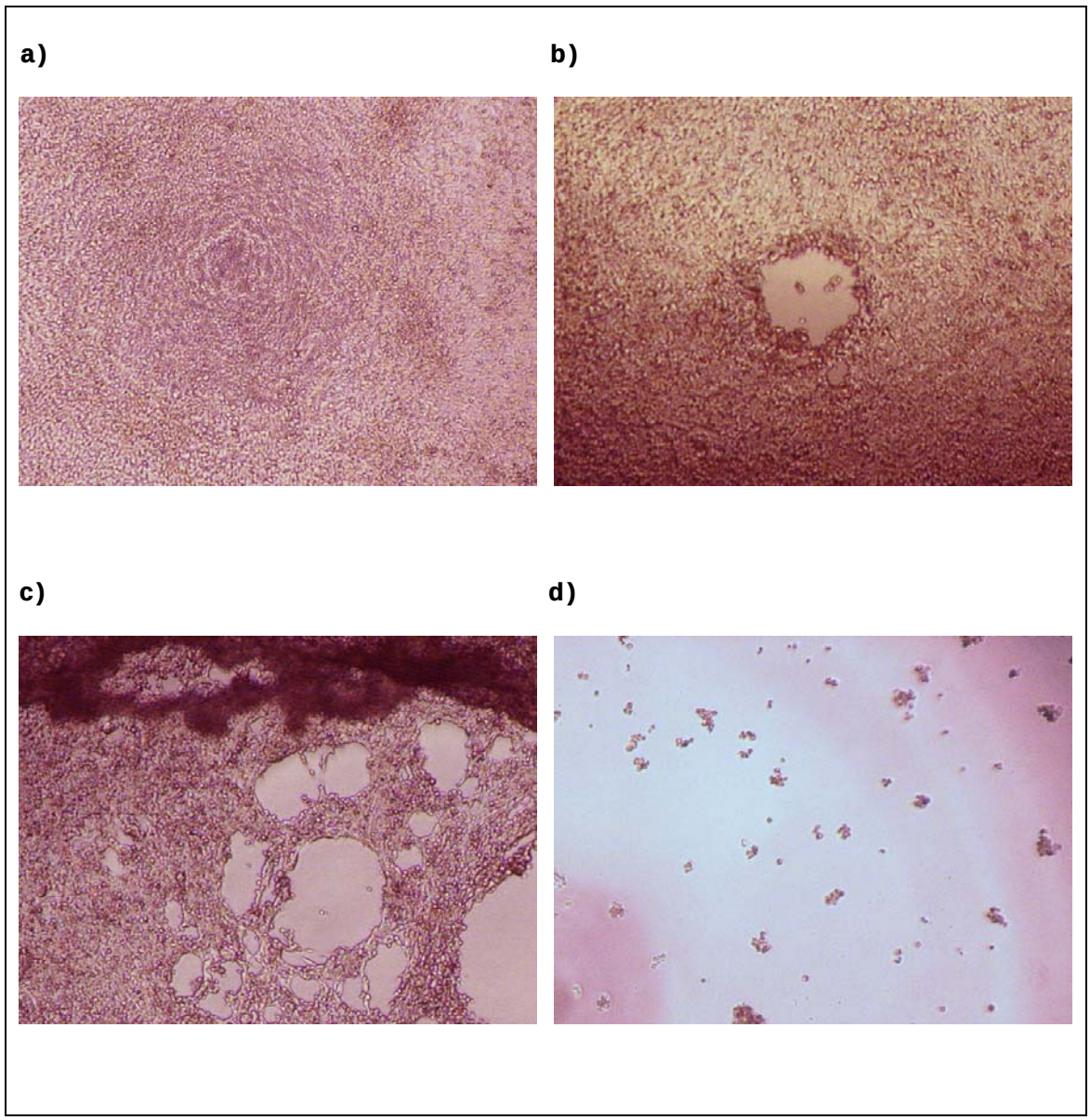


**Figure 4.2: Cytopathic effects of adenoviruses on JH-293 cells** (40x magnification). (**a**) Normal, confluent JH-293. (**b**) to (**d**) Progressive CPEs with plaque formation, cell detachment and lysis.

## 4.2 Ad11 is less effective than Ad5 in treating Ad11-insensitive MIA PaCa-2 human pancreatic cancer xenografts

To compare the *in vivo* anti-tumoural activities of Ad5 and Ad11 in an Ad11-insensitive cancer cell line, a subcutaneous MIA PaCa-2 human pancreatic cancer xenograft model was used (**Figure 4.3**). 1 x $10^7$ MIA PaCa-2 cells in 100 µl of PBS were injected into the right flanks of BALB/c nude mice. Established tumours were treated as described in 4.1. As expected, tumour growth and the number of progression-free mice were significantly better in the Ad5-treated group compared to Ad11 ($P < 0.05$).

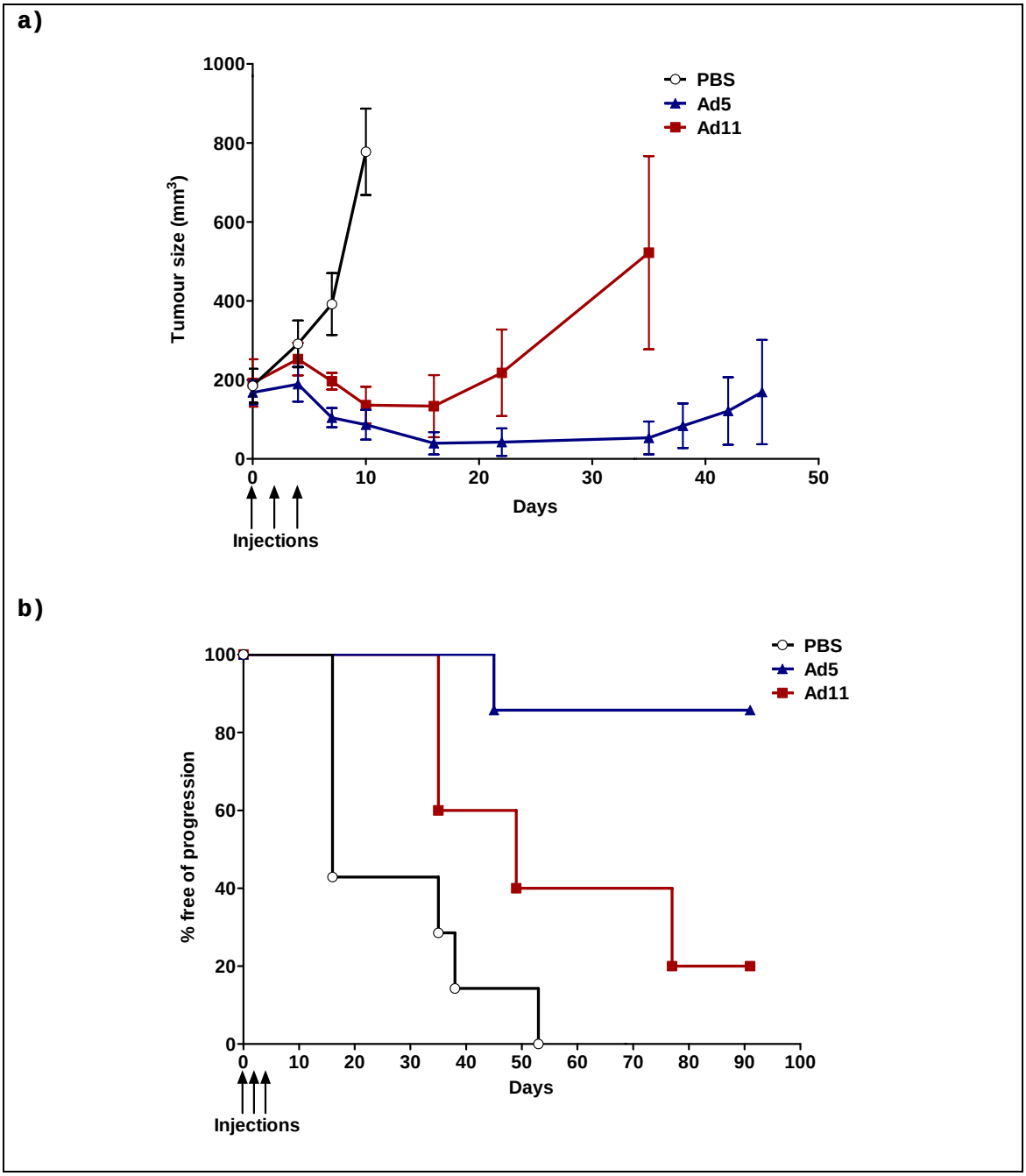


**Figure 4.3: Anti-tumoural efficacies of Ad5 and Ad11 in a MIA PaCa-2 subcutaneous xenograft model.** (**a**) Established tumours in BALB/c nude mice were given three intratumoural injections of PBS (100 µl), Ad5 or Ad11 (1 x $10^{10}$ particles/injection). Tumours were measured until the first mouse in each group has a tumour dimension of > 1.44 $cm^2$. Data represent means ± SEM ($n$ = 8 per group). On day 35, there was significant difference between the Ad-treated groups ($P < 0.05$). (**b**) Percentage of progression-free mice using the Kaplan-Meier method (logrank $P < 0.05$ between Ad5 and Ad11).

## 4.3 Summary of Chapter 4

Consistent with the *in vitro* results in Chapter 3, Ad11 showed superior efficacy in treating the Ad5-insensitive PC-3 human prostate cancer cell line in a subcutaneous xenograft model (**Figures 4.1a and b**). Higher levels of Ad11 DNA were found in the tumours from six to 96 hours after a single intratumoural virus injection, indicating that its DNA replicated more efficiently than that of Ad5 (**Figure 4.1c**). Although a fixed amount of DNA was used for qPCR and the results were normalised against total DNA, the use of an internal control, such as the housekeeping gene of glyceraldehyde 3-phosphate dehydrogenase (GAPDH), would further improve the accuracy of the results. Despite the high viral DNA levels, a significantly higher number of infectious Ad11 particles were only observed at 96 hours (**Figure 4.1d**). This could be due to a delay in Ad11 protein synthesis, as demonstrated *in vitro* in Chapter 5.

Treatment of the Ad11-insensitive MIA PaCa-2 human pancreatic cancer xenografts with Ad11 resulted in faster tumour growth compared to Ad5 (**Figure 4.3**), although this was less than expected given the more remarkable *in vitro* result (**Figure 3.2**). The reason for this is unknown, although it could be explained by the slower clearance of Ad11 in nude mice where CAR, but not CD46, is expressed.

# CHAPTER 5

# Mechanisms of Ad11's attenuated oncolytic potency in insensitive cancer cell lines

As shown in Chapter 3, there appears to be no correlation between viral receptor expression in cancer cells and their sensitivity to killing by Ad5 and Ad11. In particular, Ad11 was not always more effective than Ad5 despite the abundant expression of CD46 compared to CAR. Other factors must be involved. Dissection of the Ad infectious cycle is therefore needed, which generally involves the following steps: attachment of virus to the cellular receptor followed by internalisation, trafficking of the virus to the nucleus, expression of early gene products, cell entry into S phase and viral DNA amplification, viral structural protein synthesis, virion assembly, cell death and release of progeny viruses. For this, the cancer cell lines Capan-2, PC-3 (both Ad11-sensitive), MIA PaCa-2 and LNCaP (both Ad5-sensitive) were studied in more detail.

## 5.1 Ad11 has higher infectivity than Ad5 in cancer cell lines

Equal amounts of Ad5 and Ad11 were incubated with the fluorophore Alexa Fluor 555 carboxylic acid, succinimidyl ester, which bound to primary amines on adenoviral coat proteins. Excess dye was removed by dialysis. The conjugated viruses were used to infect cells, seeded in Lab-Tek II Chamber Slide Systems, at 4 °C for an hour to allow attachment to surface receptors but not internalisation. Unbound viruses were washed away with PBS, and this was followed by incubation at 37 °C for an hour which resulted in virus internalisation and trafficking to the nuclei. Cells were subsequently fixed with methanol, stained with anti-α-tubulin mouse antibody and Alexa Fluor 488 donkey anti-mouse IgG (cytoplasmic tubulins), and DAPI (nuclei). Images were then taken using a confocal microscope (**Figure 5.1**). In separate experiments, unlabelled Ads were used to infect suspended cells (in cold buffer of 1% BSA in PBS) at 1,000 particles/cell. Cells were infected at 4 °C for an hour (attachment), and after washing away unattached viruses, incubated at 37 °C for 30, 60 and 120 minutes, respectively. DNA was obtained from cellular nuclear extracts for qPCR using *E1A* primers and probes (**Figure 5.1**). Consistent with CAR and CD46 expression levels, significantly more Ad11 than Ad5 were found to attach to the pancreatic cancer cell lines Capan-2 and MIA PaCa-2 (**Figures 5.1a and b**), as well as

the prostate cancer cell lines PC-3 and LNCaP (**Figures 5.1c and d**). The attached Ad11 were effectively trafficked to the nuclei of these cells. Fluctuations seen in nuclear localisation were likely the result of multiphasic nuclear transport of Ads[210]. As Ad11 was much more infective than Ad5 even in the Ad11-insensitive cell lines (MIA PaCa-2 and LNCaP), downstream events are therefore responsible for its attenuated oncolytic potency.

**a) Capan-2 (Ad11-sensitive)**

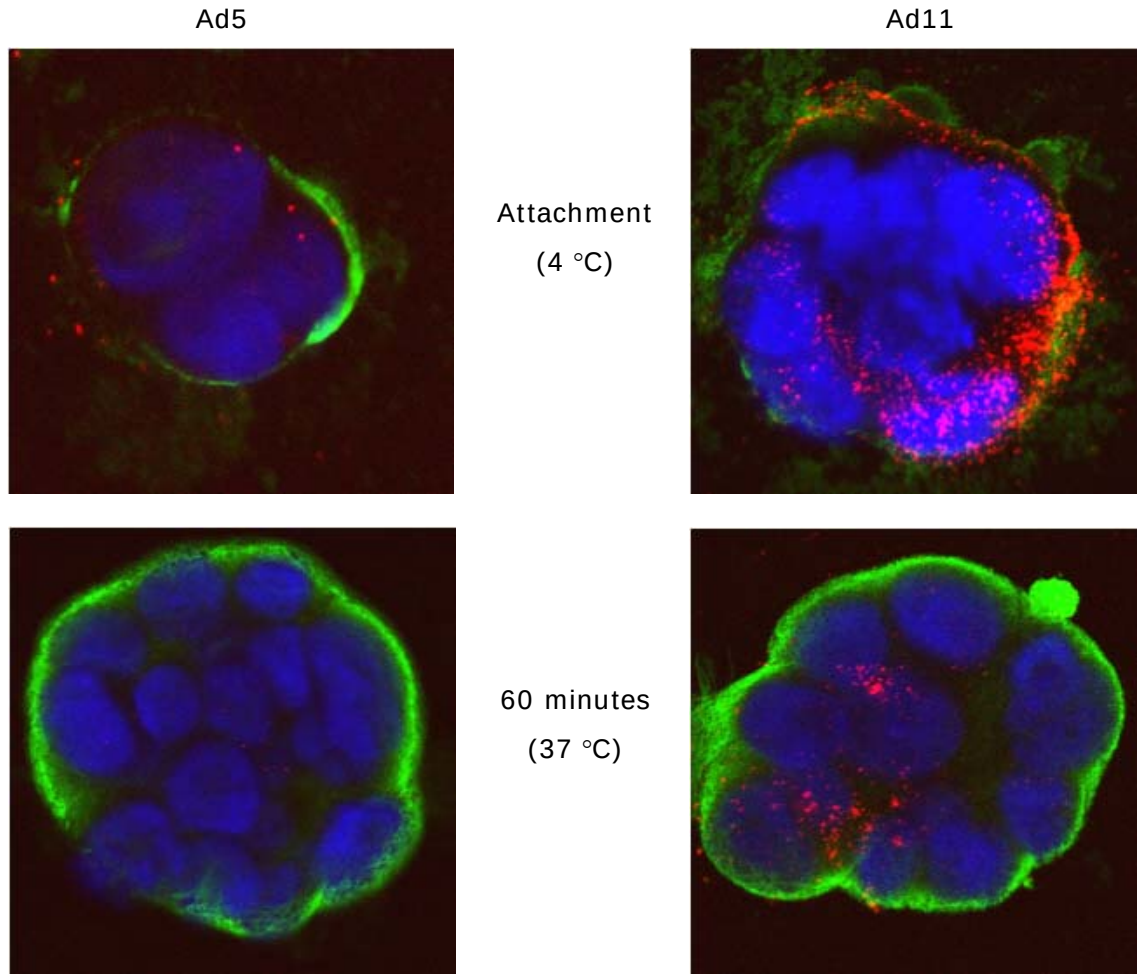


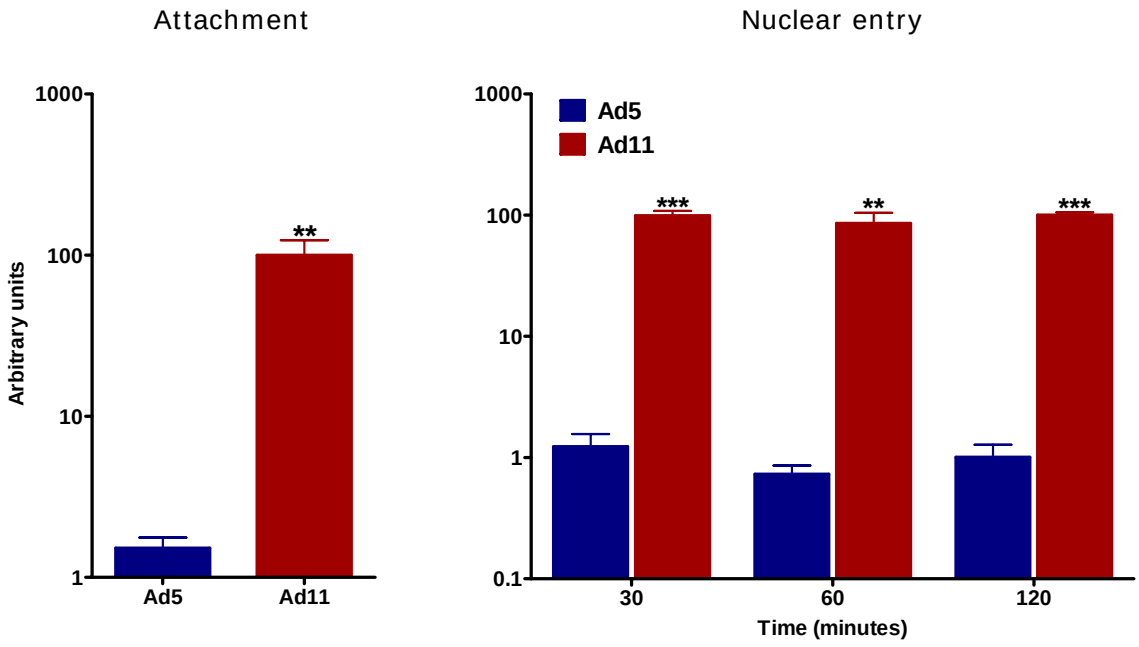

**b) MIA PaCa-2 (Ad5-sensitive)**

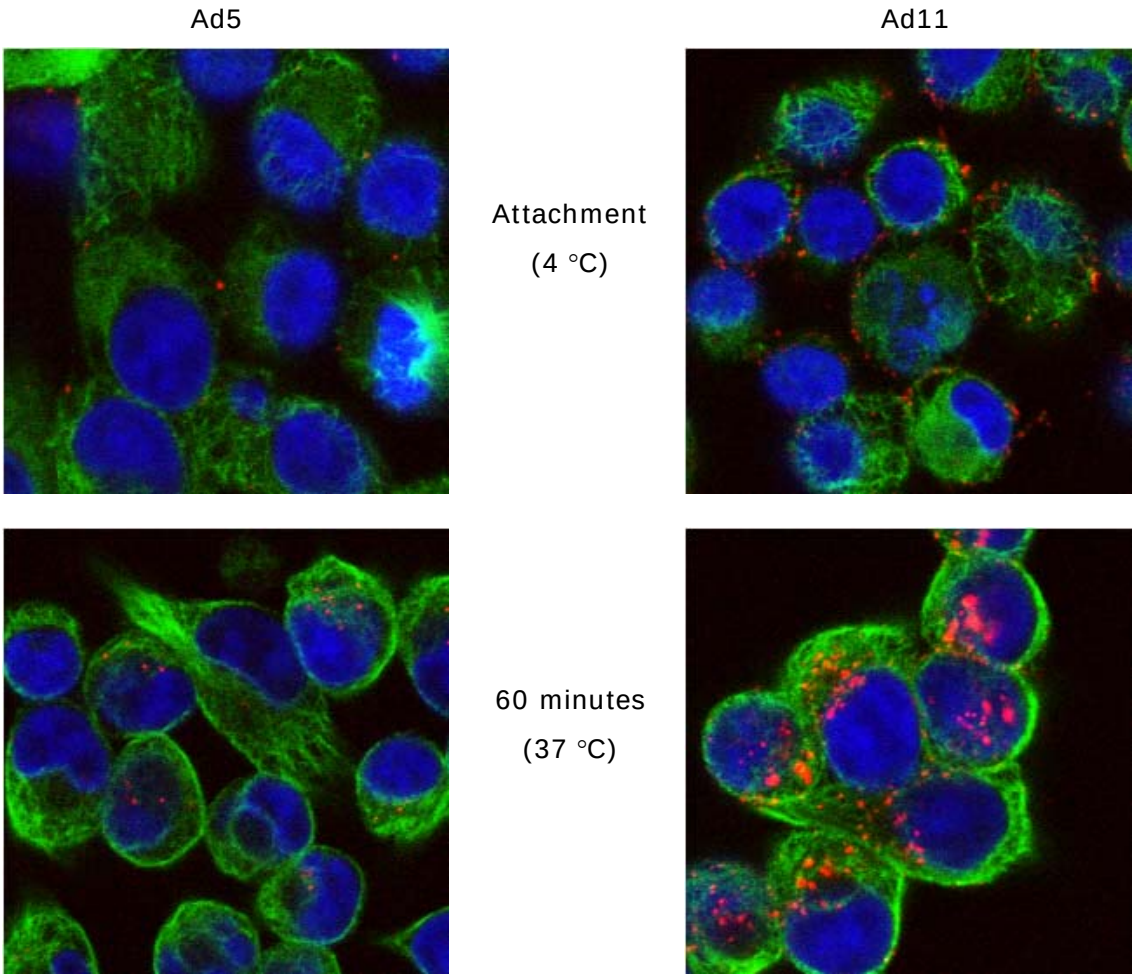


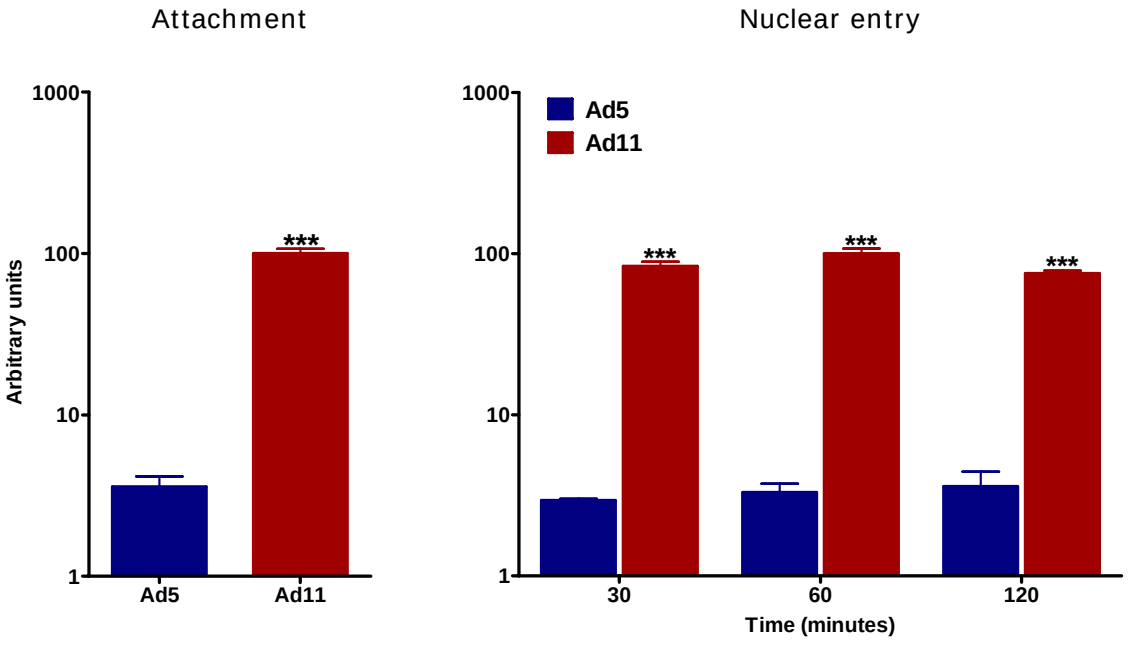

**c) PC-3 (Ad11-sensitive)**

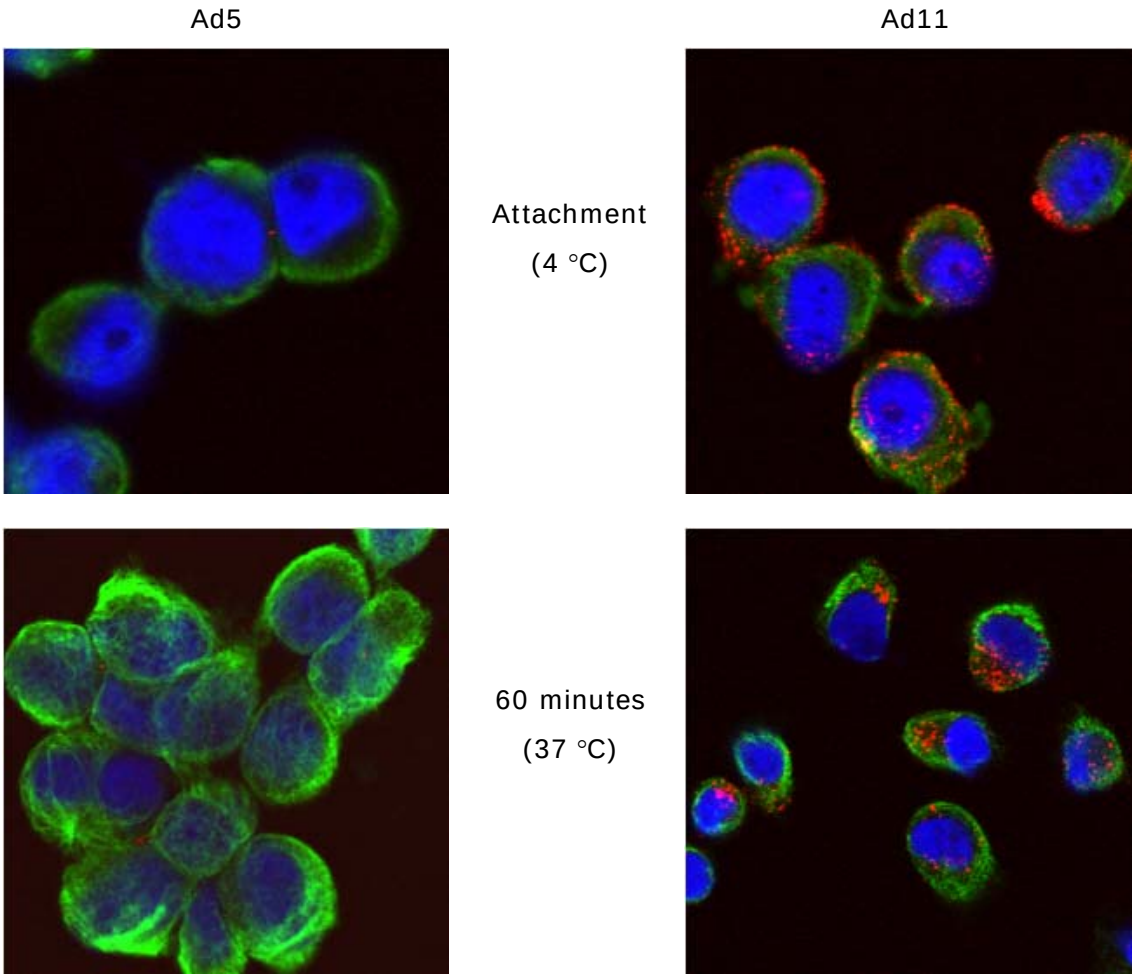


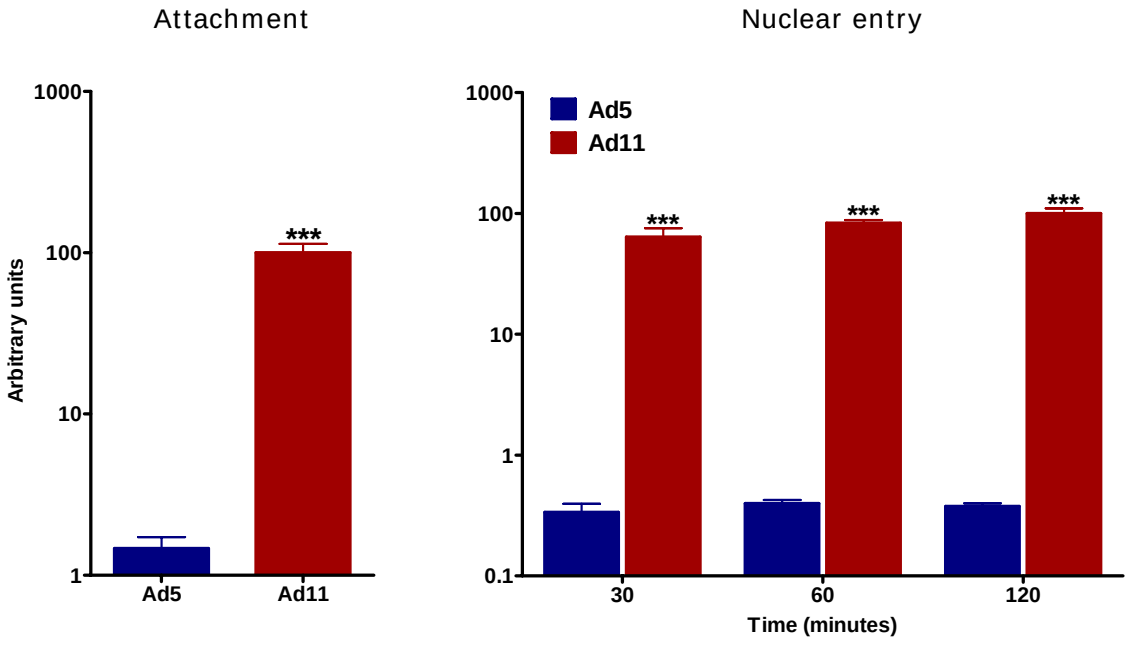

**d) LNCaP (Ad5-sensitive)**

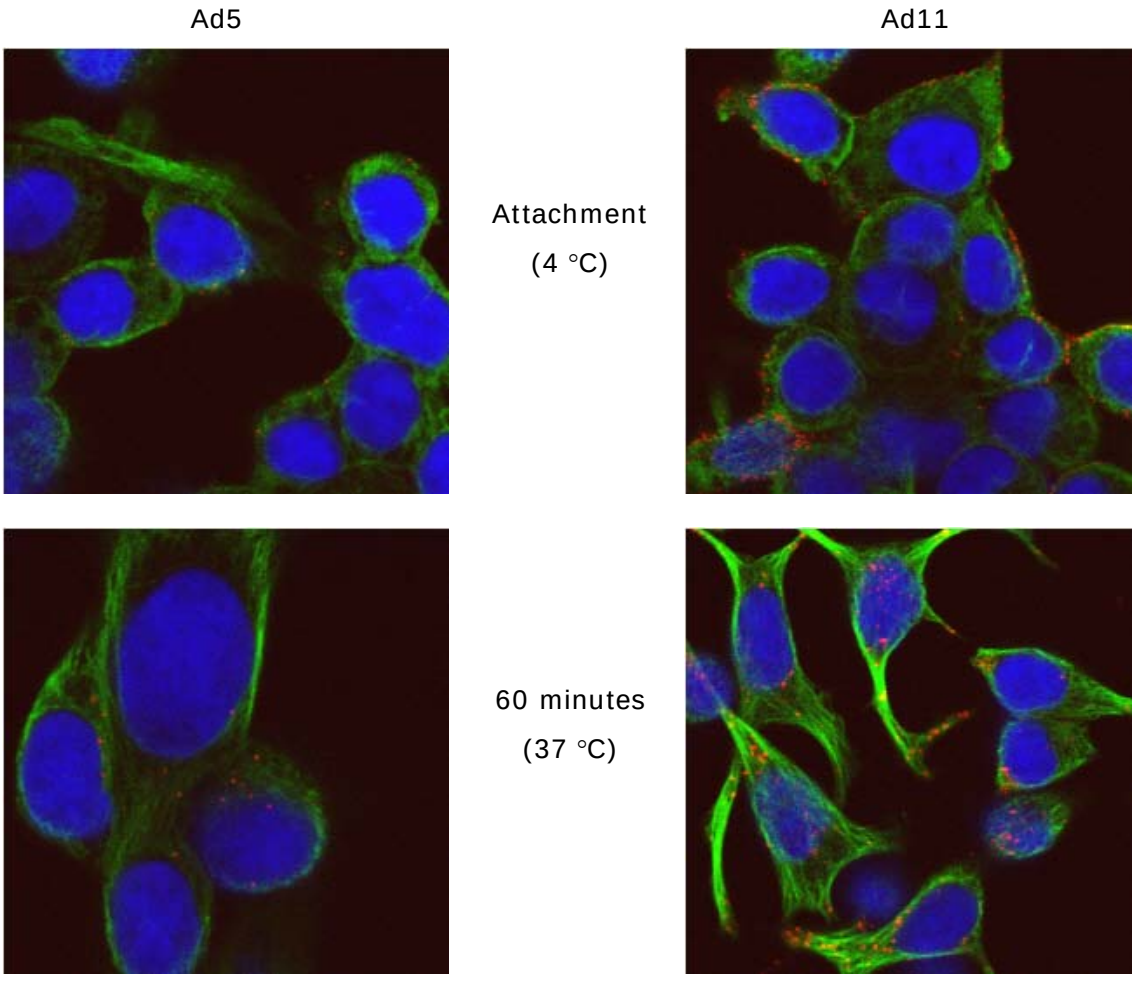


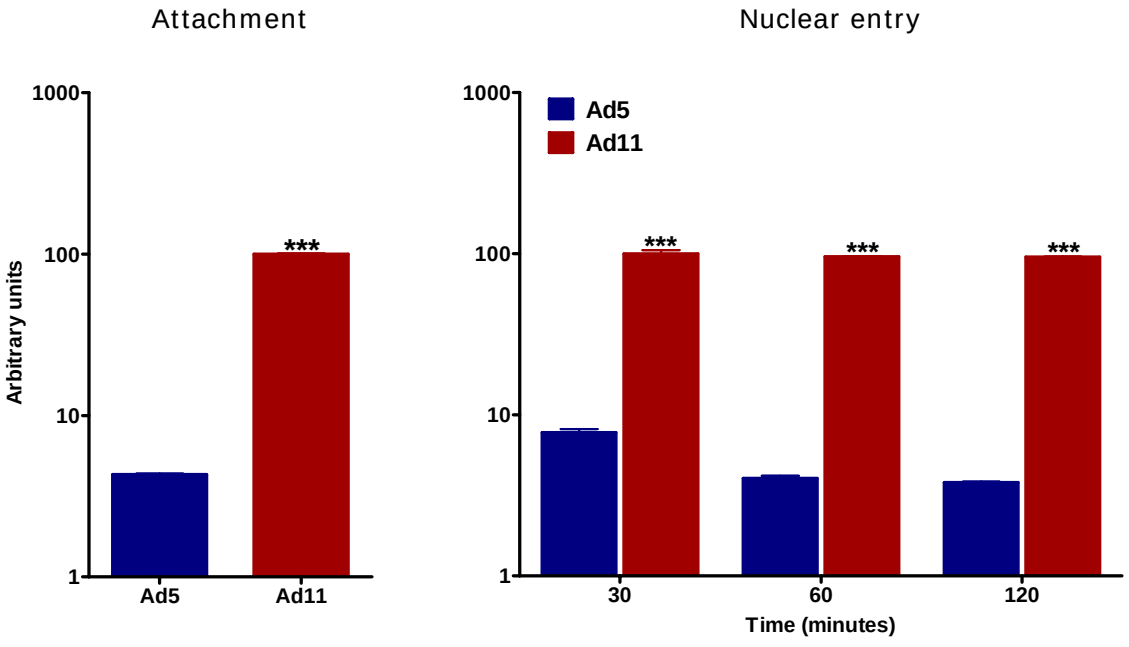

**Figure 5.1: Infectivities of Ad5 and Ad11 in Capan-2, MIA PaCa-2, PC-3 and LNCaP.** The pancreatic cancer cell lines (**a**) Capan-2 (Ad11-sensitive) and (**b**) MIA PaCa-2 (Ad5-sensitive), and the prostate cancer cell lines (**c**) PC-3 (Ad11-sensitive) and (**d**) LNCaP (Ad5-sensitive), were used. Representative confocal microscopy images are shown for virus attachment (4 °C) and trafficking 60 minutes after unbound viruses were washed off (37 °C). Cells were seeded and infected in Lab-Tek II Chamber Slide Systems. Adenoviral capsids were labelled with Alexa Fluor 555 prior to infection (red). Nuclei were stained blue by DAPI and cytoplasmic α-tubulins were stained green by Alexa Fluor 488. The graphs show qPCR results of viral DNA using *E1A* primers and probes, for viruses attached to the cellular membrane (4 °C) and those in the nuclei at 30, 60 and 120 minutes post-attachment (37 °C). Cells (suspended in 1% BSA in PBS) were infected with viruses at 1,000 particles/cell. Results represent means of triplicate experiments and are shown in arbitrary units ± SEM, with the highest value in each graph set to 100. ** $P < 0.01$, *** $P < 0.001$.

## 5.2 Ad11 DNA amplification is attenuated in Ad11-insensitive cell lines

To measure the amount of viral DNA in infected cells, MIA PaCa-2, LNCaP, Capan-2 and PC-3 were first infected with Ads in serum-free medium for two hours, which was then replaced by medium with 5% FBS. The cells and media were harvested at 24, 48, 72 and 96 hours post-infection. DNA was extracted and the amount of viral DNA was determined by qPCR using *E1A* primers and probes. Despite the presence of more Ad11 in MIA PaCa-2 and LNCaP (**Figures 5.1b and d**), their DNA levels were significantly lower than those of Ad5 (**Figure 5.2a**). Ad11 DNA amplified to a much greater extent than Ad5's in the Ad11-sensitive cell lines Capan-2 and PC-3 (**Figure 5.2b**).

**a) Ad11-insensitive cell lines**

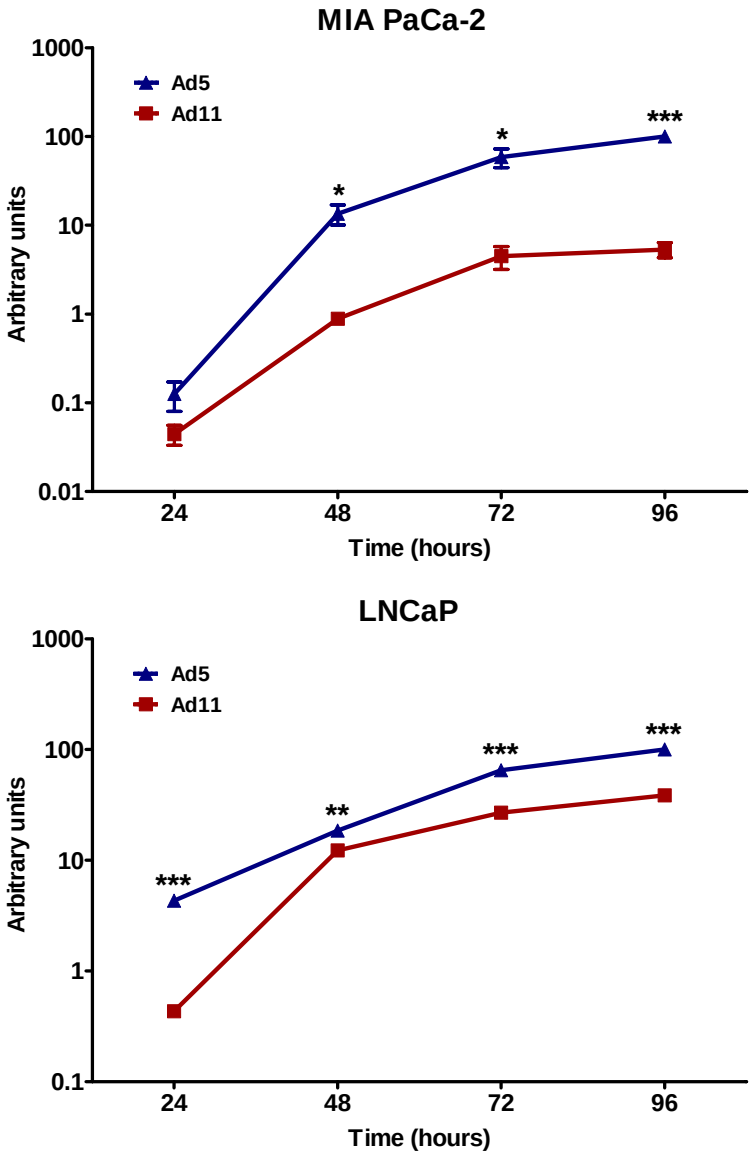


**b) Ad11-sensitive cell lines**

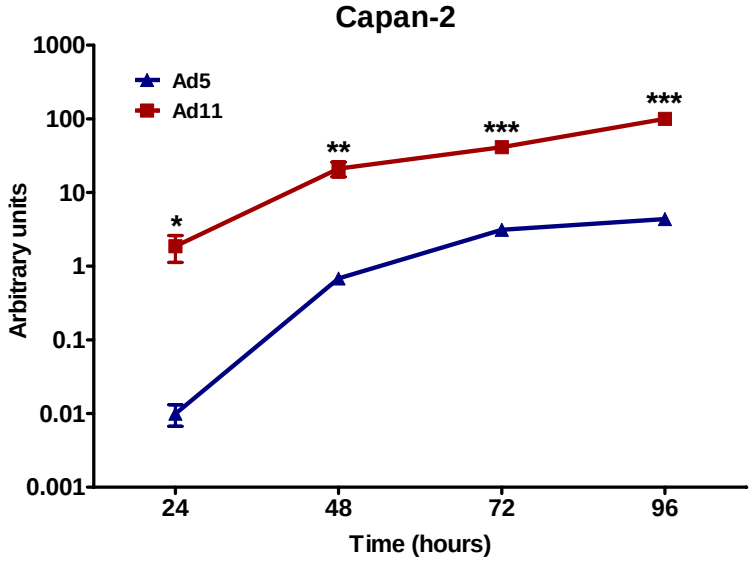

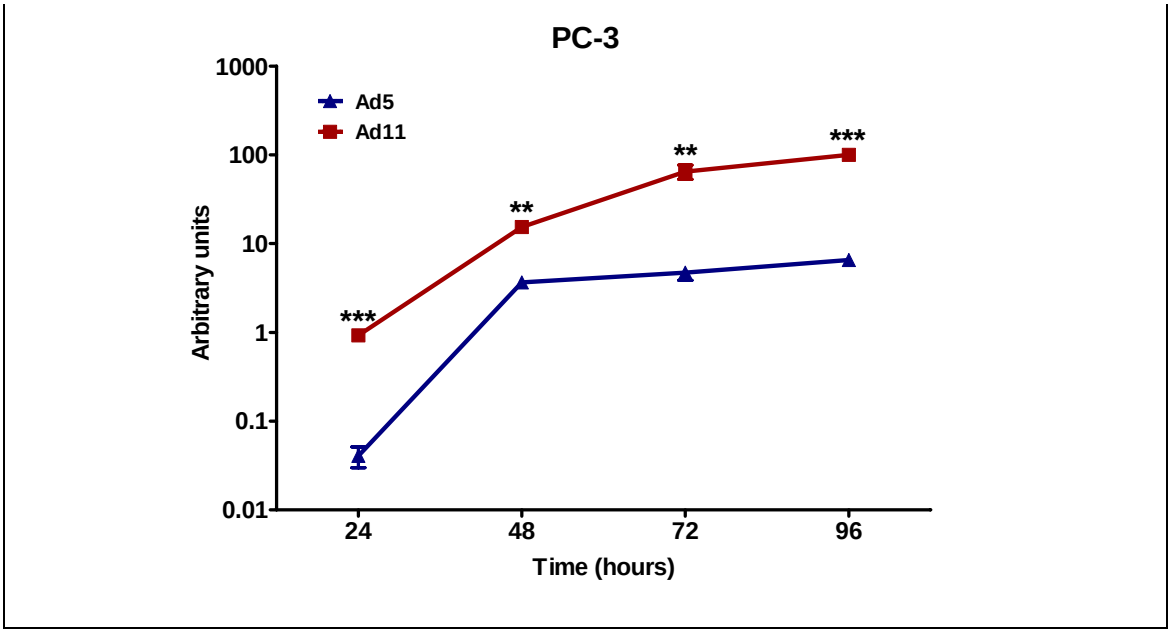


**Figure 5.2: Ad5 and Ad11 DNA amplification in (a) MIA PaCa-2, LNCaP, (b) Capan-2 and PC-3.** Cells were infected in 6-well plates with viruses at 100 particles/cell in serum-free medium. After two hours, this was replaced by medium with 5% FBS. At the stated time points post-infection, cells and media were collected and DNA was extracted for qPCR using *E1A* primers and probes. Results represent means of triplicate experiments and are shown in arbitrary units ± SEM, with the highest value in each graph set to 100. * $P < 0.05$, ** $P < 0.01$, *** $P < 0.001$.

## 5.3 Ad11 hexon protein synthesis is reduced in Ad11-insensitive cell lines

Hexon is a major constituent of the adenoviral capsid and is transcribed late in the infectious cycle. To analyse its expression, Western blotting was performed on infected cell lysates using Ad goat polyclonal antibody (for Ad5 hexon) or Ad11 hexon rabbit polyclonal antibody (for Ad11 hexon). Equal loading was checked using anti-PCNA antibody. As expected from the DNA amplification results (**Figure 5.2**), Ad11 hexon expression was lower in the Ad11-insensitive LNCaP and was hardly detectable in MIA PaCa-2 (**Figure 5.3a**). In the Ad11-sensitive Capan-2, more Ad11 hexon was expressed, certainly from 48 hours post-infection (**Figure 5.3b**). Curiously in PC-3, Ad5 hexon appears to be expressed at a higher level than that of Ad11 at 48 hours, although they became similar at 72 hours (**Figure 5.3b**). This could be due to a delay in Ad11 protein synthesis despite a high viral DNA level (see below).

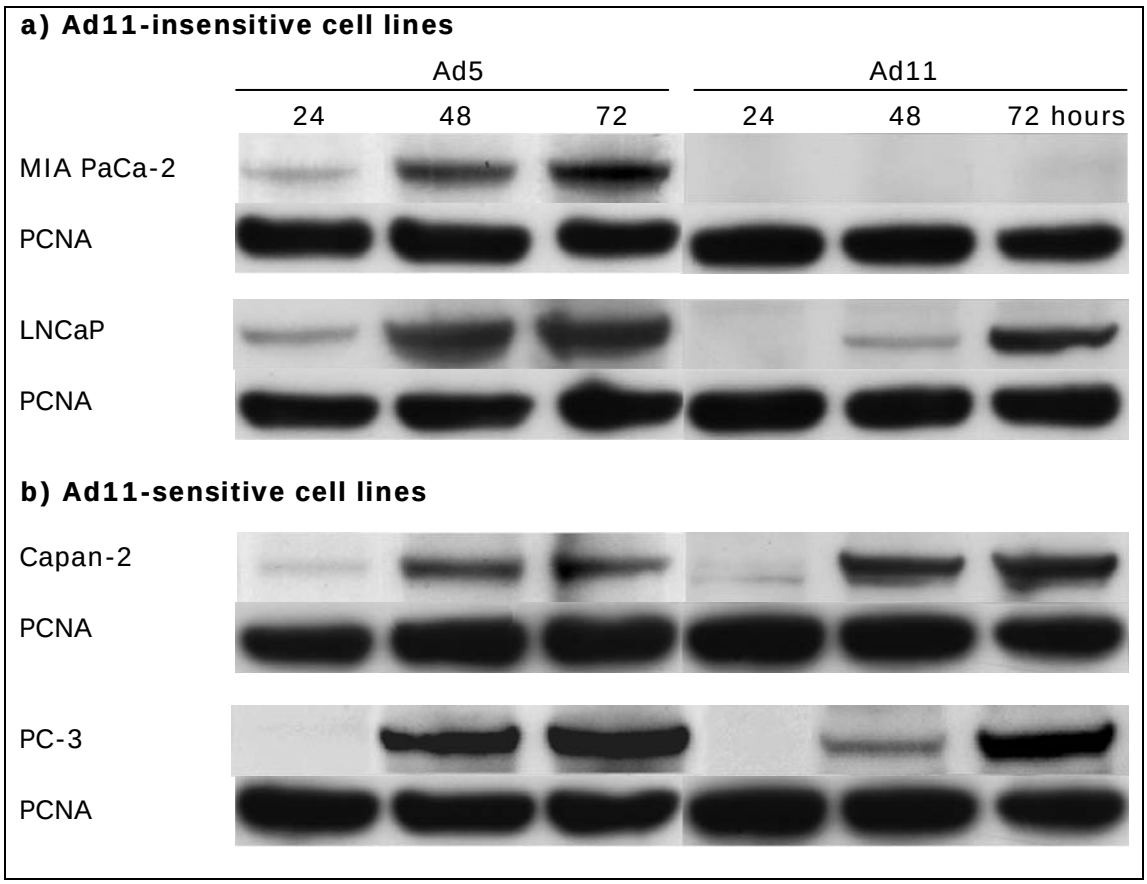


**Figure 5.3: Western blots of adenoviral hexon proteins in infected (a) MIA PaCa-2, LNCaP, (b) Capan-2 and PC-3.** Cells were infected in 6-well plates with viruses at 200 particles/cell in serum-free medium. After two hours, this was replaced by medium supplemented with 5% FBS. At the stated time points post-infection, cells were harvested with lysis buffer. Proteins were separated by SDS-PAGE and blotted onto PVDF transfer membrane. Immunodetection was performed using Ad goat polyclonal antibody or Ad11 hexon rabbit polyclonal antibody. The hexon band is located between the 102 and 150-kDa markers. Equal loading was checked using anti-PCNA antibody.

## 5.4 Lower amounts of infectious Ad11 particles are produced in Ad11-insensitive cell lines

The final step of the Ad life cycle is the production of encapsulated, infectious progeny viruses. To examine this, cells were first infected with Ads in serum-free medium for two hours, which was then replaced by medium with 5% FBS. The cells and media were harvested at 24, 48, 72 and 96 hours post-infection. These were frozen and thawed three times in liquid nitrogen and at 37 °C, respectively. The resultant lysates were used to infect the JH-293 indicator cells in 96-well plates at six 1:10 serial dilutions. Inspection for CPE was performed 11 days post-infection and the $TCID_{50}$ and number of PFUs/cell (cell count on the day of infection) were calculated using the Reed-Muench accumulative method. Consistent with the results from viral DNA amplification and hexon protein expression, cells that were sensitive to Ad5 but not to Ad11 (MIA PaCa-2 and LNCaP) showed much higher levels of Ad5 production compared to Ad11 (**Figure 5.4a**). Ad11 replicated much better than Ad5 in Capan-2 (**Figure 5.4b**). Although Ad11 DNA replicated better than Ad5's in PC-3 from 24 hours post-infection, this was only reflected in infectious virus production from 72 hours (**Figure 5.4b**). Similar findings have also been found for the breast and pancreatic cancer cell lines MCF7 (**Figure 5.5**) and PaTu 8988s (**Figure 5.8b**), respectively. This has several explanations. Firstly, complex intracellular events post-DNA replication such as structural protein synthesis and virion assembly have to be considered. The delay in Ad11 hexon expression compared to Ad5 in PC-3 cells seems to support this (**Figure 5.3b**). Secondly JH-293, the indicator cell line used in the virus replication assay, was less sensitive to Ad11 killing than to Ad5 (**Figure 5.6**; $EC_{50}$ of 0.02676 and 0.5982 virus particles/cell for Ad5 and Ad11, respectively; $P < 0.01$). Thirdly, Ad5 and Ad11 each produces different cytopathic appearances on JH-293 cells, which might contribute to the results seen.

**a) Ad11-insensitive cell lines**

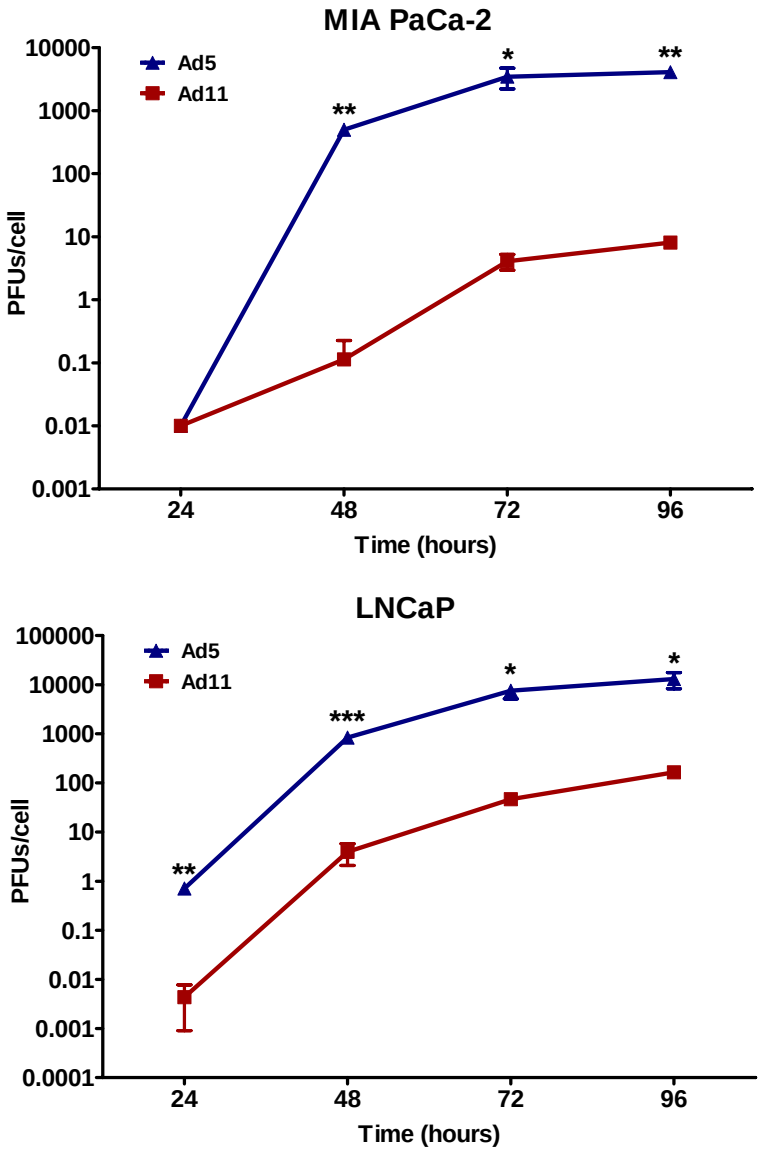


**b) Ad11-sensitive cell lines**

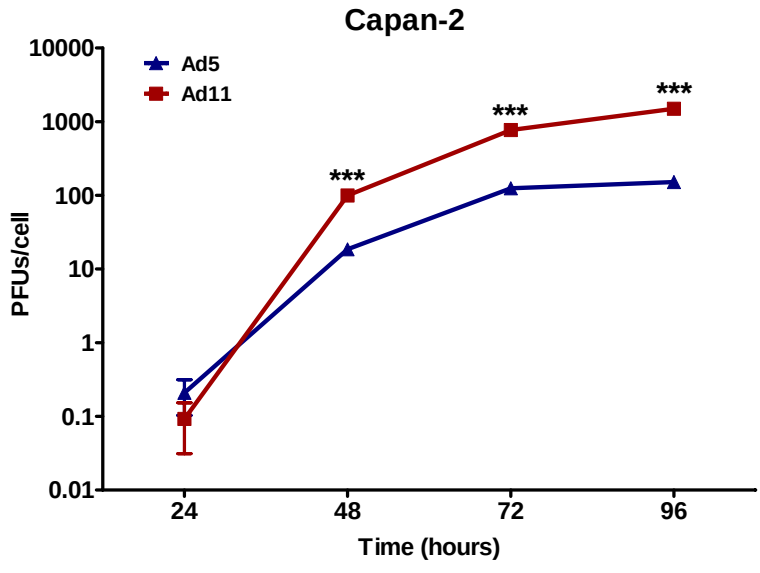

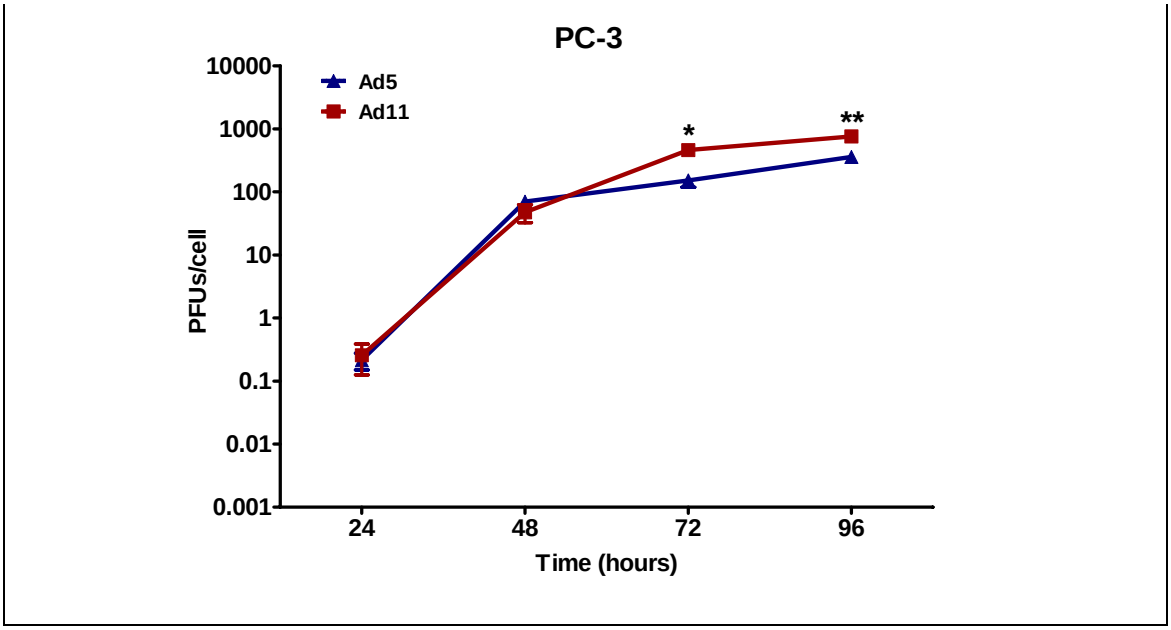


**Figure 5.4: Production of infectious Ad5 and Ad11 by (a) MIA PaCa-2, LNCaP, (b) Capan-2 and PC-3.** Cells were infected in 6-well plates with viruses at 100 particles/cell in serum-free medium. After two hours, this was replaced by medium with 5% FBS. At the stated time points post-infection, cells and media were collected, frozen and thawed three times in liquid nitrogen and at 37 °C, respectively. These were used to infect an indicator cell line, JH-293, in 96-well plates at six 1:10 serial dilutions. The cells were inspected for CPE 11 days later. The $TCID_{50}$ and number of PFUs/cell (cell count on the day of infection) were calculated using the Reed-Muench accumulative method. Results represent means of triplicate experiments ± SEM. * $P < 0.05$, ** $P < 0.01$, *** $P < 0.001$.

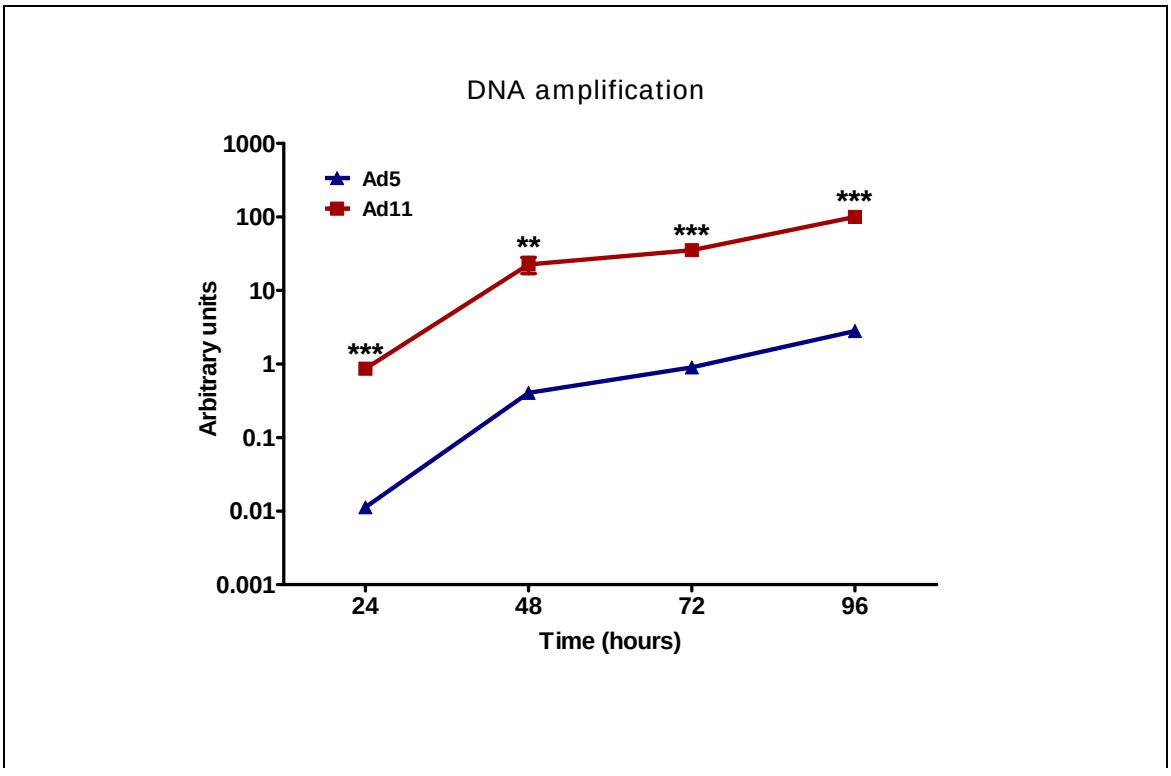

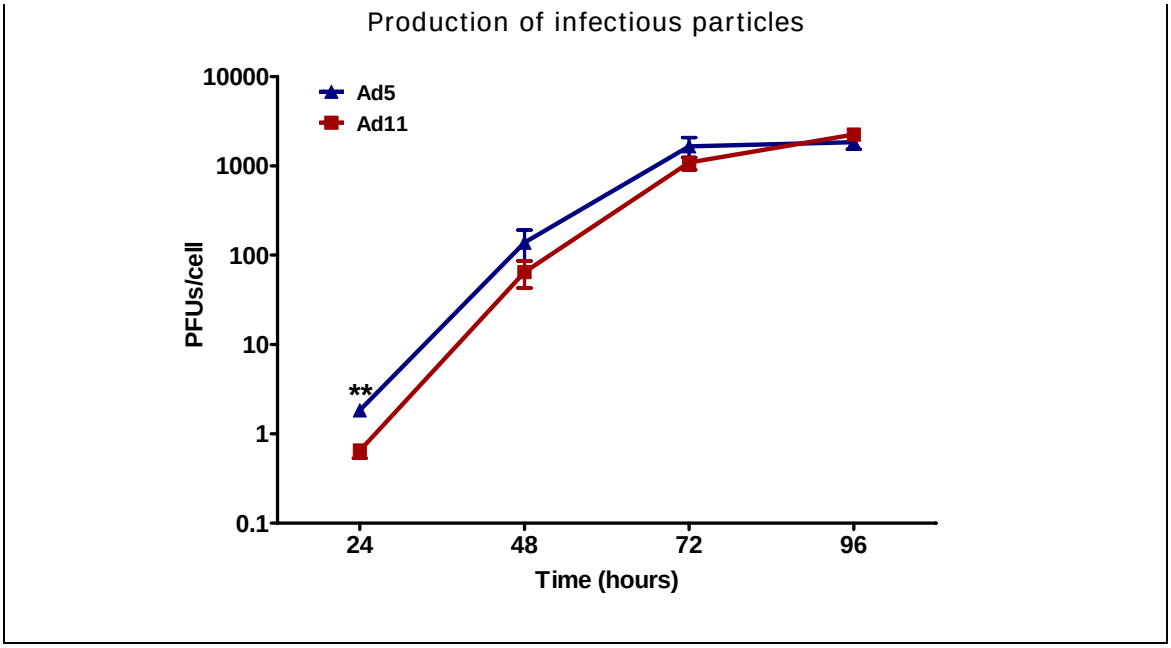


**Figure 5.5: Ad5 and Ad11 DNA amplification and production of infectious particles in MCF7.** Experiments and analyses were performed as described in **Figures 5.2 and 5.4**. Results represent means of triplicate experiments ± SEM. ** $P < 0.01$, *** $P < 0.001$.

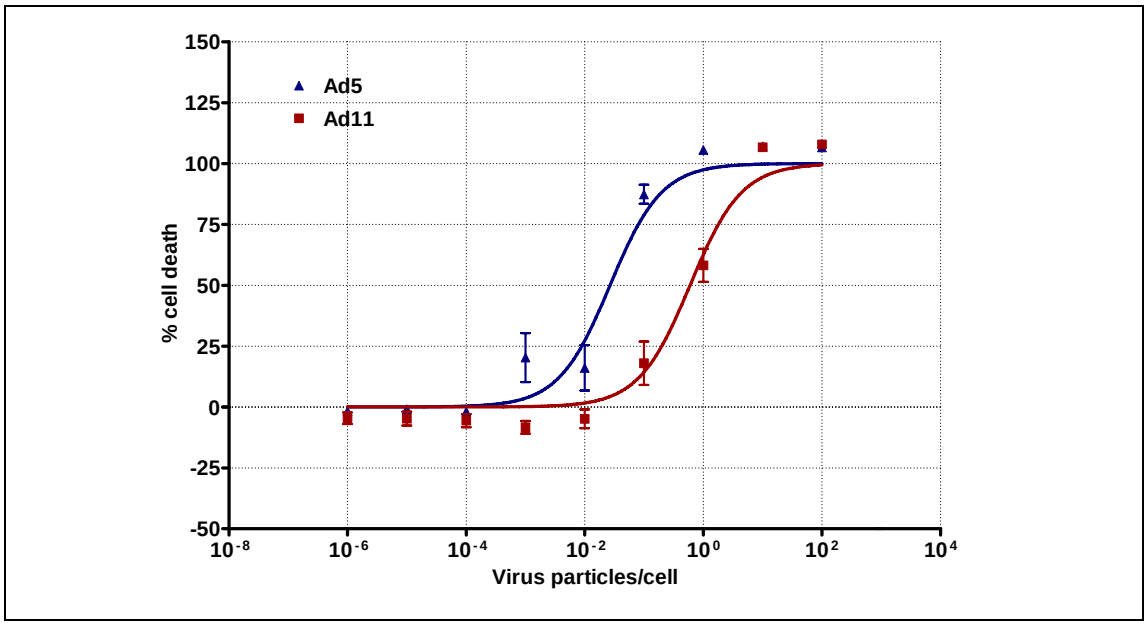


**Figure 5.6: Dose-response curves of Ad5 and Ad11 cytotoxicities in JH-293.** Cells were infected in 96-well plates. Cell viability was measured on day six after infection by the MTS assay. Data represent means ± SEM from duplicate experiments (with each concentration of virus in sextuplicates).

## 5.5 Ad11-insensitive cell lines have lower levels of Ad11 *E1A* mRNA

It is now evident that events after virus entry to the nucleus, but prior to viral DNA replication, are responsible for the attenuated potency of Ad11 in the insensitive cell lines MIA PaCa-2 and LNCaP. One such event is the expression of the adenoviral *E1A* gene. E1A proteins force quiescent cells into S phase and induce the expression of delayed-early proteins encoded by the *E1B*, *E2*, *E3* and *E4* transcriptional units, most of which are crucial for subsequent viral DNA replication.

To examine the levels of *E1A* mRNA, RNAs of virus-infected MIA PaCa-2, LNCaP, Capan-2 and PC-3 were extracted and cDNA was obtained by reverse transcription. qPCR was performed using *E1A* primers and probes, and 18S rRNA was used as an endogenous control. In the Ad11-insensitive MIA PaCa-2 and LNCaP, Ad11 *E1A* mRNA levels were significantly lower than those of Ad5 from eight hours post-infection (**Figure 5.7a**). The higher levels for Ad11 at two hours were probably due to the presence of more Ad11 in the nuclei (**Figures 5.1b and d**). In contrast, the Ad11-sensitive Capan-2 and PC-3 have more Ad11 *E1A* mRNAs throughout (**Figure 5.7b**). Attempts have been made to analyse the expression of Ad11 E1A proteins by Western blotting but there was no specific antibody available, and the proteins could not be detected by antibodies raised against Ad2 or Ad5 E1A (results not shown).

These results suggest that the level of *E1A* mRNA is a major determinant of Ad11's replicative ability and oncolytic potency. Attenuated *E1A* transcription could be responsible for the subsequent reduction in viral DNA amplification, structural protein synthesis and the production of infectious virus particles. These findings have been further extended to the Ad11-insensitive and -sensitive pancreatic cancer cell lines PANC-1 and PaTu 8988s, respectively (**Figure 5.8**) Further understanding of this is crucial and could have important implications for the future development of oncolytic Ad11.

**a) Ad11-insensitive cell lines**

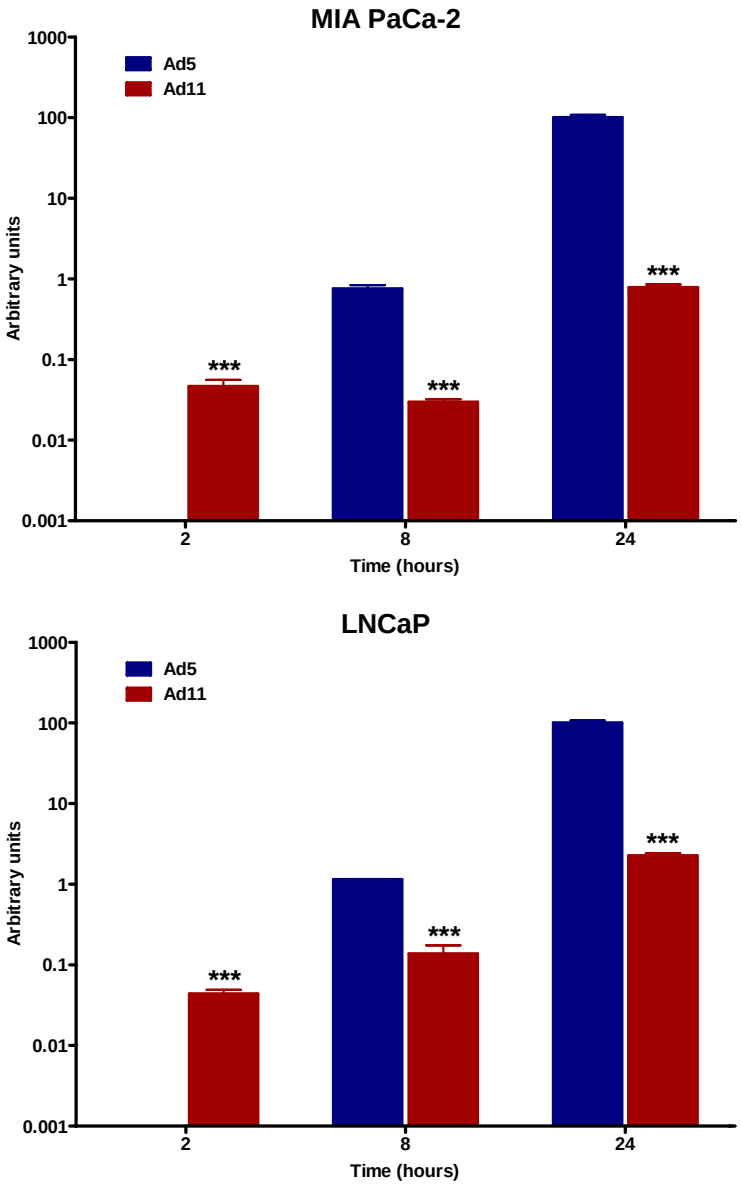


**b) Ad11-sensitive cell lines**

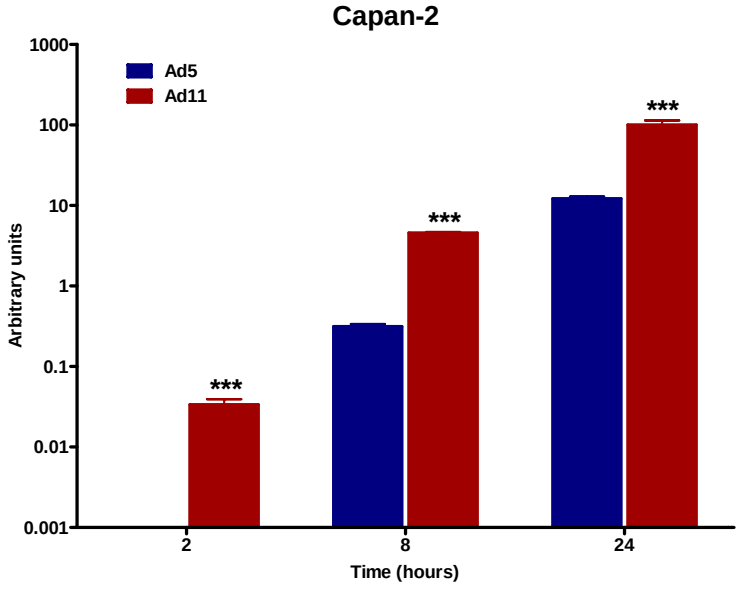

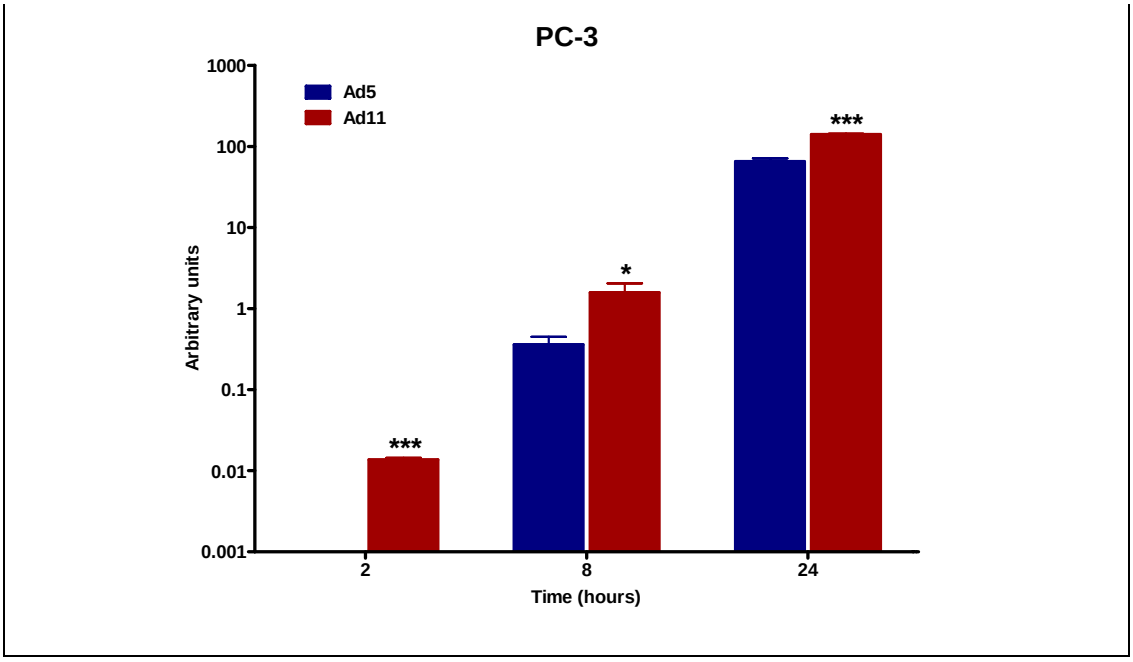


**Figure 5.7: Ad5 and Ad11 *E1A* mRNA levels in (a) MIA PaCa-2, LNCaP, (b) Capan-2 and PC-3.** Cells were infected in 6-well plates with viruses at 100 particles/cell in serum-free medium. After two hours, this was replaced by medium with 5% FBS. At the stated time points post-infection, RNAs were extracted using TRIzol Reagent, chloroform and isopropanol precipitation. cDNA was obtained by reverse transcription, followed by qPCR using *E1A* primers and probes. Results represent means of triplicate experiments normalised against 18S rRNAs and are shown in arbitrary units ± SEM, with the highest value in each graph set to 100. * $P < 0.05$, *** $P < 0.001$.

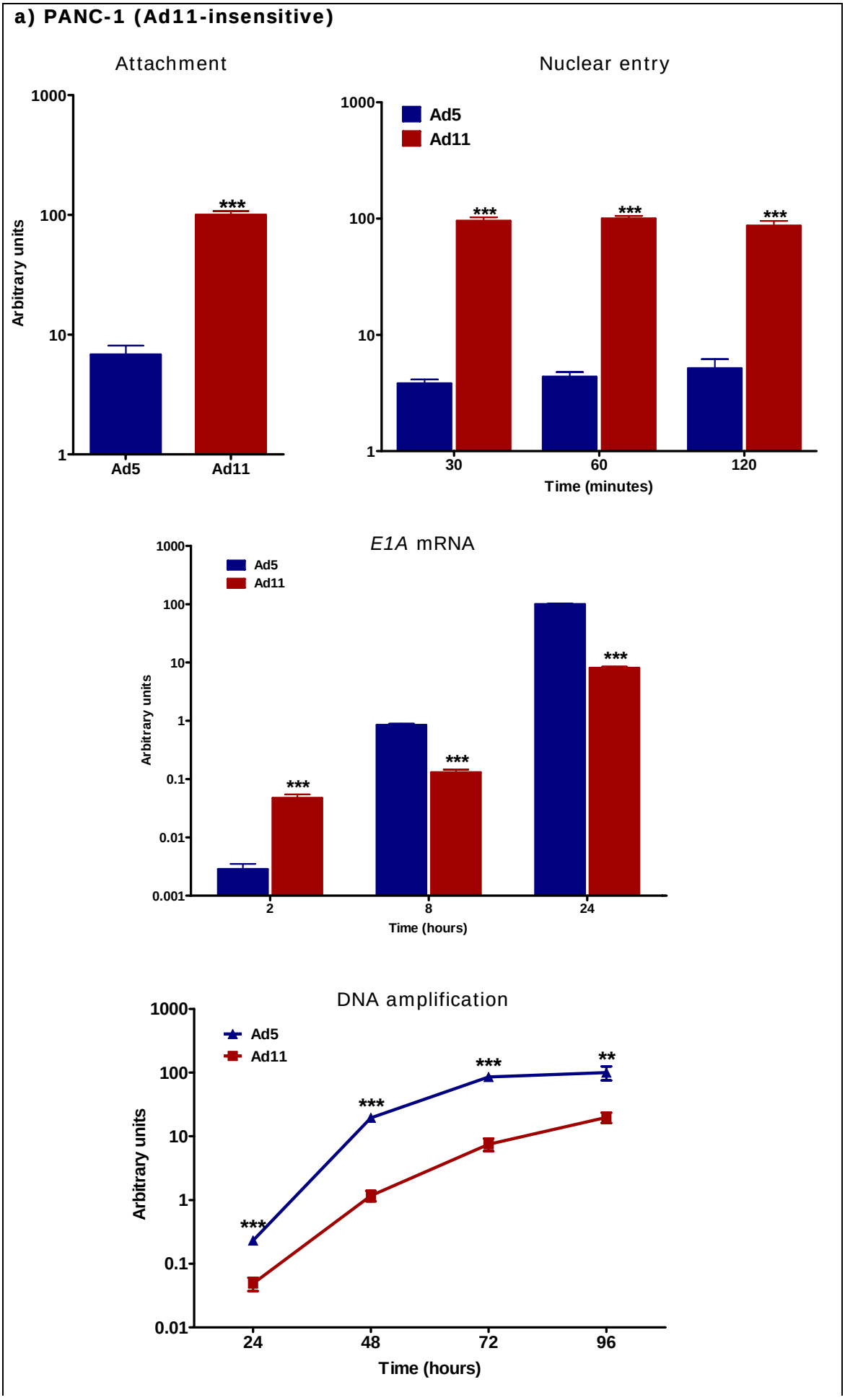
a) PANC-1 (Ad11-insensitive)
Attachment
Nuclear entry
Arbitrary units
1000
100
10
1
Ad5
Ad11
***
Ad5
Ad11
30
60
120
Time (minutes)
E1A mRNA
0.001
0.01
0.1
2
8
24
Time (hours)
DNA amplification
**
24
48
72
96

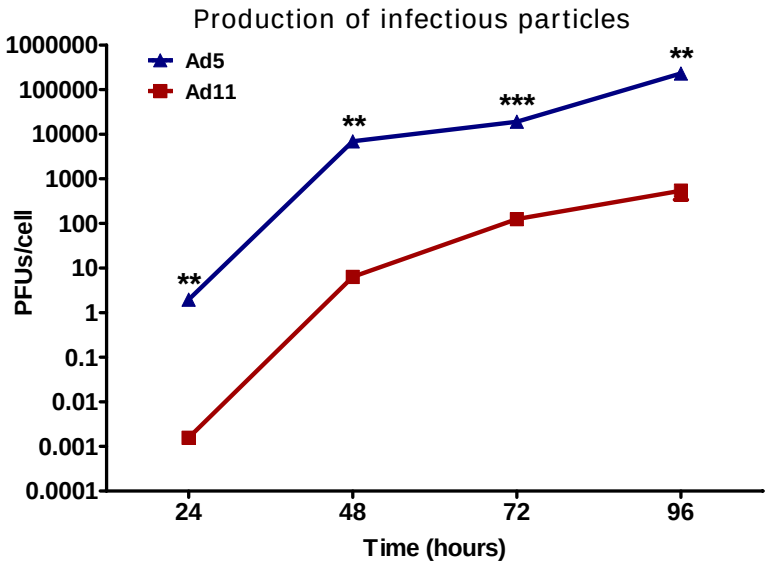


**b) PaTu 8988s (Ad11-sensitive)**

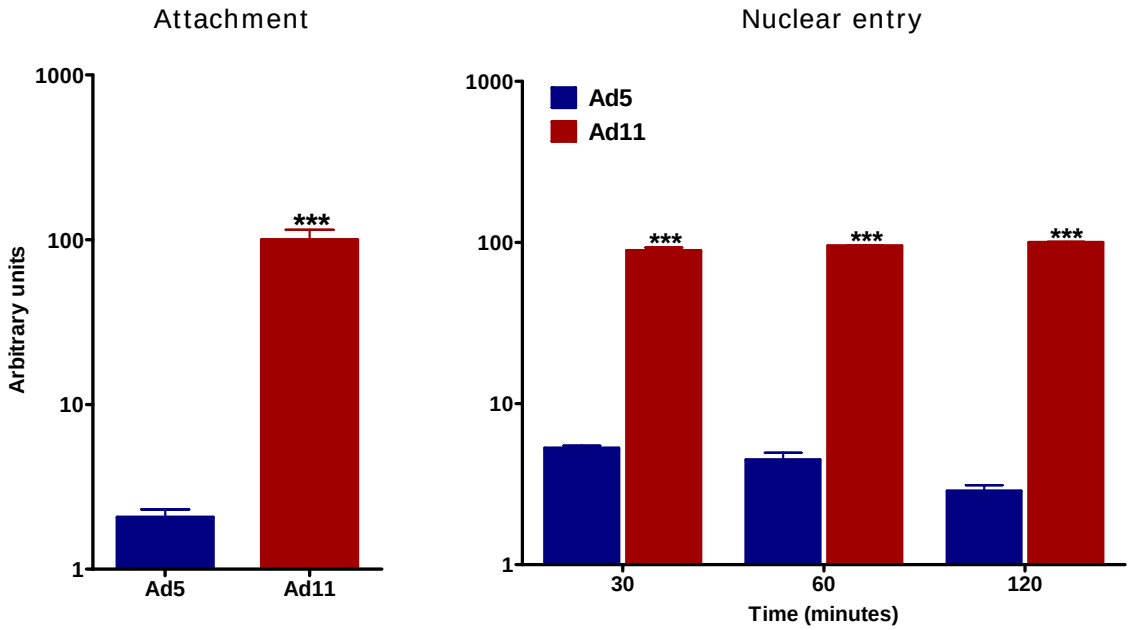


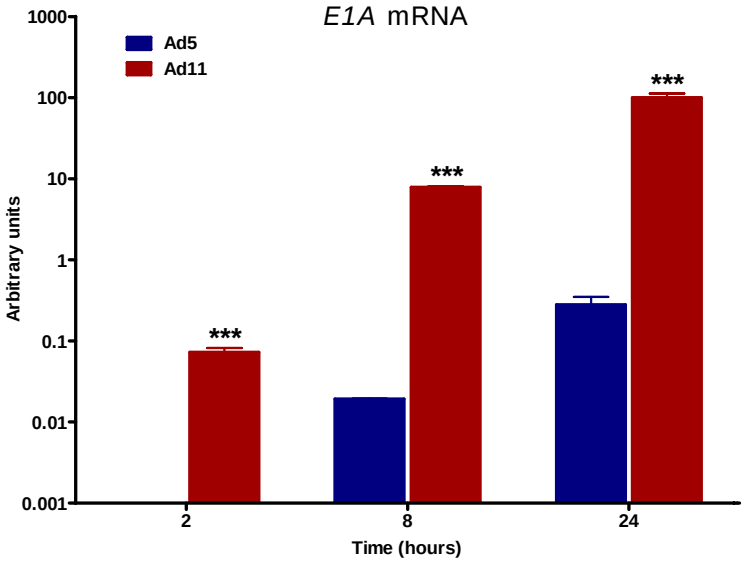

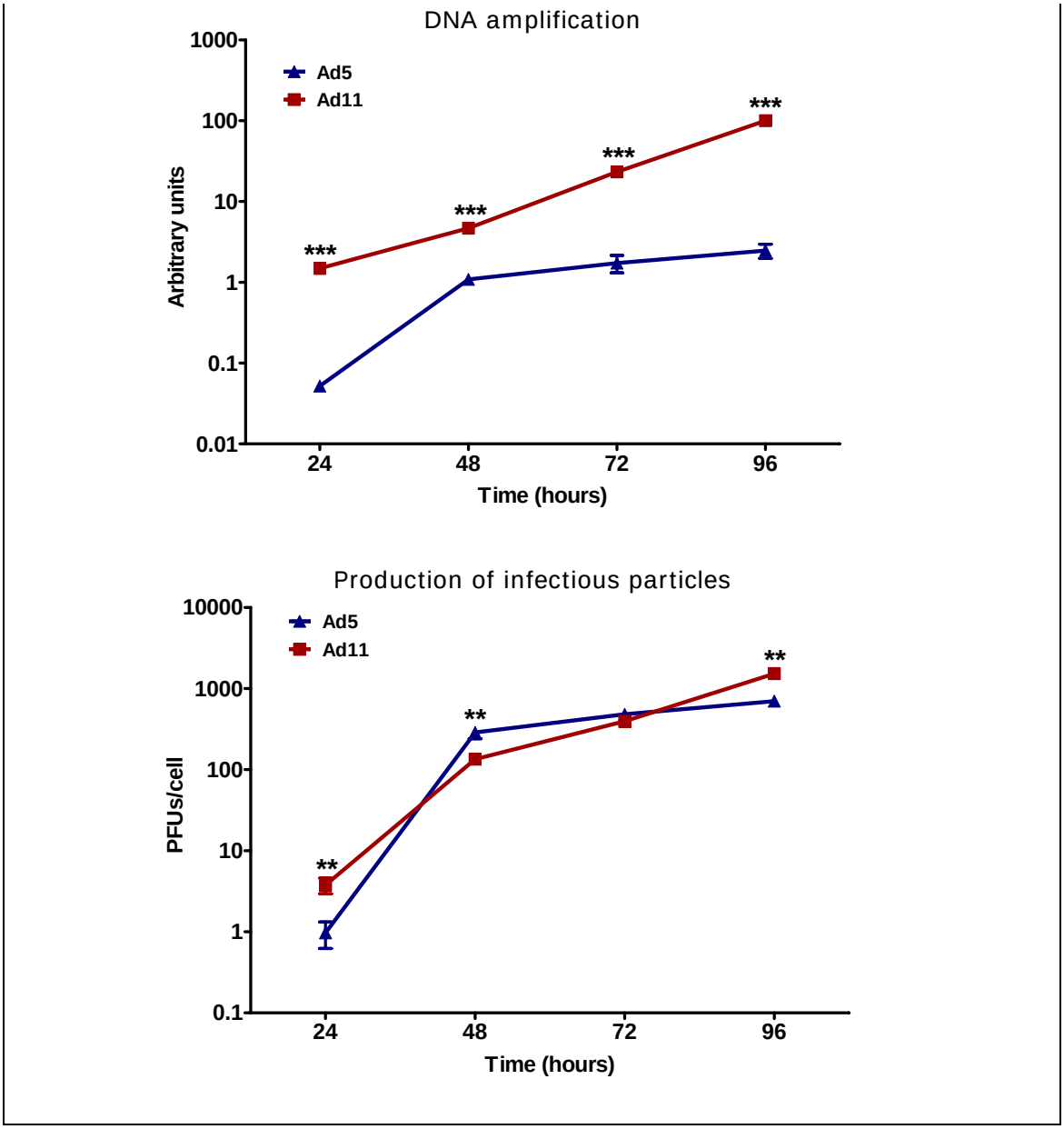


**Figure 5.8: Ad5 and Ad11's infectivities, *E1A* mRNA levels, DNA amplification and infectious particle production in (a) PANC-1 and (b) PaTu 8988s.** These are pancreatic cancer cell lines that are insensitive and sensitive to Ad11, respectively. Experiments and analyses were performed as described in **Figures 5.1, 5.2, 5.4 and 5.7**. Results represent means of triplicate experiments ± SEM. ** $P < 0.01$, *** $P < 0.001$.

## 5.6 Summary of Chapter 5

The higher expression of CD46, as demonstrated in Chapter 3, is consistent with the much greater infectivity of Ad11, with significantly more virus particles attaching to the cellular membrane and entering the nucleus. In **Figure 5.1**, it was assumed that the fluorophore used had no effect on the normal functioning of the viruses. However, this could be tested quite simply by comparing labelled and unlabelled viruses in activities such as virus replication and cell killing. It has been reported that after internalisation into the cell, certain subgroup B Ads (Ad3, -7 and -35) accumulate in lysosomes whereas subgroup C viruses (Ad2 and Ad5) traffic rapidly to the nuclear envelope, because the former group requires a lower pH in the endosomal compartments to escape into the cytosol[211-214]. Surprisingly, results in **Figures 5.1 and 5.8** appear to suggest that a significant number of Ad11 can enter the nucleus as early as 30 minutes post-infection. It is likely that the percentage of nuclear entry relative to the total membrane-associated viruses is lower for Ad11 compared to Ad5, but the absolute number of Ad11 in the nucleus is still much higher.

*E1A* transcription is the first event to occur after virus entry into the nucleus, and the E1A proteins are important at inducing the expression of *E1B*, *E2*, *E3* and *E4*, most of which are crucial for virus replication. In cells that were insensitive to Ad11 cytotoxicity and in spite of its higher infectivity (**Figures 5.1b, d and 5.8a**), Ad11 *E1A* mRNA levels were much lower than those of Ad5 (**Figures 5.7a and 5.8a**), producing a negative effect on viral DNA amplification (**Figures 5.2a and 5.8a**), structural protein synthesis (**Figure 5.3a**), progeny production (**Figures 5.4a and 5.8a**) and cell killing (**Figure 3.2**). Cells that were sensitive to Ad11 cytotoxicity showed higher levels of *E1A* mRNA after Ad11 infection (**Figures 5.7b and 5.8b**). This suggests that the regulation of *E1A* transcription in cancer cells is related to the ability of Ad11 to replicate and kill these cells. This has important implications for the optimisation of Ad11 for cancer therapy and warrants further investigations.

# CHAPTER 6

# *E1A* upstream transcriptional regulatory regions of Ad5 and Ad11

Results in Chapter 5 demonstrated that Ad11 has much higher infectivity than Ad5 in human cancer cell lines. Stepwise investigations of the virus life cycle revealed that the levels of *E1A* mRNA have a direct effect on subsequent virus replication and killing of cancer cells by Ad11. The adenoviral E1A proteins have a crucial role of pushing quiescent cells into S phase and induce the expression other early viral genes so that its DNA can be replicated. In cells insensitive to Ad11-mediated cytotoxicity, low levels of *E1A* mRNA were observed despite the presence of a high number of Ad11 in the nuclei. Conversely, cells that were sensitive to Ad11 showed higher levels of *E1A* mRNA after Ad11 infection. Cell-dependent regulation of *E1A* transcription is likely to be involved. This chapter examines the transcription-enhancing activities of regions upstream of the *E1A* gene in cells sensitive and insensitive to Ad11, respectively.

## 6.1 EF-1A expression is not a major regulator of Ad11 *E1A* transcription

An *E1A* transcriptional enhancer region is known to be located between 194 and 358 bp of the Ad5 genome[55, 56]. The transcription factor EF-1A binds to this enhancer and further upstream regions[54]. When the enhancer region was compared to the corresponding region in Ad11, Mei *et al.*[169] found little similarity in the EF-1A binding sites. Analysis of the entire sequence upstream of *E1A* using the Transcription Element Search System (TESS; www.cbil.upenn.edu/cgi-bin/tess/tess)[215] also revealed significantly more EF-1A binding sites in Ad5 compared to Ad11 (data not shown).

To determine if differences in EF-1A expression could explain the variability in *E1A* mRNA levels, Western blotting was performed using GABPA mouse monoclonal antibody and equal loading was checked using anti-PCNA antibody (**Figure 6.1**). No definite pattern in EF-1A expression between Ad11-sensitive and -insensitive cancer cell lines was observed before and after Ad infection. The lack of EF-1A in Capan-2 could explain this cell's preference to transcribe Ad11 *E1A* over Ad5's, although this did not apply to the other Ad11-sensitive cell line PC-3 (**Figure 6.1b**).

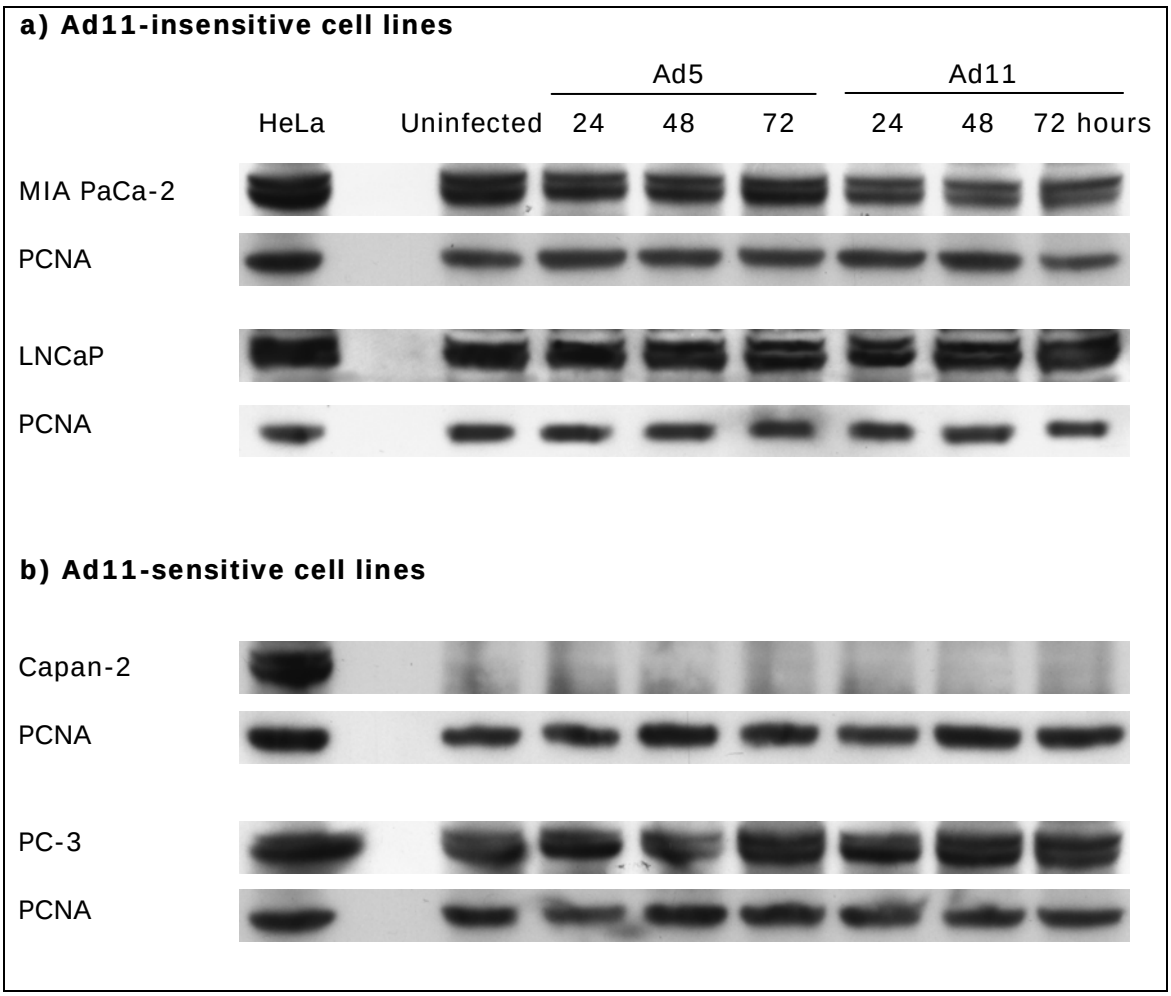


**Figure 6.1: EF-1A expression in (a) MIA PaCa-2, LNCaP, (b) Capan-2 and PC-3.** Cells were infected in 6-well plates with viruses at 100 particles/cell in serum-free medium. After two hours, this was replaced by medium with 5% FBS. At the stated time points post-infection, cells were harvested with lysis buffer. Uninfected cells and HeLa cells (positive control) were also included. Proteins were separated by SDS-PAGE and blotted onto PVDF transfer membrane. Immunodetection was performed using GABPA mouse monoclonal antibody. EF-1A is approximately 60 kDa in size. Equal loading was checked using anti-PCNA antibody.

## 6.2 Transcription-regulating activities of regions upstream of *E1A* by luciferase reporter assay

### 6.2.1 Luciferase plasmid construction

The coding sequences of *E1A* (from the ATG start codons) begin at 560 and 568 bp relative to the left ends of the Ad5 and Ad11 genomes, respectively. Besides the promoter sequence situated immediately upstream of this, the *E1A* transcriptional enhancer region is located between 194 and 358 bp in Ad5[55, 56].

To test the contribution of these regions in regulating *E1A* transcription, six plasmids were constructed. Sequences were inserted between the BglII and HindIII restriction sites in the firefly (*Photinus pyralis*) luciferase-encoding pGL3-Control Vector, replacing the SV40 promoter (**Figure 6.2**). p5-L and p11-L each contains the entire region upstream of the *E1A*-coding sequence (up to and including 559 and 567 bp for Ad5 and Ad11, respectively) ("left end"); p5-EP and p11-EP each has the sequence from 195 bp up to the *E1A*-coding sequence ("enhancer-promoter"); p5-P and p11-P each contains the region immediately after the adenoviral packaging signal up to the *E1A*-coding sequence, *i.e.* from 378 and 393 bp for Ad5 and Ad11, respectively ("promoter").

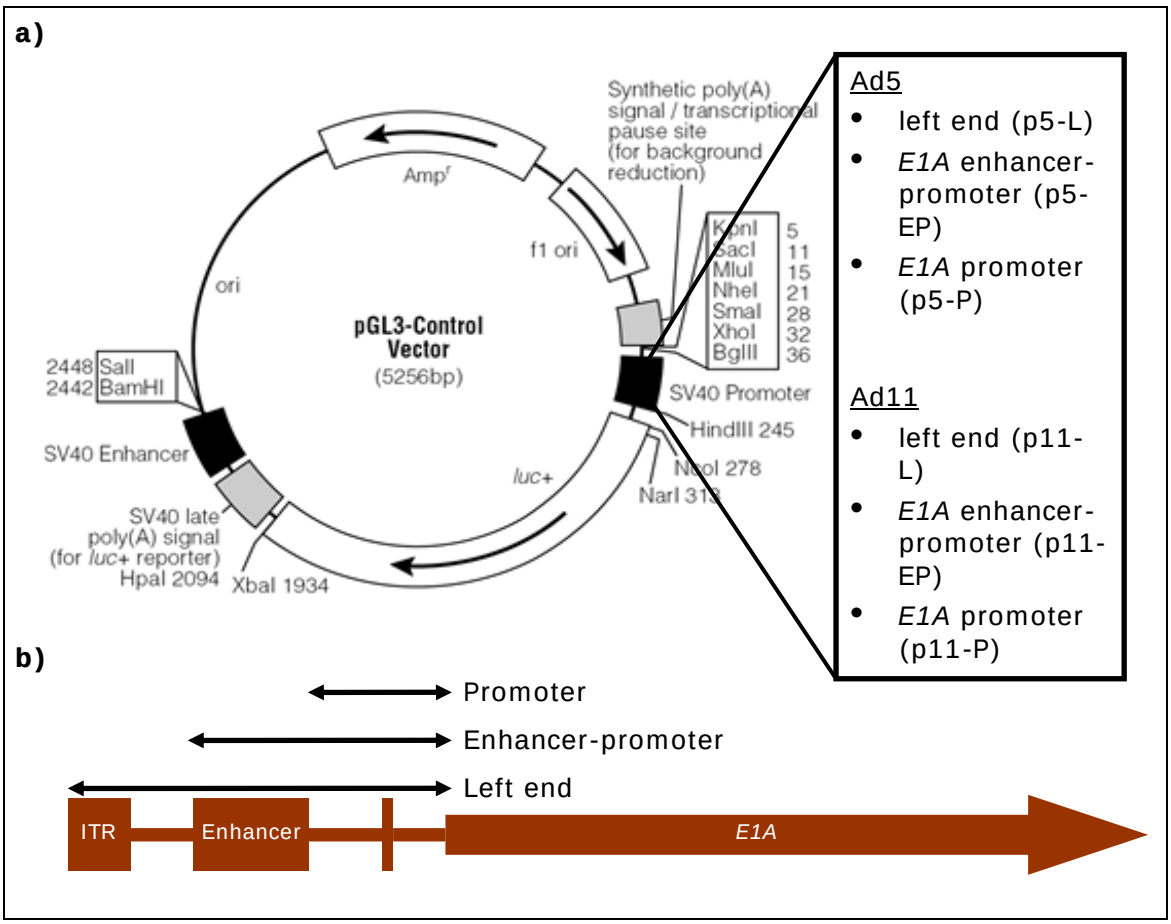


**Figure 6.2: Modification of pGL3 with regions upstream of *E1A* driving luciferase expression.** (**a**) Six plasmids were constructed by replacing the SV40 promoter in pGL3-Control Vector (between BglII and HindIII restriction sites) with the following sequences from Ad5 and Ad11 genomes: (**b**) "left end" is the entire region upstream of the *E1A*-coding sequence (up to and including 559 and 567 bp for Ad5 and Ad11, respectively); "enhancer-promoter" is taken from 195 bp up to the *E1A*-coding sequence; "promoter" is the region immediately after the adenoviral packaging signal up to the *E1A*-coding sequence, *i.e.* from 378 and 393 bp for Ad5 and Ad11, respectively. Abbreviations: amp$^r$, ampicillin resistance; *luc*+, firefly luciferase reporter gene; ori, origin of replication; poly(A), polyadenylation; SV40, Simian vacuolating virus 40.

Using primers described in 2.11.1, the required fragments were cloned from pBGwtAd11 (wild-type Ad11 plasmid) and pTG3602 (wild-type Ad5 plasmid) (**Figure 6.3**) and subsequently digested with BglII and HindIII. pGL3-Control Vector was also digested with BglII and HindIII, releasing its SV40 promoter (**Figure 6.4**). Fragments were ligated to pGL3 followed by transformation of chemically competent *E. coli*. Bacterial colonies were screened by PCR using the same primers (**Figure 6.5**). Correct plasmids were purified and confirmed by sequencing (performed by the Genome Centre; results not shown).

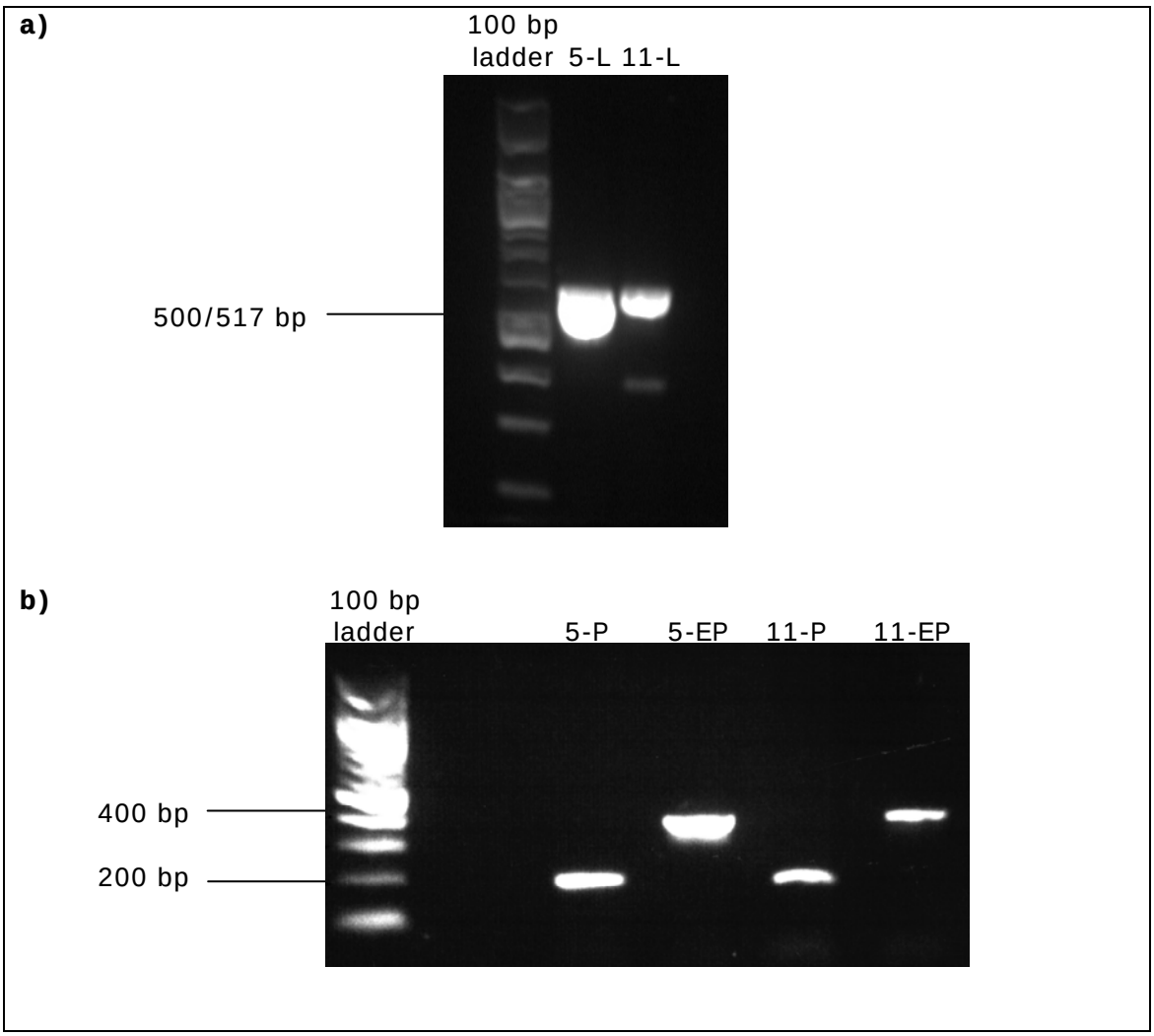


**Figure 6.3: PCR-amplified fragments of *E1A* upstream regions.** (**a**) "Left ends" of Ad5 (5-L – 579 bp) and Ad11 (11-L – 585 bp). (**b**) "Promoters" (5-P – 182 bp; 11-P – 175 bp) and "enhancer-promoters" (5-EP – 365 bp; 11-EP – 372 bp) of Ad5 and Ad11. These fragments were extracted and ligated to pGL3.

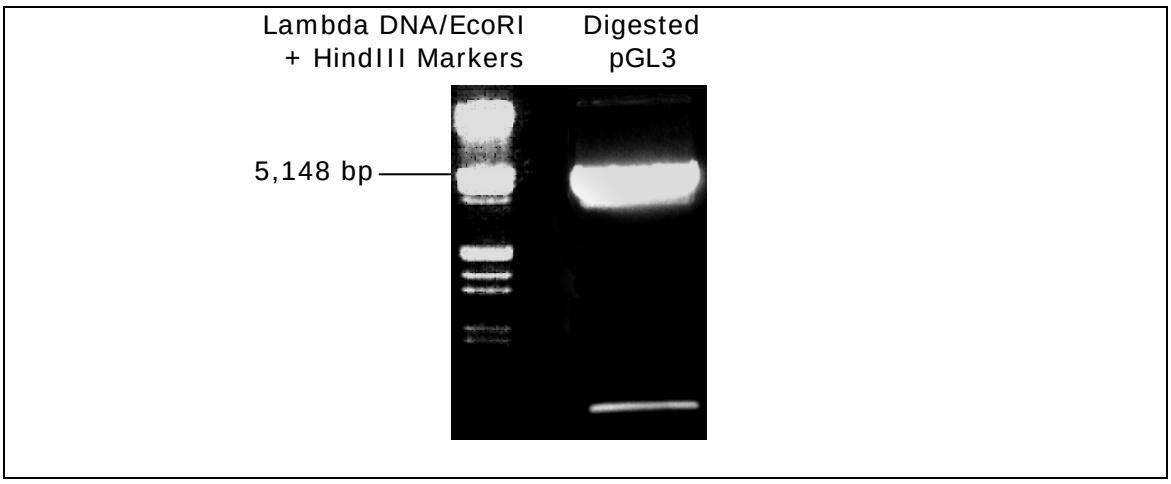


**Figure 6.4: Digestion of pGL3-Control Vector.** Digestion was done using BglII and HindIII. The upper band of linearised plasmid (5,047 bp) was extracted. The lower band (209 bp) is the released SV40 promoter.

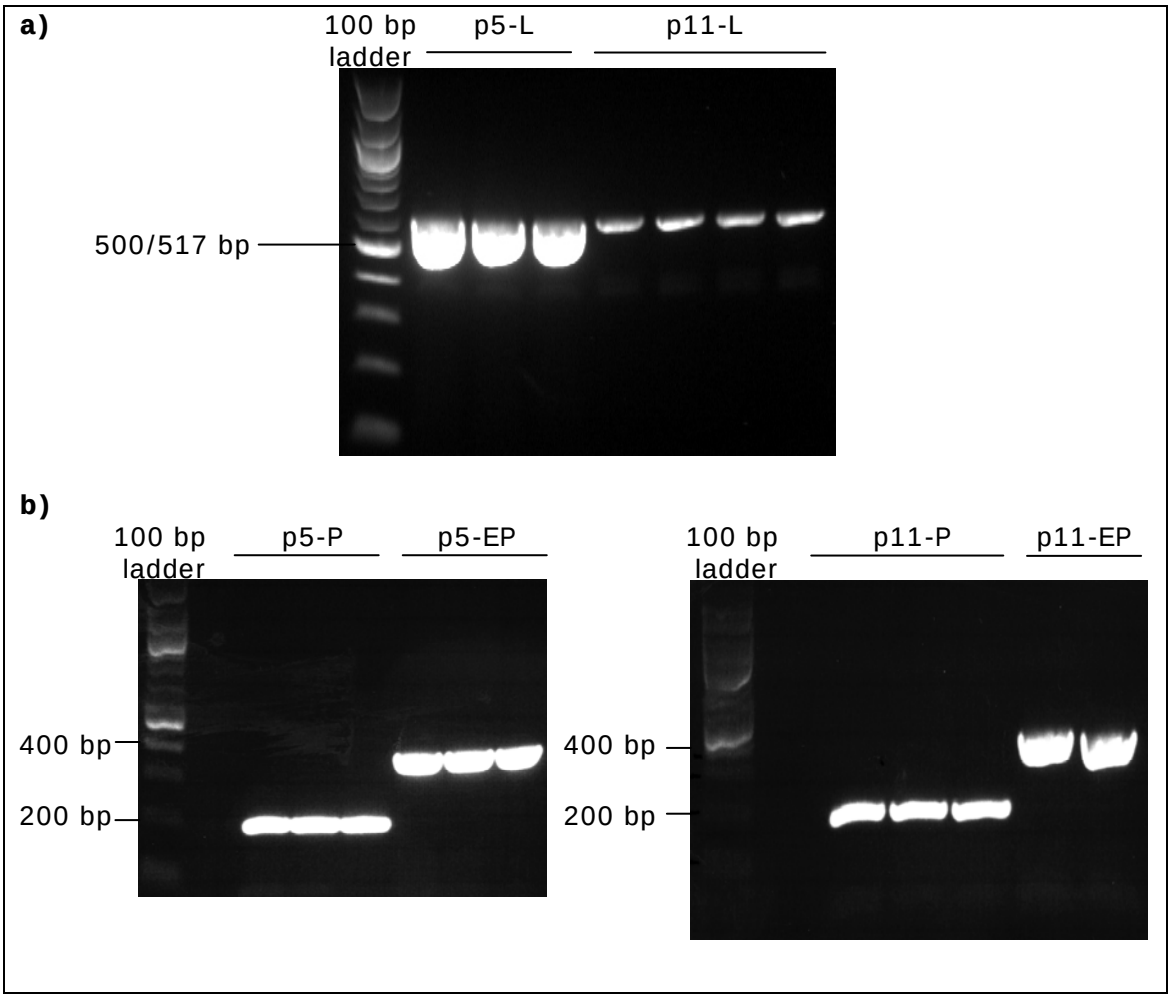


**Figure 6.5: Confirmation of successful ligation of *E1A* upstream regions to pGL3.** Primers listed in 2.11.1 were used. (**a**) "Left end"-ligated p5-L and p11-L were confirmed by PCR-amplified fragments of 579 and 585 bp, respectively. (**b**) "Promoter"-ligated p5-P and

p11-P (fragments of 182 and 175 bp, respectively) and "enhancer-promoter"-ligated p5-EP and p11-EP (fragments of 365 and 372 bp, respectively). All colonies showed the correct inserts. Further confirmation was done by DNA sequencing using RVprimer3 and GLprimer2.

### 6.2.2 Ad5 *E1A* upstream regions have higher transcription-enhancing activities than Ad11's

The constructed p5-L, p11-L, p5-EP, p11-EP, p5-P and p11-P plasmids were used to cotransfect MIA PaCa-2, LNCaP, Capan-2 and PC-3, with pRL-SV40 Vector. The sequences of *E1A* upstream regions would result in different expressions of the firefly luciferase enzyme, which oxidises luciferin to produce luminescence. To control for variability such as transfection efficiency and cell number, the cotransfected pRL-SV40 acted as an internal control. pRL-SV40 produces luciferase from *Renilla reniformis* (sea pansy), driven by the SV40 enhancer/promoter. Luciferase reporter assays were performed using the Dual-Luciferase Reporter Assay System. 18 hours after transfection, luminescence produced by the firefly luciferase was measured first. This reaction was then quenched, followed by the quantitation of luminescence from *Renilla* luciferase. Results were normalised by dividing firefly luminescence by *Renilla* luminescence.

Generally, the longest sequence (i.e. "left end") has the highest transcription-enhancing activity. The "enhancer-promoter" sequence has slightly higher or similar activity compared to the "promoter". As expected, Ad5 *E1A* upstream regions have higher activities than Ad11's in the Ad5-sensitive cell lines MIA PaCa-2 and LNCaP (**Figure 6.6a**). Surprisingly, the Ad11-sensitive Capan-2 and PC-3 also showed similar results (**Figure 6.6b**).

**a) Ad11-insensitive cell lines**

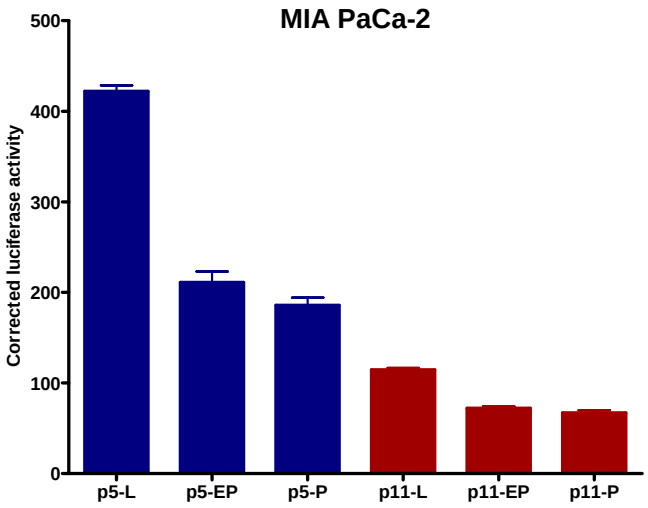


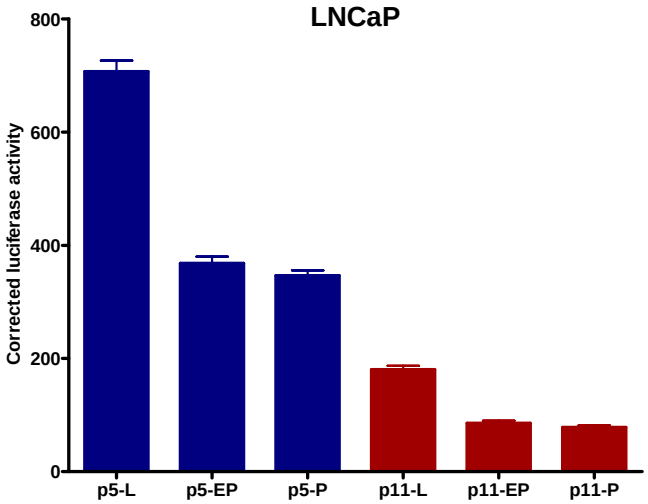


**b) Ad11-sensitive cell lines**

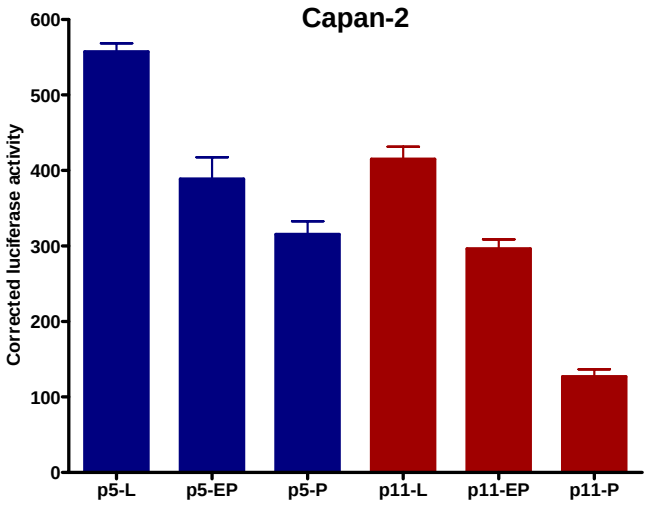

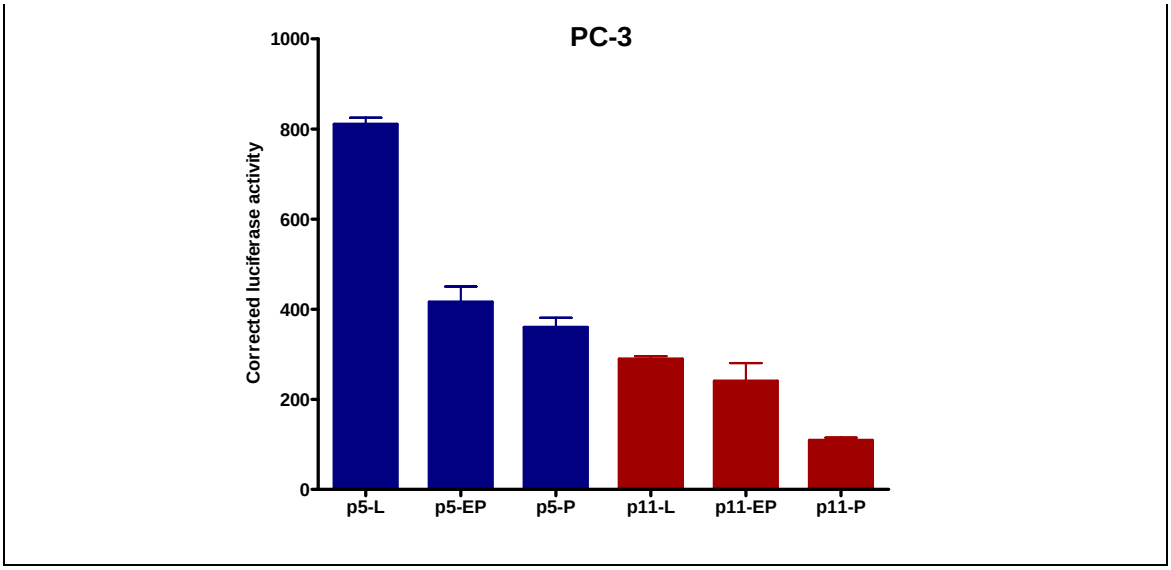


**Figure 6.6: Luciferase reporter assays of *E1A* upstream regions in (a) MIA PaCa-2, LNCaP, (b) Capan-2 and PC-3.** Cells in 24-well plates were cotransfected with plasmids described in **Figure 6.2** and the pRL-SV40 control plasmid. Luciferase reporter assays were performed 18 hours later. Luciferase activity was normalised by dividing firefly luminescence by *Renilla* luminescence of pRL-SV40. Results represent means of triplicate experiments ± SEM.

### 6.2.3 Transcription-enhancing activity of Ad11 *E1A* upstream region increases after Ad11 infection in Capan-2 but not PC-3

To determine if Ad infection could affect the *E1A* regulatory region, MIA PaCa-2, LNCaP, Capan-2 and PC-3 were infected with Ad5 or Ad11 and left for four hours prior to transfection with p5-L or p11-L. Luciferase reporter assays were performed 18 hours after transfection. As shown in **Figure 6.7**, Ad infection upregulated the transcription-enhancing activities of *E1A* upstream regions compared to mock infection. Expectedly, Ad5 infection has a greater effect than Ad11 on both Ad5's and Ad11's regulatory regions in MIA PaCa-2 and LNCaP (**Figure 6.7a**). In Capan-2, although the baseline activity of Ad11 *E1A* upstream region was weaker than that of Ad5, this increased dramatically after Ad11 infection. This level was higher than that of Ad5 after Ad5 infection, although this was not statistically significant ($P = 0.1612$) (**Figure 6.7b**). The fact that the infectivity of Ad11 was much higher in this cell line (**Figure 5.1a**) could be the reason behind the higher levels of *E1A* mRNA observed (**Figure 5.7b**). Nevertheless in PC-3, the activity of Ad5's regulatory region was still much higher than that of Ad11 after infection (**Figure 6.7b**), even though more Ad11 *E1A* mRNAs were found (**Figure 5.7b**). The reason is unknown at present, although factors such as

differences in *E1A* mRNA stability and regulatory feedback by E1A proteins (a time-dependent event) could be involved.

This luciferase reporter experiment was also performed on the Ad11-insensitive and -sensitive pancreatic cancer cell lines PANC-1 and PaTu 8988s. The results of PANC-1 were similar to those of MIA PaCa-2 and LNCaP (**Figure 6.8a**). The results of PaTu 8988s, however, were distinctive from Capan-2 and PC-3 (**Figure 6.8b**). Ad11 *E1A* upstream regions have significantly higher activities compared to Ad5's with or without infection. This could explain the observation that PaTu 8988s showed the greatest difference amongst the Ad11-sensitive cell lines in its Ad5 and Ad11 *E1A* mRNA levels (**Figures 5.7b and 5.8b**).

**a) Ad11-insensitive cell lines**

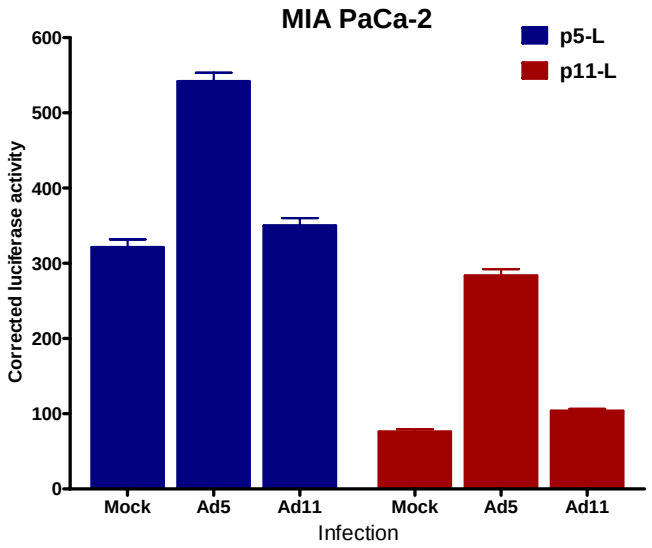


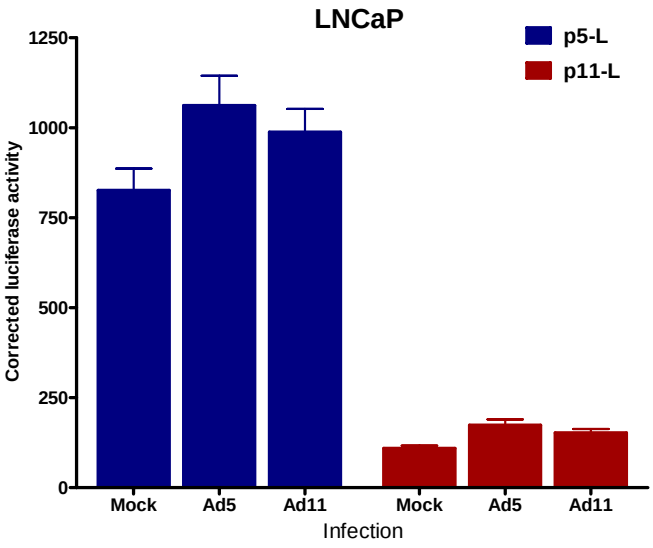


**b) Ad11-sensitive cell lines**

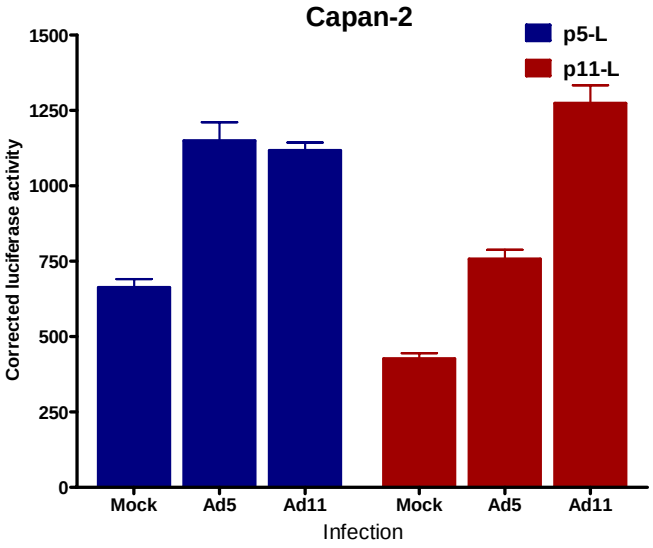

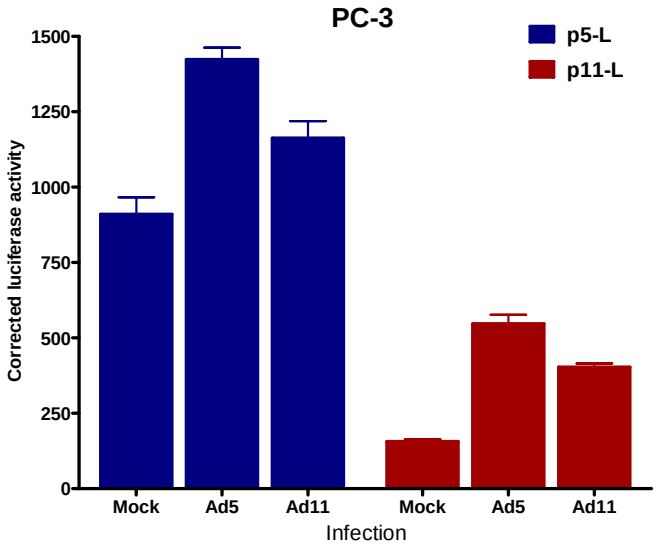


**Figure 6.7: Luciferase reporter assays of *E1A* upstream regions in (a) MIA PaCa-2, LNCaP, (b) Capan-2 and PC-3 after infection.** Cells in 24-well plates were infected with viruses at 100 particles/cell, or mock infected, in serum-free medium. After two hours, this was replaced by medium with 5% FBS. Cotransfection with p5-L or p11-L and pRL-SV40 was performed after an additional two hours. Luciferase reporter assays were performed 18 hours later. Luciferase activity was normalised by dividing firefly luminescence by *Renilla* luminescence of pRL-SV40. Results represent means of triplicate experiments ± SEM.

**a) PANC-1 (Ad11-insensitive)**

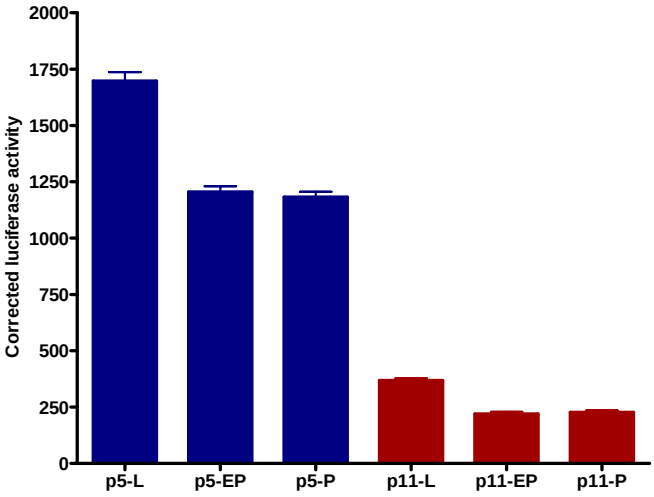


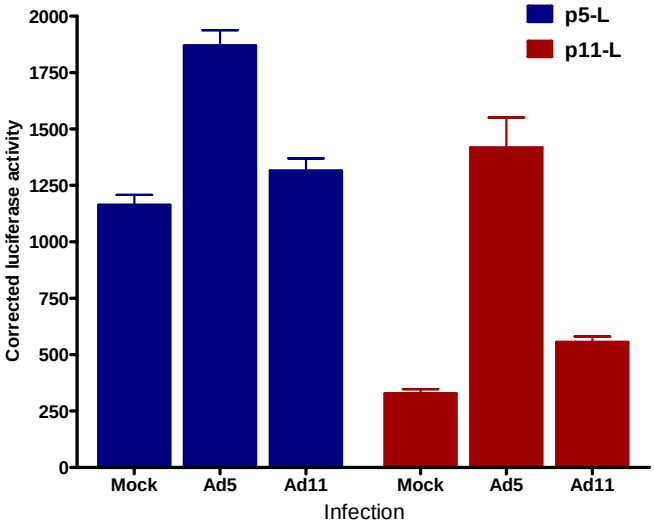


**b) PaTu 8988s (Ad11-sensitive)**

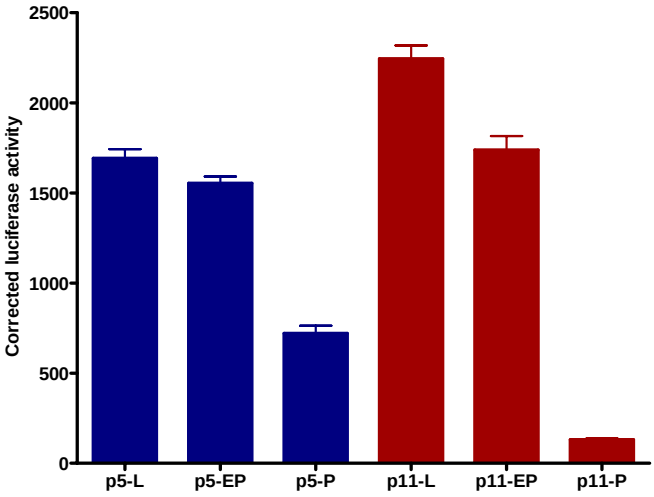

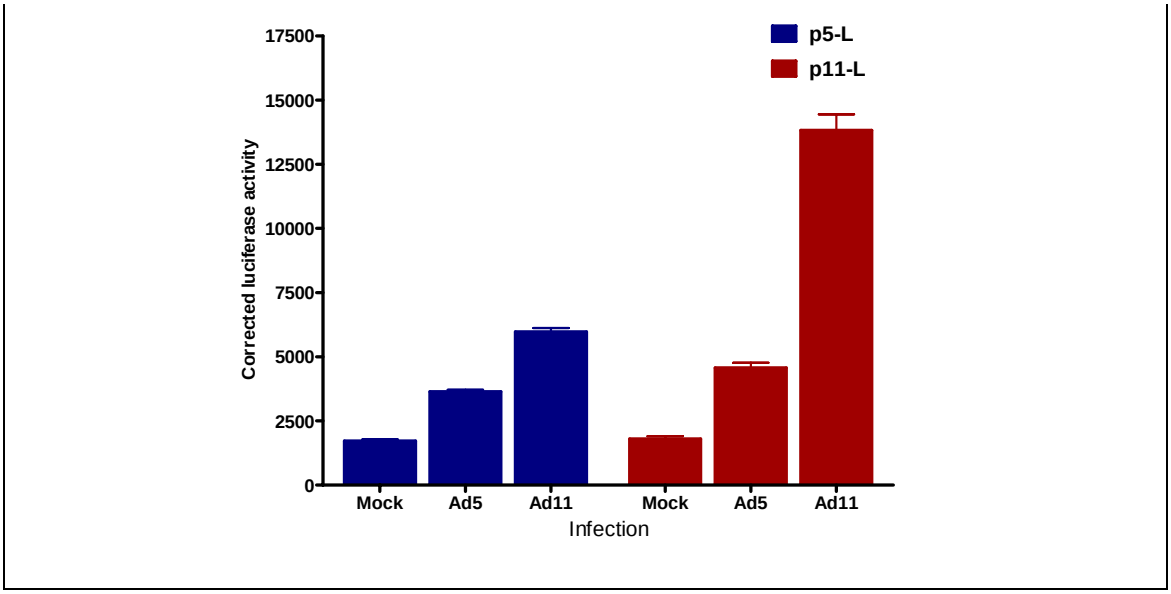


**Figure 6.8: Luciferase reporter assays of *E1A* upstream regions in (a) PANC-1 and (b) PaTu 8988s with or without infection.** Experiments and analyses were performed as described in **Figures 6.6 and 6.7**. Results represent means of triplicate experiments ± SEM.

## 6.3 Summary of Chapter 6

A transcriptional enhancer of *E1A* is known to be located between 194 and 358 bp of the Ad5 genome[55, 56]. The transcription factor EF-1A binds to this enhancer and further upstream regions[54]. In contrast to Ad5, the *E1A* enhancer region of Ad11 does not contain binding sites for EF-1A. Cellular EF-1A expression alone, however, could not completely explain the variation in *E1A* mRNA levels seen. As shown in **Figure 6.1**, the absence of EF-1A in the Ad11-sensitive Capan-2 could explain this cell's preference to transcribe Ad11 *E1A* to Ad5's. This was not shown in the Ad11-sensitive PC-3, where EF-1A expression was similar to those of the Ad5-sensitive MIA PaCa-2 and LNCaP.

The transcription-enhancing activities of regions upstream of *E1A* were examined by the inserting these sequences into pGL3 (**Figure 6.2**) and measuring the firefly luciferase activity of transfected cells. As expected, Ad5 *E1A* upstream regions have higher transcription-enhancing activities than Ad11's in the Ad5-sensitive cell lines (**Figures 6.6a, 6.7a and 6.8a**). Surprisingly except for PaTu 8988s (**Figure 6.8b**), the regions upstream of Ad5 *E1A* appear to have higher activities than that of Ad11 even in cells that showed higher levels of Ad11 *E1A* mRNA (i.e. Capan-2 and PC-3) (**Figures 6.6b**). After Ad11 infection in Capan-2, the activity of Ad11 *E1A* upstream region became similar or possibly higher than that of Ad5 after Ad5 infection, although this was not the case for PC-3 (**Figure 6.7b**). Perhaps the Ad5 *E1A* regulatory region was indeed more active than that of Ad11 in PC-3, but there was a difference in *E1A* mRNA stability and its rate of degradation. Nonetheless, as discussed in more detail in Chapter 9, this luciferase reporter assay has its limitations as it is only a surrogate measure of activities of the *E1A* regulatory regions. It is known that the E1A proteins can enhance or repress their own expression in a time-dependent manner[216]. Moreover, region within the E1A protein-coding sequence also has a regulatory role[217]. These complex and interacting factors make the luciferase reporter results difficult to interpret.

# CHAPTER 7

# Production of recombinant Ad11 with Ad5 *E1A* enhancer and/or promoter

As shown in Chapter 5, the levels of *E1A* mRNA appear to determine the replicative ability and potency of Ad11 in cancer cell lines. This is particular important in cells insensitive to Ad11-mediated cytotoxicity where despite its high infectivity, the levels of Ad11 *E1A* mRNA were significantly lower than that of Ad5. As such, it was hypothesised that Ad11's oncolytic potency in the insensitive cancer cells could be improved by increasing *E1A* transcription. Because the region upstream of Ad5 *E1A* has higher transcription-enhancing activity (see Chapter 6), this region was used in place of Ad11's to drive the expression of *E1A.* This chapter describes the construction of two Ad11 mutants – Ad11-Ad5-P has the Ad11 *E1A* promoter replaced by that of Ad5, whilst Ad11-Ad5-EP has the whole Ad5 *E1A* enhancer and promoter substituting the corresponding region of Ad11 (**Figure 7.1**).

## 7.1 Shuttle plasmid construction and homologous recombination

As described earlier, the Ad5 *E1A* transcriptional enhancer region is located between 194 and 358 bp of the Ad5 genome[55, 56]. However, the adenoviral packaging sequence, needed to direct the encapsidation of the viral DNA, also lies within this region (240-377 bp in Ad5 and 249-392 bp in Ad11, respectively)[57, 58, 169, 170]. As a small number of mutations in part of this region could dramatically reduce the packaging efficiency, it is probable that this domain is not compatible across the two species[58]. For this reason, the virus Ad11-Ad5-P was designed to have only the region downstream of the packaging signal up to the *E1A*-coding sequence replaced by the corresponding region from Ad5 (**Figure 7.1a**). The region from 195 bp up to the *E1A*-coding sequence (559 bp) of Ad5 was used to replace the corresponding region in Ad11 to produce Ad11-Ad5-EP. (**Figure 7.1b**)

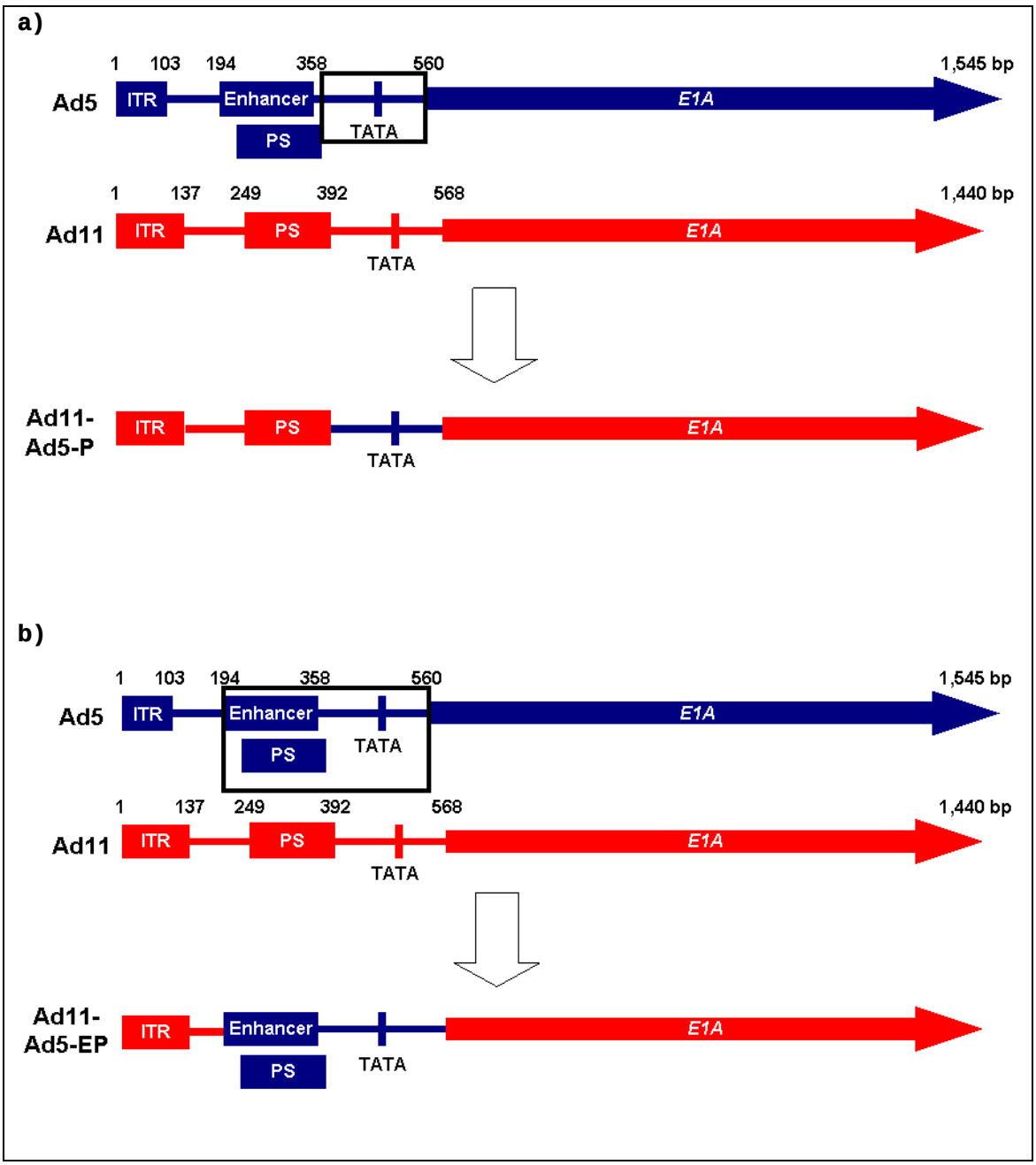


**Figure 7.1: Construction of recombinant Ad11 with Ad5 *E1A* enhancer and/or promoter.** (**a**) The region between Ad11 packaging signal (PS) and the start of *E1A*-coding sequence (393-567 bp) was replaced by the corresponding region of Ad5 (378-559 bp) to generate Ad11-Ad5-P. (**b**) The Ad5 *E1A* enhancer region up to the start of *E1A*-coding sequence (195-559 bp) was used to replace the corresponding region in Ad11 (196-567 bp) to produce Ad11-Ad5-EP.

### 7.1.1 Cloning of fragments and ligation to pUC18

The primers described in 2.13.1 were used to amplify different fragments from the wild-type Ad11 plasmid (pBGwtAd11) and Ad5 DNA (**Figure 7.2**).

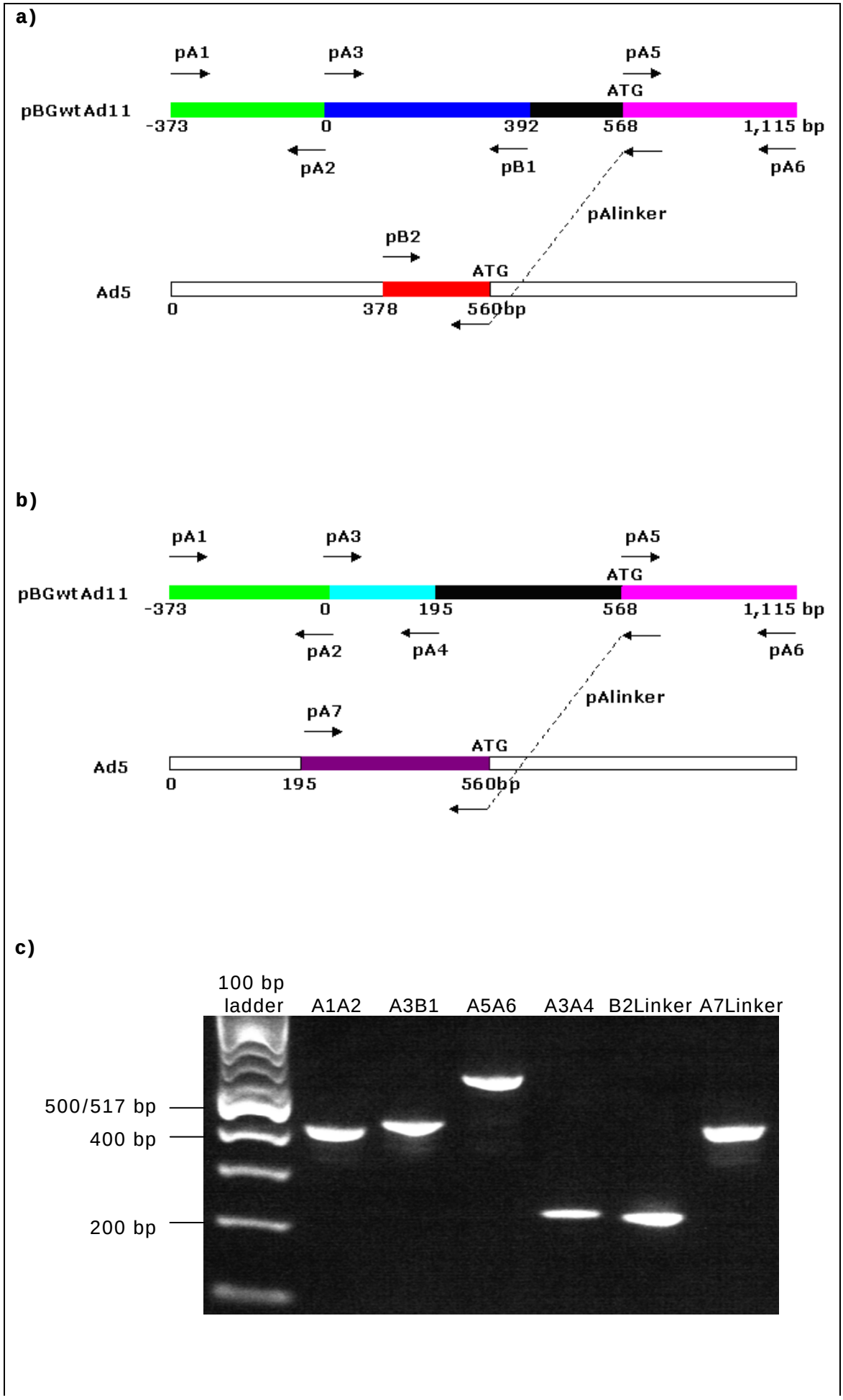
a)
pA1
pA3
pA5
ATG
pBGwtAd11
-373
0
392
568
1,115 bp
pA2
pB1
pA6
pAlinker
pB2
ATG
Ad5
0
378
560bp
b)
pA1
pA3
pA5
ATG
pBGwtAd11
-373
0
195
568
1,115 bp
pA2
pA4
pA6
pAlinker
pA7
ATG
Ad5
0
195
560bp
c)
100 bp ladder
A1A2
A3B1
A5A6
A3A4
B2Linker
A7Linker
500/517 bp
400 bp
200 bp

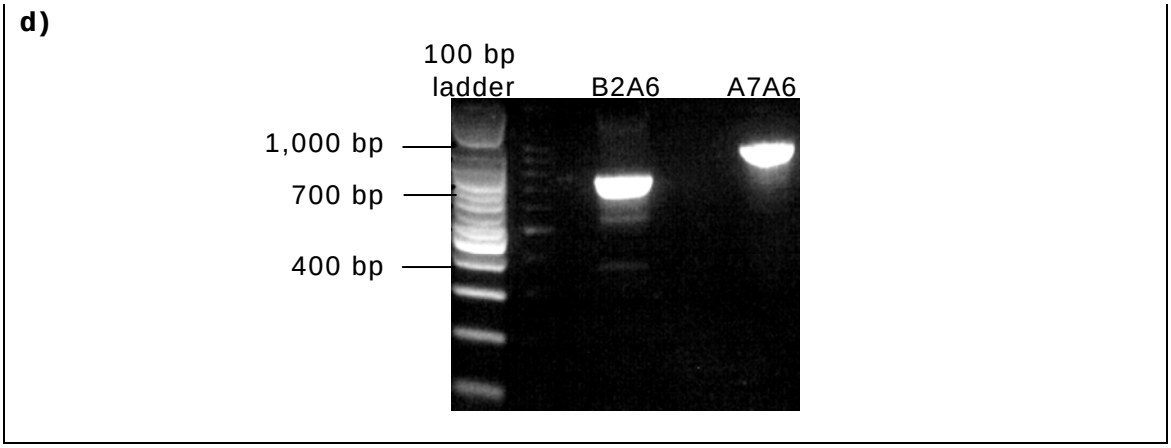


**Figure 7.2: Cloning of fragments for recombinant Ad11 construction.** Fragments needed for the construction of (**a**) Ad11-Ad5-P and (**b**) Ad11-Ad5-EP were amplified by PCR from pBGwtAd11 and Ad5 DNA. '0' represents the start of the adenoviral genome and ATG is the start of the *E1A*-coding sequence. The primers pA1-7 and pB1-2 and their directions are shown. The primer pAlinker has half of its sequence complementary to the 21 bp immediately before Ad5 *E1A*, and the other half to the 22 bp of Ad11 *E1A*. (**c**) Agarose gel electrophoresis showing the correct fragment sizes: A1A2 (405 bp), A3B1 (423 bp), A5A6 (566 bp), A3A4 (226 bp), B2Linker (219 bp) and A7Linker (402 bp). A1A2 and A3B1, and A1A2 and A3A4 were obtained separately (instead of using pA1 and pB1, and pA1 and pA4, respectively) in order to introduce a NotI restriction site. B2Linker and A7Linker contain the Ad5 *E1A* promoter and enhancer-promoter, respectively. (**d**) To join B2Linker and A7Linker to the left end of Ad11 *E1A*-coding sequence (A5A6), they were each placed in a PCR reaction with A5A6 only. The resultant mixtures were further amplified using pB2 or pA7 with pA6, to generate B2A6 (759 bp) and A7A6 (943 bp).

All fragments were extracted and subsequently digested as follows: A1A2 (HindIII and XbaI), A3B1, A3A4, B2A6 and A7A6 (HindIII and BamHI). These were ligated to HindIII and XbaI- and HindIII and BamHI-digested pUC18, respectively, to produce pUCA1A2, pUCA3B1, pUCA3A4, pUCB2A6 and pUCA7A6. These were used to transform chemically competent *E. coli* and verified by PCR (**Figure 7.3**). The correct plasmids were confirmed by sequencing using M13 forward and reverse primers (performed by the Genome Centre; results not shown).

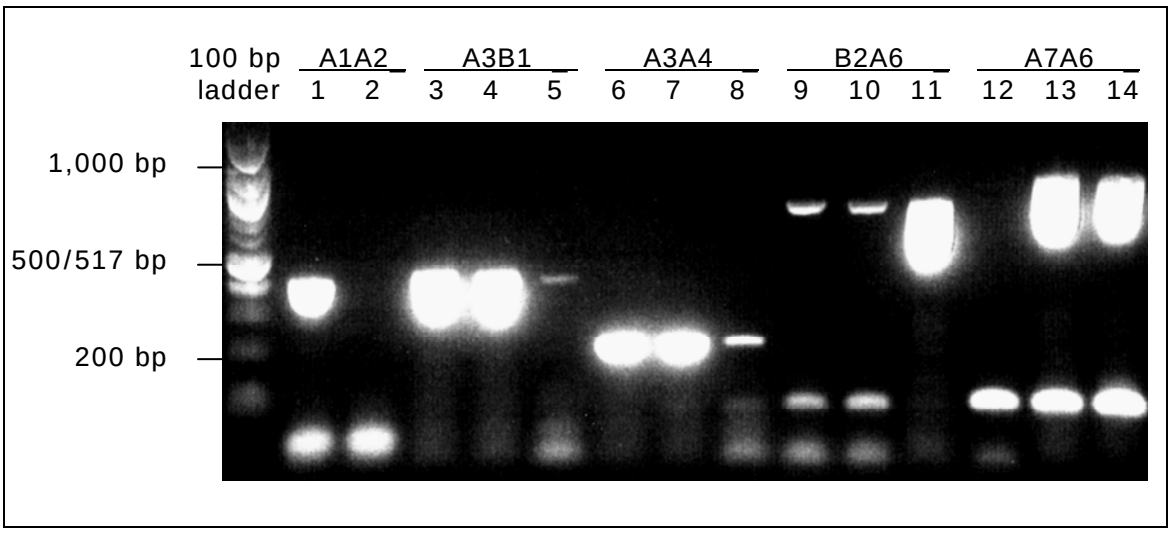


**Figure 7.3: Confirmation of successful ligation of adenoviral DNA fragments to pUC18.** Colonies of transformed chemically competent *E. coli* were picked and PCR was performed using the corresponding primer pairs for each fragment. The correct sizes are: 405 bp (A1A2), 423 bp (A3B1), 226 bp (A3A4), 759 bp (B2A6) and 943 bp (A7A6). Cultures of clones shown in lanes 1, 3, 6, 11 and 13 were selected. The plasmids were extracted and sent for sequencing.

### 7.1.2 Shuttle vector production using pSS

pUCA1A2 was digested with NotI and BamHI. A1A2 was then joined with the fragments A3B1 and A3A4 (released from pUCA3B1 and pUCA3A4 by NotI and BamHI digestion), producing the plasmids pUCA1B1 and pUCA1A4 (**Figure 7.4**). This produced the 'left arms' for subsequent homologous recombination, containing the regions -373-392 bp (A1B1) and -373-195 bp (A1A4) of pBGwtAd11, with a NotI site introduced at position '0' (**Figures 7.2a and b**).

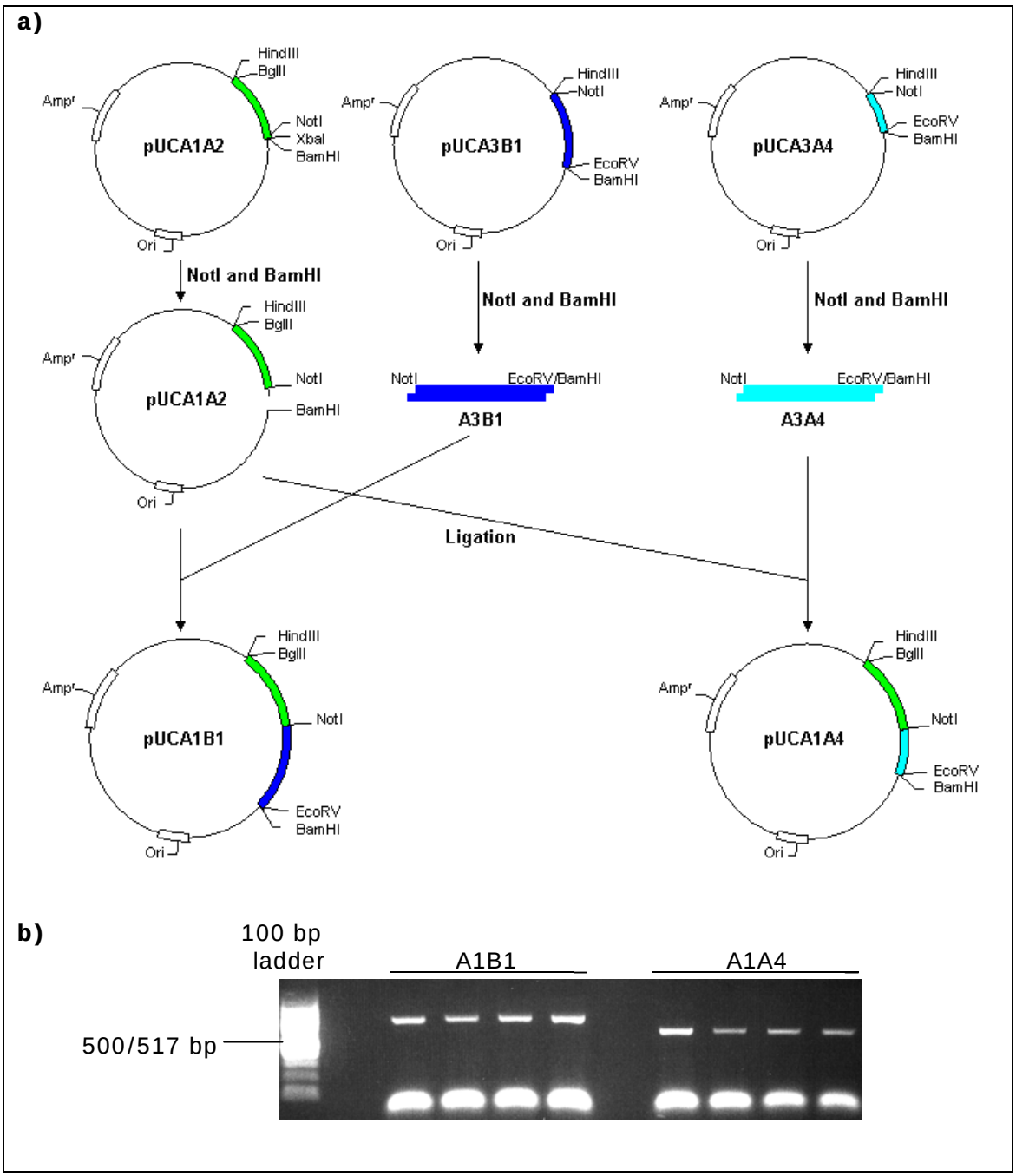


**Figure 7.4: Ligation of A3B1 and A3A4 to pUCA1A2.** (**a**) pUCA1A2, pUCA3B1 and pUCA3A4 were digested with NotI and BamHI. Ligation produced the plasmids pUCA1B1 and pUCA1A4. A NotI site was introduced at the start of the Ad11 genomic sequence. (**b**) After transformation of competent *E. coli*, successful ligation was confirmed by PCR using pA1, pB1 and pA4 primers. All colonies showed the correct inserts: 802 (A1B1) and 605 bp (A1A4).

A1B1 and A1A4 were inserted into linearised pSS (1,904 bp in size) after digestion with BglII and EcoRV, producing pSSA1B1 and pSSA1A4, respectively (**Figure 7.5**).

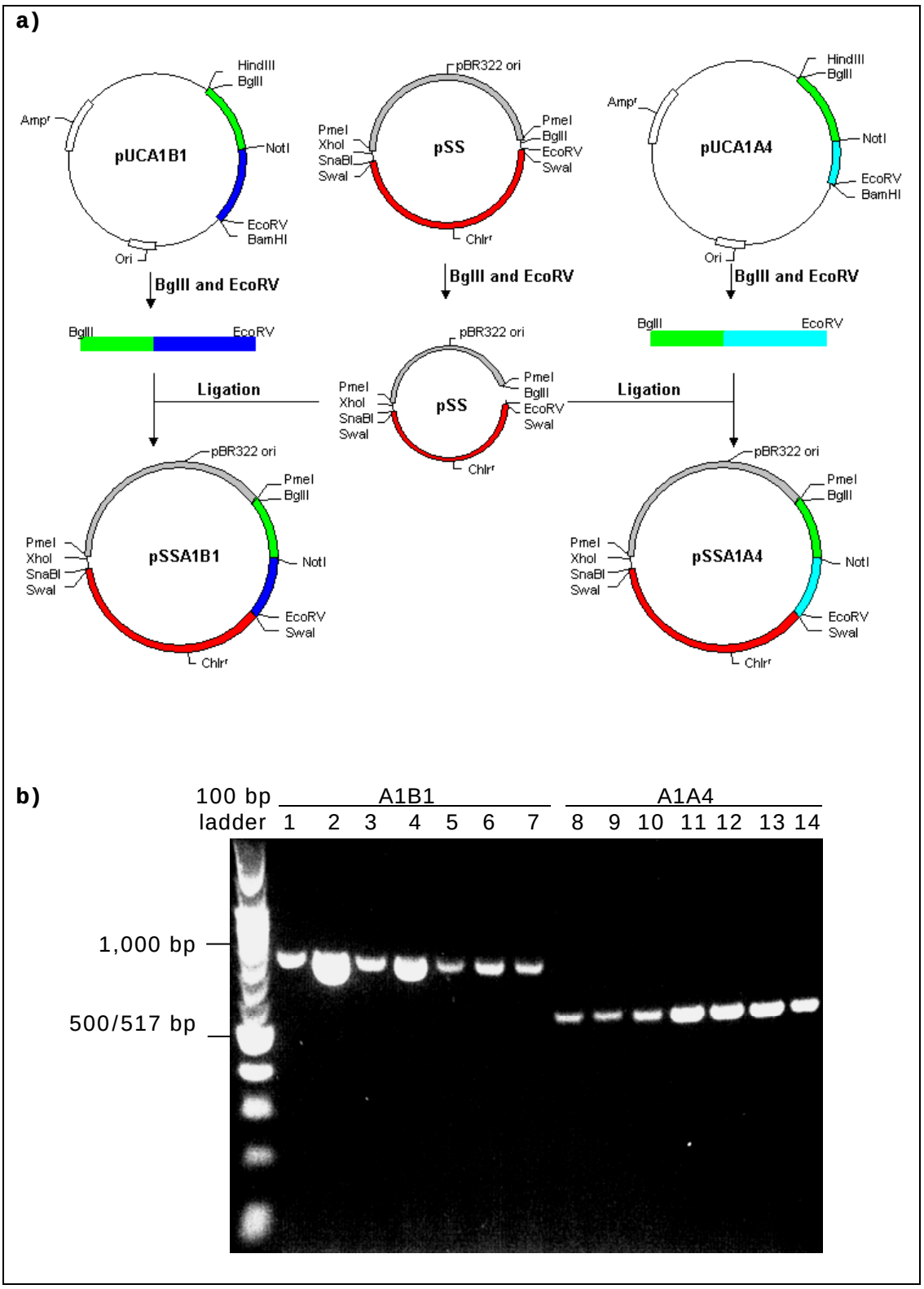


**Figure 7.5: Ligation of A1B1 and A1A4 to pSS.** (**a**) pSS, pUCA1B1 and pUCA1A4 were digested with BglII and EcoRV. Ligation produced the plasmids pSSA1B1 and pSSA1A4. (**b**) After transformation of competent *E. coli*, successful ligation was confirmed by PCR using pA1, pB1 and pA4 primers. All colonies showed the correct inserts: 802 (A1B1) and 605 bp (A1A4). Abbreviation: chlr$^r$, chloramphenicol resistance.

To join the "right arm" and "left arm" to the pSS shuttle vector, B2A6 (from pUCB2A6) was inserted into pSSA1B1 after digestion with SnaBI and XhoI. This produced the shuttle plasmid pSSA1B1B2A6 (for Ad11-Ad5-P), with the chloramphenicol resistance gene separating the two arms (**Figure 7.6**). Confirmation of successful ligation was performed by restriction digestions using SnaBI and XhoI (to release B2A6) and BglII and EcoRV (to release A1B1). Similarly, pSSA1A4A7A6 (for Ad11-Ad5-EP) was produced from pSSA1A4 and pUCA7A6 (**Figure 7.7**).

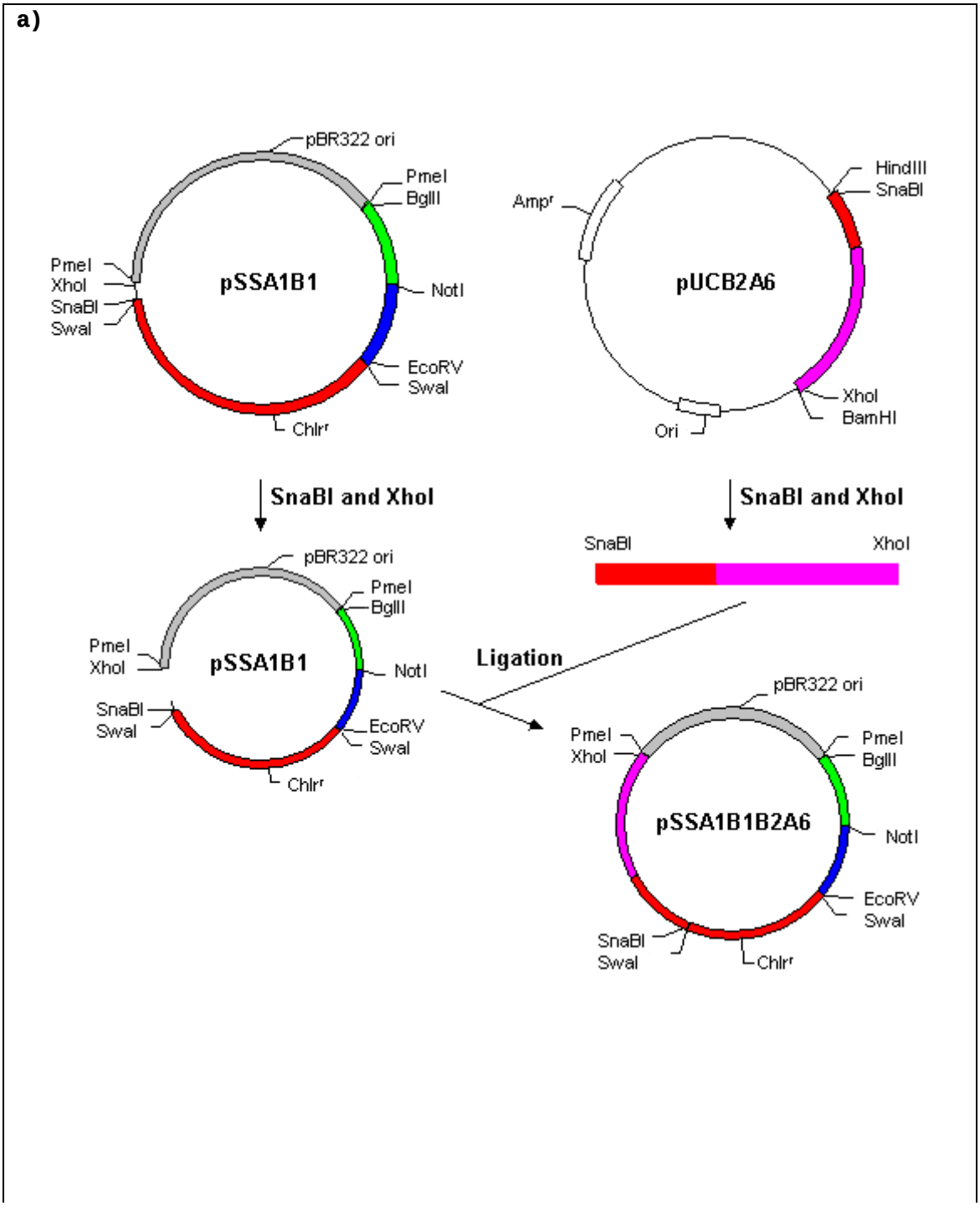

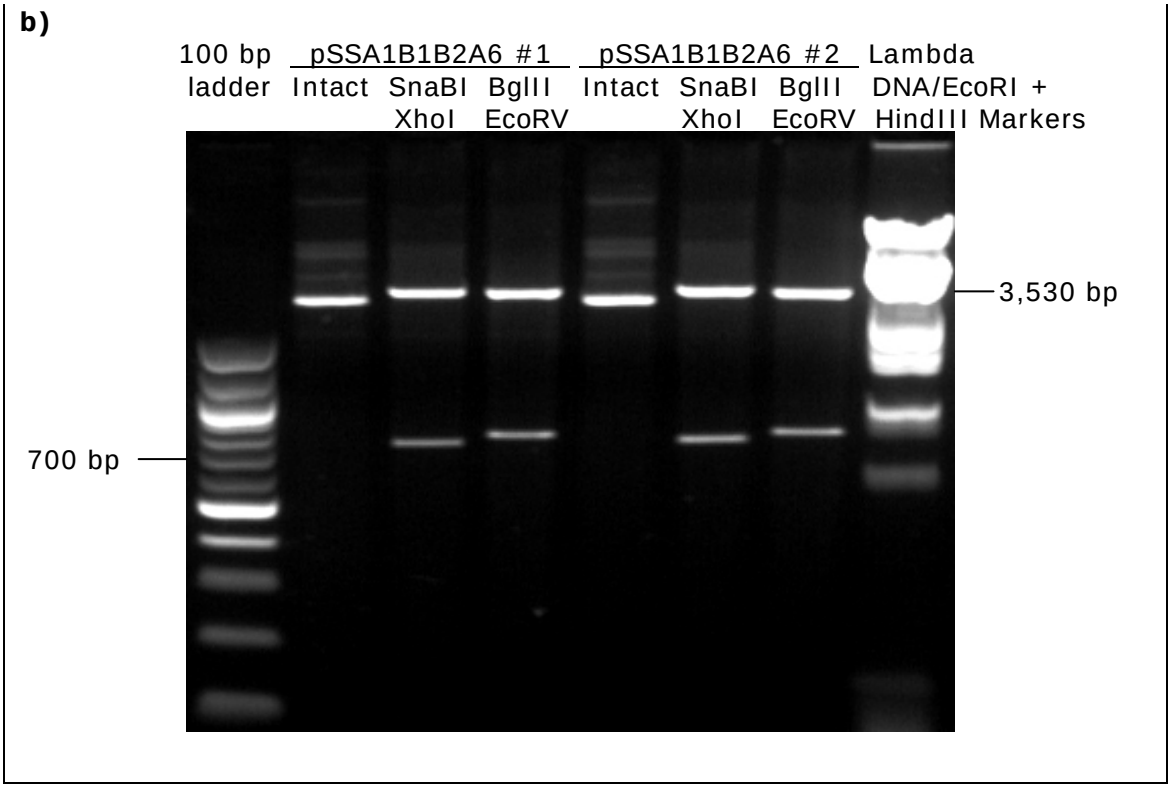


**Figure 7.6: Ligation of B2A6 to pSSA1B1.** (**a**) pSSA1B1 and pUCB2A6 were digested with SnaBI and XhoI. Ligation produced the plasmid pSSA1B1B2A6. (**b**) After transformation of competent *E. coli*, two colonies were expanded and the plasmids were extracted. These were run on an agarose gel either intact (3,375 bp), digested with SnaBI and XhoI (742 bp of B2A6), or with BglII and EcoRV (784 bp of A1B1). Both colonies showed the correct inserts.

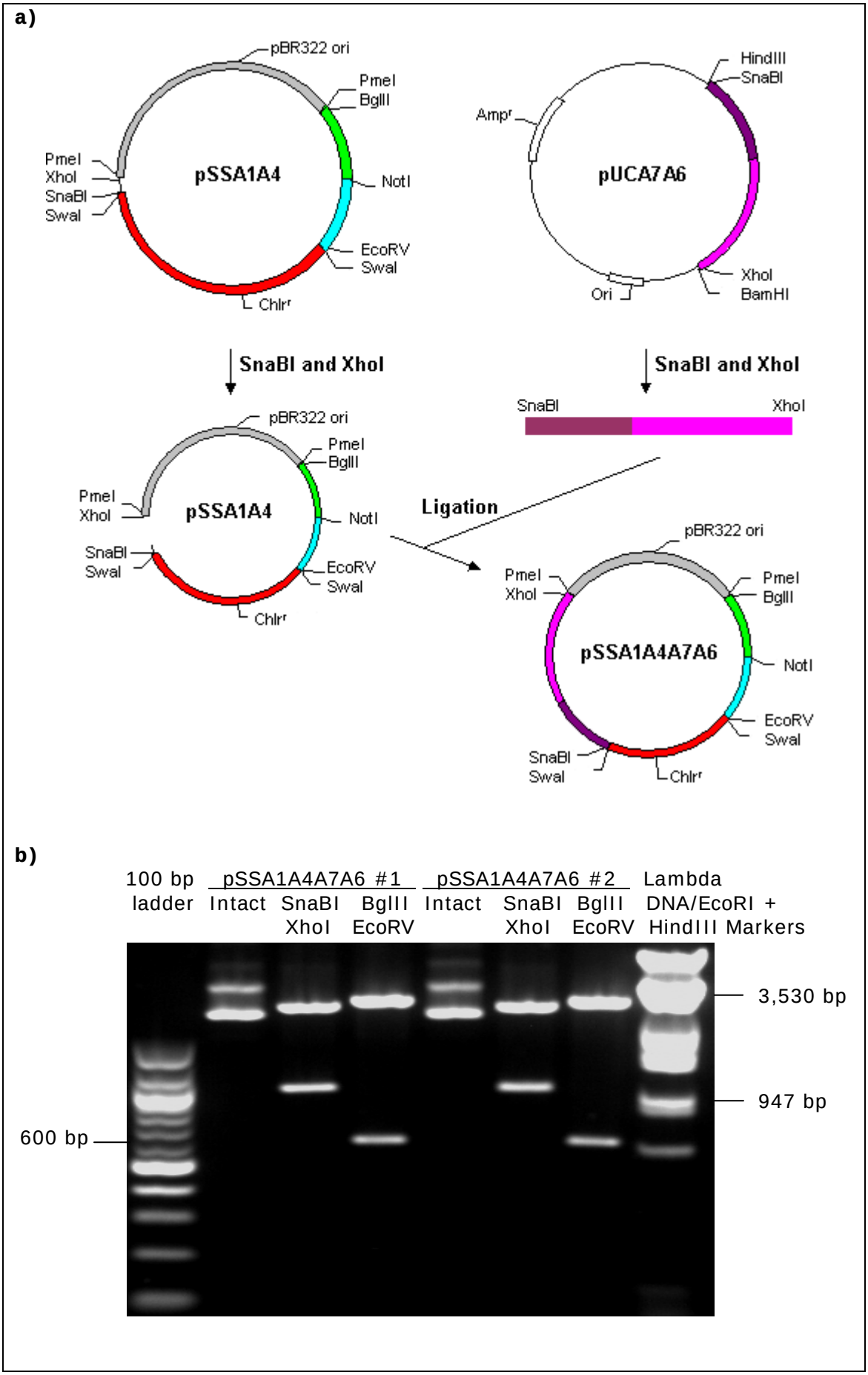
a)
pBR322 ori
PmeI
BglII
NotI
EcoRV
SwaI
ChlR
PmeI
XhoI
SnaBI
SwaI
pSSA1A4
HindIII
SnaBI
Ampr
pUCA7A6
Ori
XhoI
BamHI
SnaBI and XhoI
SnaBI and XhoI
SnaBI
XhoI
Ligation
pSSA1A4
pSSA1A4A7A6
b)
100 bp ladder
pSSA1A4A7A6 #1
Intact
SnaBI XhoI
BglII EcoRV
pSSA1A4A7A6 #2
Intact
SnaBI XhoI
BglII EcoRV
Lambda DNA/EcoRI + HindIII Markers
3,530 bp
947 bp
600 bp

**Figure 7.7: Ligation of A7A6 to pSSA1A4.** (**a**) pSSA1A4 and pUCA7A6 were digested with SnaBI and XhoI. Ligation produced the plasmid pSSA1A4A7A6. (**b**) After transformation of competent *E. coli*, two colonies were expanded and the plasmids were extracted. These were run on an agarose gel either intact (3,361 bp), digested with SnaBI and XhoI (925 bp of A7A6), or with BglII and EcoRV (587 bp of A1A4). Both colonies showed the correct inserts.

### 7.1.3 Homologous recombination in BJ5183 cells

pSSA1B1B2A6 was digested with PmeI before transforming the electroporation competent BJ5183 *E. coli*, together with the wild-type Ad11 plasmid pBGwtAd11. BJ5183 contains the enzyme recombinase A (RecA) needed for homologous recombination, *i.e.* the pairing between a DNA molecule (pSSA1B1B2A6) and a homologous sequence in another DNA molecule (pBGwtAd11). As such the region between the 'left' and 'right' arms from pSSA1B1B2A6 (containing the chloramphenicol resistance gene and Ad5 *E1A* promoter) would replace the corresponding region in pBGwtAd11 (**Figure 7.8**). Transformed cells were selected by ampicillin (from pBGwtAd11) and chloramphenicol resistance and checked by PCR (**Figure 7.8b**). Plasmid was extracted from the correct BJ5183 culture and used to transform One Shot TOP10 electrocompetent *E. coli* before further expansion as undesirable recombination might occur if left a long time in BJ5183. Subsequent confirmation was done by restriction digestions (**Figure 7.8c**).

Homologous recombination of pSSA1A4A7A6 (containing the Ad5 *E1A* enhancer-promoter) with pBGwtAd11 was done in the same way (**Figure 7.9**).

**a)**

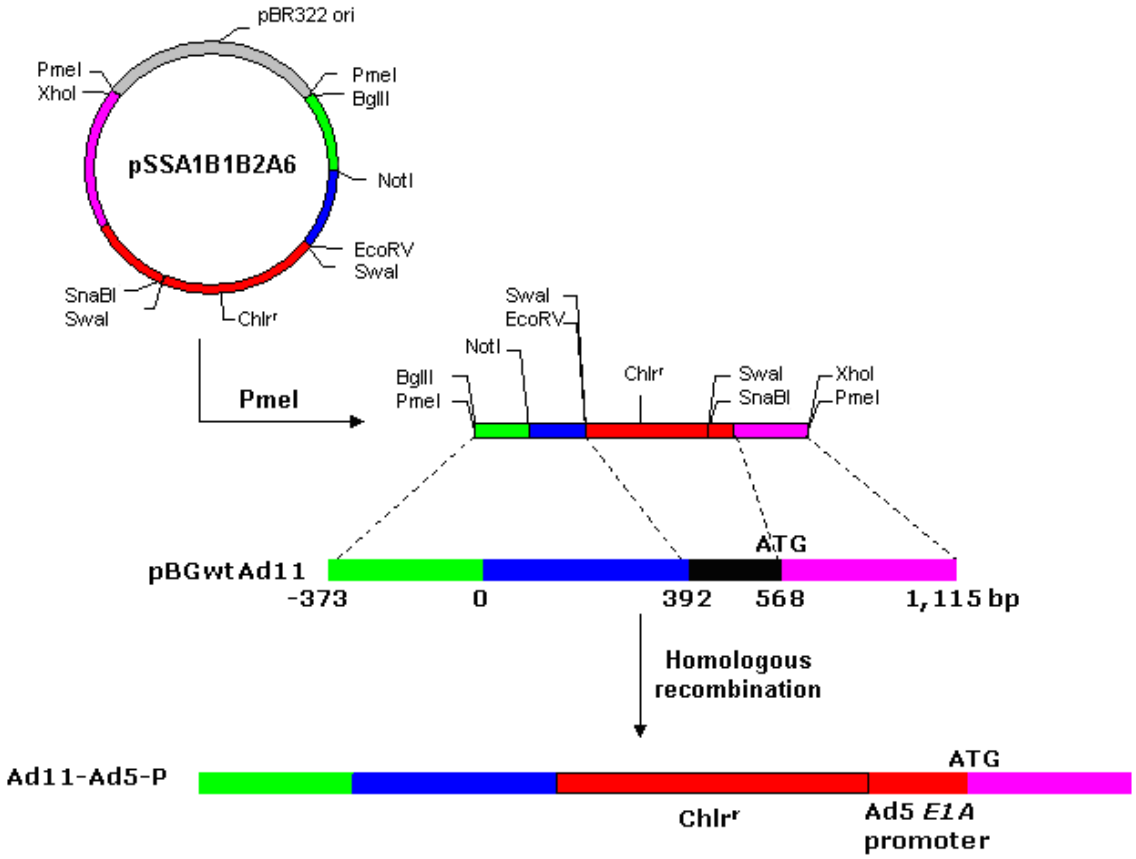
pBR322 ori
PmeI
XhoI
PmeI
BglII
pSSA1B1B2A6
NotI
EcoRV
SwaI
SnaBI
SwaI
Chlr
PmeI
SwaI
EcoRV
NotI
BglII
PmeI
Chlr
SwaI
SnaBI
XhoI
PmeI
ATG
pBGwtAd11
-373
0
392
568
1,115 bp
Homologous recombination
ATG
Ad11-Ad5-P
Chlr
Ad5 E1A promoter

**b)**

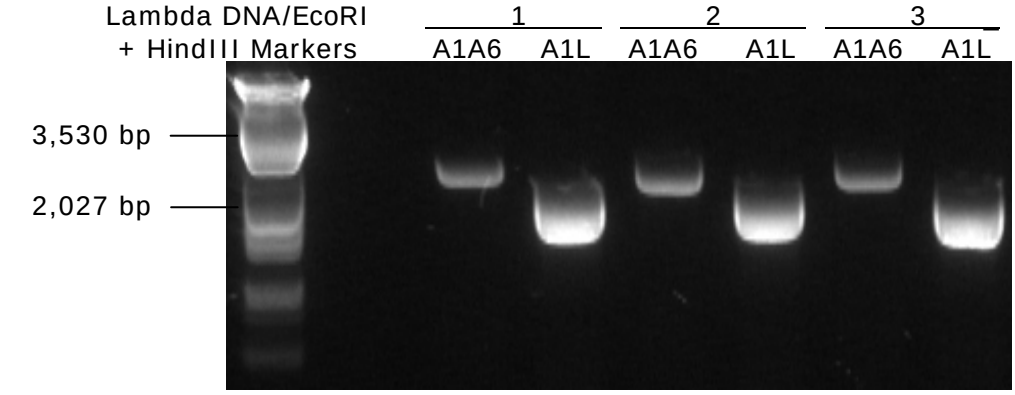
Lambda DNA/EcoRI + HindIII Markers
1
2
3
A1A6
A1L
A1A6
A1L
A1A6
A1L
3,530 bp
2,027 bp

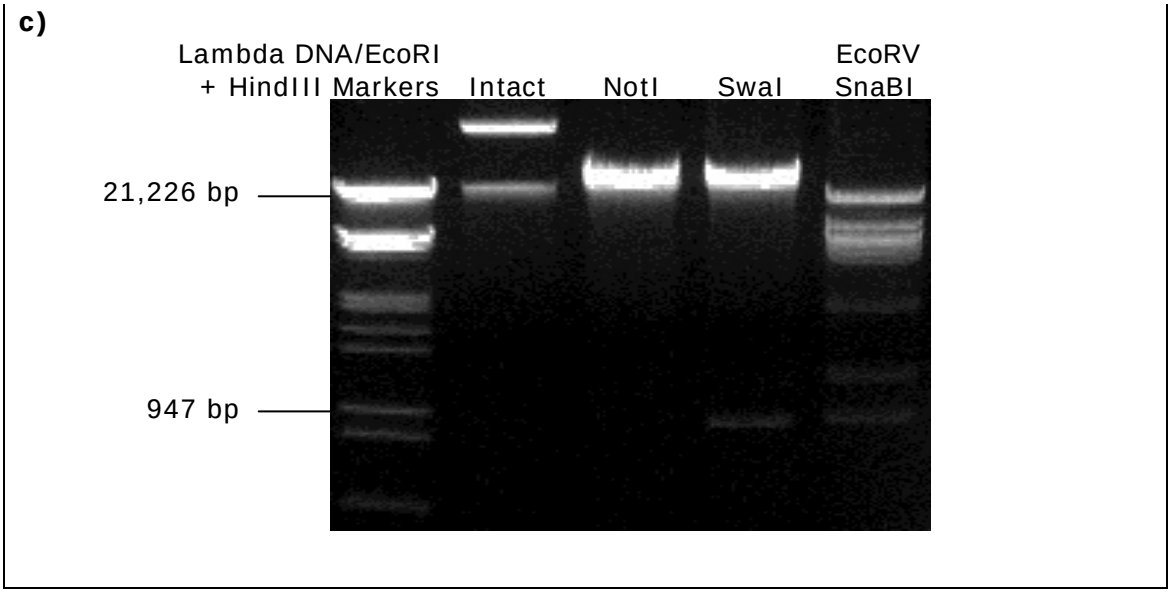


**Figure 7.8: Homologous recombination of pSSA1B1B2A6 with pBGwtAd11.** (**a**) pSSA1B1B2A6 was digested with PmeI and underwent homologous recombination in BJ5183 *E. coli* with pBGwtAd11 at -373-392 and 568-1,115 bp. The region between 392 and 568 bp was replaced by the chlr$^r$ gene and Ad5 *E1A* promoter. Transformed cells were selected by ampicillin (from pBGwtAd11) and chloramphenicol. (**b**) Confirmation of successful recombination by PCR using the primer pairs pA1 and pA6 (A1A6 – 2,462 bp) and pA1 and pAlinker (A1L – 1,922 bp). All three colonies showed the correct bands. (**c**) Further confirmation of selected culture by digestions with NotI (linearised plasmid), SwaI, and EcoRV and SnaBI (releasing the 919 bp chlr$^r$ gene).

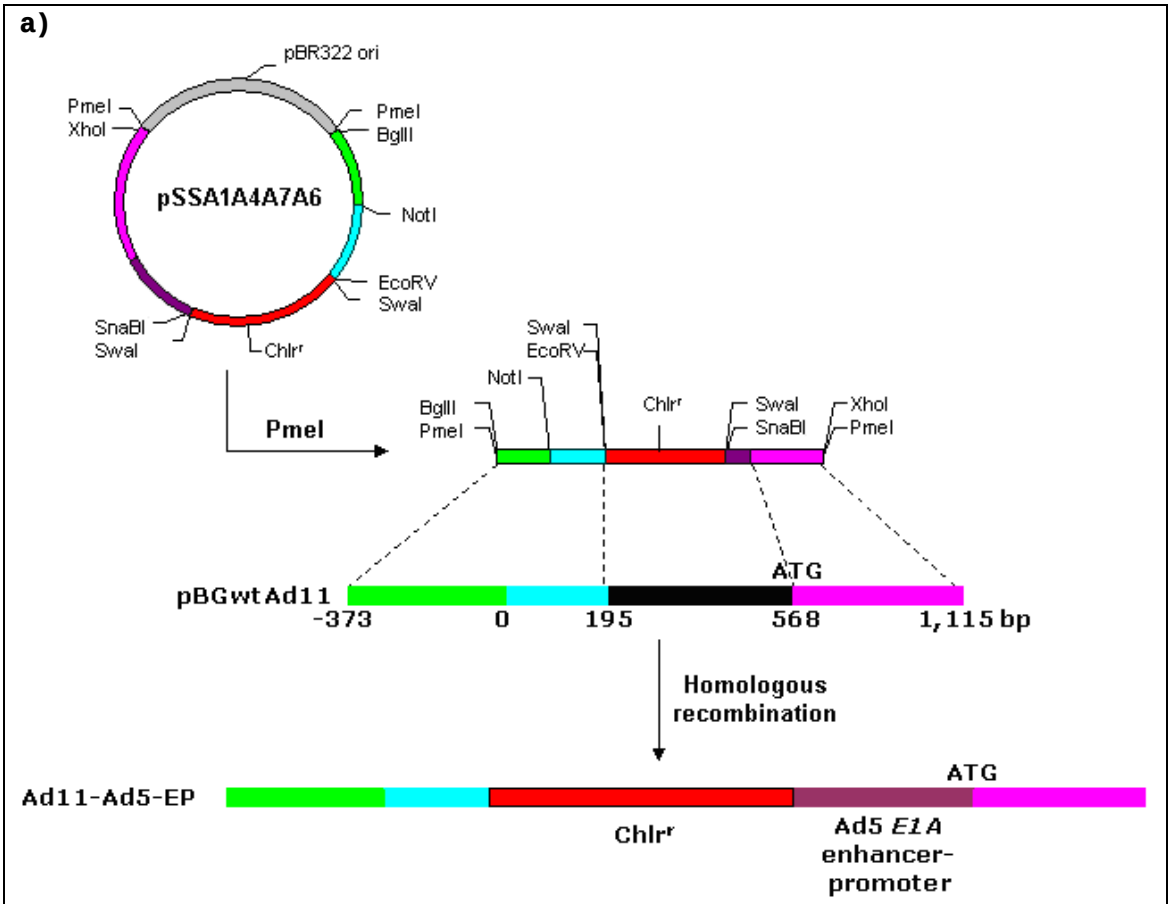
a)
pBR322 ori
PmeI
XhoI
PmeI
BglII
pSSA1A4A7A6
NotI
EcoRV
SwaI
SnaBI
SwaI
Chlr
PmeI
SwaI
EcoRV
NotI
BglII
PmeI
Chlr
SwaI
SnaBI
XhoI
PmeI
ATG
pBGwtAd11
-373
0
195
568
1,115 bp
Homologous recombination
ATG
Ad11-Ad5-EP
Chlr
Ad5 E1A enhancer-promoter

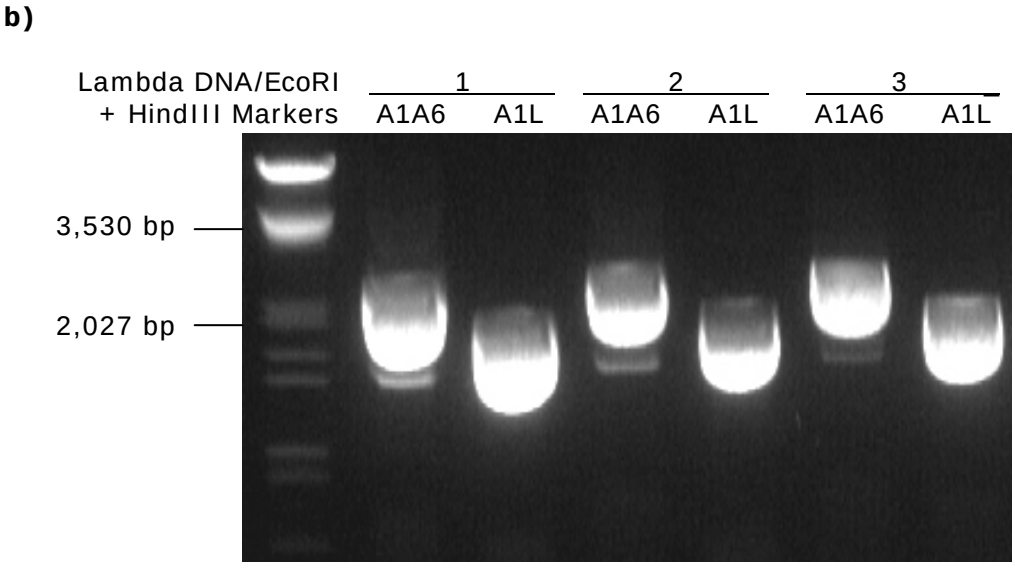
b)
Lambda DNA/EcoRI + HindIII Markers
1
2
3
A1A6
A1L
A1A6
A1L
A1A6
A1L
3,530 bp
2,027 bp

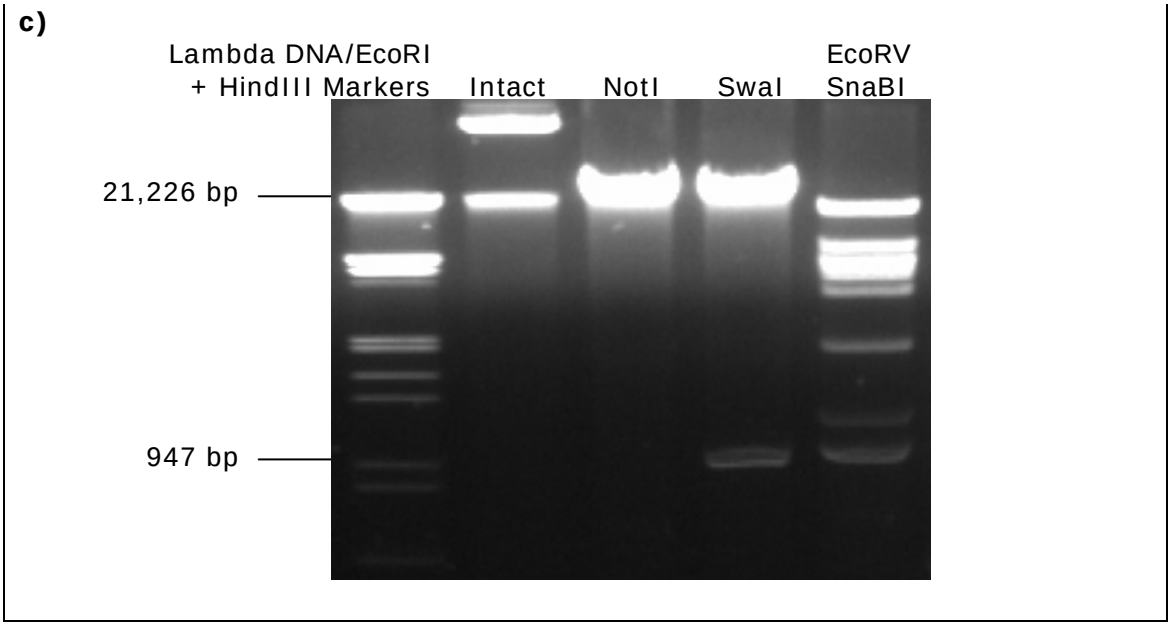


**Figure 7.9: Homologous recombination of pSSA1A4A7A6 with pBGwtAd11.** (**a**) pSSA1A4A7A6 was digested with PmeI and underwent homologous recombination in BJ5183 *E. coli* with pBGwtAd11 at -373-195 and 568-1,115 bp. The region between 195 and 568 bp was replaced by the chlr$^r$ gene and Ad5 *E1A* enhancer-promoter. Transformed cells were selected by ampicillin (from pBGwtAd11) and chloramphenicol. (**b**) Confirmation of successful recombination by PCR using the primer pairs pA1 and pA6 (A1A6 – 2,449 bp) and pA1 and pAlinker (A1L – 1,908 bp). All three colonies showed the correct bands. (**c**) Further confirmation of selected culture by digestions with NotI (linearised plasmid), SwaI, and EcoRV and SnaBI (releasing the 919 bp chlr$^r$ gene).

### 7.1.4 Removal of chloramphenicol resistance gene

The recombinant Ad11 plasmids were digested with SwaI to remove the chloramphenicol resistance genes. The plasmids were religated and used to transform electrocompetent *E. coli*. Correct colonies were identified by PCR and further confirmation of the plasmids was performed by restriction digestions (**Figures 7.10 and 7.11**).

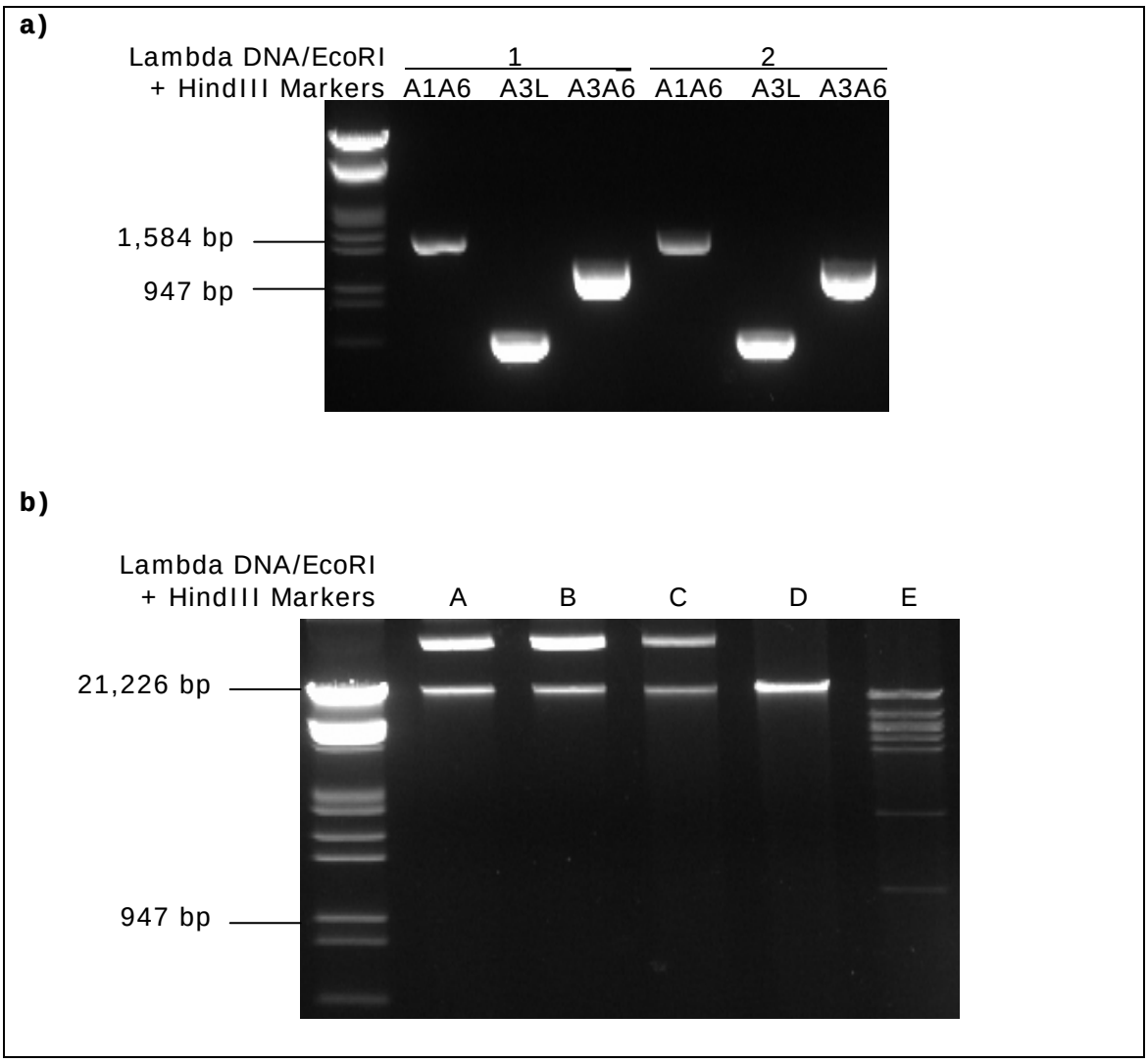


**Figure 7.10: Removal of chloramphenicol resistance gene from pBGwtAd11-Ad5-*E1A*-promoter.** (**a**) After the removal of the chlr$^r$ gene by SwaI digestion, the plasmid was religated and transformed into electrocompetent *E. coli*. Correct colonies were identified using the primer pairs pA1 and pA6 (A1A6 – 1,543 bp), pA3 and pAlinker (A3L – 624 bp), and pA3 and pA6 (A3A6 – 1,164 bp). Both samples showed the correct bands. (**b**) Confirmation of chlr$^r$ gene removal by restriction digestions. Lanes A and B are pBGwtAd11 and pBGwtAd11-Ad5-*E1A*-promoter-chlr$^r$, respectively. pBGwtAd11-Ad5-*E1A*-promoter with the chlr$^r$ gene removed (lane C) was digested with NotI (linearised, lane D), and EcoRV and SnaBI (no 919 bp band of the chlr$^r$ gene seen, lane E).

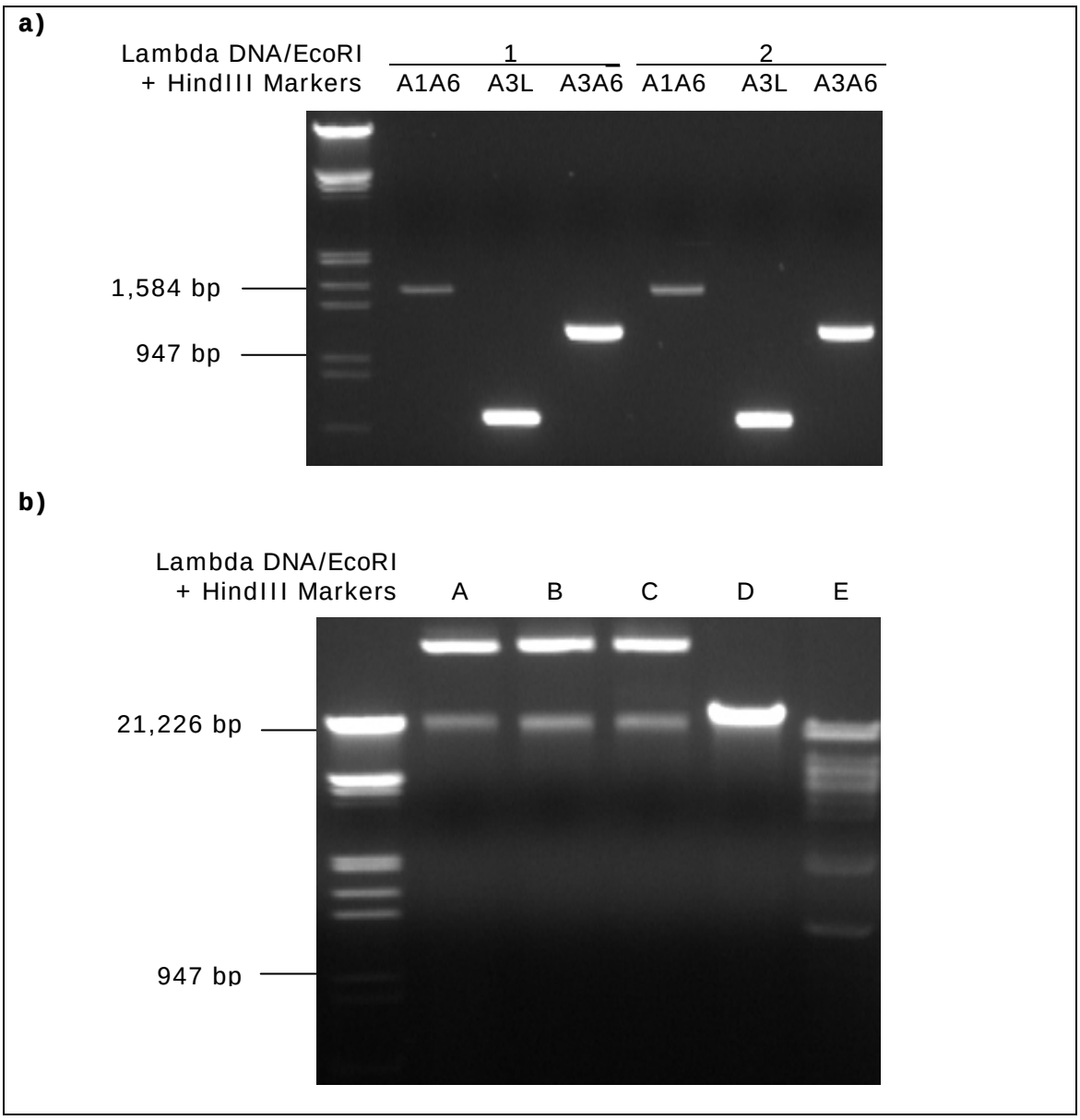


**Figure 7.11: Removal of chloramphenicol resistance gene from pBGwtAd11-Ad5-*E1A*-enhancer-promoter.** (**a**) After the removal of the chlr$^r$ gene by SwaI digestion, the plasmid was religated and transformed into electrocompetent *E. coli*. Correct colonies were identified using the primer pairs pA1 and pA6 (A1A6 – 1,530 bp), pA3 and pAlinker (A3L – 610 bp), and pA3 and pA6 (A3A6 – 1,151 bp). Both samples showed the correct bands. (**b**) Confirmation of chlr$^r$ gene removal by restriction digestions. Lanes A and B are pBGwtAd11 and pBGwtAd11-Ad5-*E1A*-enhancer-promoter-chlr$^r$, respectively. pBGwtAd11-Ad5-*E1A*-enhancer-promoter with the chlr$^r$ gene removed (lane C) was digested with NotI (linearised, lane D), and EcoRV and SnaBI (no 919 bp band of the chlr$^r$ gene seen, lane E).

## 7.2 Virus production after transfection of HEK-293 cells

The above plasmids were linearised by NotI digestion prior to transfection of HEK-293 cells, as described in 2.13.7. The presence of CPE indicated the production of infectious virus particles and this occurred about seven days post-transfection (a negative control was also set up whereby no DNA was added during the transfection process, as sometimes the transfection reagent alone could produce CPE) (**Figure 7.12**). Large scale virus production and determination of concentration are described in 2.13.7 to 2.13.9. Concentrations and titres of Ad11-Ad5-P and Ad11-Ad5-EP are shown in **Table 7.1**.

**a)**

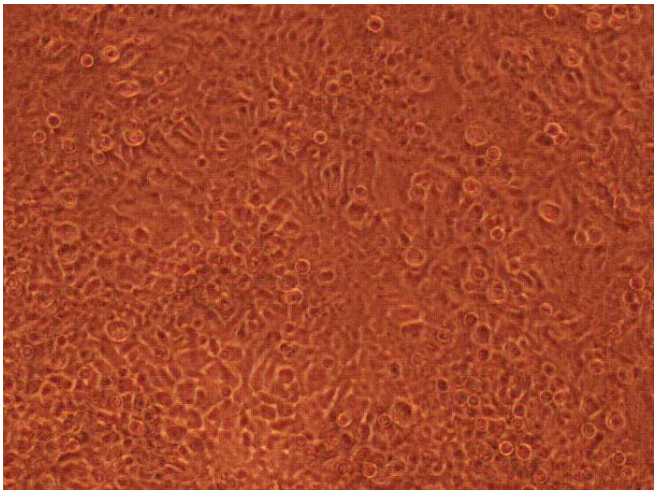

**b)**

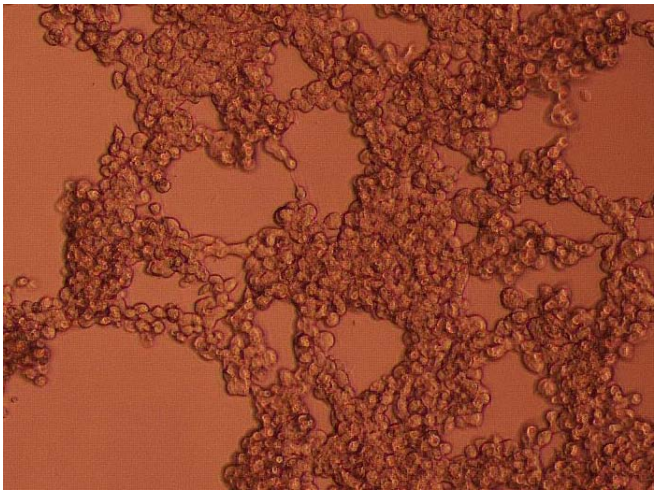

**c)**

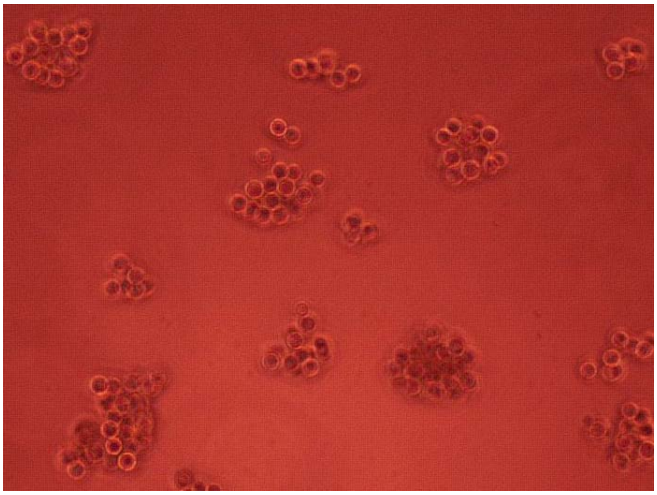

**Figure 7.12: Production of recombinant Ad11 using HEK-293 cells** (40x magnification). (**a**) Normal, confluent HEK-293 after mock transfection. (**b**) to (**c**) Progressive CPEs after transfection with recombinant Ad11 plasmid.

**Table 7.1: Concentrations and titres of Ad11-Ad5-P and Ad11-Ad5-EP**

| Virus | Particles/ml | PFUs/ml | Particles/PFU |
|---|---|---|---|
| Ad11-Ad5-P | $1.01 \times 10^{12}$ | $5.90 \times 10^{9}$ | 171.2 |
| Ad11-Ad5-EP | $2.10 \times 10^{11}$ | $1.30 \times 10^{9}$ | 161.5 |

## 7.3 Sequence confirmation of recombinant Ad11

To confirm that the correct sequence has been inserted into Ad11-Ad5-P, primers were designed to amplify the region from approximately 150 bp upstream of Ad11 *E1A* promoter to the first 150 bp of *E1A* (see 2.13.10). PCR was performed on the DNA of Ad11-Ad5-P and wild-type Ad11 (control) (**Figure 7.13**). The fragments were sent to the Genome Centre for sequencing using the forward primer. Result for the Ad11-Ad5-P fragment is shown in **Figure 7.14**.

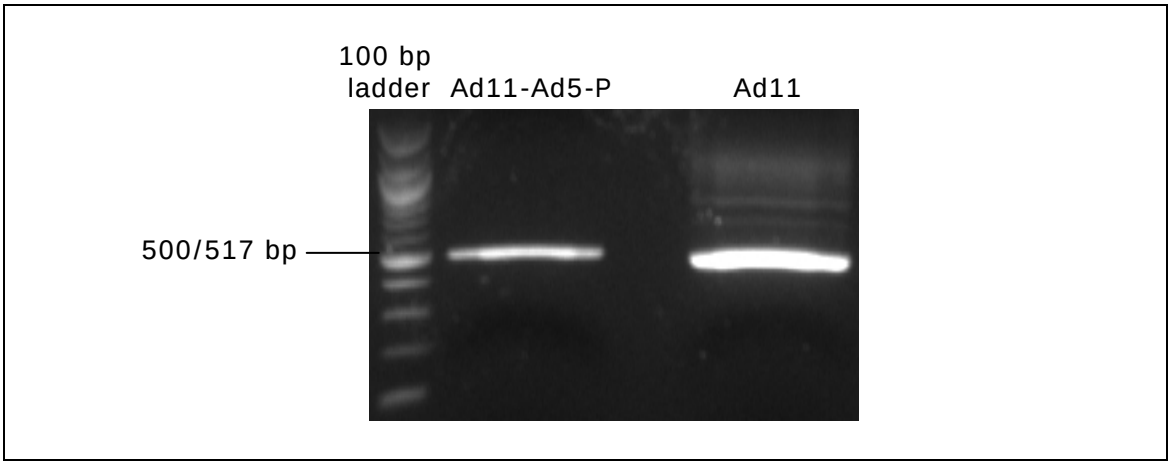


**Figure 7.13: Amplification of Ad11-Ad5-P fragment by PCR for sequencing.** Primers were designed to amplify the region from approximately 150 bp upstream of Ad11 *E1A* promoter to the first 150 bp of *E1A*. Both bands (Ad11-Ad5-P – 494 bp; Ad11 – 475 bp) were extracted and sent for sequencing.

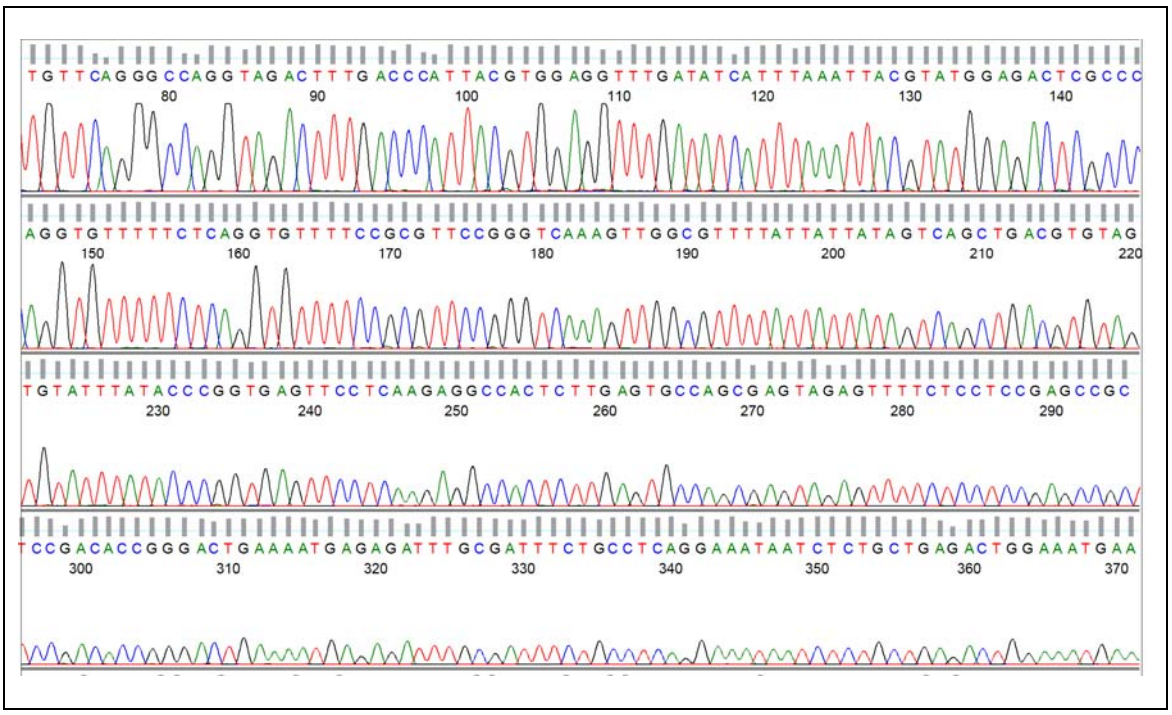


**Figure 7.14: Sequencing result of Ad11-Ad5-P fragment.** Nucleotides < 113 – right part of the first 392 bp of the Ad11 genome (see **Figure 7.2a**); 113-132 – EcoRV, SwaI and SnaBI restriction sites; 133-314 – Ad5 *E1A* promoter; > 314 – start of the Ad11 *E1A*-coding sequence.

As the region upstream of Ad11 *E1A* enhancer is very close to the virus 5'-ITR, primers that bind to this area cannot be used reliably for sequencing. As such primers were designed to amplify the region near the start of the *E1A* enhancer (to avoid the ITR) and the first 58 bp of *E1A* (see 2.13.10). These primers have the restriction sites HindIII and XbaI, respectively, introduced. The amplified fragments of Ad11-Ad5-EP and wild-type Ad11 were digested with HindIII and XbaI and inserted into pUC18. Transformation of chemically competent *E. coli* was done and colonies were identified by PCR using the same primers (**Figure 7.15**). Plasmids were extracted and sent to the Genome Centre for sequencing using M13 forward and reverse primers. Results for the Ad11-Ad5-EP fragment are shown in **Figure 7.16**.

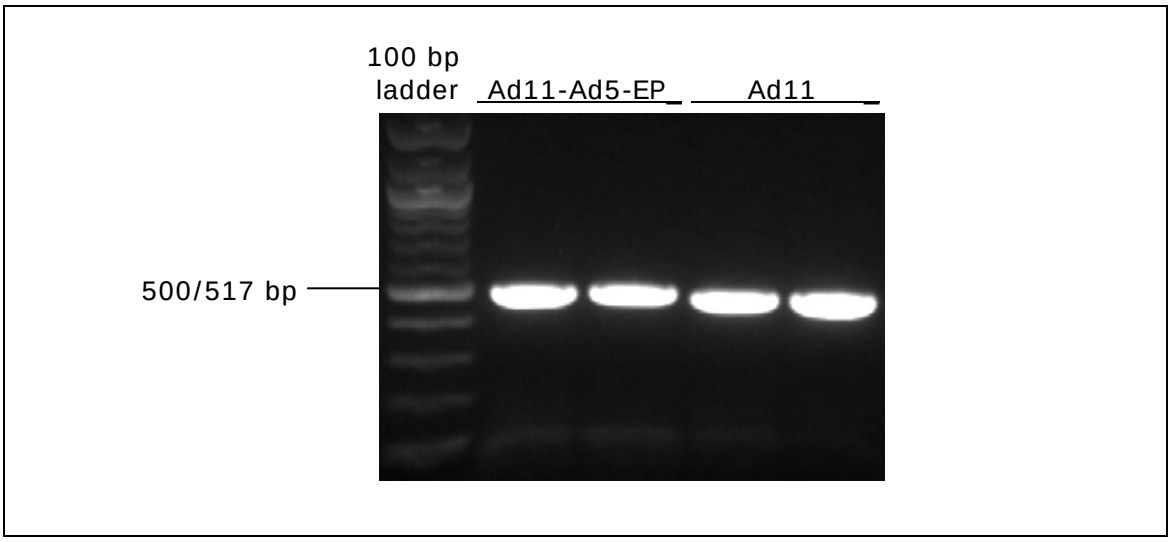


**Figure 7.15: Amplification of Ad11-Ad5-EP fragment by PCR for sequencing.** Primers that amplify the region near the start of the *E1A* enhancer and the first 58 bp of *E1A* were used, with the introduction of HindIII and XbaI restriction sites, respectively. The fragments were ligated to pUC18. After transformation of chemically competent *E. coli*, colonies were identified by PCR using the same primers. Both colonies from each group showed the correct bands (Ad11-Ad5-EP – 490 bp; Ad11 – 485 bp).

**a)**

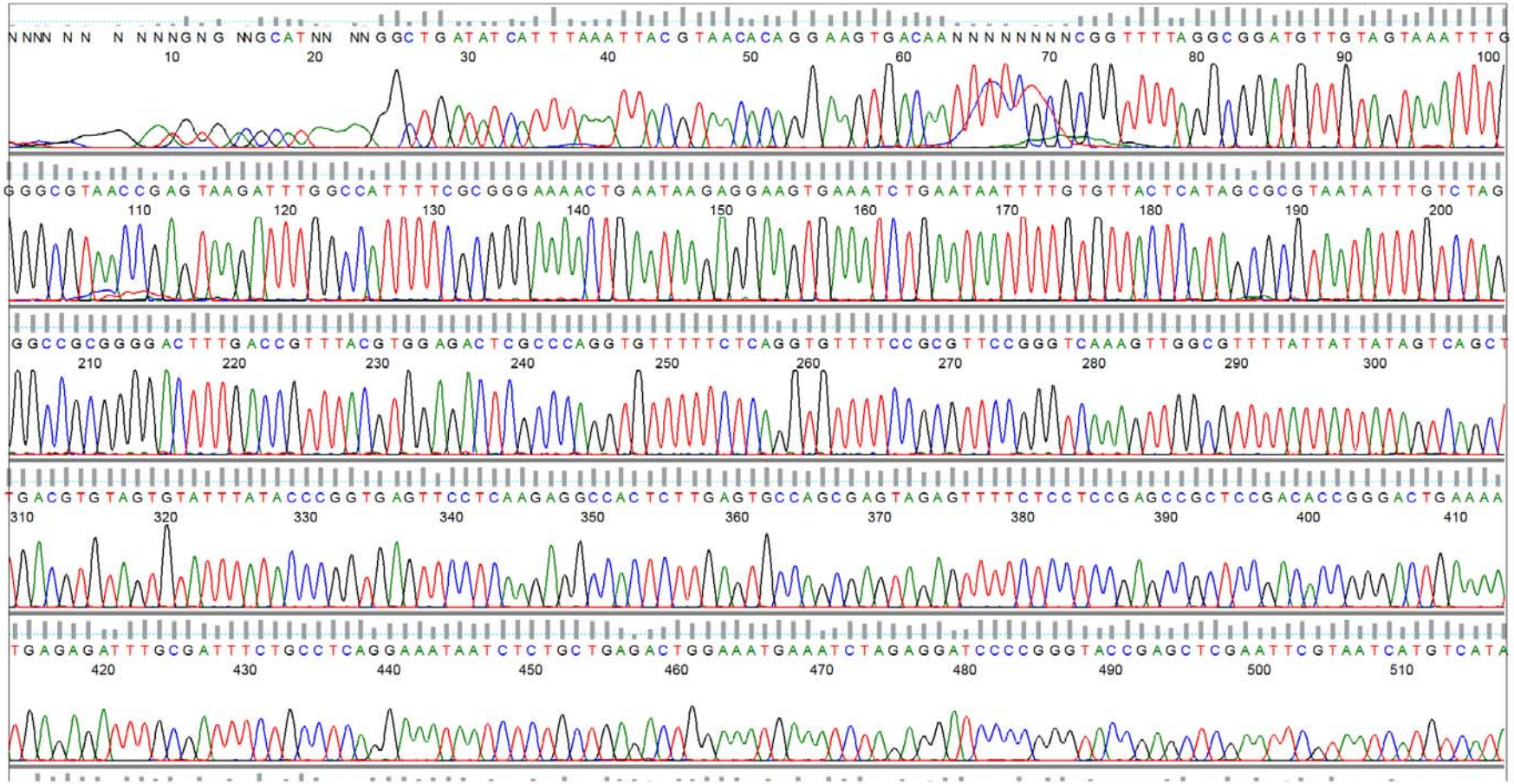
NNNN N N N N NNGNG NNGCATNN NNGGCTGATATCATTTAAATTACGTAACACAGGAAGTGACAANNNNNNNNNCGGTTTTAGGCGGATGTTGTAGTAAATTTG
10 20 30 40 50 60 70 80 90 100
GGGCGTAACCGAGTAAGATTTGGCCATTTTCGCGGGAAAACTGAATAAGAGGAAGTGAAATCTGAATAATTTTGTGTTACTCATAGCGCGTAATATTTGTCTAG
110 120 130 140 150 160 170 180 190 200
GGCCGCGGGGGACTTTGACCGTTTACGTGGAGACTCGCCCAGGTGTTTTTCTCAGGTGTTTTCCGCGTTCCGGGTCAAAGTTGGCGTTTTATTATTATAGTCAGCT
210 220 230 240 250 260 270 280 290 300
TGACGTGTAGTGTATTTATACCCGGTGAGTTCCTCAAGAGGCCACTCTTGAGTGCCAGCGAGTAGAGTTTTCTCCTCCGAGCCGCTCCGACACCGGGGACTGAAAA
310 320 330 340 350 360 370 380 390 400 410
TGAGAGATTTGCGATTTCTGCCTCAGGAAATAATCTCTGCTGAGACTGGAAATGAAATCTAGAGGATCCCCGGGTACCGAGCTCGAATTCGTAATCATGTCATA
420 430 440 450 460 470 480 490 500 510

**b)**

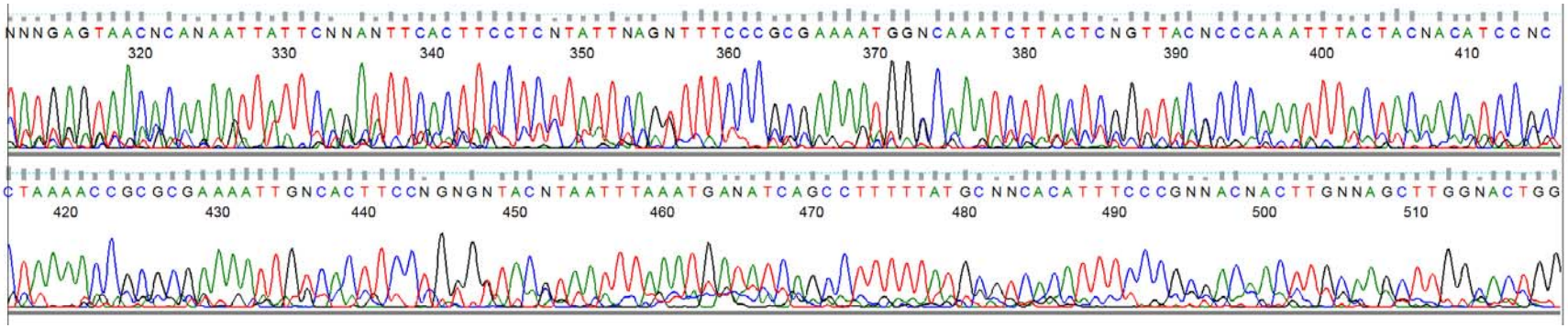


**Figure 7.16: Sequencing results of Ad11-Ad5-EP fragment inserted into pUC18.** (**a**) Sequence obtained using M13 forward primer. Nucleotides 28-47 – EcoRV, SwaI and SnaBI restriction sites; 48-412 – Ad5 *E1A* enhancer-promoter; 413-470 – start of the Ad11 *E1A*-coding sequence, interrupted by an XbaI restriction site at 471-476 where the fragment was inserted into pUC18. (**b**) Sequence obtained using M13 reverse primer. Nucleotides < 449 – part of Ad5 *E1A* enhancer-promoter; 449-468 – SnaBI, SwaI and EcoRV restriction sites; 469-505 – right part of the first 195 bp of the Ad11 genome (see **Figure 7.2b**), interrupted by a HindIII restriction site at 506-511 where the fragment was inserted into pUC18.

## 7.4 Recombinant Ad11 preparations are not contaminated by Ad5 nor by wild-type Ad11

To rule out contamination of the recombinant Ad11-Ad5-P and Ad11-Ad5-EP by Ad5 and Ad11, PCR was performed on the extracted DNA of these viruses. The primers are listed in 2.13.11. The primer pairs used are: 5P-F and 5P-R (Ad5 *E1A* promoter to just immediately before *E1A*), 11P-F and 11P-R (Ad11 *E1A* promoter to part of *E1A*), 5H-F and 5H-R (region within the Ad5 hexon-coding sequence), 5E-F and 5P-R (Ad5 *E1A* enhancer to just immediately before *E1A*), 11E-F and 11P-R (Ad11 *E1A* enhancer to part of *E1A*). The expected fragment sizes are shown in **Table 7.2**. In the latter pair, fragment sizes between Ad11 and Ad11-Ad5-P are different due to the slightly larger size of Ad5 *E1A* promoter in Ad11-Ad5-P. **Figure 7.17** shows no contamination of these viruses.

**Table 7.2: Expected sizes of PCR fragments for recombinant Ad11 purity check**

| | Ad5 | Ad11 | Ad11-Ad5-EP | Ad11-Ad5-P |
|---|---|---|---|---|
| 5P-F<br>5P-R | 184 bp | - | 184 bp | 184 bp |
| 11P-F<br>11P-R | - | 298 bp | - | - |
| 5H-F<br>5H-R | 472 bp | - | - | - |
| 5E-F<br>5P-R | 352 bp | - | 352 bp | - |
| 11E-F<br>11P-R | - | 487 bp | - | 506 bp |

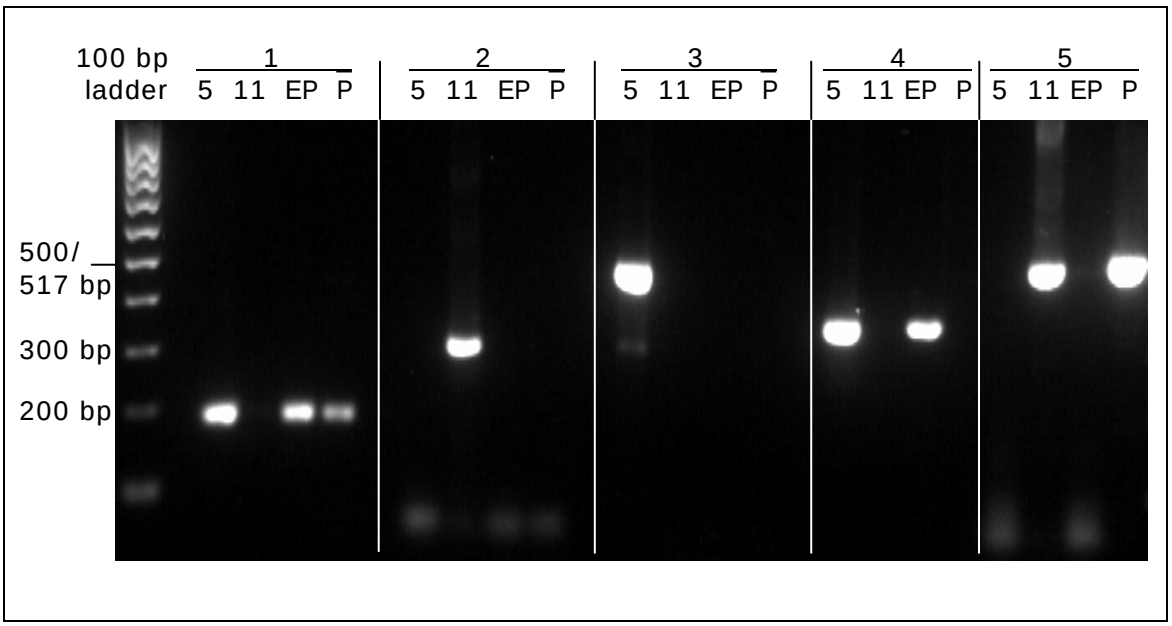


**Figure 7.17: Purity check of Ad11-Ad5-P and Ad11-Ad5-EP.** The primer pairs listed in **Table 7.2** were used: (**1**) 5P-F and 5P-R (Ad5 *E1A* promoter), (**2**) 11P-F and 11P-R (Ad11 *E1A* promoter), (**3**) 5H-F and 5H-R (Ad5 hexon), (**4**) 5E-F and 5P-R (Ad5 *E1A* enhancer), and (**5**) 11E-F and 11P-R (Ad11 *E1A* enhancer). 5, 11, EP and P are the DNA of Ad5, Ad11, Ad11-Ad5-EP and Ad11-Ad5-P, respectively. All samples showed the expected bands.

## 7.5 Summary of Chapter 7

To test the hypothesis that increasing Ad11 *E1A* transcription would result in better oncolytic potency in Ad11-insensitive cancer cells, two recombinant Ad11 were constructed. Ad11-Ad5-P has the Ad11 *E1A* promoter region substituted by that of Ad5, conserving its own packaging signal and enhancer region. Ad11-Ad5-EP on the other hand has the whole Ad5 *E1A* enhancer (including the packaging signal) and promoter replacing the corresponding region of Ad11 (**Figure 7.1**). These two viruses were successfully produced (**Table 7.1**), their sequences confirmed (**Figures 7.14 and 7.16**) and contamination with other viruses ruled out (**Figure 7.17**).

# CHAPTER 8

## Oncolytic potencies of Ad11-Ad5-P and Ad11-Ad5-EP

Results from the previous chapters have shown that Ad11 has significantly higher infectivity than Ad5 in human cancer cell lines. However in some cells, low levels of Ad11 *E1A* mRNA appear to have a negative effect on subsequent on viral DNA amplification, structural protein synthesis, infectious particle production and cell killing. To test the hypothesis that Ad11's oncolytic potency in these cells could be improved by increasing *E1A* transcription, two recombinant Ad11 were produced (see Chapter 7). Ad11-Ad5-P has the Ad11 *E1A* promoter region replaced by that of Ad5, whilst Ad11-Ad5-EP has the whole Ad5 *E1A* enhancer (including the packaging sequence) and promoter substituting the corresponding region of Ad11. In this chapter, the oncolytic potencies of these two viruses were tested *in vitro* and *in vivo* in comparison to Ad5 and Ad11.

### 8.1 Infectivities of Ad11-Ad5-P and Ad11-Ad5-EP are better than Ad5's but similar to that of wild-type Ad11

In order to check that infectivities of the recombinant viruses were unaltered by genetic manipulations, MIA PaCa-2 cells were tested. As described in detail in 5.1, cells were infected with viruses and analysed by qPCR using *E1A* primers and probes. Because the particle-to-PFU ratios of Ad11-Ad5-P (171.2 particles/PFU) and Ad11-Ad5-EP (161.5 particles/PFU) are much higher than those of Ad5 (8.9 particles/PFU) and Ad11 (36.9 particles/PFU), infection was done using 100 PFUs/cell instead of particle count. The particle-to-PFU ratio is the proportion of the total number of virus particles to encapsulated, infectious particles. Receptor attachment was performed for an hour at 4 °C, whilst nuclear trafficking was done at 37 °C for 30, 60 and 120 minutes, respectively. Consistent with results demonstrated earlier (**Figure 5.1b**), Ad11, Ad11-Ad5-P and Ad11-Ad5-EP attached and translocated to the nuclei more efficiently than Ad5 ($P < 0.001$) (**Figure 8.1**). No significant differences were noted between the recombinant viruses and wild-type Ad11.

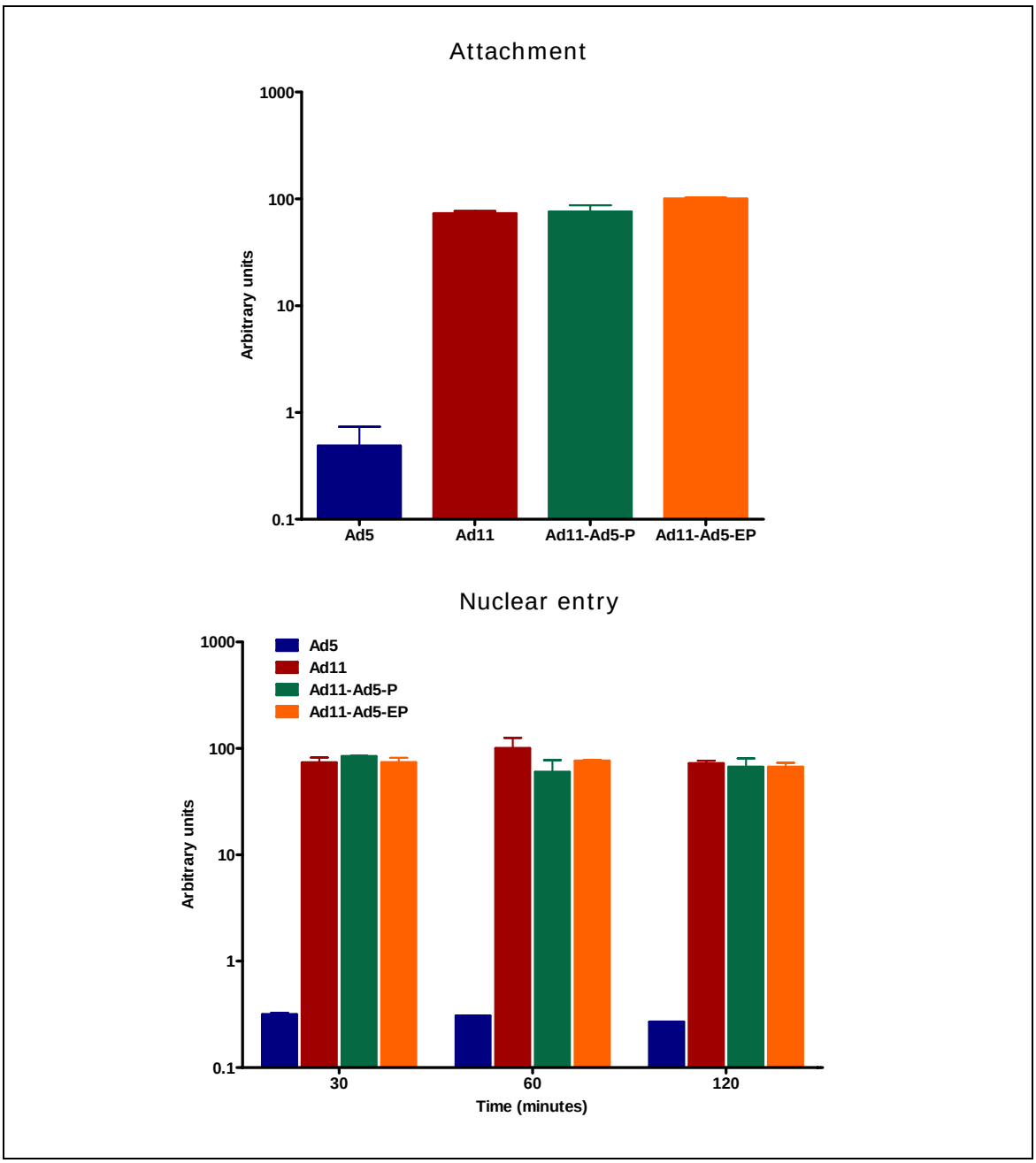


**Figure 8.1: Infectivities of Ad5, Ad11, Ad11-Ad5-P and Ad11-Ad5-EP in MIA PaCa-2.** Experiments and analyses were performed as in **Figure 5.1**, except that cells were infected with viruses at 100 PFUs/cell. Results represent means of triplicate experiments ± SEM.

## 8.2 *In vitro* oncolytic potencies of Ad11-Ad5-P and Ad11-Ad5-EP

Oncolytic potencies of the recombinant viruses were compared to those of Ad5 and Ad11 in Capan-2, MIA PaCa-2, PANC-1, PaTu 8988s (pancreas), LNCaP and PC-3 (prostate) cancer cell lines using the MTS assay. The dose-response curves are shown in **Figure 8.2** and the $EC_{50}$ are summarised in **Figure 8.3a**. In the Ad11-insensitve MIA PaCa-2, PANC-1 and LNCaP, there was a statistically significant improvement in cell killing by Ad11-Ad5-EP compared to Ad11. Ad5 remains the most potent virus in these cells. Surprisingly, Ad11-Ad5-EP was more efficient than Ad11 in killing the Ad11-sensitive Capan-2, PaTu 8988s and PC-3. The potency of Ad11-Ad5-P was variable compared to that of Ad11, but was considerably weaker in Capan-2.

As described in 8.1, the particle-to-PFU ratios of Ad11-Ad5-P and Ad11-Ad5-EP are much higher than of Ad5 and Ad11. When corrections were made such that cells were infected using PFUs rather than virus particles, further improvements in oncolytic potencies of the recombinant viruses were observed (**Figure 8.3b**). Ad11-Ad5-EP was still significantly more potent than Ad11 in all the cell lines, and was even better than Ad5 in killing MIA PaCa-2. Ad11-Ad5-P was similar (in Capan-2) or more potent than Ad11, but less so when compared to Ad11-Ad5-EP.

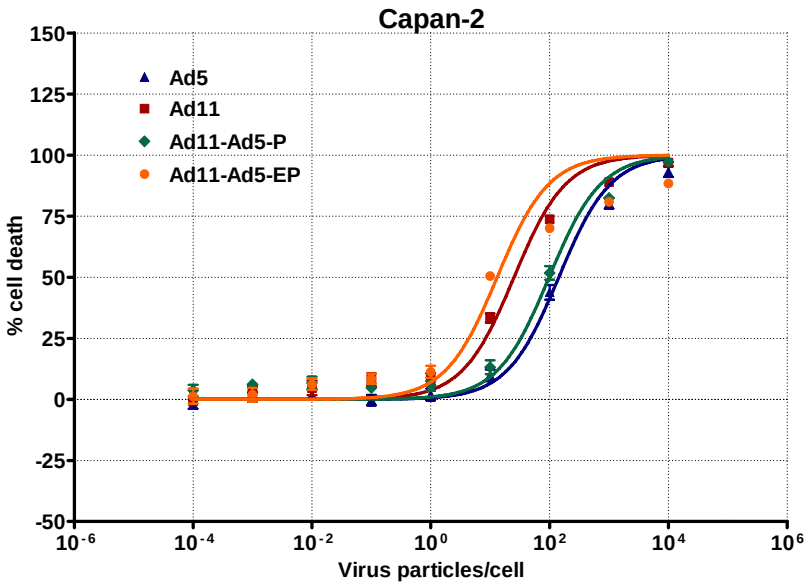
Capan-2
Ad5
Ad11
Ad11-Ad5-P
Ad11-Ad5-EP
% cell death
Virus particles/cell

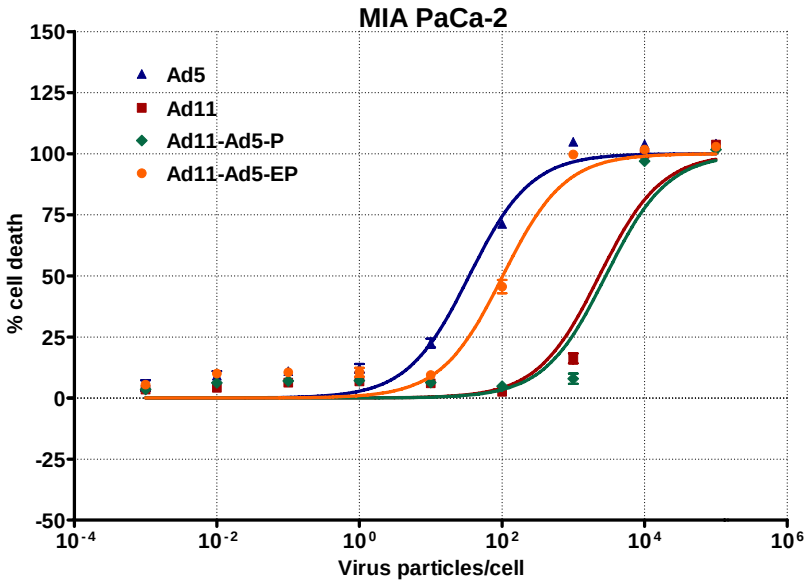
MIA PaCa-2
Ad5
Ad11
Ad11-Ad5-P
Ad11-Ad5-EP
% cell death
Virus particles/cell

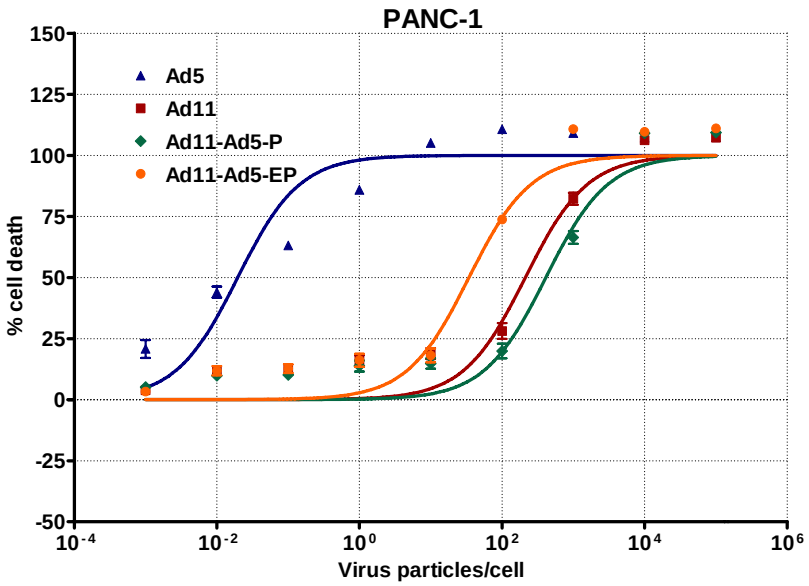
PANC-1
Ad5
Ad11
Ad11-Ad5-P
Ad11-Ad5-EP
% cell death
Virus particles/cell

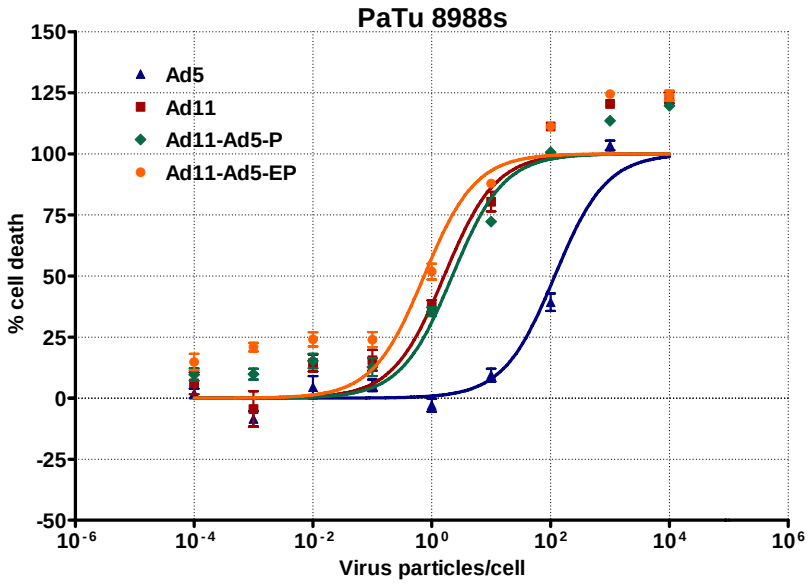
PaTu 8988s
Ad5
Ad11
Ad11-Ad5-P
Ad11-Ad5-EP
% cell death
Virus particles/cell

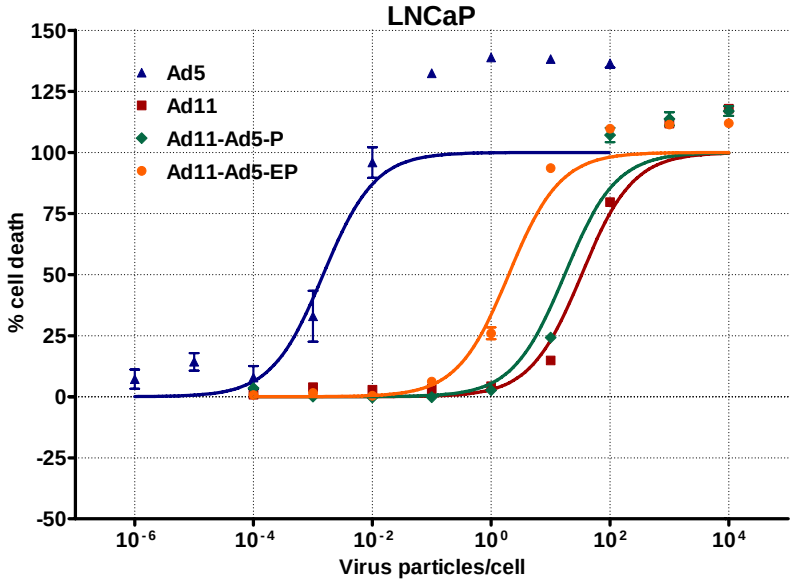
LNCaP
Ad5
Ad11
Ad11-Ad5-P
Ad11-Ad5-EP
% cell death
Virus particles/cell

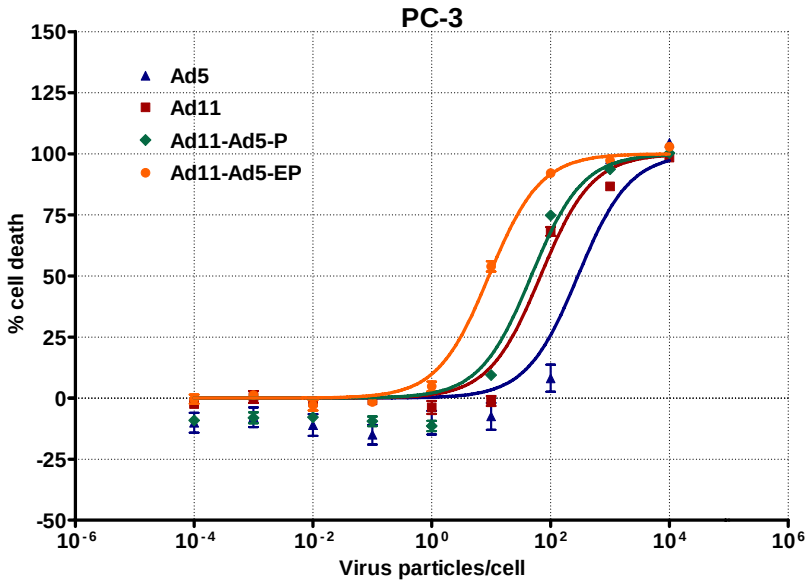
PC-3
Ad5
Ad11
Ad11-Ad5-P
Ad11-Ad5-EP
% cell death
Virus particles/cell

**Figure 8.2: Dose-response curves of Ad5, Ad11, Ad11-Ad5-P and Ad11-Ad5-EP cytotoxicities in Capan-2, MIA PaCa-2, PANC-1, PaTu 8988s, LNCaP and PC-3.** Cells were infected in 96-well plates. Cell viability was measured on day six after infection by the MTS assay. Data represent means ± SEM from duplicate experiments (with each concentration of virus in sextuplicates).

a)

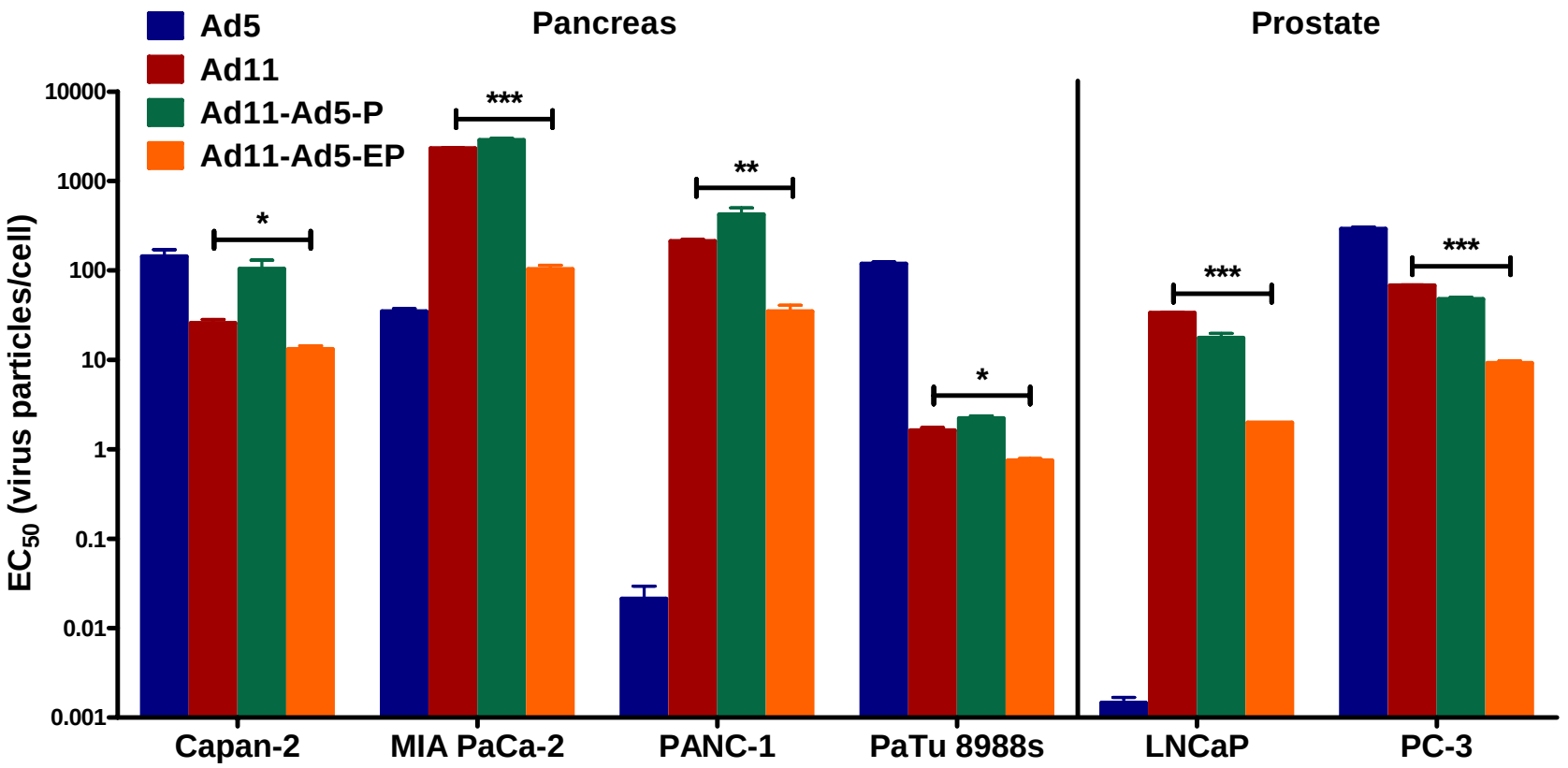
Ad5
Ad11
Ad11-Ad5-P
Ad11-Ad5-EP
Pancreas
Prostate
EC50 (virus particles/cell)
10000
1000
100
10
1
0.1
0.01
0.001
*
***
**
*
***
***
Capan-2
MIA PaCa-2
PANC-1
PaTu 8988s
LNCaP
PC-3

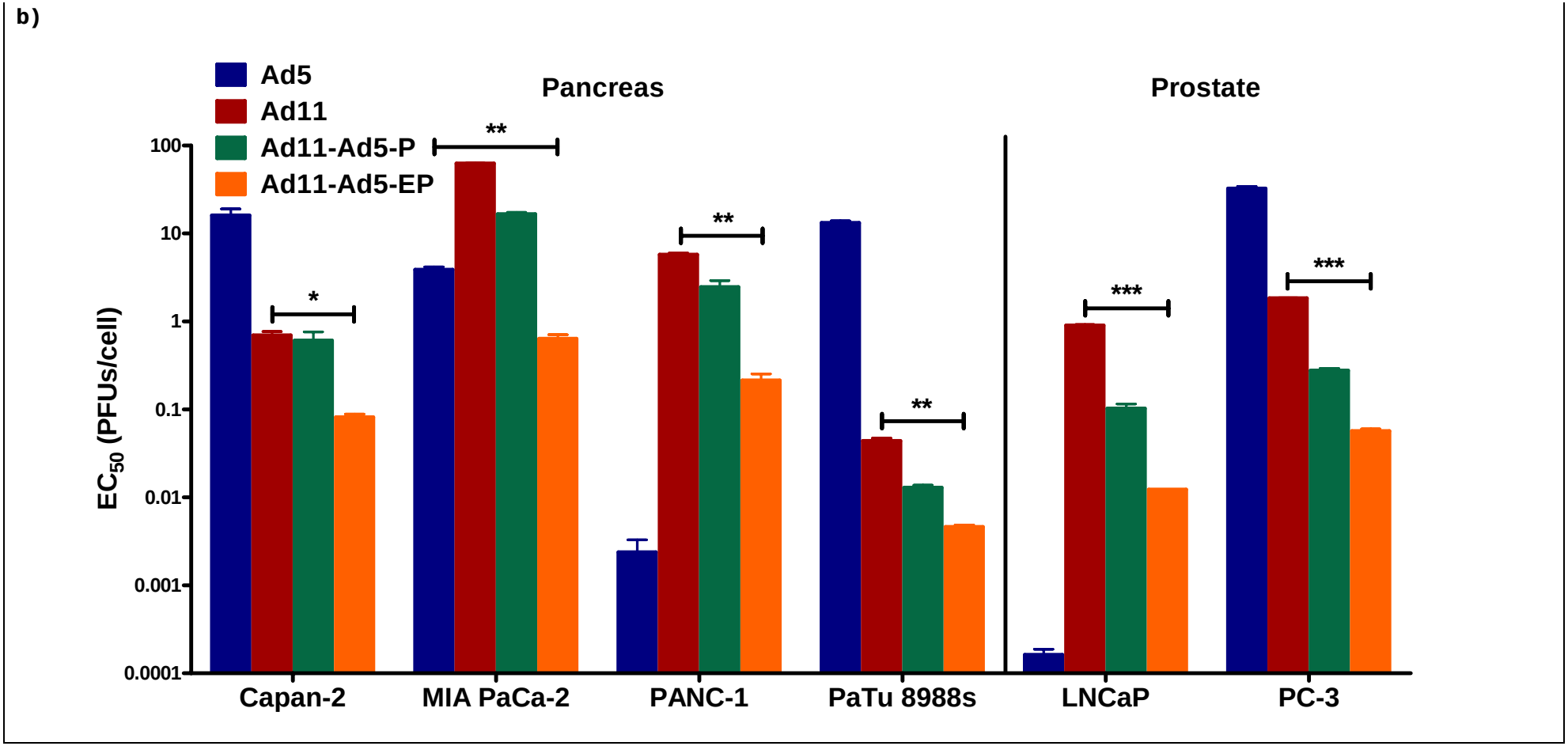


**Figure 8.3: $EC_{50}$ of Ad5, Ad11, Ad11-Ad5-P and Ad11-Ad5-EP in Capan-2, MIA PaCa-2, PANC-1, PaTu 8988s, LNCaP and PC-3.** (**a**) $EC_{50}$ in virus particles/cell. (**b**) $EC_{50}$ adjusted to PFUs/cell by dividing the $EC_{50}$ in (**a**) with the particle-to-PFU ratios of each of the viruses. A lower $EC_{50}$ indicates better cell killing. Data are presented as means ± SEM. * $P < 0.05$, ** $P < 0.01$, *** $P < 0.001$.

The potencies of these viruses were further tested on other cancer cell lines, namely MCF7, MDA-MB-231 (breast), HT-29, HCT 116 (colon), OVCAR-3 (ovary) and A549 (lung) (**Figures 8.4 and 8.5a**). There was a significant improvement in $EC_{50}$ with Ad11-Ad5-EP compared to Ad11. Ad11-Ad5-EP was even more potent than Ad11 in the Ad11-sensitive MCF7 and HT-29. There were no significant differences between Ad11-Ad5-EP and Ad5 in MDA-MB-231 and HCT 116. Ad11-Ad5-EP was slightly better than Ad11 in OVCAR-3, but Ad5 remains the most potent. Interestingly A549 was most sensitive to Ad11-Ad5-EP, with its $EC_{50}$ nearly 30 times less than that of Ad5. Ad11-Ad5-P was largely comparable to Ad11 in its potency, except that it was much less effective against MCF7 and MDA-MB-231.

Again, when the $EC_{50}$ in virus particles/cell were adjusted to PFUs/cell, there were further improvements in oncolytic potencies of the recombinant viruses (**Figure 8.5b**). Ad11-Ad5-EP was still significantly more potent than Ad11, and was more effective than Ad5 in killing MDA-MB-231 and HCT 116. The potency Ad11-Ad5-P was variable, being more potent than Ad11 in most cells but still weaker in MCF7.

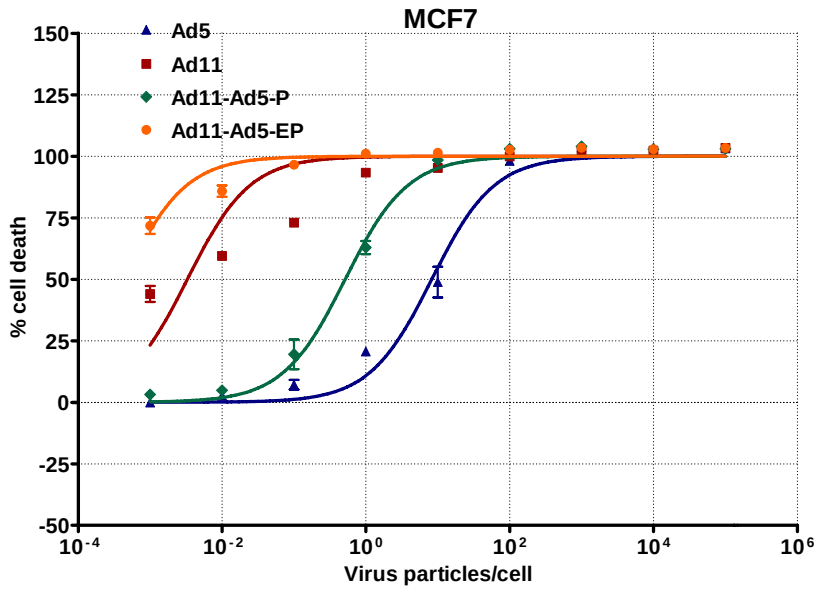
MCF7
Ad5
Ad11
Ad11-Ad5-P
Ad11-Ad5-EP
% cell death
Virus particles/cell

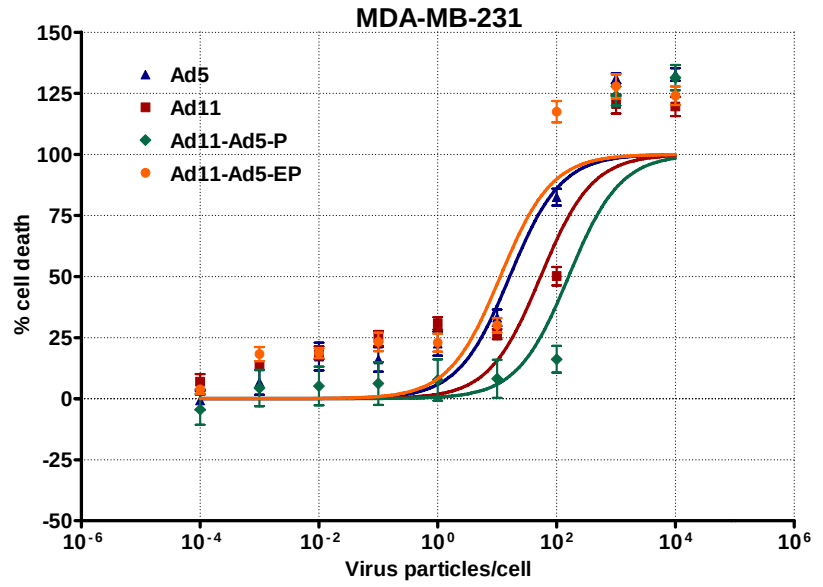
MDA-MB-231
Ad5
Ad11
Ad11-Ad5-P
Ad11-Ad5-EP
% cell death
Virus particles/cell

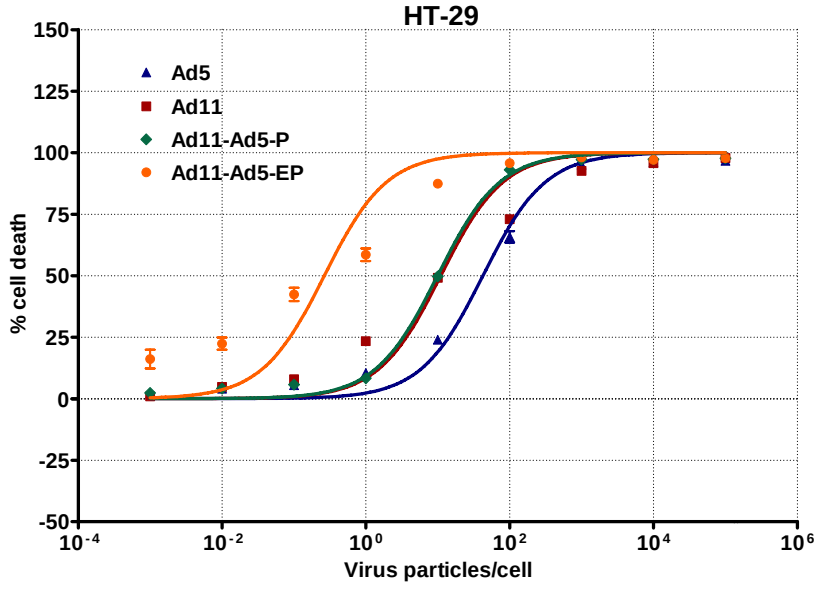
HT-29
Ad5
Ad11
Ad11-Ad5-P
Ad11-Ad5-EP
% cell death
Virus particles/cell

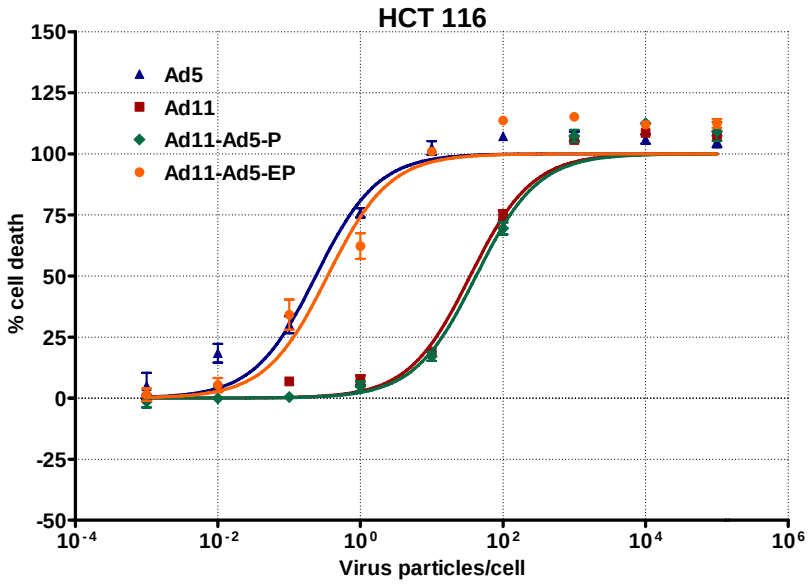
HCT 116
Ad5
Ad11
Ad11-Ad5-P
Ad11-Ad5-EP
% cell death
Virus particles/cell

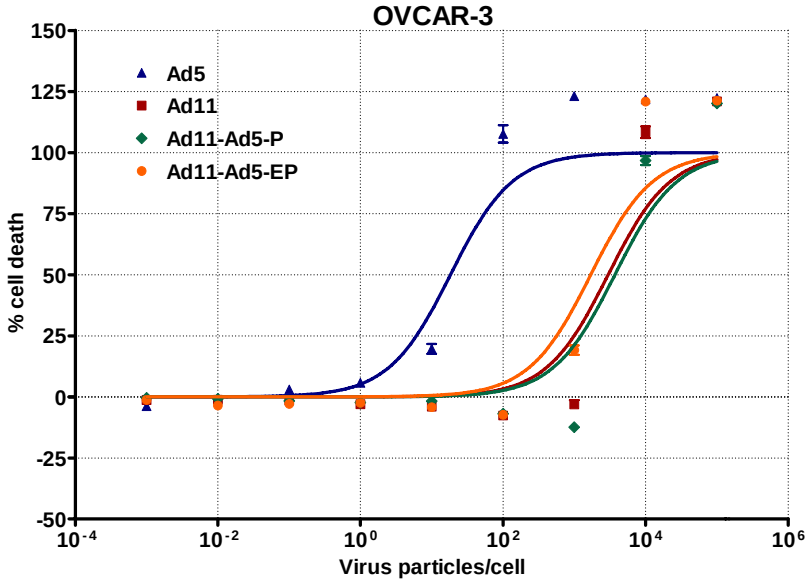
OVCAR-3
Ad5
Ad11
Ad11-Ad5-P
Ad11-Ad5-EP
% cell death
Virus particles/cell

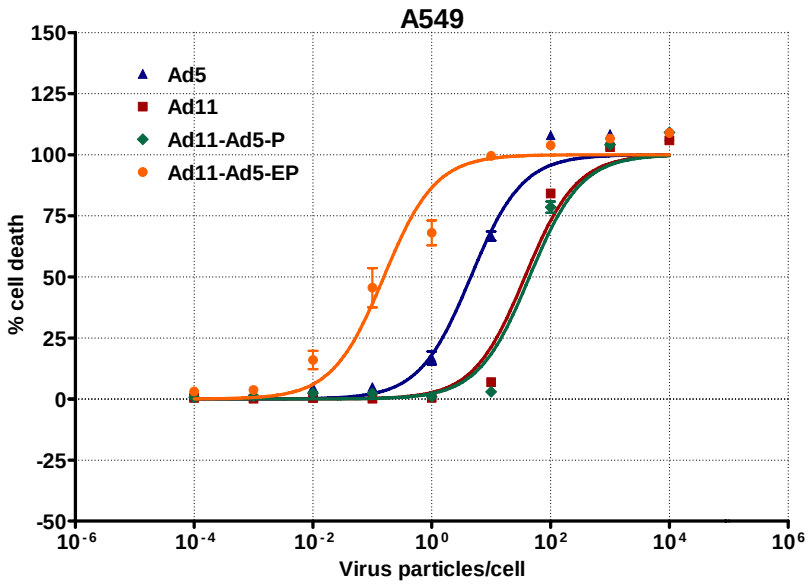
A549
Ad5
Ad11
Ad11-Ad5-P
Ad11-Ad5-EP
% cell death
Virus particles/cell

**Figure 8.4: Dose-response curves of Ad5, Ad11, Ad11-Ad5-P and Ad11-Ad5-EP cytotoxicities in MCF7, MDA-MB-231, HT-29, HCT 116, OVCAR-3 and A549.** Cells were infected in 96-well plates. Cell viability was measured on day six after infection by the MTS assay. Data represent means ± SEM from duplicate experiments (with each concentration of virus in sextuplicates).

a)

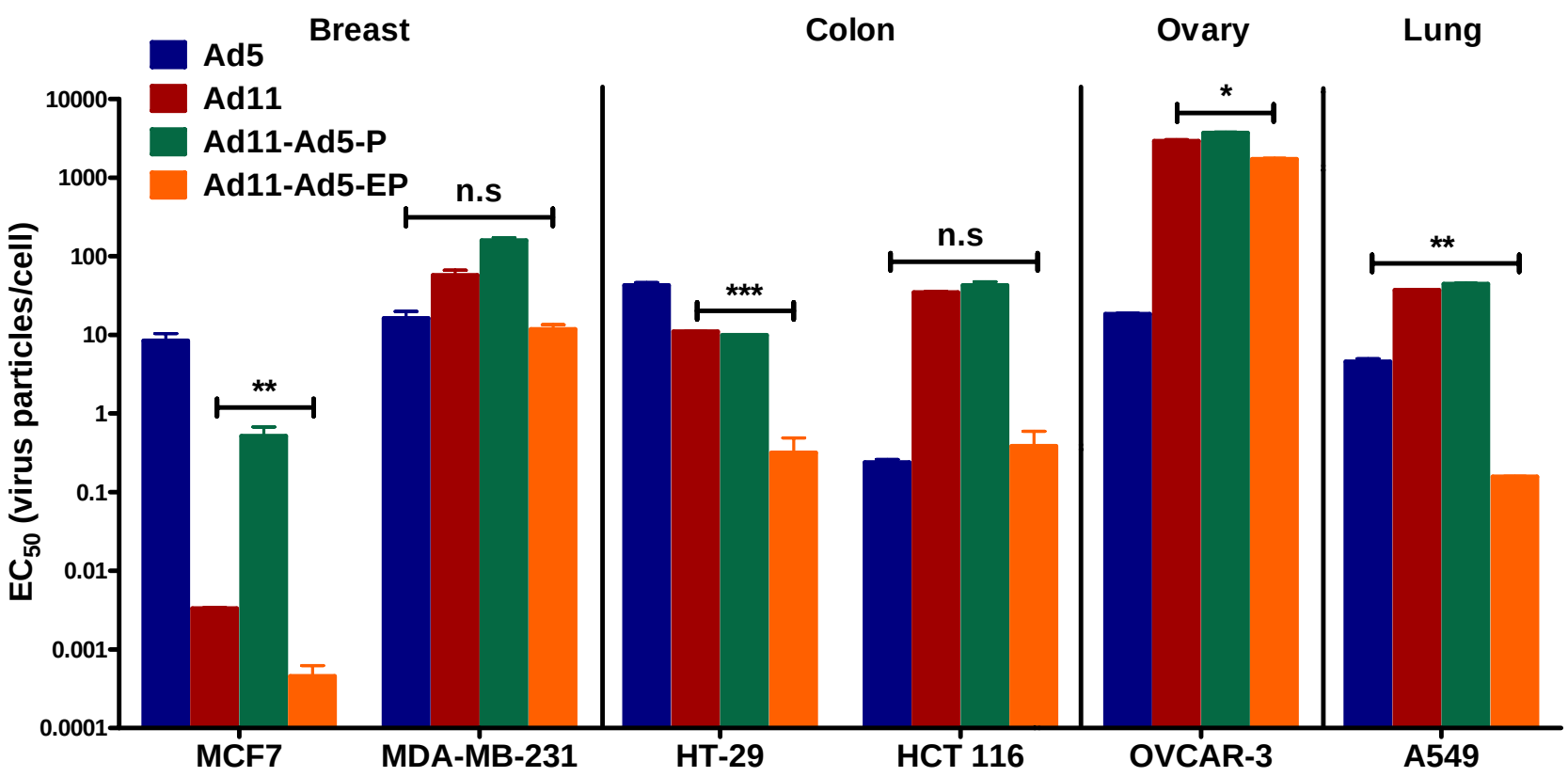
Breast
Colon
Ovary
Lung
Ad5
Ad11
Ad11-Ad5-P
Ad11-Ad5-EP
EC50 (virus particles/cell)
10000
1000
100
10
1
0.1
0.01
0.001
0.0001
**
n.s
***
n.s
*
**
MCF7
MDA-MB-231
HT-29
HCT 116
OVCAR-3
A549

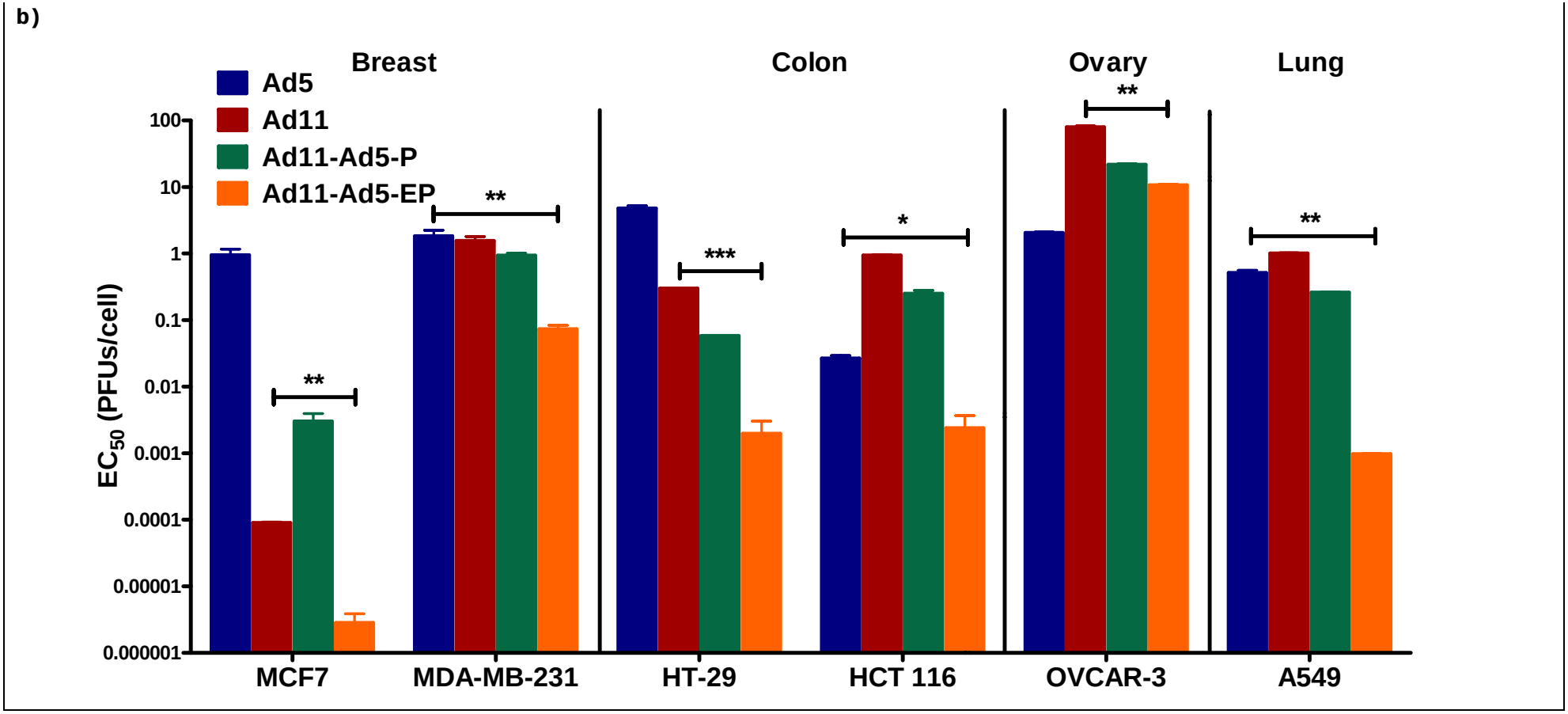


**Figure 8.5: $EC_{50}$ of Ad5, Ad11, Ad11-Ad5-P and Ad11-Ad5-EP in MCF7, MDA-MB-231, HT-29, HCT 116, OVCAR-3 and A549.** (**a**) $EC_{50}$ in virus particles/cell. (**b**) $EC_{50}$ adjusted to PFUs/cell by dividing the $EC_{50}$ in (**a**) with the particle-to-PFU ratios of each of the viruses. A lower $EC_{50}$ indicates better cell killing. Data are presented as means ± SEM. * $P < 0.05$, ** $P < 0.01$, *** $P < 0.001$, n.s – not significant.

## 8.3 Ad11-Ad5-EP has the highest DNA amplification independent of its *E1A* mRNA level but this does not always correlate with its oncolytic potency

Results so far have demonstrated that Ad11-Ad5-EP is a more potent virus than Ad11-Ad5-P and Ad11. It was even more effective than Ad11 in killing the Ad11-sensitive cancer cell lines (*e.g.* Capan-2, PC-3, MCF7, HT-29). Its effects on the Ad11-insensitive cell lines were variable, for it was either weaker (*e.g.* MIA PaCa-2), similar (*e.g.* MDA-MB-231, HCT 116), or stronger (*e.g.* A549) than Ad5. To understand this, MIA PaCa-2, PC-3 and A549 were examined further by the stepwise analysis described in Chapter 5, namely the determination of *E1A* mRNA levels, DNA amplification, structural protein synthesis and production of infectious particles.

In MIA PaCa-2, *E1A* mRNA levels from Ad11-Ad5-EP were higher than those of Ad11 and lower than those of Ad5, respectively (**Figure 8.6**). This is consistent with the luciferase reporter results (**Figures 6.6a and 6.7a**), indicating that the Ad5 *E1A* enhancer has a higher transcription-enhancing activity than Ad11's. The Ad5 *E1A* promoter alone did not enhance *E1A* transcription, as shown by its lower mRNA levels from Ad11-Ad5-P. Unexpectedly, Ad11-Ad5-EP DNA amplified at the highest level, even greater than that of Ad5 for which MIA PaCa-2 cells were most sensitive to. Thus there appears to be no direct correlation between *E1A* mRNA levels and the ability of viral DNA to replicate, contradicting the results shown previously (**Figures 5.2 and 5.7**). Despite the higher amount of DNA, hexon protein synthesis and the number of infectious Ad11-Ad5-EP produced were less than Ad5 (**Figure 8.6**), leading to the observed MTS result (**Figure 8.2**).

*E1A* mRNA

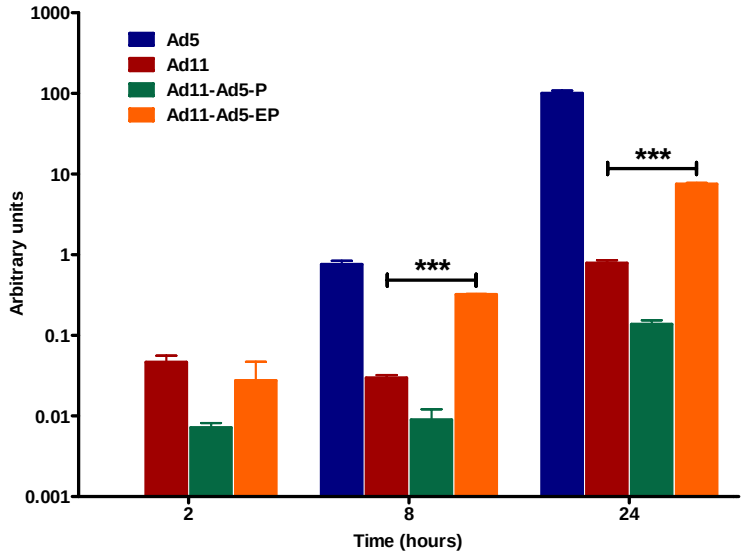


DNA amplification

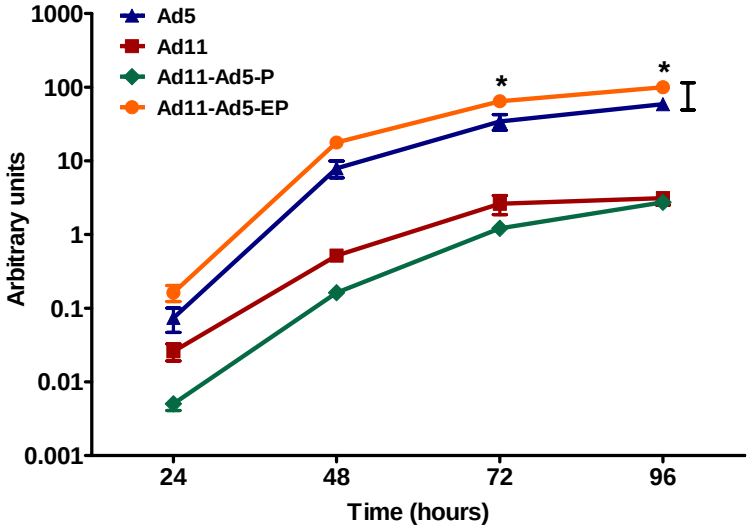


Hexon protein expression

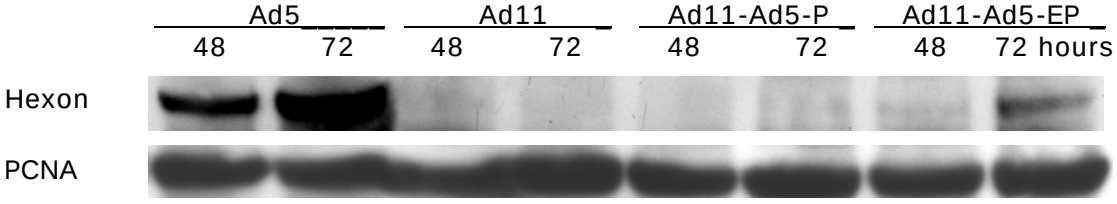

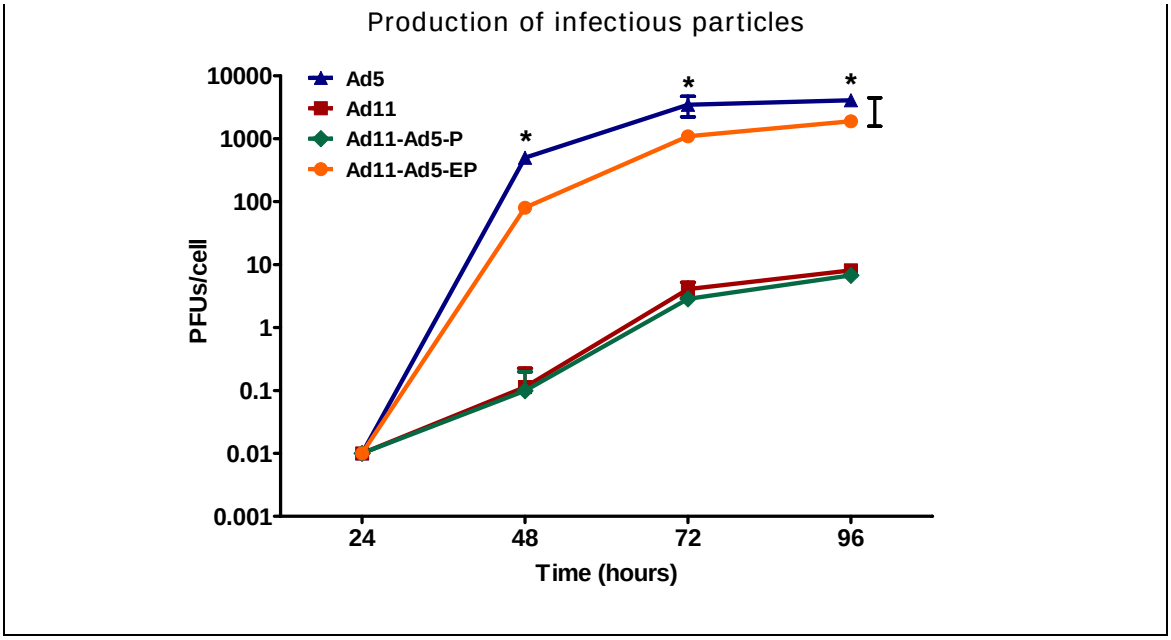


**Figure 8.6: *E1A* mRNA levels, DNA amplification, hexon expression and production of infectious particles in MIA PaCa-2 after Ad5, Ad11, Ad11-Ad5-P or Ad11-Ad5-EP infection.** Cytotoxicities from the MTS assay are Ad5 > Ad11-Ad5-EP > Ad11 > Ad11-Ad5-P. Experiments and analyses were performed as in **Figures 5.2-5.4 and 5.7**. Graph results represent means of triplicate experiments ± SEM. * $P < 0.05$, *** $P < 0.001$.

*E1A* mRNA levels of Ad11-Ad5-EP in PC-3 were the highest, followed by Ad11's, resulting in higher levels of viral DNA and infectious particle production (**Figure 8.7**). Again, this could be explained by the higher transcription-enhancing activity of Ad5 *E1A* enhancer, as demonstrated by the luciferase reporter assays (**Figures 6.6b and 6.7b**). Although the high *E1A* mRNA levels from Ad11-Ad5-EP and Ad11 corresponded to subsequent DNA amplification, this did not apply to Ad11-Ad5-P. Its *E1A* mRNA levels were similar to or lower than those of Ad5, yet significantly more Ad11-Ad5-P DNA, hexon protein and infectious particles were produced (**Figure 8.7**).

*E1A* mRNA

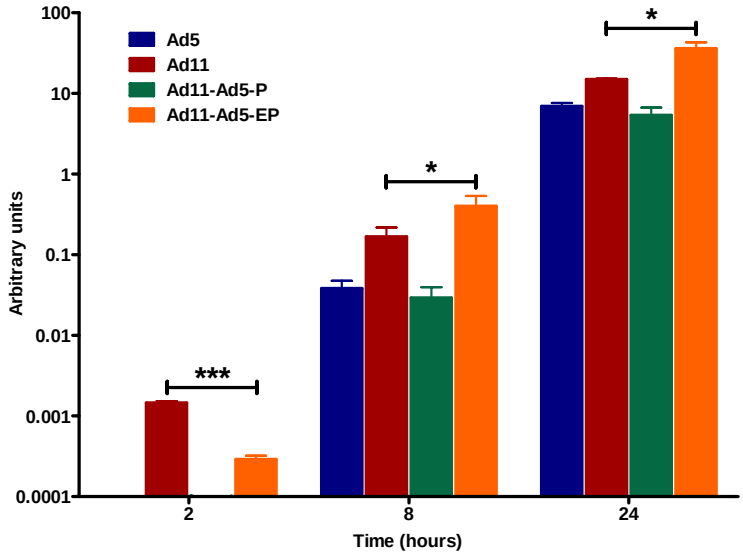


DNA amplification

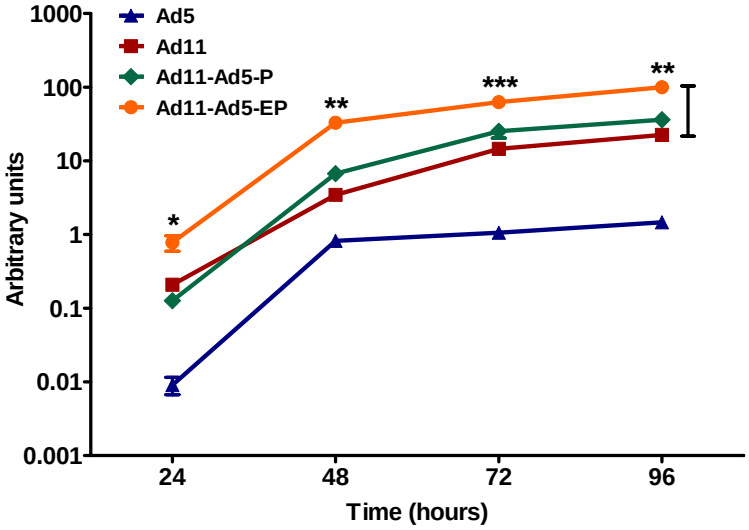


Hexon protein expression

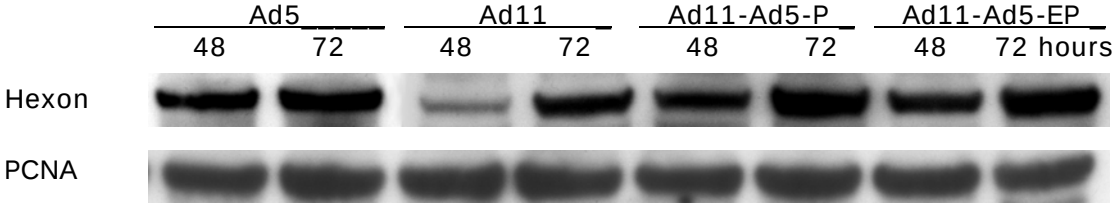

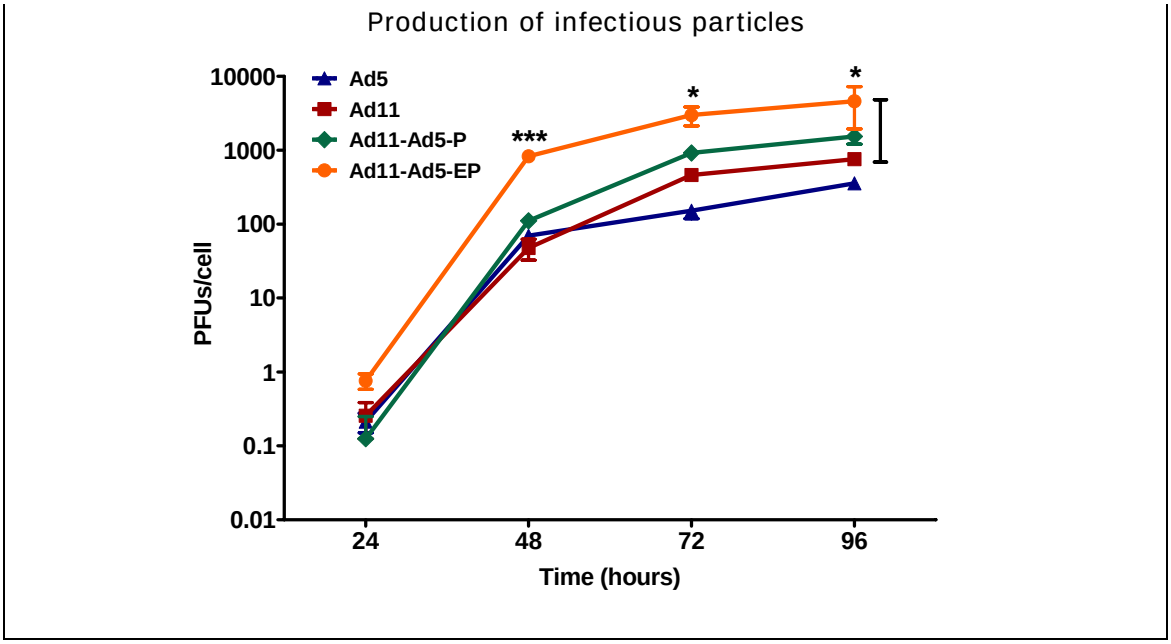


**Figure 8.7: *E1A* mRNA levels, DNA amplification, hexon expression and production of infectious particles in PC-3 after Ad5, Ad11, Ad11-Ad5-P or Ad11-Ad5-EP infection.** Cytotoxicities from the MTS assay are Ad11-Ad5-EP > Ad11-Ad5-P > Ad11 > Ad5. Experiments and analyses were performed as in **Figures 5.2-5.4 and 5.7**. Graph results represent means of triplicate experiments ± SEM. * $P < 0.05$, ** $P < 0.01$, *** $P < 0.001$.

The results for A549 cells are of particular interest. In disagreement with results from other cell lines tested, Ad11 *E1A* mRNA levels were the highest, even though it was much less sensitive to Ad11 killing compared to Ad5 (**Figure 8.8**). Ad11 DNA amplified to a greater extent than Ad5's, yet similar to Ad11-Ad5-EP in MIA PaCa-2, events post-DNA replication, such as a decrease in hexon protein synthesis, resulted in lower amounts of infectious Ad11 particles produced. In contrast, Ad11-Ad5-EP *E1A* mRNA levels were lower than those of Ad11, yet its DNA replicated most efficiently. More hexon and infectious Ad11-Ad5-EP particles were subsequently produced resulting in efficient cell killing. The drop in infectious Ad11-Ad5-EP particles at 96 hours occurred because all the cells were dead, limiting any further virus replication.

*E1A* mRNA

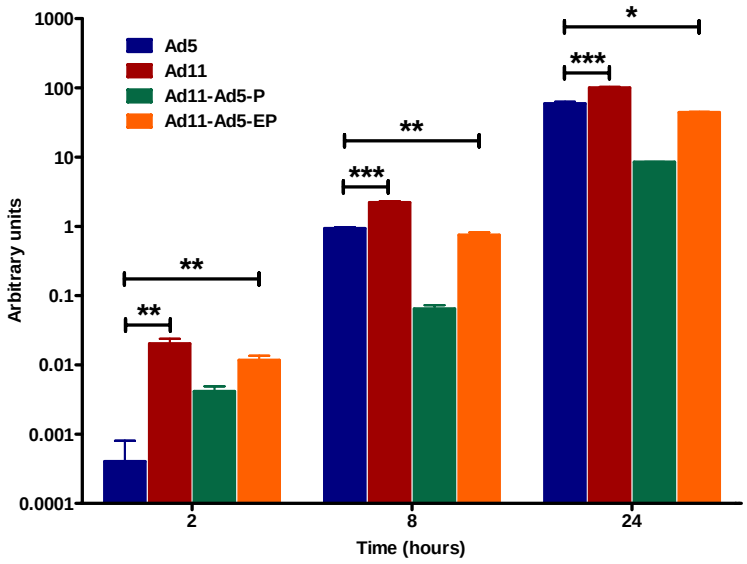


DNA amplification

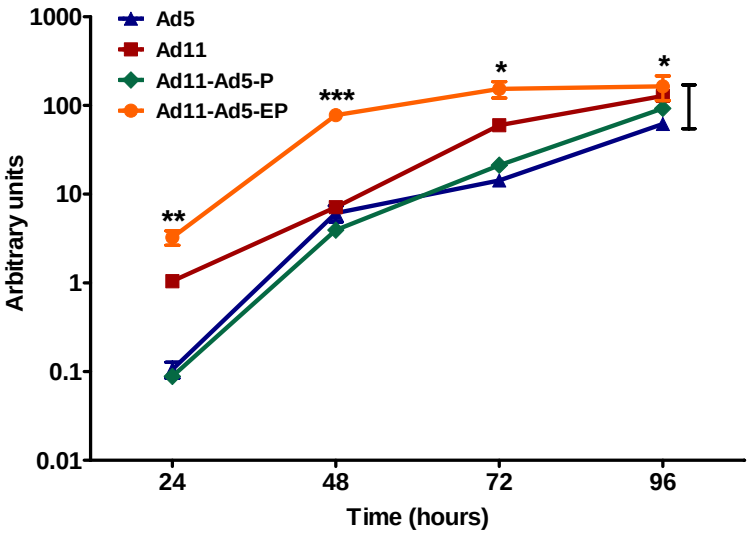


Hexon protein expression

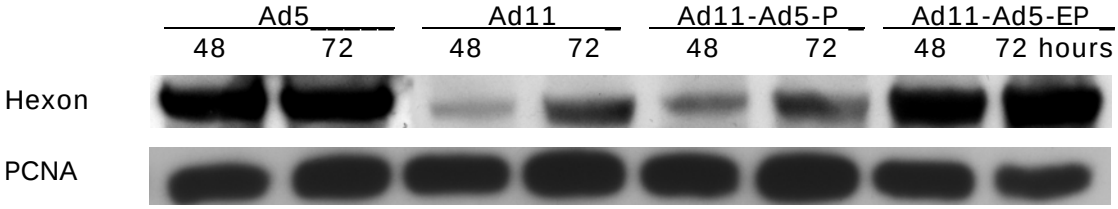

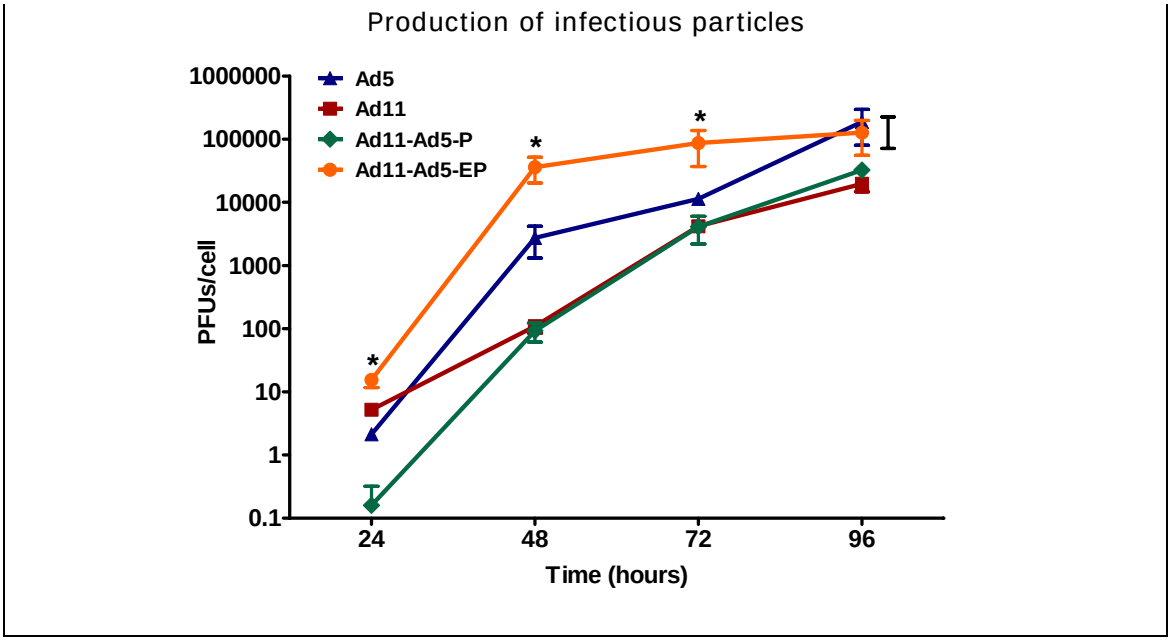


**Figure 8.8: *E1A* mRNA levels, DNA amplification, hexon expression and production of infectious particles in A549 after Ad5, Ad11, Ad11-Ad5-P or Ad11-Ad5-EP infection.** Cytotoxicities from the MTS assay are Ad11-Ad5-EP > Ad5 > Ad11 > Ad11-Ad5-P. Experiments and analyses were performed as in **Figures 5.2-5.4 and 5.7**. Graph results represent means of triplicate experiments ± SEM. * $P < 0.05$, ** $P < 0.01$, *** $P < 0.001$.

## 8.4 Ad11-Ad5-EP is as effective as Ad5 in treating MIA PaCa-2 human pancreatic cancer xenografts

The *in vivo* efficacies of Ad11-Ad5-P and Ad11-Ad5-EP were compared to those of Ad5 and Ad11 in a MIA PaCa-2 human pancreatic cancer subcutaneous xenograft model. Establishment of tumours and virus injections were conducted as described in Chapter 4. As shown in **Figure 8.9a**, Ad11-Ad5-EP was as effective as Ad5 in reducing tumour growth, culminating in similar progression-free rates that were significantly better than the Ad11-treated group (logrank $P < 0.05$) (**Figure 8.9b**). Ad11-Ad5-P was comparable to Ad11. *In vivo* DNA amplification and production of infectious Ad11-Ad5-EP were significantly higher than Ad11 (**Figures 8.9c and d**). Reflective of the *in vitro* findings (**Figure 8.6**), Ad11-Ad5-EP showed the highest amount of viral DNA but came second to Ad5 in virus production (**Figures 8.9c and d**).

a)

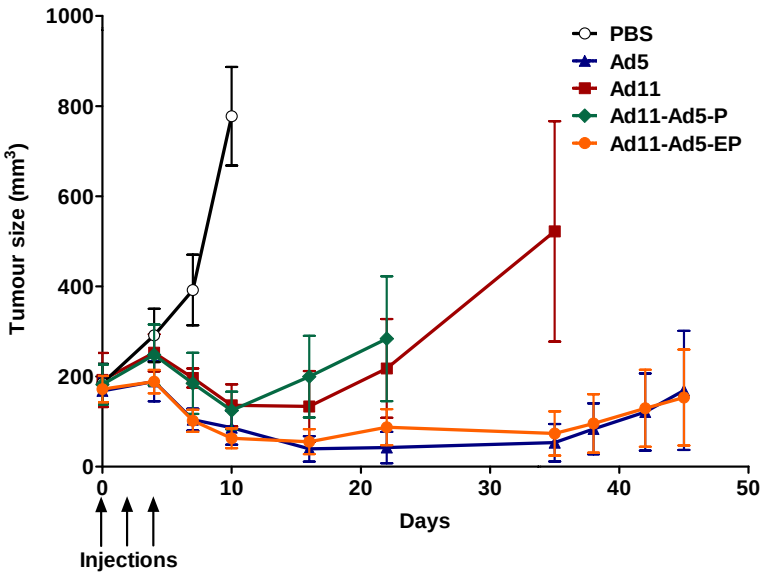
1000
800
600
400
200
0
Tumour size (mm3)
0
10
20
30
40
50
Days
Injections
PBS
Ad5
Ad11
Ad11-Ad5-P
Ad11-Ad5-EP

b)

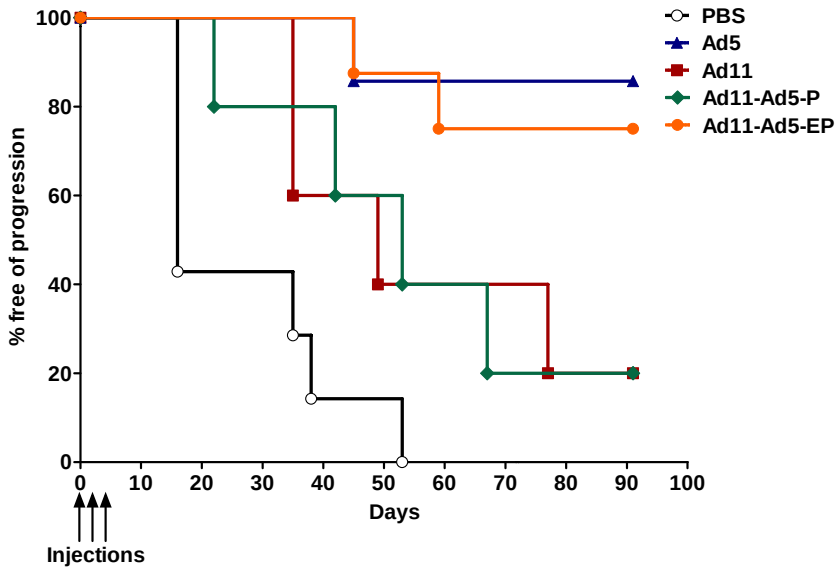
100
80
60
40
20
0
% free of progression
0
10
20
30
40
50
60
70
80
90
100
Days
Injections
PBS
Ad5
Ad11
Ad11-Ad5-P
Ad11-Ad5-EP

c)

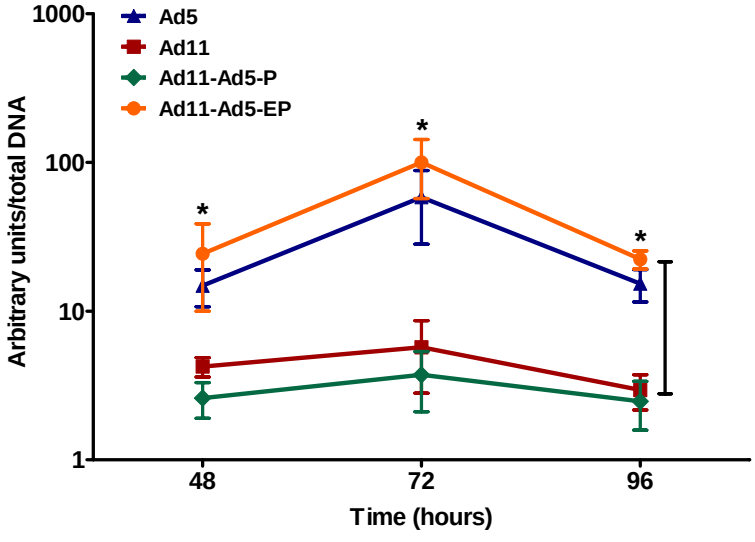
1000
100
10
1
Arbitrary units/total DNA
48
72
96
Time (hours)
*
*
*
Ad5
Ad11
Ad11-Ad5-P
Ad11-Ad5-EP

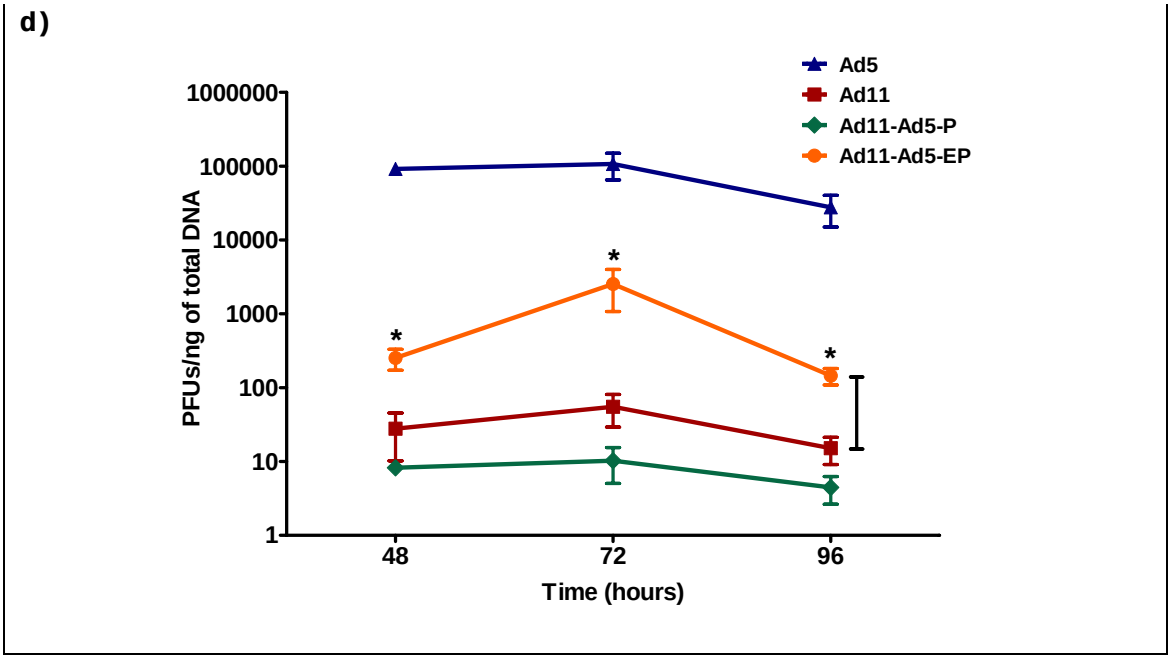


**Figure 8.9: Anti-tumoural efficacies of Ad5, Ad11, Ad11-Ad5-P and Ad11-Ad5-EP in a MIA PaCa-2 subcutaneous xenograft model.** (**a**) Tumour growth in BALB/c nude mice after three intratumoural injections of PBS (100 µl) or viruses (1 x $10^{10}$ particles/injection). Tumours were measured until the first mouse in each group has a tumour dimension of > 1.44 $cm^2$. Data represent means ± SEM ($n$ = 8 per group). On day 35, significant difference was observed between the Ad11-treated group and the Ad5- or Ad11-Ad5-EP-treated group ($P$ < 0.05). (**b**) Percentage of progression-free mice using the Kaplan-Meier method (logrank $P$ < 0.05 between Ad5 or Ad11-Ad5-EP and Ad11). (**c**) Established tumours were injected once with 1 x $10^{10}$ virus particles. At the stated time points, tumours were harvested in triplicates, homogenised in 2 ml of DMEM, frozen and thawed three times in liquid nitrogen and at 37 °C, respectively prior to DNA extraction. qPCR was performed using *E1A* primers and probes. Results are presented as average arbitrary units ± SEM, normalised against total DNA, with the highest value arbitrarily set to 100. (**d**) The above cell lysates were used to infect an indicator cell line, JH-293, in 96-well plates at six 1:10 serial dilutions. The cells were inspected for CPE 11 days later. The $TCID_{50}$ and number of PFUs were calculated using the Reed-Muench accumulative method. Results are presented as PFUs/ng of total DNA ± SEM. * $P$ < 0.05.

## 8.5 Summary of Chapter 8

The oncolytic potencies of the Ad11 mutants Ad11-Ad5-P (with the Ad11 *E1A* promoter replaced by that of Ad5) and Ad11-Ad5-EP (with the Ad5 *E1A* enhancer and promoter substituting the corresponding region of Ad11) were compared to those of Ad5 and Ad11. Ad11-Ad5-EP was significantly more potent than Ad11 in all the cancer cell lines tested, even in those that were already sensitive to Ad11 (**Figures 8.3 and 8.5**). There was a vast improvement in cytotoxicity of Ad11-Ad5-EP over Ad11 in all the Ad11-insensitive cell lines. In two of these, MDA-MB-231 and HCT 116, Ad11-Ad5-EP was as efficacious as Ad5, although Ad5 remains the most potent in MIA PaCa-2, PANC-1, LNCaP and OVCAR-3. Strikingly, the lung carcinoma cell line A549 was nearly 30 times more sensitive to Ad11-Ad5-EP than to Ad5. The potency of Ad11-Ad5-P was variable in comparison to Ad11, but was always weaker than Ad11-Ad5-EP. Considering the high particle-to-PFU ratios of Ad11-Ad5-P and Ad11-Ad5-EP, their potencies were even much greater if cells were infected using PFUs instead of particles. However, due to the toxicity and immunogenicity of both infectious and non-infectious particles, particle counts rather than PFUs are normally used for experiments and clinical trials of Ads.

Ad11-Ad5-EP was as effective as Ad5, but significantly better than Ad11, in treating MIA PaCa-2 tumour xenografts (**Figures 8.9a and b**). This occurred despite the production of more Ad5 compared to Ad11-Ad5-EP (**Figure 8.9d**). This could be due to a faster clearance of Ad5 in nude mice where CAR, but not CD46, is expressed.

Results from **Figures 8.6 to 8.8** demonstrated that increased *E1A* mRNA level is important but not the sole factor required to improve Ad11 DNA replication. Higher expression of other early genes such as *E1B*, *E2* and *E4*, mediated both by E1A and the enhancer region, is likely to be involved. In some cell lines (*e.g.* Ad11-Ad5-EP in MIA PaCa-2, Ad11 in A549), events post-DNA replication become the limiting steps for effective virus production and cell killing. Regardless of the mechanisms involved, recombinant Ad11 with the Ad5 *E1A* enhancer-promoter is a more potent virus than its wild-type counterpart and should be used in the future development of oncolytic Ad11.

# CHAPTER 9

# Discussion and future direction

## 9.1 Assessment of Ad11 as a potential oncolytic virus

The failure of Ad5 in the treatment of pancreatic cancer prompted the search of an alternative oncolytic virus that could overcome some of the limitations associated with Ad5, such as the low expression and inaccessibility of its binding receptor CAR[124-126, 184, 185, 197], high prevalence of neutralising antibodies[172, 173, 201, 202] and significant liver uptake and toxicity[137]. Whilst Ad11[172, 173, 177, 218] and the chimeric Ad5/11[192, 219-221] have already been shown to be promising gene transfer vectors secondary to their high infectivity across many cell types, this study aimed to assess in detail the potential of Ad11 as an oncolytic virus.

During the timeframe of this project, three papers have reported the use of Ad11 as an oncolytic virus. Sandberg *et al*.[136] developed a recombinant Ad11 by the insertion of a cytomegalovirus (CMV) promoter-driven green fluorescent protein (GFP) with an SV40 enhancer into the Ad11 genome. They showed that this virus effectively transduced, replicated and lysed the PC-3 prostate cancer cell line *in vitro* and *in vivo*. Oncolytic capacity was independent of p53 status. However, no comparison was made with the commonly used Ad5. Shashkova *et al*.[137] compared the oncolytic efficiencies of Ad5, -6, -11 and -35 on a panel of human cancer cell lines *in vitro* as well as the DU 145 human prostate cancer cell line *in vivo*. In the latter, Ad5, -6 and -11 have similar anti-cancer activities after intratumoural or intravenous treatment, whereas Ad35 was not efficacious. Importantly they demonstrated that hepatotoxicity only developed with Ad5 in CD46-transgenic C57BL/6 mice but not with the other serotypes. Both of these studies found that the expressions of CAR and CD46 correlated with the *in vitro* cytotoxicities of different Ads in most but not all cell lines, although no molecular mechanism has been determined. More recently, Senac *et al*.[138] compared Ad5, -6, -11, -26, -35, -40, -41 and -48 in the infection and killing of multiple myeloma cells. They found that although Ad11 and Ad35 were more infective than other serotypes, their DNA failed to replicate, resulting in weak oncolytic abilities.

This study started by determining the expression levels of CAR and CD46 in eight human pancreatic cancer cell lines, as well as the prostate cancer cells DU 145,

LNCaP and PC-3, the latter two are known to be very sensitive and insensitive to Ad5 cytotoxicity, respectively. Although all the cell lines tested expressed significantly higher levels of CD46 compared to CAR (**Figure 3.1**), no correlation between receptor expression and cytotoxicity was observed (**Figure 3.3**). In fact Ad11 was less potent than Ad5 in the majority of cancer cell lines tested *in vitro* (**Figures 3.3 and 3.5**). *In vivo*, Ad11 showed superior efficacy in treating the Ad5-insensitive PC-3 cells (**Figure 4.1**). Treatment of the Ad11-insensitive MIA PaCa-2 human pancreatic cancer xenografts showed faster tumour growth with the Ad11-treated group compared to Ad5 (**Figure 4.3**), although this was less than one would expect given the more remarkable *in vitro* result (**Figure 3.2**). A similar result was demonstrated by Shashkova *et al*.[137] with the Ad11-insensitive DU 145. The reason for this is unknown, although it could be explained by the slower clearance of Ad11 in nude mice where CAR, but not CD46, is expressed. Repeating the experiment on CD46-transgenic nude mice might shed some light to this.

The higher expression of CD46 is consistent with the much greater infectivity of Ad11, with significantly more virus particles attaching to the cellular membrane and entering the nucleus (**Figures 5.1 and 5.8**). It has been reported that after internalisation into the cell, certain subgroup B Ads (Ad3, -7 and -35) accumulate in lysosomes whereas subgroup C viruses (Ad2 and Ad5) traffic rapidly to the nuclear envelope, because the former group requires a lower pH in the endosomal compartments to escape into the cytosol[211-214]. Although it is likely that the percentage of nuclear entry relative to the total membrane-associated viruses is lower for Ad11 compared to Ad5, this is perhaps of little significance given that the absolute number of Ad11 in the nucleus is still much higher.

In cells that were insensitive to Ad11 cytotoxicity and in spite of its higher infectivity (**Figures 5.1b, d and 5.8a**), Ad11 *E1A* mRNA levels were much lower than those of Ad5 (**Figures 5.7a and 5.8a**), producing a negative effect on viral DNA amplification (**Figures 5.2a and 5.8a**), structural protein synthesis (**Figure 5.3a**), progeny production (**Figures 5.4a and 5.8a**) and cell killing (**Figure 3.2**). This is summarised in **Figure 9.1** and appears to be the case for three cancer cell lines (MIA PaCa-2, PANC-1 and LNCaP. A549, however, as discovered later, does not fit into this). *E1A* transcription is the first event to occur after virus entry into the nucleus, and the E1A proteins are important at inducing the expression of *E1B*, *E2*, *E3* and *E4*, most

of which are crucial for virus replication. Cells that were sensitive to Ad11 cytotoxicity showed higher levels of *E1A* mRNA after Ad11 infection (**Figures 5.7b and 5.8b**).

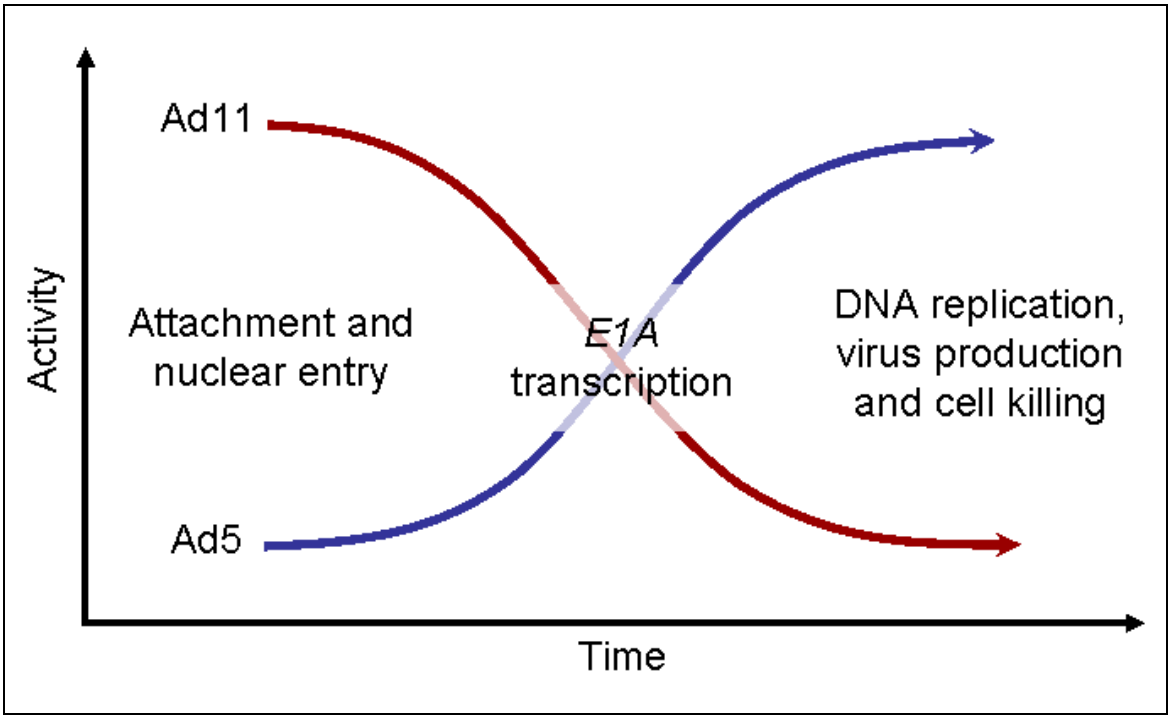


**Figure 9.1: Mechanisms of attenuated potency of Ad11 in MIA PaCa-2, PANC-1 and LNCaP.** Ad11 has higher infectivity than Ad5 but the transcription of its *E1A* gene is significantly reduced, resulting in less DNA amplification, virus production and subsequent cell killing.

## 9.2 Adenovirus *E1A* transcriptional regulation

In eukaryotes, protein-coding genes are transcribed by the enzyme RNA polymerase II. For the initiation of transcription, RNA polymerase II and transcription factors have to form a complex at the promoter region. The most highly conserved element of these promoters has the sequence TATAAA, called the TATA box, located about 25 bp upstream of the transcription start site. An enhancer is a sequence that increases the rate of transcription in an orientation- and location-independent manner.

The regulation of adenoviral *E1A* transcription is a complex issue. In Ad5, an enhancer region of *E1A* was originally identified by Hearing and Shenk in 1983[55]. This was estimated to be located between 194-358 bp relative to the left end of the viral genome, although this was later refined to 194-308 bp[56]. Deletion of this sequence could decrease transcription by a factor of 20 during the early but not late phase of infection. This region composes of element I (repeated at 200 and 300 bp), which specifically enhances *E1A* transcription, and element II (250-280 bp), which modulates in *cis* of all early viral transcriptional units[56]. A third enhancer element, the E2F binding site, is repeated at 212-219 and 275-282 bp[53]. The adenoviral packaging signal is located within the enhancer region[57, 58]. The 230-235 bp region appears to have the greatest effect on *E1A* transcription[222]. The transcription factor EF-1A was found to bind to both copies of element I and related sequences in the enhancer (200-205, 230-235 and 298-303 bp), further upstream (113-118 and 156-161 bp), as well as the *E4* enhancer region[54]. In contrast to Ad5, the *E1A* enhancer region of Ad11 does not contain binding sites for EF-1A. Cellular EF-1A expression alone, however, could not completely explain the variation in *E1A* mRNA levels seen. As shown in **Figure 6.1**, the absence of EF-1A in the Ad11-sensitive Capan-2 could explain this cell's preference to transcribe Ad11 *E1A* to Ad5's. This was not shown in the Ad11-sensitive PC-3, where EF-1A expression was similar to those of the Ad5-sensitive MIA PaCa-2 and LNCaP. EF-1A is a tetrameric protein complex composed of two α and two β subunits. The former contains the DNA-binding domain whilst the latter has the transcription-activation domain[223]. The β subunit can exist in different isoforms, but it must associate with the α subunit to interact with its target genes. Furthermore their expressions are highly concordant even when their genes are located at unlinked chromosomal loci[224]. Therefore, even though the antibody used in this study only detects the α subunit, it is believed that little extra information would be gained by using β-specific antibodies.

Besides the regulation of other early viral genes, the E1A proteins have also been found to regulate their own expression. Tibbetts *et al*.[216] found that E1A has both positive and negative effects in a temporal manner. They suggested that E1A acts to amplify *E1A* early in infection but represses transcription at later time. This is possibly related to the enhancer region[225] although no specific targets have been identified[226]. The E1A protein 243R is a repressor of transcription whereas 289R is a bifunctional activator-repressor[227]. Cogan *et al*.[228] showed that the 289R transactivating activity and the responsiveness of *E1A* promoter differ between adenoviral species. A transcriptional control region has also been found within the protein-coding sequence of Ad5 *E1A*. Osborne *et al*.[217] demonstrated that a single-base deletion 399 bases downstream from the *E1A* cap site suppressed transcription to only 2% of the wild-type rate, although Hearing *et al*.[226] found that a cellular α-globin gene substituted for *E1A* could also be positively regulated by E1A. All these factors could have played a part in the observed luciferase reporter assay results. Except for PaTu 8988s (**Figure 6.8b**), the region upstream of Ad5 *E1A* appears to have higher transcription-enhancing activity than that of Ad11, even in cells that showed higher levels of Ad11 *E1A* mRNA (**Figures 5.7b and 6.6b**). Interestingly after Ad11 infection in Capan-2, the activity of Ad11 *E1A* upstream region became similar or possibly higher than that of Ad5 after Ad5 infection (**Figure 6.7b**), possibly due to the transactivating activity of E1A proteins produced by infected cells. Nevertheless, this was not the case for PC-3, which has higher levels of Ad11 *E1A* mRNA even though its upstream region still has a much weaker activity than that of Ad5 after infection (**Figures 5.7b and 6.7b**). The reason is unknown but there are several possibilities. Perhaps this was due a higher rate of Ad5 *E1A* mRNA degradation compared to Ad11's in PC-3. As mentioned earlier the transcriptional activity of *E1A* is a time-dependent event and that the *E1A* sequence itself could play a role in its regulation. Furthermore, the higher levels of Ad11 E1A in PC-3 after infection could have negatively regulated the transcription of the luciferase reporter gene. Instead of infection, one could perhaps overcome this issue by transfecting cells with an equal amount of Ad5 or Ad11 *E1A* DNA, and measure the luciferase reporter activity at different time points. The translation of *E1A* mRNA can be downregulated by the E3 10.4K and 14.5K proteins[229], and hence it is equally important to develop an antibody against Ad11 E1A proteins so that they can be analysed by Western blotting. They could not be detected by the currently available antibodies raised against Ad2 or Ad5 E1A (results not shown). An antibody raised against the Ad11 E1A amino acid sequence with the highest surface probability (DGFPPSDEEDHEKE; produced by

GenScript) had been tested but showed significant non-specific binding even in uninfected cells (results not shown).

A previous study has shown that low levels of E1A are sufficient to initiate Ad5 replication in HeLa cells, and it was suggested that Ad5 normally produces E1A in excess of that required[230]. In an attempt to clarify this, Zheng *et al*.[231] found that high E1A levels produced by a mutant Ad5 with its *E1A* driven by the strong CMV promoter could not always enhance cytotoxicity in cancer cells. However, this work was only done on viruses lacking the *E1B 55K* gene, which has a major role in virus replication. As described in Chapter 5, mRNA levels of Ad11 *E1A* appear to correlate with viral DNA amplification. Perhaps in most cancer cells, Ad11 *E1A* expression does not reach its critical level and that by increasing this, combined with the higher of infectivity of Ad11, could result in improved virus replication and subsequent killing of cells insensitive to Ad11.

## 9.3 Recombinant Ad11 with Ad5 *E1A* enhancer and/or promoter

Given the observation that higher levels of Ad11 *E1A* mRNA are associated with better virus replication, it was hypothesised that its oncolytic potency in Ad11-insensitive cancer cells could be improved by increasing *E1A* transcription. Because the region upstream of Ad5 *E1A* has higher transcription-enhancing activity, this region was used in place of Ad11's to drive the expression of *E1A*. Ad11-Ad5-P is a recombinant Ad11 with its *E1A* promoter region replaced by that of Ad5, conserving its own packaging signal and enhancer region. Ad11-Ad5-EP on the other hand, has the whole Ad5 *E1A* enhancer (including the packaging signal) and promoter substituting the corresponding region of Ad11 (**Figure 7.1**). Contrary to the initial assumption, Ad5 packaging signal appears to work as well as its Ad11 counterpart when placed in the Ad11 backbone. The high homology of L1 52/55K between Ad5 and Ad11 might be the reason behind this[169], as it has been shown that the serotype specificity of adenoviral DNA packaging is mediated by this protein[232].

The universally-strong CMV promoter was not used to drive Ad11 *E1A* expression for a number of reasons. Firstly, Ad11-Ad5-P and Ad11-Ad5-EP were constructed to test the hypothesis that these Ad5 *E1A* regulatory regions were more active in the Ad5-sensitive cancer cell lines, given the higher levels of *E1A* mRNA observed after Ad5 infection (**Figures 5.7a and 5.8a**). Secondly the CMV promoter, unlike the *E1A* enhancer region, would not be able to modulate the expression of other early genes needed for effective virus replication. Thirdly, combining the genetic materials of two very different viruses would have safety concerns when used in future clinical studies.

Considering the high particle-to-PFU ratios of Ad11-Ad5-P (171.2 particles/PFU) and Ad11-Ad5-EP (161.5 particles/PFU) in comparison to Ad5 (8.9 particles/PFU) and Ad11 (36.9 particles/PFU), their potencies were even much greater if cells were infected using PFUs instead of particles (**Figures 8.3 and 8.5**). This ratio represents the proportion of the total number of virus particles to encapsulated, infectious particles. Due to the toxicity and immunogenicity of both infectious and non-infectious particles, particle counts rather than PFUs are normally used for experiments and clinical studies of Ads. Even when particle counts were used, the oncolytic potency of Ad11-Ad5-EP was significantly better than that of Ad11 in all the cancer cell lines tested, even in those that were already sensitive to Ad11 (**Figures 8.3 and 8.5**). There

was a vast improvement in cytotoxicity of Ad11-Ad5-EP over Ad11 in all the Ad11-insensitive cell lines. In two of these, MDA-MB-231 and HCT 116, Ad11-Ad5-EP was as efficacious as Ad5, although Ad5 remains the most potent in MIA PaCa-2, PANC-1, LNCaP and OVCAR-3. Strikingly, the lung carcinoma cell line A549 was nearly 30 times more sensitive to Ad11-Ad5-EP than to Ad5. The potency of Ad11-Ad5-P was variable in comparison to Ad11, but was always weaker than Ad11-Ad5-EP. Preliminary results with a mutant Ad11 with the Ad5 *E1A* enhancer and the human telomerase reverse transcriptase (hTERT) promoter driving *E1A* has failed to reproduce the remarkable oncolytic potency of Ad11-Ad5-EP (data not shown). This suggests that both the enhancer and promoter regions must be present for maximum efficiency.

In the Ad11-insensitive MIA PaCa-2, the *E1A* mRNA levels are Ad5 > Ad11-Ad5-EP > Ad11 > Ad11-Ad5-P (identical to the oncolytic potencies) (**Figures 8.2 and 8.6**). The reason behind the higher levels of *E1A* mRNA with Ad5 compared to those of Ad11-Ad5-EP, despite the better infectivity of the latter, is unknown. Perhaps this was due to the stronger transactivating activity of Ad5 E1A proteins on its own enhancer as well as region further upstream (**Figure 6.7a**). Intriguingly despite this, Ad11-Ad5-EP DNA amplified much more efficiently than that of Ad5 (**Figures 8.6**). As mention earlier, the *E1A* enhancer contains an element II that can increase the expression all adenoviral early transcriptional units[56]. It is possible that the small increase in Ad11 E1A proteins (which are needed for the expression of these early genes), together with the strong enhancing activity of Ad5 element II, led to a significant elevation of E1B, E2 and E4 proteins, all of which are important for viral DNA replication. As such, analysis of these proteins would be essential to determine the mechanisms involved. The subsequent production of infectious Ad11-Ad5-EP, and therefore its oncolytic potency, was however limited by events post-DNA amplification in this cell line (**Figure 8.6**). Western blot showed that the amount of hexon protein was significantly reduced.

The results with Ad11-Ad5-EP in the Ad11-sensitive cell lines Capan-2, PC-3, PaTu 8988s, MCF7 and HT-29 were unexpected (**Figures 8.3 and 8.5**). In PC-3, the oncolytic potency rankings are Ad11-Ad5-EP > Ad11-Ad5-P > Ad11 > Ad5 (consistent with viral DNA amplification and production of infectious particles), but the *E1A* mRNA levels are Ad11-Ad5-EP > Ad11 > Ad5 = Ad11-Ad5-P (**Figures 8.2 and 8.7**). The Ad11 *E1A* enhancer should theoretically be stronger given the mRNA levels

observed after Ad5 and Ad11 infections (**Figure 5.7b**). But based on the luciferase reporter assay results (**Figures 6.6b and 6.7b**), it is probable that the Ad5 *E1A* enhancer was indeed more active in PC-3, but there was a higher rate of Ad5 *E1A* mRNA degradation compared to Ad11's. Possibly by a combination of good infectivity, more stable Ad11 *E1A* mRNAs, strong Ad5 *E1A* enhancer coupled with the higher transactivating activity of Ad11 E1A proteins, Ad11-Ad5-EP managed to achieve the highest DNA amplification and virus production. The reason behind the higher replication of Ad11-Ad5-P compared to Ad11, despite its lower *E1A* mRNA levels, is unknown (**Figure 8.7**). It is possible that in PC-3, a moderate amount of Ad11 E1A was sufficient for maximum virus replication, and that the Ad5 *E1A* promoter has transcription-enhancing activity of other early viral genes.

Results with the A549 lung cancer cell line are more complicated. The oncolytic potency rankings are Ad11-Ad5-EP > Ad5 > Ad11 > Ad11-Ad5-P (**Figure 8.4**). The *E1A* mRNA and viral DNA levels are in the order of Ad11 > Ad5 > Ad11-Ad5-EP > Ad11-Ad5-P, and Ad11-Ad5-EP > Ad11 > Ad11-Ad5-P > Ad5, respectively (**Figure 8.8**). The *E1A* mRNA levels could be the result of the complex interactions between the different transactivating activities of E1A proteins and the regions at which they bind to. Also it is not known if the mRNA levels were reflective of the E1A protein levels. The highest level of Ad11-Ad5-EP DNA again was probably due to the effect of Ad5 element II on other viral early gene expression. Nevertheless, unlike in MIA PaCa-2 cells, Ad11-Ad5-EP still produced the highest number of infectious particles. This is in contrast to Ad11 and Ad11-Ad5-P, which despite having more viral DNA than Ad5, lower amounts of infectious particles were produced. Western blot showed that the synthesis of hexon protein was significantly reduced with these two viruses (**Figure 8.8**). The reason for this is unknown. It is possible that differential expressions of the E1B 55K protein, controlled by E1A and the enhancer region, might have affected the export of viral RNAs and subsequent protein translation[233]. Another probable explanation is the different packaging signals – perhaps the less efficient packaging of Ad11 and Ad11-Ad5-P resulted in rapid degradation of the empty adenoviral capsids. The adenoviral packaging domain consists of seven functional units called the A repeats because of their AT-rich nature[57, 58]. Other cellular and viral proteins can regulate the packaging of viral DNA, as observed by Grable and Hearing[234], where the activity of Ad5 packaging domain could be competed in *trans* by unlinked copies of packaging sequences. It is now known that the viral proteins IVa2, L1 52/55K and L4 22K bind to

this domain and play a key role in virion assembly[235-237]. The chicken ovalbumin upstream promoter-transcription factor (COUP-TF), Oct-1 and CCAAT displacement protein (CDP) are some of the cellular proteins that bind to the packaging elements[238, 239], although later studies have suggested that they are unlikely to be involved in packaging function[240]. Other yet unidentified proteins could well be involved[57, 237]. As the packaging signal is located within the enhancer region, regulatory proteins that bind to the enhancer could also have a dual role in transcription as well as packaging. This is an area of interest and warrants further studies.

In summary, increased *E1A* mRNA level is important, though not the sole factor, in improving viral DNA replication. Higher expression of other early genes such as *E1B*, *E2* and *E4*, mediated by the enhancer region, is likely to be involved. In some cell lines (*e.g.* Ad11-Ad5-EP in MIA PaCa-2, Ad11 in A549), events post-DNA replication become the limiting steps for effective virus production and cell killing. Regardless of the mechanisms involved, recombinant Ad11 with the Ad5 *E1A* enhancer-promoter is a more potent virus than its wild-type counterpart and should be used in the future development of oncolytic Ad11.

## 9.4 Safety issues of Ad11

Having demonstrated that Ad11 is a promising oncolytic virus, the safety concerns of Ad11 need to be addressed. Ad11 is a recognised cause of urinary tract infection, haemorrhagic cystitis and acute haemorrhagic conjunctivitis. Infection results in mild symptoms in healthy individuals but could be more severe in immunocompromised patients[241-243]. Rarely, cases of acute respiratory disease, caused by Ad11a (BC34 strain) have been reported[166-168]. There is no evidence of Ad11 oncogenicity in humans, allaying any concerns over its transforming potential[172, 244]. The ubiquitous presence of CD46 in humans suggests that it could infect any cell in the body. In human CD46-transgenic mice, Ad11 sequestration was higher than Ad5 in the lung, kidney and spleen 30 minutes after intravenous delivery, but this was not detectable at 72 hours[172]. It was rapidly cleared from the liver with no Ad11 vector-mediated transduction of hepatocytes.

The effects of Ad11 in the induction of inflammatory reactions are poorly understood. Compared to Ad5, some subgroup B Ads (Ad16 and Ad35) have been found to reduce cytokine production (interleukin (IL)-1, -6 and -12) by human peripheral blood mononuclear cells stimulated with IFN-γ and lipopolysaccharide[245]. This appears to be the result of fibre-CD46 interaction leading to the inhibition of CCAAT-enhancer-binding protein β (C/EBPβ) transcription factor expression. However, study by the same group also showed that these viruses preferentially induce Toll-like receptor-9 (TLR-9)-mediated events such as NF-κB (nuclear factor κ-light-chain-enhancer of activated B cells) activation and IFN-β expression in HeLa cells, despite the lower frequency of stimulatory cytosine-phosphate-guanine (CpG) motifs in their genomes compared to Ad5[246]. In CD46-transgenic mice, Ad11 induced more pro-inflammatory cytokines and chemokines (IL-6 and monocyte chemoattractant protein-1) than Ad5 after intravenous injection, although this was lower with the chimeric Ad5/11[147]. However, doses used are comparatively much higher ($4 \times 10^{12}$ particles/kg, assuming a mouse weighs 25 g) than those of Ad5 used in clinical trials (maximum doses of $2.5\text{-}7.5 \times 10^{10}$ particles/kg, assuming a human weighs 80 kg), where it has been well tolerated[122, 247-249].

## 9.5 Disadvantages of Ad11

The particle-to-PFU ratios of wild-type and mutant Ad11 are higher than that of Ad5. For example, the viruses used in this study have the following ratios: Ad5 (8.9 particles/PFU), Ad11 (36.9 particles/PFU), Ad11-Ad5-P (171.2 particles/PFU) and Ad11-Ad5-EP (161.5 particles/PFU). This is a drawback in terms of high-titre production. Importantly, immune responses are activated by both infectious and non-infectious particles and therefore a low particle-to-PFU ratio is desirable. Nonetheless, one could argue that the use of JH-293 cells in determining this ratio may not be most suitable for Ad11. JH-293 has been shown to be less sensitive to Ad11 than to Ad5 (**Figure 5.6**). Furthermore, plaques formed by Ad11-infected cells are less transparent than those caused by Ad5. These could have led to an overestimation of the ratio.

Although Ad11 has benefit over Ad5 in terms of the lower prevalence of serum neutralising antibodies, $CD4^+$ helper and cytotoxic T cells against one human Ad serotype may cross-react with other serotypes, resulting in virus clearance and limiting its therapeutic efficacy[250, 251]. The significance of this is unknown but it could actually be beneficial. Evidence suggests that although the innate immune response plays an important role in virus clearance, T cell-mediated responses are largely responsible for the anti-tumoural effect[81, 148, 252-254]. It is therefore possible that the presence of Ad11 antigens on infected tumour cells would be recognised by pre-existing CTLs and result in better tumour eradication.

In CD46-transgenic mice, Ad11 was found to bind to blood cells and persist much longer in the circulation than Ad5 after intravenous injection[147, 172]. This was likely to be mediated by the hexon and/or penton proteins rather than fibres, as the chimeric Ad5/11 did not show the same level of association. Binding to blood cells may decrease access of the virus to extravascular targets and thus reduce its therapeutic activity. In a study conducted by Lyons *et al.*[142], samples from a patient to whom Ad5 was administered in a clinical trial showed that > 98% of viral genomes in the blood were cell-associated, whereas nearly all viral DNA in murine blood was free in the plasma. It is therefore reasonable to conclude that the comparison between Ad5- and Ad11-blood cell association in CD46-transgenic mice cannot be extrapolated to clinical contexts. It is possible that the levels of such association may be similar between these viruses in humans. Clearly this requires additional investigation.

## 9.6 Comparison with Ad35

Ad35 was first isolated from a renal transplant recipient with interstitial pneumonia[255], and like Ad11 is mainly associated with infections of the urinary tract and in immunocompromised patients. It is a much better gene transfer vector than Ad5[202]. Ad11 and Ad35 both bind to CD46[175] and they have comparable prevalence of neutralising antibodies in the human population (7-25% and 10-31% for Ad35 and Ad11, respectively)[172, 173, 201, 202, 256, 257]. Both belong to subgroup B2 and have an overall DNA homology of > 98%, but the majority of base pair mismatches lie within the hexon and fibre genes[170]. This might explain why Ad11 is able to bind to receptor(s) other than CD46. Surprisingly Ad5/35 seems to have a higher infectivity than Ad5/11 in a number of cancer cell lines[192, 219]. The reason for this is unknown. With regards to safety, blood clearance of Ad35 was much quicker and but has significantly higher levels of sequestration in the lung and spleen of CD46-transgenic mice after intravenous injection. The levels of pro-inflammatory cytokines induced were probably similar to those of Ad11[147], so were its affinity to factor X[153] and liver toxicity[137]. To compare the oncolytic potencies of Ad11 and Ad35, MIA PaCa-2, PANC-1 (pancreatic) and PC-3 (prostate) cancer cell lines were tested (**Figure 9.2**). Ad35 caused significantly less cytotoxicity than Ad11, although this was likely due to the high particle-to-PFU ratio of Ad35 (2170.2 particles/PFU). *In vivo* efficacy of Ad35 in treating a DU 145 tumour model was reported to be the weakest in comparison to Ad5, -6 and -11[137]. Given these findings the assessment of Ad35 as an oncolytic virus was abandoned.

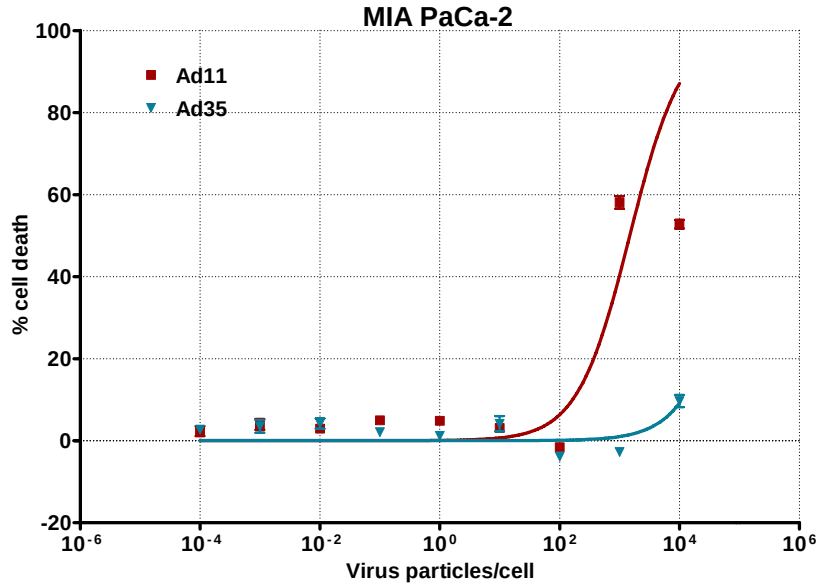

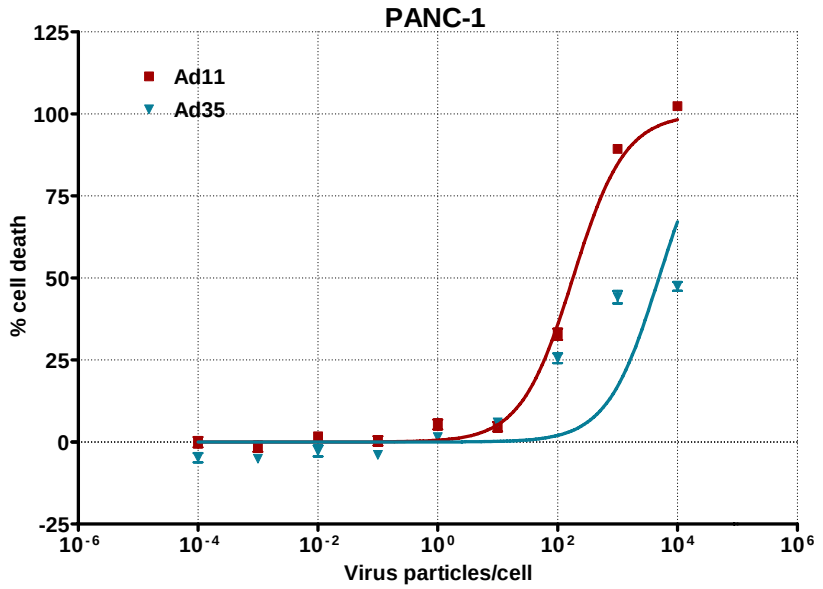


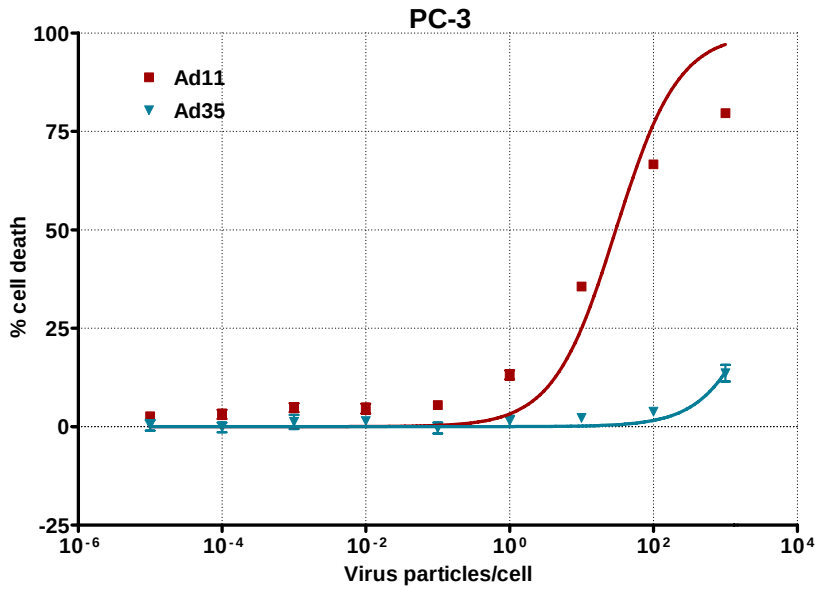


**Figure 9.2: Dose-response curves of Ad11 and Ad35 cytotoxicities in MIA PaCa-2, PANC-1 and PC-3.** Cells were infected in 96-well plates. Cell viability was measured on day six after infection by the MTS assay. Data represent means ± SEM from duplicate experiments (with each concentration of virus in sextuplicates).

## 9.7 Future direction

The potential of Ad11 as an effective oncolytic virus cannot be ignored. The much better infectivity of Ad11 compared to Ad5 means that inserted therapeutic genes would have much higher levels of expression. A variety of anti-cancer genes can be exploited, such as tumour suppressor, pro-apoptotic and anti-angiogenic genes, but for a better systemic response, immunomodulatory genes should be considered. Arming Ad11 with tumour-specific antigen is also an attractive option, given that it is more effective in transducing DCs[172, 173] and could result in a stronger immune response. Deletion of Ad11 genes such as *E3 18.5K* (*18.4K*; equivalent to *E3 gp19K* of Ad5), *20.3K* (*20.1K*) and *20.6K* (*20.8K*) (possibly involved in immune-response evasion and therefore dispensable)[169, 170, 258] could provide additional space for transgene insertion. This study has also shown that the oncolytic potency of Ad11 could be improved by replacing its *E1A* enhancer-promoter region with that from Ad5. It is believed that this should form the backbone of any future oncolytic Ad11 mutants.

Tumour selectivity is of particular importance due to the ubiquitous expression of CD46. Although CD46 was reported to be upregulated in a number of malignancies[186-188], its level in immortalised human pancreatic ductal epithelium was similar to those in the pancreatic cancer cell lines (**Figures 3.1 and 9.3**). Ad11 also replicated better than Ad5 in primary human epithelial cells (**Figure 9.4**). Approaches to improve its tumour selectivity include the deletion of the pRb-binding region of *E1A*, *E1B 55K* or *E1B 21K* (*20K*; equivalent to Ad5 *E1B 19K*)[169, 170]. As listed in **Table 1.3**, it has benefits over Ad5 in terms of attachment receptor, prevalence of neutralising antibodies and liver toxicity. It is conceivable that after achieving tumour selectivity, Ad11 would be a much safer and effective alternative to Ad5 when given intravenously to treat local and metastatic diseases. The Ad5 *10.5K* (ADP) gene, responsible for efficient lysis and release of progeny viruses from infected cells[82], is absent in Ad11[169]. As overexpression of this gene in Ad5 was found to increase cell lysis and virus spread[84, 85], this could be done for Ad11 as well.

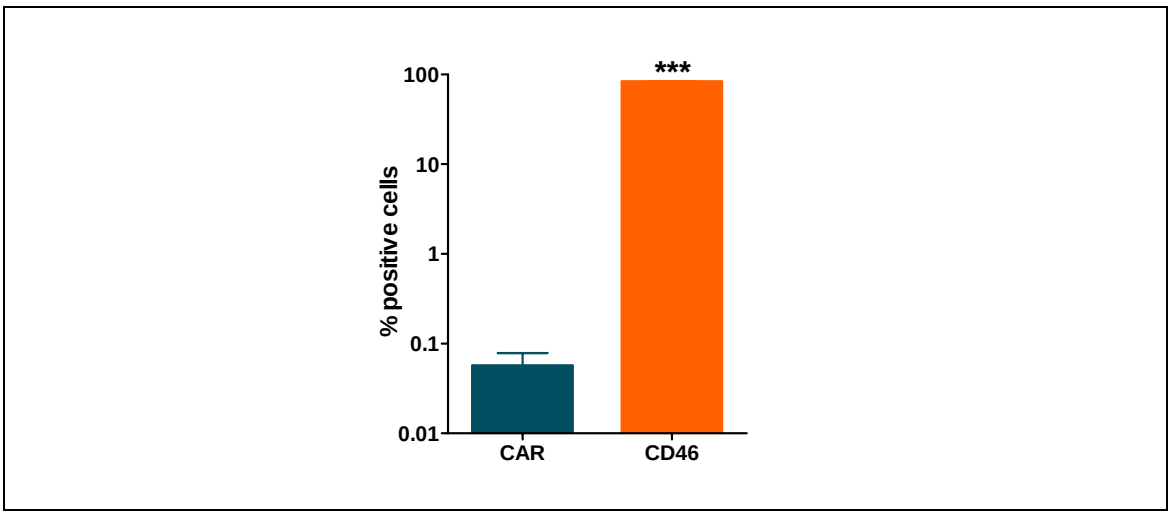


**Figure 9.3: CAR and CD46 expression levels in immortalised human pancreatic ductal epithelium.** Results represent means of triplicate readings ± SEM from flow cytometric analysis and were corrected for non-specific staining using control antibodies. Dead cells were excluded by PI staining. *** $P < 0.001$.

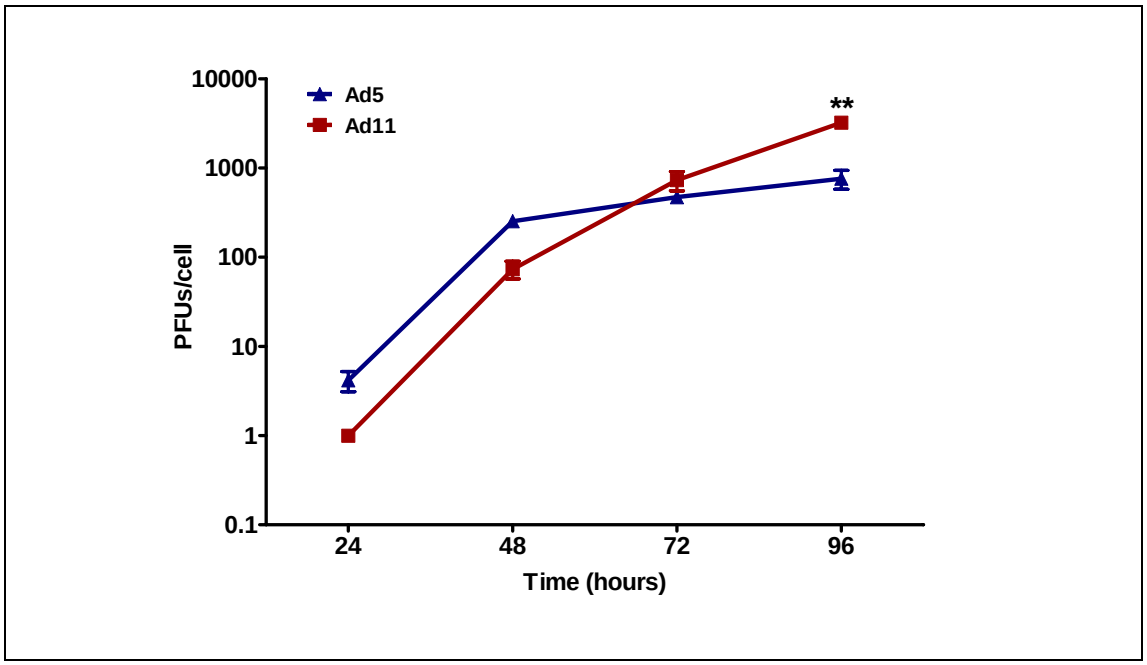


**Figure 9.4: Production of infectious Ad5 and Ad11 in normal bronchial/tracheal epithelial cells.** Cells were infected in 6-well plates with viruses at 100 particles/cell in BEGM. After two hours, this was replaced by fresh BEGM. At the stated time points post-infection, cells and media were collected, frozen and thawed three times in liquid nitrogen and at 37 °C, respectively. These were used to infect an indicator cell line, JH-293, in 96-well plates at six 1:10 serial dilutions. The cells were inspected for CPE 11 days later. The $TCID_{50}$ and number of PFUs/cell (cell count on the day of infection) were calculated using the Reed-Muench accumulative method. Results represent means of triplicate experiments ± SEM. ** $P < 0.01$.

In contrast to Ad2 and Ad5, the biology of Ad11 is less well understood. Many of its properties need to be elucidated before its full potential could be taken advantage of. These include its interactions with the host cell, *e.g.* the identity of receptor X, virus entry and trafficking, regulation of gene expression and virus replication. Greig *et al.*[259] recently demonstrated that in addition to internalisation via CD46, the presence of physiological levels of factor X can enhance Ad35 entry secondary to interaction with HSPGs. However, intracellular trafficking appears to be hindered by this HSPG pathway compared to the CD46 pathway (*i.e.* with no factor X added). It is not known if this also applies to Ad11. As shown in this study, events post-DNA replication such as virion assembly and mode of cell killing are worth exploring given that they appear to govern its oncolytic potency in some cell lines. Some Ad11 genes are of unknown function and certainly need investigating, *i.e. 20.3K* (*20.1K*), *20.6K* (*20.8K*) and *L6*[169, 170] . Its *in vivo* characteristics also require further clarification, preferably in an animal species closer to humans. Intravenous injections of chimeric Ad5/35 and Ad5/11 have been tested in baboons, in which they showed less uptake by most organs and lower levels of pro-inflammatory cytokine production (IL-6 and TNF-α) than Ad5, with the latter causing widespread endothelial damage and inflammation[260].

A major hurdle for the study of Ad11 is the lack of a suitable immunocompetent model. The use of non-human primates (such as gorillas, which unlike baboons but similar to humans, do not have CD46 on their erythrocytes[261]), although ideal, is often difficult and not practical. CD46 is widely expressed in humans, but in mice it is only found in the testes, and the homology between human and rodent CD46 is low[206, 262]. It follows that murine cells and tumours would be resistant to Ad11 infection and cytotoxicity, as shown in **Figure 9.5** with the C57BL strain-derived CMT-93 rectal carcinoma cell line. One possible method to circumvent this problem is to use human CD46-transgenic mice together with tumours engineered to express this molecule. Not only could Ad11 be tested with an intact immune system by this method, but with a CD46 expression more reflective of humans, its biodistribution and toxicity profile could be examined as well. A further improvement to this would be the use of immunodeficient CD46-transgenic mice reconstituted with human bone marrow cells (humanised mice)[263, 264]. However, the fact that Ad11 could enter a CD46-expressing murine cell does not mean that it could support virus replication, a phenomenon well known with Ad5[47, 265, 266]. Thomas *et al.*[267] reported in 2006 the use of Syrian hamster as a permissive immunocompetent model for Ad5. For this, three Syrian hamster cell lines

have been tested, namely HaK (kidney), HAP-T1 and HPD-1NR (pancreatic carcinoma), but minimal cytotoxicity was observed with Ad11 in comparison to Ad5 (**Figure 9.5**). Again this is likely to be related to CD46. Transfecting these cell lines with CD46 is a possibility, although the use of CD46-transgenic Syrian hamsters has yet to be reported.

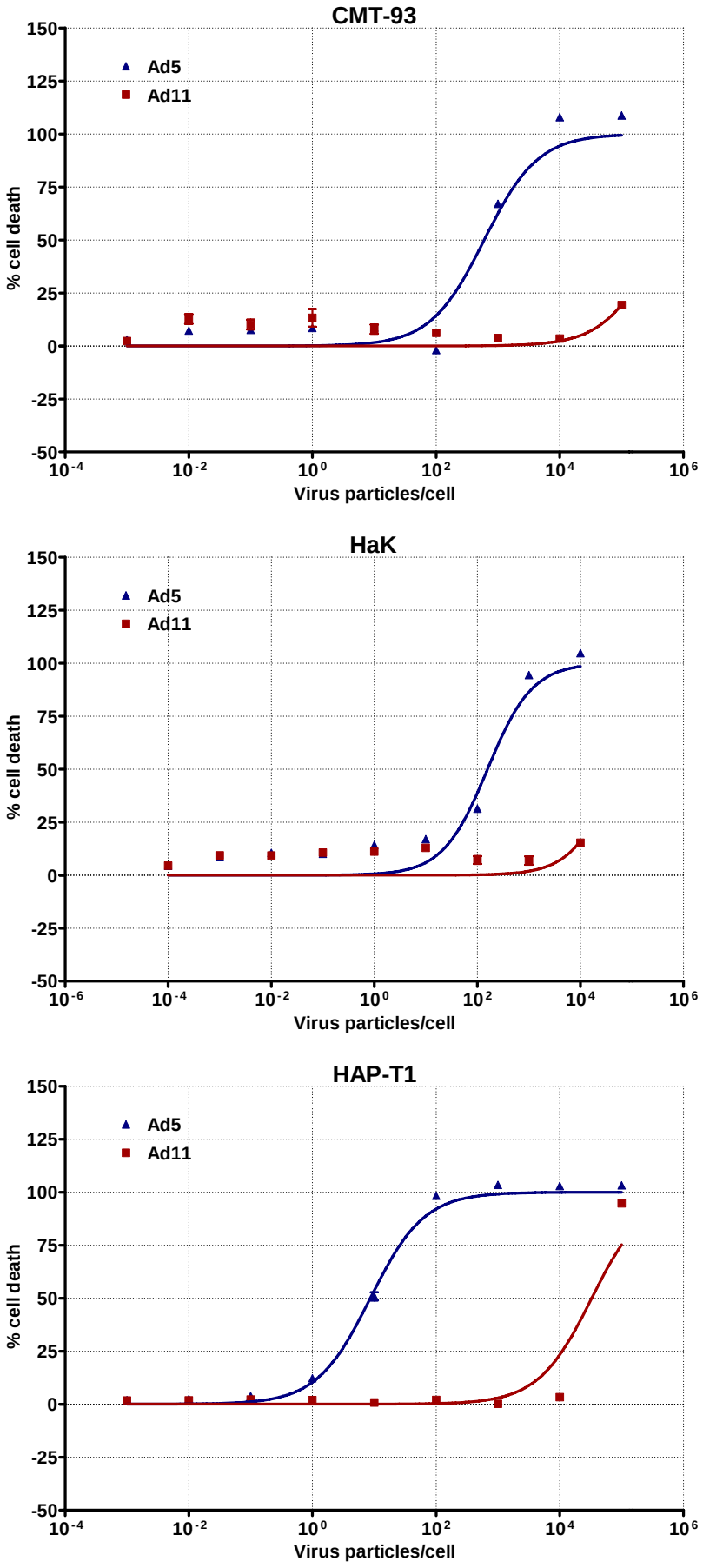
CMT-93
Ad5
Ad11
% cell death
150
125
100
75
50
25
0
-25
-50
10-4
10-2
100
102
104
106
Virus particles/cell
HaK
Ad5
Ad11
% cell death
150
125
100
75
50
25
0
-25
-50
10-6
10-4
10-2
100
102
104
106
Virus particles/cell
HAP-T1
Ad5
Ad11
% cell death
150
125
100
75
50
25
0
-25
-50
10-4
10-2
100
102
104
106
Virus particles/cell

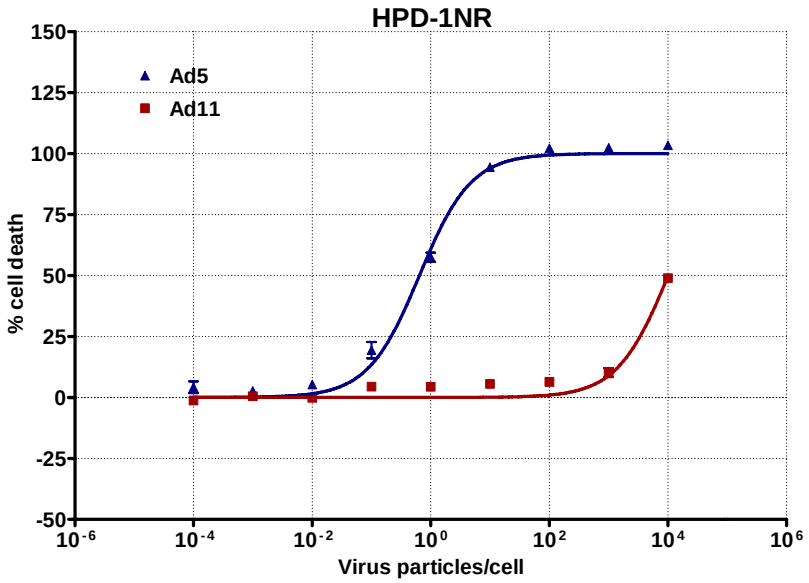


**Figure 9.5: Dose-response curves of Ad5 and Ad11 cytotoxicities in murine and Syrian (golden) hamster cell lines.** The murine CMT-93 (rectal carcinoma), the Syrian hamster HaK (kidney), HAP-T1 and HPD-1NR (exocrine pancreatic carcinoma) cell lines were infected in 96-well plates. Cell viability was measured on day six after infection by the MTS assay. Data represent means ± SEM from duplicate experiments (with each concentration of virus in sextuplicates).

# REFERENCES


1. Sultana, A. et al. Systematic review, including meta-analyses, on the management of locally advanced pancreatic cancer using radiation/combined modality therapy. *Br J Cancer* **96**, 1183-1190 (2007).
2. Jemal, A. et al. Cancer statistics, 2009. *CA Cancer J Clin* **59**, 225-249 (2009).
3. Guidelines for the management of patients with pancreatic cancer periampullary and ampullary carcinomas. *Gut* **54 Suppl 5**, v1-16 (2005).
4. Moore, M.J. et al. Erlotinib plus gemcitabine compared with gemcitabine alone in patients with advanced pancreatic cancer: a phase III trial of the National Cancer Institute of Canada Clinical Trials Group. *J Clin Oncol* **25**, 1960-1966 (2007).
5. Wong, H.H. & Lemoine, N.R. Pancreatic cancer: molecular pathogenesis and new therapeutic targets. *Nat Rev Gastroenterol Hepatol* **6**, 412-422 (2009).
6. Kelly, E. & Russell, S.J. History of oncolytic viruses: genesis to genetic engineering. *Mol Ther* **15**, 651-659 (2007).
7. Kirn, D. Replication-selective oncolytic adenoviruses: virotherapy aimed at genetic targets in cancer. *Oncogene* **19**, 6660-6669 (2000).
8. Everts, B. & van der Poel, H.G. Replication-selective oncolytic viruses in the treatment of cancer. *Cancer Gene Ther* **12**, 141-161 (2005).
9. DePace, N. Sulla scomparsa di un enorme cancro vegetante del collo dell'utero senza cura chirurgica. *Ginecologia* **9**, 82-89 (1912).
10. Hoster, H.A., Zanes, R.P., Jr. & Von Haam, E. Studies in Hodgkin's syndrome; the association of viral hepatitis and Hodgkin's disease; a preliminary report. *Cancer Res* **9**, 473-480 (1949).
11. Huebner, R.J., Rowe, W.P., Schatten, W.E., Smith, R.R. & Thomas, L.B. Studies on the use of viruses in the treatment of carcinoma of the cervix. *Cancer* **9**, 1211-1218 (1956).
12. Zielinski, T. & Jordan, E. [Remote results of clinical observation of the oncolytic action of adenoviruses on cervix cancer]. *Nowotwory* **19**, 217-221 (1969).
13. Georgiades, J., Zielinski, T., Cicholska, A. & Jordan, E. Research on the oncolytic effect of APC viruses in cancer of the cervix uteri; preliminary report. *Biul Inst Med Morsk Gdansk* **10**, 49-57 (1959).
14. Martuza, R.L., Malick, A., Markert, J.M., Ruffner, K.L. & Coen, D.M. Experimental therapy of human glioma by means of a genetically engineered virus mutant. *Science* **252**, 854-856 (1991).
15. Garber, K. China approves world's first oncolytic virus therapy for cancer treatment. *J Natl Cancer Inst* **98**, 298-300 (2006).
16. McCart, J.A. et al. Systemic cancer therapy with a tumor-selective vaccinia virus mutant lacking thymidine kinase and vaccinia growth factor genes. *Cancer Res* **61**, 8751-8757 (2001).
17. Huch, M. et al. Urokinase-type plasminogen activator receptor transcriptionally controlled adenoviruses eradicate pancreatic tumors and liver metastasis in mouse models. *Neoplasia* **11**, 518-528 (2009).
18. Pan, W., Bodempudi, V., Esfandyari, T. & Farassati, F. Utilizing ras signaling pathway to direct selective replication of herpes simplex virus-1. *PLoS One* **4**, e6514 (2009).

19. Doloff, J.C., Waxman, D.J. & Jounaidi, Y. Human telomerase reverse transcriptase promoter-driven oncolytic adenovirus with E1B-19 kDa and E1B-55 kDa gene deletions. *Hum Gene Ther* **19**, 1383-1400 (2008).
20. Hsu, K.F. et al. Conditionally replicating E1B-deleted adenovirus driven by the squamous cell carcinoma antigen 2 promoter for uterine cervical cancer therapy. *Cancer Gene Ther* **15**, 526-534 (2008).
21. Cafferata, E.G. et al. A novel A33 promoter-based conditionally replicative adenovirus suppresses tumor growth and eradicates hepatic metastases in human colon cancer models. *Clin Cancer Res* **15**, 3037-3049 (2009).
22. Hsieh, J.L. et al. Transthyretin-driven oncolytic adenovirus suppresses tumor growth in orthotopic and ascites models of hepatocellular carcinoma. *Cancer Sci* **100**, 537-545 (2009).
23. Shafren, D.R., Dorahy, D.J., Ingham, R.A., Burns, G.F. & Barry, R.D. Coxsackievirus A21 binds to decay-accelerating factor but requires intercellular adhesion molecule 1 for cell entry. *J Virol* **71**, 4736-4743 (1997).
24. Anderson, B.D., Nakamura, T., Russell, S.J. & Peng, K.W. High CD46 receptor density determines preferential killing of tumor cells by oncolytic measles virus. *Cancer Res* **64**, 4919-4926 (2004).
25. Nishimoto, T. et al. Oncolytic virus therapy for pancreatic cancer using the adenovirus library displaying random peptides on the fiber knob. *Gene Ther* **16**, 669-680 (2009).
26. Conner, J., Braidwood, L. & Brown, S.M. A strategy for systemic delivery of the oncolytic herpes virus HSV1716: redirected tropism by antibody-binding sites incorporated on the virion surface as a glycoprotein D fusion protein. *Gene Ther* **15**, 1579-1592 (2008).
27. Coughlan, L. et al. In vivo retargeting of adenovirus type 5 to alphavbeta6 integrin results in reduced hepatotoxicity and improved tumor uptake following systemic delivery. *J Virol* **83**, 6416-6428 (2009).
28. Gomes, E.M. et al. Antitumor activity of an oncolytic adenoviral-CD40 ligand (CD154) transgene construct in human breast cancer cells. *Clin Cancer Res* **15**, 1317-1325 (2009).
29. Piao, Y. et al. Oncolytic adenovirus retargeted to Delta-EGFR induces selective antiglioma activity. *Cancer Gene Ther* **16**, 256-265 (2009).
30. Morrison, J. et al. Virotherapy of ovarian cancer with polymer-cloaked adenovirus retargeted to the epidermal growth factor receptor. *Mol Ther* **16**, 244-251 (2008).
31. Allen, C. et al. Interleukin-13 displaying retargeted oncolytic measles virus strains have significant activity against gliomas with improved specificity. *Mol Ther* **16**, 1556-1564 (2008).
32. Ylosmaki, E. et al. Generation of a conditionally replicating adenovirus based on targeted destruction of E1A mRNA by a cell type-specific MicroRNA. *J Virol* **82**, 11009-11015 (2008).
33. Cawood, R. et al. Use of tissue-specific microRNA to control pathology of wild-type adenovirus without attenuation of its ability to kill cancer cells. *PLoS Pathog* **5**, e1000440 (2009).
34. Lee, C.Y., Rennie, P.S. & Jia, W.W. MicroRNA regulation of oncolytic herpes simplex virus-1 for selective killing of prostate cancer cells. *Clin Cancer Res* **15**, 5126-5135 (2009).
35. Edge, R.E. et al. A let-7 MicroRNA-sensitive vesicular stomatitis virus demonstrates tumor-specific replication. *Mol Ther* **16**, 1437-1443 (2008).
36. Kelly, E.J., Hadac, E.M., Greiner, S. & Russell, S.J. Engineering microRNA responsiveness to decrease virus pathogenicity. *Nat Med* **14**, 1278-1283 (2008).

37. Gurlevik, E. et al. p53-dependent antiviral RNA-interference facilitates tumor-selective viral replication. *Nucleic Acids Res* **37**, e84 (2009).
38. Lorence, R.M. et al. Complete regression of human fibrosarcoma xenografts after local Newcastle disease virus therapy. *Cancer Res* **54**, 6017-6021 (1994).
39. Coffey, M.C., Strong, J.E., Forsyth, P.A. & Lee, P.W. Reovirus therapy of tumors with activated Ras pathway. *Science* **282**, 1332-1334 (1998).
40. Kirn, D.H. & Thorne, S.H. Targeted and armed oncolytic poxviruses: a novel multi-mechanistic therapeutic class for cancer. *Nat Rev Cancer* **9**, 64-71 (2009).
41. Stojdl, D.F. et al. Exploiting tumor-specific defects in the interferon pathway with a previously unknown oncolytic virus. *Nat Med* **6**, 821-825 (2000).
42. Whitley, R.J., Kern, E.R., Chatterjee, S., Chou, J. & Roizman, B. Replication, establishment of latency, and induced reactivation of herpes simplex virus gamma 1 34.5 deletion mutants in rodent models. *J Clin Invest* **91**, 2837-2843 (1993).
43. Muster, T. et al. Interferon resistance promotes oncolysis by influenza virus NS1-deletion mutants. *Int J Cancer* **110**, 15-21 (2004).
44. Cascallo, M., Capella, G., Mazo, A. & Alemany, R. Ras-dependent oncolysis with an adenovirus VAI mutant. *Cancer Res* **63**, 5544-5550 (2003).
45. Wang, Y. et al. Virus-associated RNA I-deleted adenovirus, a potential oncolytic agent targeting EBV-associated tumors. *Cancer Res* **65**, 1523-1531 (2005).
46. Heise, C. et al. An adenovirus E1A mutant that demonstrates potent and selective systemic anti-tumoral efficacy. *Nat Med* **6**, 1134-1139 (2000).
47. Liu, T.C. et al. An E1B-19 kDa gene deletion mutant adenovirus demonstrates tumor necrosis factor-enhanced cancer selectivity and enhanced oncolytic potency. *Mol Ther* **9**, 786-803 (2004).
48. Bischoff, J.R. et al. An adenovirus mutant that replicates selectively in p53-deficient human tumor cells. *Science* **274**, 373-376 (1996).
49. Zheng, X. et al. Adenovirus E1B55K region is required to enhance cyclin E expression for efficient viral DNA replication. *J Virol* **82**, 3415-3427 (2008).
50. O'Shea, C.C. et al. Late viral RNA export, rather than p53 inactivation, determines ONYX-015 tumor selectivity. *Cancer Cell* **6**, 611-623 (2004).
51. Vellinga, J., Van der Heijdt, S. & Hoeben, R.C. The adenovirus capsid: major progress in minor proteins. *J Gen Virol* **86**, 1581-1588 (2005).
52. Russell, W.C. Update on adenovirus and its vectors. *J Gen Virol* **81**, 2573-2604 (2000).
53. Kovesdi, I., Reichel, R. & Nevins, J.R. Role of an adenovirus E2 promoter binding factor in E1A-mediated coordinate gene control. *Proc Natl Acad Sci U S A* **84**, 2180-2184 (1987).
54. Bruder, J.T. & Hearing, P. Nuclear factor EF-1A binds to the adenovirus E1A core enhancer element and to other transcriptional control regions. *Mol Cell Biol* **9**, 5143-5153 (1989).
55. Hearing, P. & Shenk, T. The adenovirus type 5 E1A transcriptional control region contains a duplicated enhancer element. *Cell* **33**, 695-703 (1983).
56. Hearing, P. & Shenk, T. The adenovirus type 5 E1A enhancer contains two functionally distinct domains: one is specific for E1A and the other modulates all early units in cis. *Cell* **45**, 229-236 (1986).
57. Grable, M. & Hearing, P. Adenovirus type 5 packaging domain is composed of a repeated element that is functionally redundant. *J Virol* **64**, 2047-2056 (1990).
58. Schmid, S.I. & Hearing, P. Bipartite structure and functional independence of adenovirus type 5 packaging elements. *J Virol* **71**, 3375-3384 (1997).

59. Moran, E., Grodzicker, T., Roberts, R.J., Mathews, M.B. & Zerler, B. Lytic and transforming functions of individual products of the adenovirus E1A gene. *J Virol* **57**, 765-775 (1986).
60. Pelka, P., Ablack, J.N., Fonseca, G.J., Yousef, A.F. & Mymryk, J.S. Intrinsic structural disorder in adenovirus E1A: a viral molecular hub linking multiple diverse processes. *J Virol* **82**, 7252-7263 (2008).
61. Frisch, S.M. & Mymryk, J.S. Adenovirus-5 E1A: paradox and paradigm. *Nat Rev Mol Cell Biol* **3**, 441-452 (2002).
62. Flint, J. & Shenk, T. Viral transactivating proteins. *Annu Rev Genet* **31**, 177-212 (1997).
63. Harada, J.N. & Berk, A.J. p53-Independent and -dependent requirements for E1B-55K in adenovirus type 5 replication. *J Virol* **73**, 5333-5344 (1999).
64. Perez, D. & White, E. TNF-alpha signals apoptosis through a bid-dependent conformational change in Bax that is inhibited by E1B 19K. *Mol Cell* **6**, 53-63 (2000).
65. Han, J., Modha, D. & White, E. Interaction of E1B 19K with Bax is required to block Bax-induced loss of mitochondrial membrane potential and apoptosis. *Oncogene* **17**, 2993-3005 (1998).
66. Han, J. et al. The E1B 19K protein blocks apoptosis by interacting with and inhibiting the p53-inducible and death-promoting Bax protein. *Genes Dev* **10**, 461-477 (1996).
67. Sundararajan, R. & White, E. E1B 19K blocks Bax oligomerization and tumor necrosis factor alpha-mediated apoptosis. *J Virol* **75**, 7506-7516 (2001).
68. Perez, D. & White, E. E1B 19K inhibits Fas-mediated apoptosis through FADD-dependent sequestration of FLICE. *J Cell Biol* **141**, 1255-1266 (1998).
69. Vijayalingam, S., Subramanian, T., Ryerse, J., Varvares, M. & Chinnadurai, G. Down-regulation of multiple cell survival proteins in head and neck cancer cells by an apoptogenic mutant of adenovirus type 5. *Virology* **392**, 62-72 (2009).
70. Robinson, M. et al. Comparison of the E3 and L3 regions for arming oncolytic adenoviruses to achieve a high level of tumor-specific transgene expression. *Cancer Gene Ther* **15**, 9-17 (2008).
71. Bett, A.J., Prevec, L. & Graham, F.L. Packaging capacity and stability of human adenovirus type 5 vectors. *J Virol* **67**, 5911-5921 (1993).
72. Bennett, E.M., Bennink, J.R., Yewdell, J.W. & Brodsky, F.M. Cutting edge: adenovirus E19 has two mechanisms for affecting class I MHC expression. *J Immunol* **162**, 5049-5052 (1999).
73. Hermiston, T.W., Tripp, R.A., Sparer, T., Gooding, L.R. & Wold, W.S. Deletion mutation analysis of the adenovirus type 2 E3-gp19K protein: identification of sequences within the endoplasmic reticulum lumenal domain that are required for class I antigen binding and protection from adenovirus-specific cytotoxic T lymphocytes. *J Virol* **67**, 5289-5298 (1993).
74. Blattman, J.N. & Greenberg, P.D. Cancer immunotherapy: a treatment for the masses. *Science* **305**, 200-205 (2004).
75. McSharry, B.P. et al. Adenovirus E3/19K promotes evasion of NK cell recognition by intracellular sequestration of the NKG2D ligands major histocompatibility complex class I chain-related proteins A and B. *J Virol* **82**, 4585-4594 (2008).
76. Bortolanza, S. et al. Deletion of the E3-6.7K/gp19K region reduces the persistence of wild-type adenovirus in a permissive tumor model in Syrian hamsters. *Cancer Gene Ther* **16**, 703-712 (2009).
77. Lichtenstein, D.L., Krajcsi, P., Esteban, D.J., Tollefson, A.E. & Wold, W.S. Adenovirus RIDbeta subunit contains a tyrosine residue that is critical for RID-

mediated receptor internalization and inhibition of Fas- and TRAIL-induced apoptosis. *J Virol* **76**, 11329-11342 (2002).
78. Gooding, L.R. Regulation of TNF-mediated cell death and inflammation by human adenoviruses. *Infect Agents Dis* **3**, 106-115 (1994).
79. Shisler, J., Duerksen-Hughes, P., Hermiston, T.M., Wold, W.S. & Gooding, L.R. Induction of susceptibility to tumor necrosis factor by E1A is dependent on binding to either p300 or p105-Rb and induction of DNA synthesis. *J Virol* **70**, 68-77 (1996).
80. Liu, T.C. et al. Functional interactions of antiapoptotic proteins and tumor necrosis factor in the context of a replication-competent adenovirus. *Gene Ther* **12**, 1333-1346 (2005).
81. Wang, Y. et al. E3 gene manipulations affect oncolytic adenovirus activity in immunocompetent tumor models. *Nat Biotechnol* **21**, 1328-1335 (2003).
82. Tollefson, A.E., Ryerse, J.S., Scaria, A., Hermiston, T.W. & Wold, W.S. The E3-11.6-kDa adenovirus death protein (ADP) is required for efficient cell death: characterization of cells infected with adp mutants. *Virology* **220**, 152-162 (1996).
83. Tollefson, A.E., Scaria, A., Saha, S.K. & Wold, W.S. The 11,600-MW protein encoded by region E3 of adenovirus is expressed early but is greatly amplified at late stages of infection. *J Virol* **66**, 3633-3642 (1992).
84. Zou, A., Atencio, I., Huang, W.M., Horn, M. & Ramachandra, M. Overexpression of adenovirus E3-11.6K protein induces cell killing by both caspase-dependent and caspase-independent mechanisms. *Virology* **326**, 240-249 (2004).
85. Doronin, K. et al. Overexpression of the ADP (E3-11.6K) protein increases cell lysis and spread of adenovirus. *Virology* **305**, 378-387 (2003).
86. Liu, H., Naismith, J.H. & Hay, R.T. Adenovirus DNA replication. *Curr Top Microbiol Immunol* **272**, 131-164 (2003).
87. Tauber, B. & Dobner, T. Molecular regulation and biological function of adenovirus early genes: the E4 ORFs. *Gene* **278**, 1-23 (2001).
88. Logan, J. & Shenk, T. Adenovirus tripartite leader sequence enhances translation of mRNAs late after infection. *Proc Natl Acad Sci U S A* **81**, 3655-3659 (1984).
89. Lutz, P. & Kedinger, C. Properties of the adenovirus IVa2 gene product, an effector of late-phase-dependent activation of the major late promoter. *J Virol* **70**, 1396-1405 (1996).
90. Lutz, P., Rosa-Calatrava, M. & Kedinger, C. The product of the adenovirus intermediate gene IX is a transcriptional activator. *J Virol* **71**, 5102-5109 (1997).
91. Schneider, R.J., Weinberger, C. & Shenk, T. Adenovirus VAI RNA facilitates the initiation of translation in virus-infected cells. *Cell* **37**, 291-298 (1984).
92. Schneider, R.J., Safer, B., Munemitsu, S.M., Samuel, C.E. & Shenk, T. Adenovirus VAI RNA prevents phosphorylation of the eukaryotic initiation factor 2 alpha subunit subsequent to infection. *Proc Natl Acad Sci U S A* **82**, 4321-4325 (1985).
93. Lei, M., Liu, Y. & Samuel, C.E. Adenovirus VAI RNA antagonizes the RNA-editing activity of the ADAR adenosine deaminase. *Virology* **245**, 188-196 (1998).
94. Desai, S.Y. et al. Activation of interferon-inducible 2'-5' oligoadenylate synthetase by adenoviral VAI RNA. *J Biol Chem* **270**, 3454-3461 (1995).
95. Andersson, M.G. et al. Suppression of RNA interference by adenovirus virus-associated RNA. *J Virol* **79**, 9556-9565 (2005).

96. Law, L.K. & Davidson, B.L. What does it take to bind CAR? *Mol Ther* **12**, 599-609 (2005).
97. Seiradake, E., Lortat-Jacob, H., Billet, O., Kremer, E.J. & Cusack, S. Structural and mutational analysis of human Ad37 and canine adenovirus 2 fiber heads in complex with the D1 domain of coxsackie and adenovirus receptor. *J Biol Chem* **281**, 33704-33716 (2006).
98. Arnberg, N., Edlund, K., Kidd, A.H. & Wadell, G. Adenovirus type 37 uses sialic acid as a cellular receptor. *J Virol* **74**, 42-48 (2000).
99. Wu, E. et al. Membrane cofactor protein is a receptor for adenoviruses associated with epidemic keratoconjunctivitis. *J Virol* **78**, 3897-3905 (2004).
100. Wickham, T.J., Filardo, E.J., Cheresh, D.A. & Nemerow, G.R. Integrin alpha v beta 5 selectively promotes adenovirus mediated cell membrane permeabilization. *J Cell Biol* **127**, 257-264 (1994).
101. Li, E. et al. Integrin alpha(v)beta1 is an adenovirus coreceptor. *J Virol* **75**, 5405-5409 (2001).
102. Li, E., Stupack, D., Bokoch, G.M. & Nemerow, G.R. Adenovirus endocytosis requires actin cytoskeleton reorganization mediated by Rho family GTPases. *J Virol* **72**, 8806-8812 (1998).
103. Rauma, T., Tuukkanen, J., Bergelson, J.M., Denning, G. & Hautala, T. rab5 GTPase regulates adenovirus endocytosis. *J Virol* **73**, 9664-9668 (1999).
104. Bai, M., Harfe, B. & Freimuth, P. Mutations that alter an Arg-Gly-Asp (RGD) sequence in the adenovirus type 2 penton base protein abolish its cell-rounding activity and delay virus reproduction in flat cells. *J Virol* **67**, 5198-5205 (1993).
105. Mathias, P., Wickham, T., Moore, M. & Nemerow, G. Multiple adenovirus serotypes use alpha v integrins for infection. *J Virol* **68**, 6811-6814 (1994).
106. Albinsson, B. & Kidd, A.H. Adenovirus type 41 lacks an RGD alpha(v)-integrin binding motif on the penton base and undergoes delayed uptake in A549 cells. *Virus Res* **64**, 125-136 (1999).
107. Dechecchi, M.C., Tamanini, A., Bonizzato, A. & Cabrini, G. Heparan sulfate glycosaminoglycans are involved in adenovirus type 5 and 2-host cell interactions. *Virology* **268**, 382-390 (2000).
108. Xie, J. et al. Novel fiber-dependent entry mechanism for adenovirus serotype 5 in lacrimal acini. *J Virol* **80**, 11833-11851 (2006).
109. Tuve, S. et al. Role of cellular heparan sulfate proteoglycans in infection of human adenovirus serotype 3 and 35. *PLoS Pathog* **4**, e1000189 (2008).
110. Leopold, P.L. & Crystal, R.G. Intracellular trafficking of adenovirus: many means to many ends. *Adv Drug Deliv Rev* **59**, 810-821 (2007).
111. Greber, U.F., Willetts, M., Webster, P. & Helenius, A. Stepwise dismantling of adenovirus 2 during entry into cells. *Cell* **75**, 477-486 (1993).
112. de Jong, R.N. & van der Vliet, P.C. Mechanism of DNA replication in eukaryotic cells: cellular host factors stimulating adenovirus DNA replication. *Gene* **236**, 1-12 (1999).
113. Pilder, S., Moore, M., Logan, J. & Shenk, T. The adenovirus E1B-55K transforming polypeptide modulates transport or cytoplasmic stabilization of viral and host cell mRNAs. *Mol Cell Biol* **6**, 470-476 (1986).
114. Hearing, P., Samulski, R.J., Wishart, W.L. & Shenk, T. Identification of a repeated sequence element required for efficient encapsidation of the adenovirus type 5 chromosome. *J Virol* **61**, 2555-2558 (1987).
115. Ostapchuk, P. & Hearing, P. Control of adenovirus packaging. *J Cell Biochem* **96**, 25-35 (2005).
116. Wong, H.H., Lemoine, N.R. & Wang, Y. Oncolytic viruses for cancer therapy: overcoming the obstacles. *Viruses* **2**, 78-106 (2010).

117. Ganly, I. et al. A phase I study of Onyx-015, an E1B attenuated adenovirus, administered intratumorally to patients with recurrent head and neck cancer. *Clin Cancer Res* **6**, 798-806 (2000).
118. Nemunaitis, J. et al. Selective replication and oncolysis in p53 mutant tumors with ONYX-015, an E1B-55kD gene-deleted adenovirus, in patients with advanced head and neck cancer: a phase II trial. *Cancer Res* **60**, 6359-6366 (2000).
119. Nemunaitis, J. et al. Phase II trial of intratumoral administration of ONYX-015, a replication-selective adenovirus, in patients with refractory head and neck cancer. *J Clin Oncol* **19**, 289-298 (2001).
120. Mulvihill, S. et al. Safety and feasibility of injection with an E1B-55 kDa gene-deleted, replication-selective adenovirus (ONYX-015) into primary carcinomas of the pancreas: a phase I trial. *Gene Ther* **8**, 308-315 (2001).
121. Hecht, J.R. et al. A phase I/II trial of intratumoral endoscopic ultrasound injection of ONYX-015 with intravenous gemcitabine in unresectable pancreatic carcinoma. *Clin Cancer Res* **9**, 555-561 (2003).
122. Nemunaitis, J. et al. Intravenous infusion of a replication-selective adenovirus (ONYX-015) in cancer patients: safety, feasibility and biological activity. *Gene Ther* **8**, 746-759 (2001).
123. Reid, T. et al. Intra-arterial administration of a replication-selective adenovirus (dl1520) in patients with colorectal carcinoma metastatic to the liver: a phase I trial. *Gene Ther* **8**, 1618-1626 (2001).
124. Anders, M., Christian, C., McMahon, M., McCormick, F. & Korn, W.M. Inhibition of the Raf/MEK/ERK pathway up-regulates expression of the coxsackievirus and adenovirus receptor in cancer cells. *Cancer Res* **63**, 2088-2095 (2003).
125. O'Prey, J., Wilkinson, S. & Ryan, K.M. Tumor antigen LRRC15 impedes adenoviral infection: implications for virus-based cancer therapy. *J Virol* **82**, 5933-5939 (2008).
126. Cohen, C.J. et al. The coxsackievirus and adenovirus receptor is a transmembrane component of the tight junction. *Proc Natl Acad Sci U S A* **98**, 15191-15196 (2001).
127. Wang, G. et al. E1B 55-kDa deleted, Ad5/F35 fiber chimeric adenovirus, a potential oncolytic agent for B-lymphocytic malignancies. *J Gene Med* **11**, 477-485 (2009).
128. Takayama, K. et al. A mosaic adenovirus possessing serotype Ad5 and serotype Ad3 knobs exhibits expanded tropism. *Virology* **309**, 282-293 (2003).
129. Douglas, J.T. et al. Targeted gene delivery by tropism-modified adenoviral vectors. *Nat Biotechnol* **14**, 1574-1578 (1996).
130. Thomas, M.A. et al. Immunosuppression enhances oncolytic adenovirus replication and antitumor efficacy in the Syrian hamster model. *Mol Ther* **16**, 1665-1673 (2008).
131. Ikeda, K. et al. Oncolytic virus therapy of multiple tumors in the brain requires suppression of innate and elicited antiviral responses. *Nat Med* **5**, 881-887 (1999).
132. Chen, Y., Yu, D.C., Charlton, D. & Henderson, D.R. Pre-existent adenovirus antibody inhibits systemic toxicity and antitumor activity of CN706 in the nude mouse LNCaP xenograft model: implications and proposals for human therapy. *Hum Gene Ther* **11**, 1553-1567 (2000).
133. Tsai, V. et al. Impact of human neutralizing antibodies on antitumor efficacy of an oncolytic adenovirus in a murine model. *Clin Cancer Res* **10**, 7199-7206 (2004).

134. Dhar, D., Spencer, J.F., Toth, K. & Wold, W.S. Effect of preexisting immunity on oncolytic adenovirus vector INGN 007 antitumor efficacy in immunocompetent and immunosuppressed Syrian hamsters. *J Virol* **83**, 2130-2139 (2009).
135. Dhar, D., Spencer, J.F., Toth, K. & Wold, W.S. Pre-existing immunity and passive immunity to adenovirus 5 prevents toxicity caused by an oncolytic adenovirus vector in the Syrian hamster model. *Mol Ther* **17**, 1724-1732 (2009).
136. Sandberg, L., Papareddy, P., Silver, J., Bergh, A. & Mei, Y.F. Replication-competent Ad11p vector (RCAd11p) efficiently transduces and replicates in hormone-refractory metastatic prostate cancer cells. *Hum Gene Ther* **20**, 361-373 (2009).
137. Shashkova, E.V., May, S.M. & Barry, M.A. Characterization of human adenovirus serotypes 5, 6, 11, and 35 as anticancer agents. *Virology* **394**, 311-320 (2009).
138. Senac, J.S. et al. Infection and killing of multiple myeloma by adenoviruses. *Hum Gene Ther* **21**, 179-190 (2010).
139. Komarova, S., Kawakami, Y., Stoff-Khalili, M.A., Curiel, D.T. & Pereboeva, L. Mesenchymal progenitor cells as cellular vehicles for delivery of oncolytic adenoviruses. *Mol Cancer Ther* **5**, 755-766 (2006).
140. Hakkarainen, T. et al. Human mesenchymal stem cells lack tumor tropism but enhance the antitumor activity of oncolytic adenoviruses in orthotopic lung and breast tumors. *Hum Gene Ther* **18**, 627-641 (2007).
141. Sonabend, A.M. et al. Mesenchymal stem cells effectively deliver an oncolytic adenovirus to intracranial glioma. *Stem Cells* **26**, 831-841 (2008).
142. Lyons, M. et al. Adenovirus type 5 interactions with human blood cells may compromise systemic delivery. *Mol Ther* **14**, 118-128 (2006).
143. Carlisle, R.C. et al. Human erythrocytes bind and inactivate type 5 adenovirus by presenting Coxsackie virus-adenovirus receptor and complement receptor 1. *Blood* **113**, 1909-1918 (2009).
144. Stone, D. et al. Adenovirus-platelet interaction in blood causes virus sequestration to the reticuloendothelial system of the liver. *J Virol* **81**, 4866-4871 (2007).
145. Huard, J. et al. The route of administration is a major determinant of the transduction efficiency of rat tissues by adenoviral recombinants. *Gene Ther* **2**, 107-115 (1995).
146. Alemany, R., Suzuki, K. & Curiel, D.T. Blood clearance rates of adenovirus type 5 in mice. *J Gen Virol* **81**, 2605-2609 (2000).
147. Stone, D. et al. Comparison of adenoviruses from species B, C, E, and F after intravenous delivery. *Mol Ther* **15**, 2146-2153 (2007).
148. Worgall, S., Wolff, G., Falck-Pedersen, E. & Crystal, R.G. Innate immune mechanisms dominate elimination of adenoviral vectors following in vivo administration. *Hum Gene Ther* **8**, 37-44 (1997).
149. Xu, Z., Tian, J., Smith, J.S. & Byrnes, A.P. Clearance of adenovirus by Kupffer cells is mediated by scavenger receptors, natural antibodies, and complement. *J Virol* **82**, 11705-11713 (2008).
150. Manickan, E. et al. Rapid Kupffer cell death after intravenous injection of adenovirus vectors. *Mol Ther* **13**, 108-117 (2006).
151. Tao, N. et al. Sequestration of adenoviral vector by Kupffer cells leads to a nonlinear dose response of transduction in liver. *Mol Ther* **3**, 28-35 (2001).
152. Hollon, T. Researchers and regulators reflect on first gene therapy death. *Nat Med* **6**, 6 (2000).

153. Waddington, S.N. et al. Adenovirus serotype 5 hexon mediates liver gene transfer. *Cell* **132**, 397-409 (2008).
154. Kalyuzhniy, O. et al. Adenovirus serotype 5 hexon is critical for virus infection of hepatocytes in vivo. *Proc Natl Acad Sci U S A* **105**, 5483-5488 (2008).
155. Shashkova, E.V., Doronin, K., Senac, J.S. & Barry, M.A. Macrophage depletion combined with anticoagulant therapy increases therapeutic window of systemic treatment with oncolytic adenovirus. *Cancer Res* **68**, 5896-5904 (2008).
156. Doronin, K., Shashkova, E.V., May, S.M., Hofherr, S.E. & Barry, M.A. Chemical modification with high molecular weight polyethylene glycol reduces transduction of hepatocytes and increases efficacy of intravenously delivered oncolytic adenovirus. *Hum Gene Ther* **20**, 975-988 (2009).
157. Shashkova, E.V., May, S.M., Doronin, K. & Barry, M.A. Expanded anticancer therapeutic window of hexon-modified oncolytic adenovirus. *Mol Ther* **17**, 2121-2130 (2009).
158. Seiradake, E. et al. The cell adhesion molecule "CAR" and sialic acid on human erythrocytes influence adenovirus in vivo biodistribution. *PLoS Pathog* **5**, e1000277 (2009).
159. Rebetz, J. et al. Fiber mediated receptor masking in non-infected bystander cells restricts adenovirus cell killing effect but promotes adenovirus host co-existence. *PLoS One* **4**, e8484 (2009).
160. Kibrick, S., Melendez, L. & Enders, J.F. Clinical associations of enteric viruses with particular reference to agents exhibiting properties of the ECHO group. *Ann N Y Acad Sci* **67**, 311-325 (1957).
161. Mufson, M.A. & Belshe, R.B. A review of adenoviruses in the etiology of acute hemorrhagic cystitis. *J Urol* **115**, 191-194 (1976).
162. Mufson, M.A., Belshe, R.B., Horrigan, T.J. & Zollar, L.M. Cause of acute hemorrhagic cystitis in children. *Am J Dis Child* **126**, 605-609 (1973).
163. Numazaki, Y. et al. Acute hemorrhagic cystitis in children. Isolation of adenovirus type II. *N Engl J Med* **278**, 700-704 (1968).
164. Shindo, K. et al. Acute hemorrhagic cystitis caused by adenovirus type 11 after renal transplantation. *Urol Int* **41**, 152-155 (1986).
165. Mei, Y.F., Lindman, K. & Wadell, G. Two closely related adenovirus genome types with kidney or respiratory tract tropism differ in their binding to epithelial cells of various origins. *Virology* **240**, 254-266 (1998).
166. Hierholzer, J.C., Pumarola, A., Rodriguez-Torres, A. & Beltran, M. Occurrence of respiratory illness due to an atypical strain of adenovirus type 11 during a large outbreak in Spanish military recruits. *Am J Epidemiol* **99**, 434-442 (1974).
167. Kajon, A.E. et al. Molecular epidemiology of adenovirus acute lower respiratory infections of children in the south cone of South America (1991-1994). *J Med Virol* **48**, 151-156 (1996).
168. Zhang, Z.J. et al. Acute respiratory infections in childhood in Beijing: An etiological study of pneumonia and bronchiolitis. *Chin Med J (Engl)* **99**, 695-702 (1986).
169. Mei, Y.F., Skog, J., Lindman, K. & Wadell, G. Comparative analysis of the genome organization of human adenovirus 11, a member of the human adenovirus species B, and the commonly used human adenovirus 5 vector, a member of species C. *J Gen Virol* **84**, 2061-2071 (2003).
170. Stone, D., Furthmann, A., Sandig, V. & Lieber, A. The complete nucleotide sequence, genome organization, and origin of human adenovirus type 11. *Virology* **309**, 152-165 (2003).

171. Crawford-Miksza, L. & Schnurr, D.P. Analysis of 15 adenovirus hexon proteins reveals the location and structure of seven hypervariable regions containing serotype-specific residues. *J Virol* **70**, 1836-1844 (1996).
172. Stone, D. et al. Development and assessment of human adenovirus type 11 as a gene transfer vector. *J Virol* **79**, 5090-5104 (2005).
173. Holterman, L. et al. Novel replication-incompetent vector derived from adenovirus type 11 (Ad11) for vaccination and gene therapy: low seroprevalence and non-cross-reactivity with Ad5. *J Virol* **78**, 13207-13215 (2004).
174. Segerman, A. et al. Adenovirus type 11 uses CD46 as a cellular receptor. *J Virol* **77**, 9183-9191 (2003).
175. Gaggar, A., Shayakhmetov, D.M. & Lieber, A. CD46 is a cellular receptor for group B adenoviruses. *Nat Med* **9**, 1408-1412 (2003).
176. Tuve, S. et al. A new group B adenovirus receptor is expressed at high levels on human stem and tumor cells. *J Virol* **80**, 12109-12120 (2006).
177. Zhang, L.Q., Mei, Y.F. & Wadell, G. Human adenovirus serotypes 4 and 11 show higher binding affinity and infectivity for endothelial and carcinoma cell lines than serotype 5. *J Gen Virol* **84**, 687-695 (2003).
178. Liszewski, M.K., Post, T.W. & Atkinson, J.P. Membrane cofactor protein (MCP or CD46): newest member of the regulators of complement activation gene cluster. *Annu Rev Immunol* **9**, 431-455 (1991).
179. Seya, T., Hirano, A., Matsumoto, M., Nomura, M. & Ueda, S. Human membrane cofactor protein (MCP, CD46): multiple isoforms and functions. *Int J Biochem Cell Biol* **31**, 1255-1260 (1999).
180. Dorig, R.E., Marcil, A., Chopra, A. & Richardson, C.D. The human CD46 molecule is a receptor for measles virus (Edmonston strain). *Cell* **75**, 295-305 (1993).
181. Santoro, F. et al. CD46 is a cellular receptor for human herpesvirus 6. *Cell* **99**, 817-827 (1999).
182. Rezcallah, M.S. et al. Engagement of CD46 and alpha5beta1 integrin by group A streptococci is required for efficient invasion of epithelial cells. *Cell Microbiol* **7**, 645-653 (2005).
183. Kallstrom, H., Liszewski, M.K., Atkinson, J.P. & Jonsson, A.B. Membrane cofactor protein (MCP or CD46) is a cellular pilus receptor for pathogenic Neisseria. *Mol Microbiol* **25**, 639-647 (1997).
184. Li, Y. et al. Loss of adenoviral receptor expression in human bladder cancer cells: a potential impact on the efficacy of gene therapy. *Cancer Res* **59**, 325-330 (1999).
185. Okegawa, T. et al. The dual impact of coxsackie and adenovirus receptor expression on human prostate cancer gene therapy. *Cancer Res* **60**, 5031-5036 (2000).
186. Fishelson, Z., Donin, N., Zell, S., Schultz, S. & Kirschfink, M. Obstacles to cancer immunotherapy: expression of membrane complement regulatory proteins (mCRPs) in tumors. *Mol Immunol* **40**, 109-123 (2003).
187. Kinugasa, N. et al. Expression of membrane cofactor protein (MCP, CD46) in human liver diseases. *Br J Cancer* **80**, 1820-1825 (1999).
188. Murray, K.P. et al. Expression of complement regulatory proteins-CD 35, CD 46, CD 55, and CD 59-in benign and malignant endometrial tissue. *Gynecol Oncol* **76**, 176-182 (2000).
189. Ganesh, S. et al. Combination therapy with radiation or cisplatin enhances the potency of Ad5/35 chimeric oncolytic adenovirus in a preclinical model of head and neck cancer. *Cancer Gene Ther* **16**, 383-392 (2009).

190. Zhu, Z.B. et al. Development of an optimized conditionally replicative adenoviral agent for ovarian cancer. *Int J Oncol* **32**, 1179-1188 (2008).
191. Chen, L. et al. Concomitant use of Ad5/35 chimeric oncolytic adenovirus with TRAIL gene and taxol produces synergistic cytotoxicity in gastric cancer cells. *Cancer Lett* **284**, 141-148 (2009).
192. Yu, L. et al. Adenovirus type 5 substituted with type 11 or 35 fiber structure increases its infectivity to human cells enabling dual gene transfer in CD46-dependent and -independent manners. *Anticancer Res* **27**, 2311-2316 (2007).
193. Short, J.J., Vasu, C., Holterman, M.J., Curiel, D.T. & Pereboev, A. Members of adenovirus species B utilize CD80 and CD86 as cellular attachment receptors. *Virus Res* **122**, 144-153 (2006).
194. Short, J.J. et al. Adenovirus serotype 3 utilizes CD80 (B7.1) and CD86 (B7.2) as cellular attachment receptors. *Virology* **322**, 349-359 (2004).
195. Di Guilmi, A.M., Barge, A., Kitts, P., Gout, E. & Chroboczek, J. Human adenovirus serotype 3 (Ad3) and the Ad3 fiber protein bind to a 130-kDa membrane protein on HeLa cells. *Virus Res* **38**, 71-81 (1995).
196. Sakurai, F., Akitomo, K., Kawabata, K., Hayakawa, T. & Mizuguchi, H. Downregulation of human CD46 by adenovirus serotype 35 vectors. *Gene Ther* **14**, 912-919 (2007).
197. Strauss, R. et al. Epithelial phenotype confers resistance of ovarian cancer cells to oncolytic adenoviruses. *Cancer Res* **69**, 5115-5125 (2009).
198. Segerman, A., Mei, Y.F. & Wadell, G. Adenovirus types 11p and 35p show high binding efficiencies for committed hematopoietic cell lines and are infective to these cell lines. *J Virol* **74**, 1457-1467 (2000).
199. Mei, Y.F. et al. Human hematopoietic (CD34+) stem cells possess high-affinity receptors for adenovirus type 11p. *Virology* **328**, 198-207 (2004).
200. Mei, Y.F., Lindman, K. & Wadell, G. Human adenoviruses of subgenera B, C, and E with various tropisms differ in both binding to and replication in the epithelial A549 and 293 cells. *Virology* **295**, 30-43 (2002).
201. Kostense, S. et al. Adenovirus types 5 and 35 seroprevalence in AIDS risk groups supports type 35 as a vaccine vector. *Aids* **18**, 1213-1216 (2004).
202. Seshidhar Reddy, P. et al. Development of adenovirus serotype 35 as a gene transfer vector. *Virology* **311**, 384-393 (2003).
203. Lemckert, A.A. et al. Immunogenicity of heterologous prime-boost regimens involving recombinant adenovirus serotype 11 (Ad11) and Ad35 vaccine vectors in the presence of anti-ad5 immunity. *J Virol* **79**, 9694-9701 (2005).
204. Sumida, S.M. et al. Neutralizing antibodies to adenovirus serotype 5 vaccine vectors are directed primarily against the adenovirus hexon protein. *J Immunol* **174**, 7179-7185 (2005).
205. Lore, K. et al. Myeloid and plasmacytoid dendritic cells are susceptible to recombinant adenovirus vectors and stimulate polyfunctional memory T cell responses. *J Immunol* **179**, 1721-1729 (2007).
206. Tsujimura, A. et al. Molecular cloning of a murine homologue of membrane cofactor protein (CD46): preferential expression in testicular germ cells. *Biochem J* **330 ( Pt 1)**, 163-168 (1998).
207. Kemper, C. et al. Membrane cofactor protein (MCP; CD46) expression in transgenic mice. *Clin Exp Immunol* **124**, 180-189 (2001).
208. Liu, N., Furukawa, T., Kobari, M. & Tsao, M.S. Comparative phenotypic studies of duct epithelial cell lines derived from normal human pancreas and pancreatic carcinoma. *Am J Pathol* **153**, 263-269 (1998).

209. Bradford, M.M. A rapid and sensitive method for the quantitation of microgram quantities of protein utilizing the principle of protein-dye binding. *Anal Biochem* **72**, 248-254 (1976).
210. Nakano, M.Y. & Greber, U.F. Quantitative microscopy of fluorescent adenovirus entry. *J Struct Biol* **129**, 57-68 (2000).
211. Miyazawa, N. et al. Fiber swap between adenovirus subgroups B and C alters intracellular trafficking of adenovirus gene transfer vectors. *J Virol* **73**, 6056-6065 (1999).
212. Miyazawa, N., Crystal, R.G. & Leopold, P.L. Adenovirus serotype 7 retention in a late endosomal compartment prior to cytosol escape is modulated by fiber protein. *J Virol* **75**, 1387-1400 (2001).
213. Defer, C., Belin, M.T., Caillet-Boudin, M.L. & Boulanger, P. Human adenovirus-host cell interactions: comparative study with members of subgroups B and C. *J Virol* **64**, 3661-3673 (1990).
214. Shayakhmetov, D.M. et al. The interaction between the fiber knob domain and the cellular attachment receptor determines the intracellular trafficking route of adenoviruses. *J Virol* **77**, 3712-3723 (2003).
215. Schug, J. Using TESS to predict transcription factor binding sites in DNA sequence. *Curr Protoc Bioinformatics* **Chapter 2**, Unit 2 6 (2008).
216. Tibbetts, C., Larsen, P.L. & Jones, S.N. Autoregulation of adenovirus E1A gene expression. *J Virol* **57**, 1055-1064 (1986).
217. Osborne, T.F., Arvidson, D.N., Tyau, E.S., Dunsworth-Browne, M. & Berk, A.J. Transcription control region within the protein-coding portion of adenovirus E1A genes. *Mol Cell Biol* **4**, 1293-1305 (1984).
218. Benlahrech, A. et al. Adenovirus vector vaccination induces expansion of memory CD4 T cells with a mucosal homing phenotype that are readily susceptible to HIV-1. *Proc Natl Acad Sci U S A* **106**, 19940-19945 (2009).
219. Yu, L. et al. Increased infectivity of adenovirus type 5 bearing type 11 or type 35 fibers to human esophageal and oral carcinoma cells. *Oncol Rep* **14**, 831-835 (2005).
220. Stecher, H., Shayakhmetov, D.M., Stamatoyannopoulos, G. & Lieber, A. A capsid-modified adenovirus vector devoid of all viral genes: assessment of transduction and toxicity in human hematopoietic cells. *Mol Ther* **4**, 36-44 (2001).
221. Yotnda, P. et al. Comparison of the efficiency of transduction of leukemic cells by fiber-modified adenoviruses. *Hum Gene Ther* **15**, 1229-1242 (2004).
222. Bruder, J.T. & Hearing, P. Cooperative binding of EF-1A to the E1A enhancer region mediates synergistic effects on E1A transcription during adenovirus infection. *J Virol* **65**, 5084-5087 (1991).
223. Rosmarin, A.G., Resendes, K.K., Yang, Z., McMillan, J.N. & Fleming, S.L. GA-binding protein transcription factor: a review of GABP as an integrator of intracellular signaling and protein-protein interactions. *Blood Cells Mol Dis* **32**, 143-154 (2004).
224. de la Brousse, F.C., Birkenmeier, E.H., King, D.S., Rowe, L.B. & McKnight, S.L. Molecular and genetic characterization of GABP beta. *Genes Dev* **8**, 1853-1865 (1994).
225. Jones, S.N. & Tibbetts, C. Upstream DNA sequences determine different autoregulatory responses of the adenovirus types 5 and 3 E1A promoters. *J Virol* **63**, 1833-1838 (1989).
226. Hearing, P. & Shenk, T. Sequence-independent autoregulation of the adenovirus type 5 E1A transcription unit. *Mol Cell Biol* **5**, 3214-3221 (1985).

227. Lillie, J.W., Loewenstein, P.M., Green, M.R. & Green, M. Functional domains of adenovirus type 5 E1a proteins. *Cell* **50**, 1091-1100 (1987).
228. Cogan, J.D., Jones, S.N., Hall, R.K. & Tibbetts, C. Functional diversity of E1A gene autoregulation among human adenoviruses. *J Virol* **66**, 3833-3845 (1992).
229. Zhang, X. et al. Down-regulation of human adenovirus E1a by E3 gene products: evidence for translational control of E1a by E3 14.5K and/or E3 10.4K products. *J Gen Virol* **75 ( Pt 8)**, 1943-1951 (1994).
230. Hitt, M.M. & Graham, F.L. Adenovirus E1A under the control of heterologous promoters: wide variation in E1A expression levels has little effect on virus replication. *Virology* **179**, 667-678 (1990).
231. Zheng, X. et al. Adenoviral E1a expression levels affect virus-selective replication in human cancer cells. *Cancer Biol Ther* **4**, 1255-1262 (2005).
232. Wohl, B.P. & Hearing, P. Role for the L1-52/55K protein in the serotype specificity of adenovirus DNA packaging. *J Virol* **82**, 5089-5092 (2008).
233. Babiss, L.E., Ginsberg, H.S. & Darnell, J.E., Jr. Adenovirus E1B proteins are required for accumulation of late viral mRNA and for effects on cellular mRNA translation and transport. *Mol Cell Biol* **5**, 2552-2558 (1985).
234. Grable, M. & Hearing, P. cis and trans requirements for the selective packaging of adenovirus type 5 DNA. *J Virol* **66**, 723-731 (1992).
235. Perez-Romero, P., Tyler, R.E., Abend, J.R., Dus, M. & Imperiale, M.J. Analysis of the interaction of the adenovirus L1 52/55-kilodalton and IVa2 proteins with the packaging sequence in vivo and in vitro. *J Virol* **79**, 2366-2374 (2005).
236. Tyler, R.E., Ewing, S.G. & Imperiale, M.J. Formation of a multiple protein complex on the adenovirus packaging sequence by the IVa2 protein. *J Virol* **81**, 3447-3454 (2007).
237. Ostapchuk, P., Anderson, M.E., Chandrasekhar, S. & Hearing, P. The L4 22-kilodalton protein plays a role in packaging of the adenovirus genome. *J Virol* **80**, 6973-6981 (2006).
238. Schmid, S.I. & Hearing, P. Cellular components interact with adenovirus type 5 minimal DNA packaging domains. *J Virol* **72**, 6339-6347 (1998).
239. Erturk, E. et al. Binding of CCAAT displacement protein CDP to adenovirus packaging sequences. *J Virol* **77**, 6255-6264 (2003).
240. Ostapchuk, P., Yang, J., Auffarth, E. & Hearing, P. Functional interaction of the adenovirus IVa2 protein with adenovirus type 5 packaging sequences. *J Virol* **79**, 2831-2838 (2005).
241. Hierholzer, J.C. Adenoviruses in the immunocompromised host. *Clin Microbiol Rev* **5**, 262-274 (1992).
242. Zahradnik, J.M., Spencer, M.J. & Porter, D.D. Adenovirus infection in the immunocompromised patient. *Am J Med* **68**, 725-732 (1980).
243. Fiala, M. et al. Role of adenovirus type 11 in hemorrhagic cystitis secondary to immunosuppression. *J Urol* **112**, 595-597 (1974).
244. Wold, W.S., Mackey, J.K., Rigden, P. & Green, M. Analysis of human cancer DNA's for DNA sequence of human adenovirus serotypes 3, 7, 11, 14, 16, and 21 in group B1. *Cancer Res* **39**, 3479-3484 (1979).
245. Iacobelli-Martinez, M., Nepomuceno, R.R., Connolly, J. & Nemerow, G.R. CD46-utilizing adenoviruses inhibit C/EBPbeta-dependent expression of proinflammatory cytokines. *J Virol* **79**, 11259-11268 (2005).
246. Iacobelli-Martinez, M. & Nemerow, G.R. Preferential activation of Toll-like receptor nine by CD46-utilizing adenoviruses. *J Virol* **81**, 1305-1312 (2007).
247. Nemunaitis, J. et al. Pilot trial of intravenous infusion of a replication-selective adenovirus (ONYX-015) in combination with chemotherapy or IL-2 treatment in refractory cancer patients. *Cancer Gene Ther* **10**, 341-352 (2003).

248. Hamid, O. et al. Phase II trial of intravenous CI-1042 in patients with metastatic colorectal cancer. *J Clin Oncol* **21**, 1498-1504 (2003).
249. Small, E.J. et al. A phase I trial of intravenous CG7870, a replication-selective, prostate-specific antigen-targeted oncolytic adenovirus, for the treatment of hormone-refractory, metastatic prostate cancer. *Mol Ther* **14**, 107-117 (2006).
250. Heemskerk, B. et al. Extensive cross-reactivity of CD4+ adenovirus-specific T cells: implications for immunotherapy and gene therapy. *J Virol* **77**, 6562-6566 (2003).
251. Smith, C.A., Woodruff, L.S., Rooney, C. & Kitchingman, G.R. Extensive cross-reactivity of adenovirus-specific cytotoxic T cells. *Hum Gene Ther* **9**, 1419-1427 (1998).
252. Wakimoto, H., Johnson, P.R., Knipe, D.M. & Chiocca, E.A. Effects of innate immunity on herpes simplex virus and its ability to kill tumor cells. *Gene Ther* **10**, 983-990 (2003).
253. Diaz, R.M. et al. Oncolytic immunovirotherapy for melanoma using vesicular stomatitis virus. *Cancer Res* **67**, 2840-2848 (2007).
254. Zamarin, D. et al. Enhancement of oncolytic properties of recombinant newcastle disease virus through antagonism of cellular innate immune responses. *Mol Ther* **17**, 697-706 (2009).
255. Stalder, H., Hierholzer, J.C. & Oxman, M.N. New human adenovirus (candidate adenovirus type 35) causing fatal disseminated infection in a renal transplant recipient. *J Clin Microbiol* **6**, 257-265 (1977).
256. Vogels, R. et al. Replication-deficient human adenovirus type 35 vectors for gene transfer and vaccination: efficient human cell infection and bypass of preexisting adenovirus immunity. *J Virol* **77**, 8263-8271 (2003).
257. Ophorst, O.J. et al. Immunogenicity and protection of a recombinant human adenovirus serotype 35-based malaria vaccine against Plasmodium yoelii in mice. *Infect Immun* **74**, 313-320 (2006).
258. Hawkins, L.K. & Wold, W.S. A 20,500-Dalton protein is coded by region E3 of subgroup B but not subgroup C human adenoviruses. *Virology* **208**, 226-233 (1995).
259. Greig, J.A. et al. Influence of coagulation factor x on in vitro and in vivo gene delivery by adenovirus (Ad) 5, Ad35, and chimeric Ad5/Ad35 vectors. *Mol Ther* **17**, 1683-1691 (2009).
260. Ni, S. et al. Evaluation of biodistribution and safety of adenovirus vectors containing group B fibers after intravenous injection into baboons. *Hum Gene Ther* **16**, 664-677 (2005).
261. Nickells, M.W. & Atkinson, J.P. Characterization of CR1- and membrane cofactor protein-like proteins of two primates. *J Immunol* **144**, 4262-4268 (1990).
262. Mead, R., Hinchliffe, S.J. & Morgan, B.P. Molecular cloning, expression and characterization of the rat analogue of human membrane cofactor protein (MCP/CD46). *Immunology* **98**, 137-143 (1999).
263. Namikawa, R., Weilbaecher, K.N., Kaneshima, H., Yee, E.J. & McCune, J.M. Long-term human hematopoiesis in the SCID-hu mouse. *J Exp Med* **172**, 1055-1063 (1990).
264. Ito, M. et al. NOD/SCID/gamma(c)(null) mouse: an excellent recipient mouse model for engraftment of human cells. *Blood* **100**, 3175-3182 (2002).
265. Duncan, S.J. et al. Infection of mouse liver by human adenovirus type 5. *J Gen Virol* **40**, 45-61 (1978).

266. Ginsberg, H.S. et al. A mouse model for investigating the molecular pathogenesis of adenovirus pneumonia. *Proc Natl Acad Sci U S A* **88**, 1651-1655 (1991).
267. Thomas, M.A. et al. Syrian hamster as a permissive immunocompetent animal model for the study of oncolytic adenovirus vectors. *Cancer Res* **66**, 1270-1276 (2006).
268. Reed, L.J. & Muench, H. A simple method of estimating fifty percent endpoints. *Am J Hyg* **27**, 493-497 (1938).

# APPENDIX

## i. Reed-Muench accumulative method for $TCID_{50}$ determination[268]

Example of a 96-well plate (+ indicates well with evidence of CPE):

| **Dilution** | | | | | | | | | | | | | **% with CPE** |
|---|---|---|---|---|---|---|---|---|---|---|---|---|---|
| $10^{-3}$ | + | + | + | + | + | + | + | + | + | + | + | + | 100% |
| $10^{-4}$ | + | + | + | + | + | + | + | + | + | + | + | + | 100% |
| $10^{-5}$ | + | + | + | + | + | + | + | + | + | + | + | + | 100% |
| $10^{-6}$ | | + | + | | | + | | + | | | | + | 42% |
| $10^{-7}$ | | | | | | | | | | | | | 0% |
| $10^{-8}$ | | | | | | | | | | | | | 0% |
| $10^{-9}$ | | | | | | | | | | | | | 0% |
| Negative controls | | | | | | | | | | | | | |

- Calculate the proportionate distance: (% next above 50% - 50%) / (% next above 50% - % next below 50%) = (100% - 50%) / (100% - 42%) = 0.86
- Calculate the 50% end point: $\log_{10}$ (dilution in which position is next above 50%) = $\log_{10}\ 10^{-5} = -5$
- Combine the values to obtain $\log_{10}\ TCID_{50} = -5 - 0.86 = -5.86$
- $TCID_{50}$ titre = $10^{-5.86}$ (or 1 in $7.24 \times 10^5$ dilution of the amount added to the top row). As 22 µl (0.022 ml) was added to the top row, $TCID_{50}$/ml = $7.24 \times 10^5 / 0.022 = 3.29 \times 10^7$
- Multiply by a constant: $3.29 \times 10^7 \times 0.69 = 2.27 \times 10^7$ PFUs/ml
- For PFUs/cell, multiply the above with the volume of virus added to each well of the 6-well plate (2 ml) and divide by the cell count on the day of infection (*e.g.* $2.4 \times 10^5$): $(2.27 \times 10^7 \times 2) / 2.4 \times 10^5 = 189$ PFUs/cell

## ii. Solutions for virus purification

a) TD solution (diluent for CsCl)

| Component | Amount (g/L) | Final concentration (mM) |
|---|---|---|
| NaCl | 0.8 | 14 |
| KCl | 0.38 | 5 |
| $Na_2HPO_4$ | 0.1 | 0.7 |
| Tris base | 3 | 25 |

pH was adjusted to 7.5 by addition of HCl and the solution made up to 1 L.

b) CsCl solutions

| Density (g/ml) | g/100 ml of TD solution |
|---|---|
| 1.25 | 36.16 |
| 1.35 | 51.2 |
| 1.4 | 62 |

c) TSG buffer

| Solution A | Final concentration (mM) |
|---|---|
| 900 ml water | - |
| 8 g NaCl | 137 |
| 0.1 g $Na_2HPO_4$ | 0.7 |
| 0.3 g KCl | 4 |
| **Solution B** | |
| 100 ml water | - |
| 2 g $MgCl_2$ | 98 |
| 2 g $CaCl_2$ | 136 |

TSG buffer was made up as follows: 700 ml solution A + 3.5 ml solution B + 300 ml glycerol. The mixture was then heated by microwave and filter sterilised.

d) Dialysis solution

| Component | Volume (ml) | Final concentration |
|---|---|---|
| 1 M Tris-HCl, pH 7.5 | 20 | 10 mM |
| 1 M $MgCl_2$ | 2 | 1 mM |
| 5 M NaCl | 60 | 150 mM |
| Glycerol | 200 | 10% |
| Water | 1718 | - |

## iii. Reagents for SDS-PAGE and Western blotting

a) 10% running gel

| Reagent | Volume |
|---|---|
| ProtoGel (30%) (National Diagnostics, Georgia, USA) – 30% (w/v) acrylamide/methylene bisacrylamide solution (37.5:1 ratio) | 2.3 ml |
| ProtoGel Resolving Buffer (4x) (National Diagnostics) – 1.5 M Tris-HCl, 0.4% SDS, pH 8.8 | 1.75 ml |
| Water | 2.842 ml |
| TEMED (Sigma-Aldrich) | 7 µl |
| 10% ammonium persulfate (Sigma-Aldrich) | 70 µl |

b) 4% stacking gel

| Reagent | Volume |
|---|---|
| ProtoGel (30%) | 0.39 ml |
| ProtoGel Stacking Buffer (4x) (National Diagnostics) – 0.5 M Tris-HCl, 0.4% SDS, pH 6.8 | 0.75 ml |
| Water | 1.83 ml |
| TEMED | 3 µl |
| 10% ammonium persulfate | 15 µl |

c) Lysis buffer: 50 mM Tris-HCl, pH 8.0, 150 mM NaCl, 1% Nonidet P-40 (Sigma-Aldrich), one Complete Protease Inhibitor Cocktail Tablet (Roche, Basel, Switzerland) – made in 50 ml volume.

d) 5x SDS-PAGE loading buffer: 2.25 ml 1 M Tris-HCl, pH 6.8, 5 ml glycerol, 0.5 g SDS, 5 mg bromophenol blue, 2.5 ml 1 M dithiolthreitol.

e) 10x SDS-PAGE running buffer: 30.3 g Tris base, 144 g glycine, 10 g SDS, 1 L water. Diluted to 1x prior to use.

f) 1x transfer buffer: 28.8 g glycine, 6.04 g Tris base, 200 ml methanol, water (to a final volume of 2 L).

g) 1x TBST: 8.8 g NaCl, 0.2 g KCl, 3 g Tris base, 500 µl Tween 20, water (to a final volume of 1 L and pH adjusted to 7.4).

## iv. Peer-reviewed publications on pancreatic cancer and oncolytic virus

# Pancreatic cancer: molecular pathogenesis and new therapeutic targets

*Han H. Wong and Nicholas R. Lemoine*

**Abstract** | Patients with pancreatic cancer normally present with advanced disease that is lethal and notoriously difficult to treat. Survival has not improved dramatically despite routine use of chemotherapy and radiotherapy; this situation signifies an urgent need for novel therapeutic approaches. Over the past decade, a large number of studies have been published that aimed to target the molecular abnormalities implicated in pancreatic tumor growth, invasion, metastasis, angiogenesis and resistance to apoptosis. This research is of particular importance, as data suggest that a large number of genetic alterations affect only a few major signaling pathways and processes involved in pancreatic tumorigenesis. Although laboratory results of targeted therapies have been impressive, until now only erlotinib, an epidermal growth factor receptor tyrosine kinase inhibitor, has demonstrated modest survival benefit in combination with gemcitabine in a phase III clinical trial. Whilst the failures of targeted therapies in the clinical setting are discouraging, lessons have been learnt and new therapeutic targets that hold promise for the future management of the disease are continuously emerging. This Review describes some of the important developments and targeted agents for pancreatic cancer that have been tested in clinical trials.

Wong, H. H. & Lemoine, N. R. *Nat. Rev. Gastroenterol. Hepatol.* **6**, 412–422 (2009); published online 9 June 2009; doi:10.1038/nrgastro.2009.89

## Introduction

Pancreatic cancer remains an important health problem. Known risk factors for the disease include cigarette smoking, chronic and hereditary pancreatitis, late-onset diabetes mellitus and familial cancer syndromes. Pancreatic cancer is one of the most difficult conditions to treat, although it only accounts for 3% of all cancers; 5-year survival is about 5% in patients with the disease and this figure has remained largely unchanged over the past 25 years.[1] The majority of patients present with locally advanced or metastatic disease, and such individuals have a median survival of 6–10 months and 3–6 months, respectively.[2] Although 10–15% of patients have potentially resectable tumors, many experience recurrence of disease following surgery. Gemcitabine is the standard chemotherapeutic drug for patients with advanced pancreatic cancer, after a phase III trial in 1997 demonstrated a modest survival advantage of this agent over 5-fluorouracil (median survival 5.65 months versus 4.41 months, $P = 0.0025$), and improved alleviation of disease-related symptoms.[3] Given the limited effect of conventional therapies, however, a desperate need for improved diagnostic and treatment modalities remains. Considerable resources have been channeled to the development of novel therapies that target the molecular aberrations of the disease (Table 1). These targeted therapies are designed to disable the cellular pathways that are essential for cancer to survive. Targeted therapies could also be used in a multimodal treatment regimen in combination with standard radiotherapy and chemotherapy to improve outcomes and overcome drug resistance. In 2008, detailed, global, genomic analyses found that a large number of genetic alterations (an average of 63) affect only a core set of 12 signaling pathways and processes that are genetically altered in 67–100% of cases of pancreatic cancer.[4] These data suggest that treatments for pancreatic cancer should target these complex and overlapping signaling pathways, rather than just the products of a single gene (Figure 1). This Review describes some of the important developments in therapies for pancreatic cancer that have been tested both in the laboratory and, most importantly, in subsequent clinical trials.

Centre for Molecular Oncology and Imaging (**H. H. Wong**), Institute of Cancer (**N. R. Lemoine**), Barts and The London School of Medicine and Dentistry, Queen Mary University of London, London, UK.

Correspondence: N. R. Lemoine, Institute of Cancer, Barts and The London School of Medicine and Dentistry, Queen Mary University of London, Charterhouse Square, London EC1M 6BQ, UK
n.r.lemoine@qmul.ac.uk

**Competing interests**
The authors declare no competing interests.

## Targeted therapies in clinical trials

### Signal-transduction pathways

#### *The Ras pathway*

*KRAS* is a member of the *Ras* family of genes, which encode membrane-bound GTP-binding proteins. When activated by signaling partners, such as the epidermal growth factor receptor (EGFR), Ras proteins release GDP in exchange for GTP, which converts the Ras protein to the 'on' state and activates downstream signaling events, such as the Raf, MAP2K, MAPK and the PI3K–Akt cascades (Figure 2). These events are usually short-lived by virtue of the intrinsic GTPase activity of Ras proteins, which switches these proteins' effects 'off'. Mutations of *KRAS*, mostly at codon 12 but also sometimes at codons 13 and 61, are exceptionally frequent in patients with pancreatic cancer.[5] Mutations in *KRAS* result in impaired



© 2009 Macmillan Publishers Limited. All rights reserved

GTPase function, which causes KRas to be locked in the GTP-bound 'on' state. This malfunction triggers a variety of cellular processes, including transcription, translation, cell-cycle progression, enhanced cell survival and motility. Oncogenic *KRAS* is involved in the initiation or early phase of pancreatic tumorigenesis.

A peptide vaccine that aims to stimulate immunity against cancer cells with mutant Ras proteins has been tested as an adjuvant treatment in patients with pancreatic cancer.[6] An extension to this research investigated the effects of combination therapy with mutant Ras peptide plus granulocyte–macrophage colony-stimulating factor[7] or interleukin (IL)-2.[8] Outcomes seemed to be favorable in these phase I–II trials, albeit only in individuals who mounted an immune response (about half of the patients).

For Ras to function, it must undergo post-translational modification so that it can attach to the cell membrane. One essential step involves the addition of a 15-carbon isoprenoid chain, mediated by farnesyltransferase. The therapeutic use of tipifarnib, a farnesyltransferase inhibitor (FTI), in combination with gemcitabine was disappointing in a phase III trial (Table 2).[9] This finding could be partly explained by the fact that KRas can be alternatively prenylated by the addition of a 20-carbon isoprenoid moiety mediated by the enzyme geranylgeranyltransferase. Moreover, FTIs work largely by inhibition of the cell cycle, but gemcitabine needs cell-cycle progression to be effective. To this end, a dual inhibitor of farnesyltransferase and geranylgeranyltransferase (L-778123) was tested in a phase I trial in combination with radiotherapy for locally advanced pancreatic cancer.[10] Inhibition of farnesylation and sensitivity to radiotherapy was demonstrated in a patient-derived cell line. Further development of this drug was, nevertheless, halted owing to adverse cardiac effects. Other compounds that are in early phases of clinical testing after yielding promising laboratory results include romidepsin, a histone deacetylase inhibitor that inhibits Ras-mediated signal transduction and thus causes cell-cycle arrest,[11] and farnesylthiosalicyclic acid (salirasib), which disrupts Ras from its membrane-binding site.[12] These compounds seem to have clinical activity in combination with gemcitabine and further studies are warranted.

Other strategies that target the Ras signaling pathway include the use of RNA-directed gene-silencing strategies, such as antisense therapy and RNA interference. Antisense therapy involves the use of oligonucleotides that have sequences complementary to a specific target messenger RNA (mRNA), which, therefore, block its translation to protein. In a phase II trial of patients with locally advanced and metastatic pancreatic cancers, the antisense inhibitor of another member of the Ras family (HRas), ISIS 2503, showed a response rate of 10.4% and a median survival of 6.6 months in combination with gemcitabine.[13] However, initial enthusiasm for this approach is diminishing following the failures of antisense inhibitors, such as ISIS 2503 and oblimersen in lung cancer and melanoma, respectively. An alternative method is RNA interference, which involves the manufacture of small interfering RNAs (siRNAs) that are specific for a particular target mRNA. These siRNAs bind to a complex of several proteins, including endoribonucleases, which is then termed the RNA-induced silencing complex. This complex identifies complementary mRNA and effects its cleavage or translational block. This technology is highly specific but has yet to

**Key points**

- Pancreatic cancer has high morbidity and mortality and is resistant to conventional treatment; therefore, an unmet need for novel therapeutic approaches exists
- Important molecular pathways and components involved in pancreatic carcinogenesis have been targeted with therapeutic intent, including Ras, EGFR, VEGF, gastrin and matrix metalloproteinases
- Good results from novel therapies have been demonstrated *in vitro* and in animal models, but results from the limited number of clinical trials are less encouraging
- Erlotinib, an EGFR tyrosine kinase inhibitor, is the only agent so far that has shown a significant (albeit small) survival benefit in a phase III clinical trial
- Potential therapeutic targets that warrant further investigation include other signal-transduction and embryonic pathways, telomerase, microRNAs and cancer stem cells
- Future development of targeted treatments should focus on inhibition of multiple signaling pathways, or blockade of one signaling pathway at multiple levels

**Table 1** | Important therapeutic targets in pancreatic cancer

| Target | Frequency of mutation or expression in pancreatic cancer (%) |
|---|---|
| Cholecystokinin B and gastrin receptor[32] | 95 |
| Ras[5] | 95 |
| Telomerase[114] | 95 |
| Vascular endothelial growth factor[37] | 93 |
| Gastrin precursors and gastrin[32] | 23–91 |
| Cyclo-oxygenase 2[67] | 90 |
| Hepatocyte growth factor receptor[80] | 78 |
| Notch3[106,107] | 70 |
| SHH[97] | 70 |
| Src[85] | 70 |
| Epidermal growth factor receptor[20] | 69 |
| β-Catenin[108] | 65 |
| Insulin-like growth factor I receptor[85] | 64 |
| Activated Akt[49] | 59 |
| SMAD4[75] | 50 |
| Focal adhesion kinase[91] | 48 |
| *AKT2*[48] | 20 |
| *TGFBR2* (transforming growth factor β receptor II)[75] | 4 |
| *TGFBR1* (transforming growth factor β receptor I)[75] | 1 |



© 2009 Macmillan Publishers Limited. All rights reserved

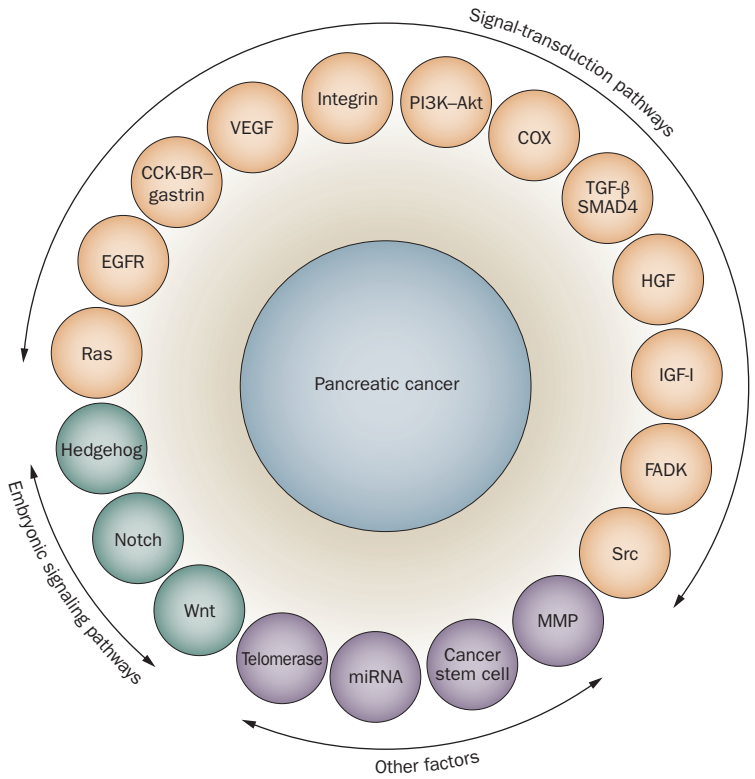


**Figure 1** | The pathways and processes involved in pancreatic carcinogenesis. Entities involved in these signal-transduction pathways have diverse roles in the promotion of tumor growth, resistance to apoptosis, invasion, metastasis and angiogenesis. Reactivation of physiological, embryonic development pathways is also frequently observed in pancreatic cancer. MMPs are important for tumor invasion and neovascularization. Telomerase is involved in the maintenance of telomeres and is activated in the majority of pancreatic cancers. The miRNAs regulate gene expression post-transcriptionally and can be either oncogenic or tumor suppressive. Cancer stem cells have been implicated in tumor progression, resistance to chemotherapy and radiotherapy and in disease relapse. Abbreviations: miRNA, microRNA; MMP, matrix metalloproteinase.

enter clinical trials, although *in vitro* and *in vivo* studies have been promising.[14,15]

MAP2K, the principal downstream component of Ras signaling, has also been the subject of targeted inhibition. In a phase II trial, the inhibitor CI-1040 (PD184532) did not demonstrate enough antitumor activity to justify further development.[16] Nevertheless, combined inhibition of MAP2K and other kinases (such as EGFR) has been effective in preclinical studies, which suggests that this approach might still have a role in therapy for pancreatic cancer.[17,18]

*The epidermal growth factor receptor pathway*

EGFR is a transmembrane receptor tyrosine kinase of the ErbB family. Upon binding to its ligands, homodimerization or heterodimerization with other members of the ErbB family occurs, which leads to phosphorylation of tyrosine residues in its intracellular domain. This process recruits intracellular proteins that cause downstream signaling events through MAPK, PI3K–AKT, and the STAT family of proteins (Figure 2). STAT proteins have roles in cell proliferation, survival, motility, invasion and adhesion. Mechanisms that lead to inappropriate activation of EGFR include receptor overexpression, activating mutations, overexpression of receptor ligands, and/or loss of their negative regulatory pathways. Overexpression of EGFR and its ligands EGF and TGF-α are frequently observed in pancreatic cancer.[19,20]

In a phase III trial in combination with gemcitabine, erlotinib, an orally active small molecule that binds to the ATP-binding site of EGFR, has demonstrated a small but significant increase in the survival of patients with advanced pancreatic cancer (Table 2).[21] In 2005, erlotinib was the first targeted therapy approved by the FDA for pancreatic cancer. However, its clinical relevance has been criticized and its cost-effectiveness has been questioned.[22] Other EGFR tyrosine kinase inhibitors that have been tested in early-phase clinical trials include gefitinib[23–25] and lapatinib.[26,27]

Although EGFR inhibitors have shown promising results, inhibition of EGFR with the monoclonal antibody cetuximab was ineffective in a phase III trial in patients with locally advanced and metastatic pancreatic cancers (Table 2).[28] No objective responses were seen in phase II trials of cetuximab in combination with gemcitabine and intensity-modulated radiotherapy or cisplatin.[29,30] A phase II trial of cetuximab in combination with docetaxel and irinotecan is ongoing.[31]

*Gastrin–cholecystokinin B receptor pathway*

The peptide hormone gastrin is secreted by G cells in the gastric antrum and duodenum, and it can act as a growth factor for gastric, colonic and pancreatic cancers. CCK-BR (the gastrin and cholecystokinin B receptor), gastrin precursors and the fully amidated gastrin are expressed in 95%, 55–91% and 23% of pancreatic cancers, respectively.[32] A selective CCK-BR antagonist, gastrazole, was tested in two small, randomized, controlled trials in patients with advanced pancreatic cancer (Table 2).[33] Gastrazole was superior to placebo, but not to 5-fluorouracil. Another inhibitor, the orally active Z-360, has demonstrated promising laboratory results[34] and is tolerated well by patients in combination with gemcitabine.[35] A phase III trial of Z-360 is being planned. An alternative approach to blockade of this pathway involves the use of gastrimmune, an immunogen that stimulates the formation of antibodies against gastrin 17 and its precursors. This agent was, however, not successful in a phase III trial (Table 2).[36]

## Angiogenesis

Angiogenesis is essential for solid tumor growth, and is principally mediated by the VEGF family of proteins and receptors (Figure 2). Stimuli that upregulate VEGF expression include hypoxia, other growth factors and oncogenic proteins (for example, TGF-β, EGF and Ras). VEGF is overexpressed in >90% of pancreatic cancers[37] and is, therefore, an appealing target for therapy.



© 2009 Macmillan Publishers Limited. All rights reserved

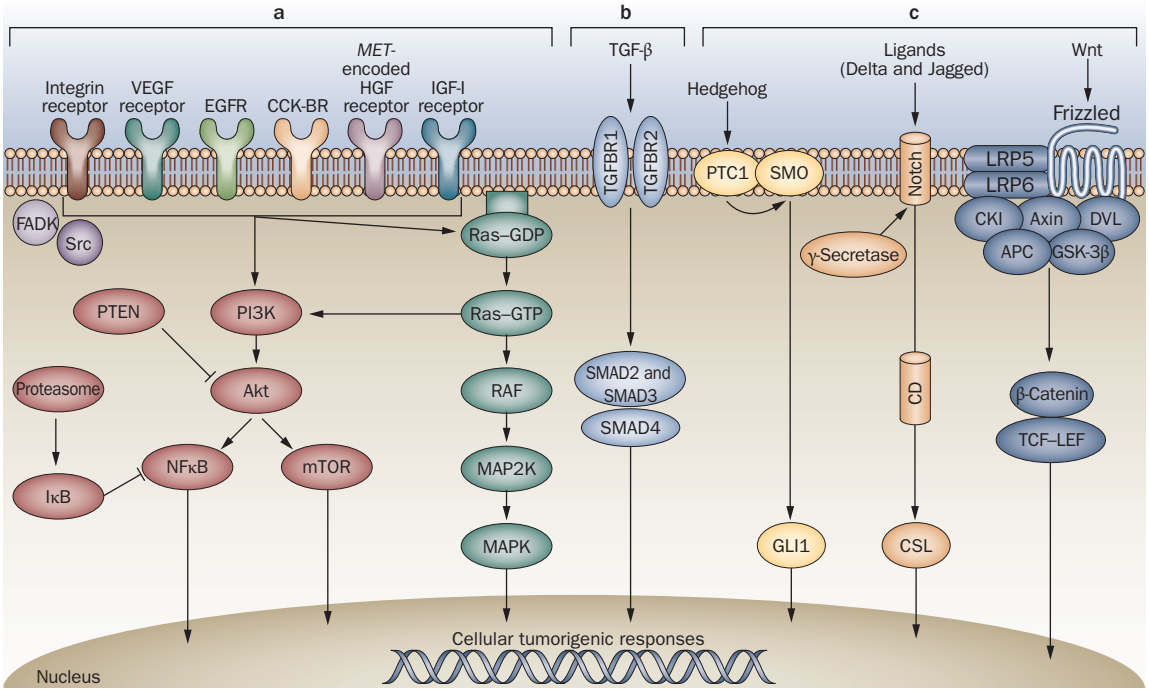


**Figure 2** | A simplified representation of oncogenic signaling cascades in pancreatic cancer. **a** | Binding of ligands to receptors for integrins, VEGF, EGFR, CCK-BR–gastrin, HGF and IGF-I activates signaling cascades including the PI3K–Akt and Ras pathways, which affect downstream targets such as NFκB, mTOR and MAPK. FADK binds to integrin receptors and Src to growth factor receptors. FADK–Src interaction increases the activity of FADK. PTEN has the opposite effect to PI3K and inhibits the Akt pathway. Proteasomes degrade IκB, which normally inhibits NFκB. **b** | Binding of TGF-β forms a complex with TGFBR1 and TGFBR2, which leads to phosphorylation of SMAD2 and SMAD3. These proteins form a complex with SMAD4, which migrates to the nucleus to activate gene transcription. **c** | The embryonic signaling pathways. Binding of hedgehog proteins to PTC1 stops inhibition of SMO, which leads to activation of downstream targets, such as GLI1. Activation of Notch by its ligands Delta and Jagged leads to its proteolytic cleavage by γ-secretase, and releases the cytoplasmic domain, which translocates to the nucleus and binds to transcription factors, such as CSL. β-Catenin is normally destined for proteasomal degradation. In the canonical Wnt–β-catenin pathway, binding of Wnt proteins stabilizes β-catenin and induces its translocation to the nucleus. β-Catenin forms a complex with the TCF–LEF transcription factors to initiate gene expression. Abbreviation: CD, cytoplasmic domain.

Bevacizumab is a humanized antibody against VEGF and is approved for use in patients with colorectal cancer. However, a phase III trial in advanced pancreatic cancer failed to show any survival benefit for bevacizumab in combination with gemcitabine (Table 2).[38] The AVITA (BO17706) phase III study of patients with metastatic pancreatic cancer reported that the addition of bevacizumab to gemcitabine and erlotinib did not significantly prolong overall survival, although a significant improvement in progression-free survival was seen (Table 2).[39] A number of other trials are being conducted to examine bevacizumab in combination with other agents or treatment modalities for pancreatic cancer; however, this agent seems unlikely to confer sufficient benefit to justify its licensing for this condition.

The failure of bevacizumab in therapeutic trials for pancreatic cancer highlighted the need for angiogenic inhibitors that could target other non-VEGF pathways and have better access to the tumor environment than an antibody. Sorafenib is a multitargeted kinase inhibitor that inhibits the VEGF receptor (VEGFR), platelet-derived growth factor receptor (PDGFR), SCFR (formerly c-KIT), Raf1 and FLT3, which are all implicated in tumor growth and angiogenesis. Sorafenib was approved in 2005 for the treatment of advanced renal-cell carcinoma. However, a phase II study concluded that, although well-tolerated, it was inactive in patients with advanced pancreatic cancer.[40] Axitinib at high concentrations is an orally active inhibitor of both VEGFR and related tyrosine kinase receptors. A median survival of 6.9 months was reported for axitinib combined with gemcitabine compared with 5.6 months for gemcitabine alone in a phase II trial in patients with advanced pancreatic cancer, but this finding was not significant.[41] Phase III trials of axitinib combined with gemcitabine are currently in progress. Aflibercept, a recombinant fusion protein that functions as a soluble decoy receptor and thereby inhibits VEGF, is another novel agent being tested in a phase III trial of patients treated with gemcitabine for metastatic pancreatic cancer.

Integrin receptors on the cell surface interact with the extracellular matrix and mediate various signaling



© 2009 Macmillan Publishers Limited. All rights reserved

**Table 2** | Completed phase III clinical trials of targeted therapies for pancreatic cancer

| Trial | Disease stage | Number of patients | Treatments investigated | Mechanism of treatment | Median survival (months) | 1-year survival (%) | PFS (months) | CR or PR (%) | Patients achieved stable disease (%) |
|---|---|---|---|---|---|---|---|---|---|
| Bramhall *et al.* (2001)[45] | Unresectable | 414 | Marimastat vs gemcitabine | MMPI | 3.4–4.1<br>5.5 | 14.0–20.0<br>19.0 | 1.8–1.9[a]<br>3.8[a] | 2.8<br>25.8 | n/a<br>n/a |
| Bramhall *et al.* (2002)[46] | Unresectable | 239 | Marimastat + gemcitabine vs gemcitabine | MMPI | 5.4<br>5.4 | 18.0<br>17.0 | 3.0<br>3.1 | 11.0<br>16.0 | 50.0<br>56.0 |
| NCIC CTG (2003)[47] | Advanced | 277 | Tanomastat vs gemcitabine | MMPI | 3.74[a]<br>6.59[a] | 10.0<br>25.0 | 1.68[a]<br>3.5[a] | 0.9<br>5.2 | 28.7<br>53.9 |
| Van Cutsem *et al.* (2004)[9] | Advanced | 688 | Tipifarnib + gemcitabine vs gemcitabine | RAS FTI | 6.3<br>6.0 | 27.0<br>24.0 | 3.7<br>3.6 | 6.0<br>8.0 | 53.0<br>52.0 |
| Shapiro *et al.* (2005)[36] | Advanced | 394 | G17DT + gemcitabine vs gemcitabine | Induction of antibodies against gastrin-17 | 5.8<br>6.6 | n/a<br>n/a | 3.9<br>3.9 | 32.0<br>36.0 | n/a<br>n/a |
| Chau *et al.* (2006)[33] | Advanced | Trial A: 18<br>Trial B: 98 | Gastrazole vs placebo<br>Gastrazole vs 5-fluorouracil | Gastrin receptor antagonist | 7.9[a]<br>4.5[a]<br>3.6<br>4.2 | 33.0[a]<br>11.0[a]<br>13.2<br>26.2 | n/a<br>n/a<br>2.3<br>2.7 | n/a<br>n/a<br>0.0<br>4.8 | n/a<br>n/a<br>28.3<br>28.6 |
| CALGB 80303 (2007)[38] | Advanced | 602 | Bevacizumab + gemcitabine vs gemcitabine | Anti-VEGF antibody | 5.7<br>6.0 | n/a<br>n/a | 4.8<br>4.3 | 13.1<br>11.3 | 40.7<br>35.7 |
| NCIC CTG (2007)[21] | Advanced | 569 | Erlotinib + gemcitabine vs gemcitabine | EGFR tyrosine kinase inhibitor | 6.24[a]<br>5.91[a] | 23.0[a]<br>17.0[a] | 3.75[a]<br>3.55[a] | 8.6<br>8.0 | 48.9<br>41.2 |
| SWOG S0205 (2007)[28] | Advanced | 766 | Cetuximab + gemcitabine vs gemcitabine | Anti-EGFR antibody | 6.5<br>6.0 | n/a<br>n/a | 3.5<br>3.0 | 12.0<br>14.0 | n/a<br>n/a |
| AVITA/ BO17706 (2008)[39] | Metastatic | 607 | Bevacizumab + erlotinib + gemcitabine vs erlotinib + gemcitabine | Anti-VEGF antibody and EGFR tyrosine kinase inhibitor | 7.1<br>6.0 | n/a<br>n/a | 4.6[a]<br>3.6[a] | 13.5<br>8.6 | n/a<br>n/a |

[a]Significant. Abbreviations: CALGB, Cancer and Leukemia Group B; CR or PR, complete or partial response; EGFR, epithelial growth factor receptor; FTI, farnesyltransferase inhibitor; MMPI, matrix metalloproteinase inhibitor; n/a, not applicable; NCIC CTG, National Cancer Institute of Canada Clinical Trials Group; PFS, progression-free survival; SWOG, Southwest Oncology Group; VEGF, vascular endothelial growth factor.

pathways (Figure 2). These receptors are involved in many neoplastic processes, including tumor survival, invasion and metastasis. The $\alpha_V\beta_3$ and $\alpha_V\beta_5$ integrins induce angiogenesis, principally via basic fibroblast growth factor and VEGF, respectively. Cilengitide inhibits these integrins, but in a phase II trial in patients with advanced pancreatic cancer it did not show significant benefit compared to gemcitabine alone.[42] Other anti-integrin agents, including an antibody against $\alpha_5\beta_1$ (volociximab)[43] and an inhibitor of α2 (E7820),[44] are in early-phase clinical trials.

### Matrix metalloproteinases

Matrix metalloproteinases (MMPs) are a family of zinc-dependent proteolytic enzymes that degrade the extracellular matrix and are essential for tumor spread and neovascularization. Imbalance between MMPs and their natural inhibitors is unsurprisingly, therefore, a frequent event in pancreatic cancer. Despite promising laboratory results, MMP inhibitors have failed to live up to their initial therapeutic expectation in three phase III clinical trials (Table 2),[45–47] although critics argued that the trials included a large number of patients with metastatic disease, which contradicts the rationale of exploiting the cytostatic effect of MMP inhibitors.

## Other potential therapeutic targets

### Signal-transduction pathways

*The PI3K–Akt pathway*

Upon activation by Ras or EGFR, PI3K activates Akt, which in turn has multiple downstream targets, including the mammalian target of rapamycin (mTOR) and the transcription factor NFκB (Figure 2). mTOR and NFκB have a variety of roles in cell proliferation, survival, resistance to apoptosis, angiogenesis and invasion. AKT2 is amplified and the PI3K–Akt pathway is activated in 20% and 59% of pancreatic cancers, respectively.[48,49] Deregulation of this pathway through aberrant expression of PTEN (phosphatase and tensin homolog, a natural antagonist of PI3K) is frequently observed in pancreatic cancer.[50] Furthermore, an architectural transcription factor, HMGA-1, is overexpressed in pancreatic cancer.[51] This transcription factor activates PI3K–Akt signaling and seems to mediate resistance to gemcitabine,[52] which, therefore, provides another target for inhibition therapy.[53,54]

Temsirolimus is an mTOR inhibitor approved for the treatment of renal-cell carcinoma, but use of this agent in pancreatic cancer has been limited.[55] Other agents, including everolimus and sirolimus, are currently being



© 2009 Macmillan Publishers Limited. All rights reserved

studied in phase II clinical trials.[56] A combination of an mTOR inhibitor with other standard or targeted therapies might be needed,[57,58] as mTOR expression does not correlate with survival of patients.[59]

Curcumin, which is derived from the spice turmeric, can inhibit NFκB and, therefore, the expression of regulated gene products, such as Bcl2, BclXL, COX2, cyclin D1 and survivin, which all have a role in the survival of pancreatic cancer cells.[60,61] Curcumin can also alter the expression of miRNAs (microRNAs, see below) in pancreatic cancer cells.[62] Phase II trials of curcumin with and without gemcitabine showed that it was well-tolerated and might have some biological activity in patients with pancreatic cancer.[63,64] The oral inhibitor of NFκB–STAT3, RTA 402, is being examined in a phase I–II trial. Bortezomib is a proteosome inhibitor that prevents the degradation of IκBβ, which in turn is an endogenous inhibitor of NFκB (Figure 2). Bortezomib is licensed for the treatment of refractory multiple myeloma, but unfortunately it failed to show any benefit—either alone or in combination with gemcitabine—in a phase II trial.[65] This finding could be related to the fact that proteosome inhibition paradoxically activates other antiapoptotic and mitogenic signaling pathways in pancreatic cancer.[66]

### *The cyclo-oxygenase pathway*

The COX enzymes have principal roles in the conversion of arachidonic acid into prostaglandins. COX1 is constitutively expressed and has a homeostatic role. COX2 is inducible by growth factors, cytokines and tumor promoters, and its expression is upregulated in 90% of pancreatic cancers.[67] The mechanisms of COX-mediated and prostaglandin-mediated pancreatic cancer development are complex; they involve multiple mitogenic signaling pathways and molecules that mediate resistance to apoptosis, cell migration, invasion, angiogenesis, immunosuppression, the production of free radicals and peroxidation of procarcinogens to carcinogens.[68] Inhibition of COX2 by NSAIDs has suppressed proliferation of pancreatic cancer cells and angiogenesis, both *in vitro* and *in vivo*.[68,69] Interestingly, Chang and colleagues reported in 2008 that the antitumor activity of celecoxib does not correlate with its inhibition of COX2, which suggests the involvement of alternative mechanisms.[70] Nonetheless, phase II trials of gemcitabine in combination with celecoxib 400 mg twice daily have been conducted, but results were inconclusive. For 20 evaluable patients with metastatic pancreatic cancer, the reported median survival was 6.2 months and survival at 3 months was 72%.[71] For patients with locally advanced or metastatic disease, one study showed an median survival of 9.1 months and overall clinical response of 54.7%,[72] but another study concluded that the addition of celecoxib had no significant benefit.[73] The combination of celecoxib, gemcitabine and irinotecan resulted in a median survival of 13 months and 1-year survival of 64%, and was associated with improvement of pain and quality of life.[74] A phase III trial of gemcitabine, celecoxib and curcumin is in progress.

### *The TGF-β–SMAD4 pathway*

TGF-β is a cytokine secreted by epithelial, endothelial, hematopoietic and mesenchymal cells. Binding of TGF-β forms a heteromeric complex with the type I and type II TGFBR triggers the phosphorylation of cytoplasmic SMAD2 and SMAD3. In turn, these SMAD proteins form a complex with SMAD4, which translocates into the nucleus to activate gene transcription (Figure 2). TGF-β can also signal via SMAD-independent pathways that involve Ras, PI3K and MAPK. TGF-β mediates a wide range of physiological processes, such as embryonic development, tissue repair, angiogenesis and immunosuppression. TGF-β also has a complex role in tumorigenesis, as it is tumor-suppressive in epithelial cells, but promotes invasion and metastasis during the late stages of cancer progression. Mutations of the *TGFBR1*, *TGFBR2* and *SMAD4* genes are found in about 1%, 4% and 50% of patients with pancreatic cancers, respectively.[75] Inactivation of SMAD4 abolishes TGF-β-mediated tumor-suppressive functions while it maintains some tumor-promoting TGF-β responses, such as epithelial–mesenchymal transition, which makes cells migratory and invasive.[76]

TGF-β-based therapeutic strategies are currently in development, including inhibitors of TGFBR1 and TGFBR2.[77,78] AP 12009, an antisense oligonucleotide specific to TGF-β2, is currently being tested in a phase I–II study of malignant melanoma, pancreatic cancer and colorectal carcinomas. One patient with advanced pancreatic cancer was still alive 128 weeks after complete regression of liver metastases.[79]

### *The hepatocyte growth factor receptor pathway*

The *MET* oncogene encodes the receptor for hepatocyte growth factor (HGF) and is overexpressed in 78% of pancreatic cancers.[80] HGF is normally produced by mesenchymal cells and acts on epithelial cells to promote tissue regeneration. In hypoxic conditions, however, tumor-associated fibroblasts produce HGF, which stimulates angiogenesis, tumor growth, cell motility and extracellular matrix breakdown and leads to invasion and metastasis (Figure 2). Targeting the HGF pathway with use of a synthetic competitive antagonist of HGF[81,82] and an antibody against the MET receptor[83] has yielded encouraging results in the laboratory setting. ARQ 197 is a MET receptor tyrosine kinase inhibitor that is currently being tested in a phase II trial. A phase I study showed that it was tolerated well by patients.[84]

### *The insulin-like growth factor pathway*

The insulin-like growth factor I (IGF-I) receptor, a transmembrane receptor tyrosine kinase, is overexpressed in 64% of pancreatic cancers.[85] The IGF-I receptor has antiapoptotic and growth-promoting effects and acts via multiple signaling cascades, including the PI3K–Akt, MAPK and STAT pathways (Figure 2). Inhibition of the IGF-I receptor by the tyrosine kinase inhibitor NVP-AEW541, a dominant-negative mutant and RNA interference have



© 2009 Macmillan Publishers Limited. All rights reserved

all been shown to reduce the growth of pancreatic cancer cells *in vitro* and *in vivo*, and increase chemotherapy-induced or radiation-induced apoptosis.[86,87] Concomitant inhibition of KRas increases the therapeutic effect of this inhibitor.[88] Human anti-IGF-I receptor antibodies have been reported to increase the antitumor effects of gemcitabine and EGFR inhibition *in vivo*.[89,90] As a result of these findings, phase I–II trials of cixutumumab and MK-0646 with gemcitabine and erlotinib have now commenced for pancreatic cancer.

*The focal adhesion kinase pathway*

Focal adhesion kinase (FADK) is a cytoplasmic non-receptor tyrosine kinase that mediates functions involved in cell motility and survival and is closely related to the integrin signaling pathway (Figure 2). 48% of pancreatic cancers[91] express FADK and, importantly, it shares a common pathway with IGF-I receptor.[92] The dual IGF-I receptor–FADK inhibitor NVP-TAE226 has shown significant tumor-suppressive activity *in vivo*.[93]

*The Src pathway*

Src is one of nine members of the Src family of non-receptor protein tyrosine kinases. In normal conditions, Src is maintained in a phosphorylated and inactive form, but is activated in a number of malignancies, including in 70% of pancreatic cancers.[85] Src has diverse roles in cell proliferation, survival, motility, invasiveness, resistance to chemotherapy and angiogenesis. This protein acts via multiple signaling pathways and, therefore, is an ideal target for therapeutic intervention (Figure 2). Src kinase inhibitors have been effective in suppressing pancreatic tumor growth and metastasis *in vivo*.[94–96] Dasatinib is an orally active multitargeted kinase inhibitor of Src, BCR–ABL, PDGFR, ephrin type A receptor 2 and SCFR, and is licensed for the treatment of chronic myelogenous and acute lymphoblastic leukemias. Dasatinib is being examined in a phase II trial in patients with metastatic pancreatic cancer, as is the related compound saracatinib.

## Embryonic signaling pathways

*The hedgehog pathway*

Three mammalian hedgehog homolog proteins have been identified—DHH, IHH and SHH. These proteins are secreted and specify the organization and structure of many tissues during embryonic development. Activation of the hedgehog signaling pathway is controlled by two transmembrane proteins, the tumor-suppressor PTC1 protein and the oncogenic SMO protein (Figure 2). PTC1 normally suppresses SMO, but mechanisms, such as an inactivating mutation of *PTC1* and the binding of hedgehog proteins to PTC1, relieves this inhibition, which leads to SMO activation of transcriptional responses. SHH is expressed in 70% of human pancreatic adenocarcinomas.[97] IHH expression is increased 35-fold in pancreatic cancer cells compared with in normal tissues.[98] Mechanisms of tumorigenesis include the effects of hedgehog proteins on the cell-cycle regulators, protection from apoptosis via PI3K–Akt signaling and stabilization of Bcl2 and BclXL and collaboration with activated KRas and angiogenesis. The hedgehog signaling pathway can be inhibited by cyclopamine, which binds to SMO. Laboratory work has demonstrated the effectiveness of cyclopamine in a wide range of digestive-tract tumors, including pancreatic cancer.[99] Cyclopamine can enhance sensitivity to radiotherapy and chemotherapy and suppress metastatic spread[100,101] as well as improving antitumor activity when combined with an EGFR inhibitor.[102] A downstream target of the SHH pathway, the transcription factor GLI1, can also be inhibited by miRNA.[103]

*The Notch pathway*

The four known human Notch genes encode heterodimeric transmembrane receptors, which are important in the development of organs, tissue proliferation, differentiation and apoptosis. Activation of the Notch signaling pathway leads to proteolytic cleavage of the transmembrane receptors by γ-secretase; the released cytoplasmic domain then migrates to the nucleus and binds to transcription factors, which leads to the expression of a variety of genes (Figure 2). Notch signaling occurs downstream of Ras, EGFR and TGF-β signaling in pancreatic tumorigenesis and promotes tumor vascularization. Downregulation of Notch 1 with siRNA or curcumin (owing to the crosstalk between Notch and NFκB signaling pathways) can inhibit cell growth and induce apoptosis in pancreatic cancer cell lines *in vitro*.[104,105] Notch 3 is expressed in around 70% of pancreatic cancers and can be inhibited by siRNA and γ-secretase inhibitors (GSI and L-685,458).[106,107]

*The Wnt pathway*

19 human Wnt genes each encode a lipid-modified secreted glycoprotein. Wnt signaling is involved in normal embryonic development and homeostatic self-renewal of a number of adult tissues. There are three Wnt signaling cascades, namely the canonical Wnt–β-catenin, the planar-cell polarity, and the Wnt–$Ca^{2+}$ pathways. The former is the best known and has been implicated in a variety of cancers, including liver, colorectal, breast, prostate, renal and hematological malignancies. Normally, β-catenin is phosphorylated and targeted for degradation. However, binding of Wnt proteins results in activation of intracellular pathways that cause β-catenin to enter the nucleus, where its interaction with the T-cell factor and lymphoid enhancer factor families of transcription factors leads to targeted gene expression (Figure 2). Any gain-of-function mutation of activators or loss-of-function mutation of inhibitors of Wnt signaling could lead to aberrant activation of these signaling pathways, which could result in carcinogenesis and progression. Aberrant activation occurs in 65% of pancreatic cancers.[108] Inhibition of Wnt signaling to reduce proliferation and increase apoptosis of pancreatic cancer cells has been achieved in the laboratory setting by a variety of methods, including the use



© 2009 Macmillan Publishers Limited. All rights reserved

**Table 3** | Ongoing phase III clinical trials of targeted therapies for pancreatic cancer

| Treatment | Target | Disease stage |
|---|---|---|
| Erlotinib, capecitabine and gemcitabine | EGFR | Locally advanced or metastatic |
| Curcumin, celecoxib and gemcitabine | NFκB and COX2 | Locally advanced or metastatic |
| Axitinib and gemcitabine | VEGF receptor and other tyrosine kinases | Locally advanced or metastatic |
| Sorafenib and gemcitabine | VEGF receptor and other tyrosine kinases | Locally advanced or metastatic |
| GV1001, capecitabine and gemcitabine | Telomerase | Locally advanced or metastatic |
| Aflibercept and gemcitabine | VEGF | Metastatic |

of β-catenin-interacting protein 1, a dominant-negative mutant of lymphoid enhancer factor, and siRNA against β-catenin or extracellular sulfatases.[109,110] Wnt signaling is positively regulated by the hedgehog and SMAD4 signaling pathways,[109,111] which could be targets for a combined inhibitory therapeutic strategy.

The CXC-chemokine receptor 4 (CXCR 4) and its ligand, SDF-1 have a role in tumor growth, angiogenesis and, in particular, metastatic spread. *In vitro* blockade of CXCR 4 could inhibit pancreatic cancer growth through inhibition of the canonical Wnt pathway.[112] Furthermore, plerixafor, an antagonist of CXCR 4, reduces metastasis by pancreatic cancer cells that are positive for the markers CXCR 4 and CD133 (the latter is a marker of pancreatic cancer stem cells) *in vivo*.[113]

### Telomerase

The telomeres located at the end of chromosomes normally shrink with each cell division and thereby impose a finite lifespan on the cell. Most malignant cells have detectable activity of telemerase, a reverse transcriptase that contains an RNA template and acts to elongate telomeres. Telomerase is overexpressed in 95% of pancreatic cancers[114] which provides a rationale for the development of antitelomerase agents. GV1001 is a telomerase peptide vaccine that has shown some promising results in phase I/II studies.[115,116] This vaccine is being tested in the large (>1,000 patients), phase III, TeloVac trial with gemcitabine and capecitabine in locally advanced and metastatic pancreatic cancers.

### MicroRNAs

The miRNAs are small, endogenous, noncoding RNA molecules that regulate gene expression and are important for developmental and physiological processes. These molecules all negatively regulate gene expression post-transcriptionally and can be either oncogenic or tumor-suppressive, depending on their target mRNAs.[117] Expression profiling showed that at least 100 miRNA precursors are aberrantly expressed in pancreatic cancer or desmoplasia.[118,119] Anticancer miRNA-based therapy has the theoretical advantage of having multiple targets that are controlled by an individual miRNA by virtue of its post-transcriptional modulation. Therapeutic strategies include the reconstitution of tumor-suppressive miRNAs and the knockdown of oncogenic miRNAs by coding vectors or anti-miRNA oligonucleotides. Studies of these treatment approaches have been limited in pancreatic cancer but have yielded promising results in breast cancer and glioma.

### Cancer stem cells

Cancer stem cells possess important properties associated with their normal counterparts, namely the ability for self-renewal and differentiation. Pancreatic cancer stem cells are identified by their surface markers, such as CD133, CD44, CD24 and flotillin 2 epithelial-specific antigen. Evidence suggests that such cells form a small subset in the heterogenous tumor population, and contribute to neoplastic progression, metastasis and resistance to chemotherapy and radiotherapy.[113,120] For this reason, cancer stem cells are thought to be responsible for relapse of disease after clinical remission. Dysregulation of various signaling cascades, including the PTEN, SHH, Notch and Wnt pathways, are frequently observed in cancer stem cells, which provides further rationale for use of these pathways as a target for therapeutic purposes. Further studies are still needed to understand the genetic and biological properties of cancer stem cells for the development of effective treatment modalities.

## Conclusions

Although targeted therapies for pancreatic cancer have yielded encouraging results *in vitro* and in animal models, these findings have not been translated to improved outcomes in clinical trials. Reasons for this failure might include an incomplete understanding of the biology of pancreatic cancer, the selection of poor active agents, problems with trial design (such as inappropriate therapeutic end points or patient selection) and the rapidity with which agents move into randomized, controlled trials without the extensive early testing necessary to optimize treatment regimens. Furthermore, preclinical studies performed on mouse models do not always recapitulate the human condition, which is a particular problem with human pancreatic cancer xenografts in immunodeficient mice. Despite these setbacks, lessons have been learnt, and our collective effort has generated a substantial platform of knowledge from which further work could spring. Genetically engineered immunocompetent mice, such as those with *KRAS* or *TP53* mutations, have been developed and they hold promise for the future studies of the disease.[121] The bioavailability of compounds such as antisense oligonucleotides and siRNAs in



© 2009 Macmillan Publishers Limited. All rights reserved

humans remains a big hurdle, which will require further improvement of gene-delivery strategies.

The individualization of therapy for patients is possible if factors that predict treatment response, such as biological markers, could be determined accurately. Alternatively, resected tumors could be grown in laboratory mice and treated with a series of drugs, and the most effective agent subsequently administered to the patient. This concept is currently being tested in a phase II trial at Johns Hopkins Hospital, MD, US. Until this strategy is proven effective in the clinical setting, multimodal approaches will remain the mainstay of treatment for advanced pancreatic cancer. These approaches are likely to comprise a mixture of targeted agents in combination with conventional chemotherapy and radiotherapy. For a clinically relevant effect to be achieved, treatment strategies should either be in the form of a 'horizontal' approach, in which several oncogenic pathways are inhibited, or a 'vertical' approach, whereby multiple levels of a major pathway are targeted. One example currently being investigated in a phase III trial is the treatment combination of celecoxib, curcumin and gemcitabine for advanced pancreatic cancer. Besides the synergistic antiproliferative and proapoptotic effects of curcumin and celecoxib,[122] these agents also potentiate the antitumor activity of gemcitabine.[123,124] Combination therapies, together with improved diagnostic tools and predictive markers, are ultimately hoped to improve the bleak outlook for patients diagnosed with pancreatic cancer. For now, the results of a number of phase III trials are eagerly awaited (Table 3).

**Review criteria**

PubMed was searched in November 2008 for English-language publications, using the terms "pancreatic", "pancreas", "carcinoma", "cancer", "therapy", "treatment" and those listed in the articles' subheadings. Published reports and abstracts from the American Society of Clinical Oncology and the American Association for Cancer Research meetings, were also searched. No exclusion criteria were used. Articles were selected on the basis of relevance and additional papers were identified from their reference lists. The National Cancer Institute website was searched for ongoing clinical trials.


1. Jemal, A. *et al.* Cancer statistics, 2008. *CA Cancer J. Clin.* **58**, 71–96 (2008).
2. Pancreatic section, British Society of Gastroenterology *et al.* Guidelines for the management of patients with pancreatic cancer periampullary and ampullary carcinomas. *Gut* **54 (Suppl. 5)**, v1–v16 (2005).
3. Burris, H. A. 3rd *et al.* Improvements in survival and clinical benefit with gemcitabine as first-line therapy for patients with advanced pancreas cancer: a randomized trial. *J. Clin. Oncol.* **15**, 2403–2413 (1997).
4. Jones, S. *et al.* Core signaling pathways in human pancreatic cancers revealed by global genomic analyses. *Science* **321**, 1801–1806 (2008).
5. Almoguera, C. *et al.* Most human carcinomas of the exocrine pancreas contain mutant c-K-ras genes. *Cell* **53**, 549–554 (1988).
6. Toubaji, A. *et al.* Pilot study of mutant Ras peptide-based vaccine as an adjuvant treatment in pancreatic and colorectal cancers. *Cancer Immunol. Immunother.* **57**, 1413–1420 (2008).
7. Gjertsen, M. K. *et al.* Intradermal Ras peptide vaccination with granulocyte-macrophage colony-stimulating factor as adjuvant: clinical and immunological responses in patients with pancreatic adenocarcinoma. *Int. J. Cancer* **92**, 441–450 (2001).
8. Achtar, M. S. *et al.* Phase II clinical trial of mutant Ras peptide vaccine in combination with GM-CSF and IL-2 in advanced cancer patients [Abstract]. *J. Clin. Oncol.* **25**, a3067 (2007).
9. Van Cutsem, E. *et al.* Phase III trial of gemcitabine plus tipifarnib compared with gemcitabine plus placebo in advanced pancreatic cancer. *J. Clin. Oncol.* **22**, 1430–1438 (2004).
10. Martin, N. E. *et al.* A phase I trial of the dual farnesyltransferase and geranylgeranyltransferase inhibitor L-778 123 and radiotherapy for locally advanced pancreatic cancer. *Clin. Cancer Res.* **10**, 5447–5454 (2004).
11. Doss, H. H. *et al.* A phase I trial of romidepsin in combination with gemcitabine in patients with pancreatic and other advanced solid tumors [Abstract]. *J. Clin. Oncol.* **26**, a2567 (2008).
12. Rudek, M. A. *et al.* Integrated development of S-*trans*. Trans-farnesylthiosalicyclic acid (FTS, salisarib) in pancreatic cancer [Abstract]. *J. Clin. Oncol.* **26**, a4626 (2008).
13. Alberts, S. R. *et al.* Gemcitabine and ISIS-2503 for patients with locally advanced or metastatic pancreatic adenocarcinoma: a North Central Cancer Treatment Group phase II trial. *J. Clin. Oncol.* **22**, 4944–4950 (2004).
14. Rejiba, S., Wack, S., Aprahamian, M. & Hajri, A. K-ras oncogene silencing strategy reduces tumor growth and enhances gemcitabine chemotherapy efficacy for pancreatic cancer treatment. *Cancer Sci.* **98**, 1128–1136 (2007).
15. Brummelkamp, T. R., Bernards, R. & Agami, R. Stable suppression of tumorigenicity by virus-mediated RNA interference. *Cancer Cell* **2**, 243–247 (2002).
16. Rinehart, J. *et al.* Multicenter phase II study of the oral MEK inhibitor, CI-1040, in patients with advanced non-small-cell lung, breast, colon, and pancreatic cancer. *J. Clin. Oncol.* **22**, 4456–4462 (2004).
17. Jimeno, A. *et al.* Dual mitogen-activated protein kinase and epidermal growth factor receptor inhibition in biliary and pancreatic cancer. *Mol. Cancer Ther.* **6**, 1079–1088 (2007).
18. Takayama, Y. *et al.* MEK inhibitor enhances the inhibitory effect of imatinib on pancreatic cancer cell growth. *Cancer Lett.* **264**, 241–249 (2008).
19. Korc, M. *et al.* Overexpression of the epidermal growth factor receptor in human pancreatic cancer is associated with concomitant increases in the levels of epidermal growth factor and transforming growth factor alpha. *J. Clin. Invest.* **90**, 1352–1360 (1992).
20. Bloomston, M., Bhardwaj, A., Ellison, E. C. & Frankel, W. L. Epidermal growth factor receptor expression in pancreatic carcinoma using tissue microarray technique. *Dig. Surg.* **23**, 74–79 (2006).
21. Moore, M. J. *et al.* Erlotinib plus gemcitabine compared with gemcitabine alone in patients with advanced pancreatic cancer: a phase III trial of the National Cancer Institute of Canada Clinical Trials Group. *J. Clin. Oncol.* **25**, 1960–1966 (2007).
22. Grubbs, S. S., Grusenmeyer, P. A., Petrelli, N. J. & Gralla, R. J. Is it cost-effective to add erlotinib to gemcitabine in advanced pancreatic cancer? [Abstract]. *J. Clin. Oncol.* **24**, a6048 (2006).
23. Fountzilas, G. *et al.* Gemcitabine combined with gefitinib in patients with inoperable or metastatic pancreatic cancer: a phase II study of the Hellenic Cooperative Oncology Group with biomarker evaluation. *Cancer Invest.* **26**, 784–793 (2008).
24. Ignatiadis, M. *et al.* A multicenter phase II study of docetaxel in combination with gefitinib in gemcitabine-pretreated patients with advanced/metastatic pancreatic cancer. *Oncology* **71**, 159–163 (2006).
25. Blaszkowsky, L. S. *et al.* A phase II study of docetaxel in combination with ZD1839 (gefitinib) in previously treated patients with metastatic pancreatic cancer [Abstract]. *J. Clin. Oncol.* **25**, a15080 (2007).
26. Safran, H. *et al.* Lapatinib/gemcitabine and lapatinib/gemcitabine/oxaliplatin: a phase I study for advanced pancreaticobiliary cancer. *Am. J. Clin. Oncol.* **31**, 140–144 (2008).
27. Midgley, R. *et al.* Phase I study of GW572016 (lapatinib), a dual kinase inhibitor, in combination with irinotecan (IR), 5-fluorouracil (FU) and leucovorin (LV). *J. Clin. Oncol.* **23**, 3086–3093 (2005).
28. Philip, P. A. *et al.* Phase III study of gemcitabine [G] plus cetuximab [C] versus gemcitabine in patients [pts] with locally advanced or metastatic pancreatic adenocarcinoma [PC]: SWOG S0205 study [Abstract]. *J. Clin. Oncol.* **25**, 4509 (2007).




© 2009 Macmillan Publishers Limited. All rights reserved

29. Cascinu, S. *et al.* Cetuximab plus gemcitabine and cisplatin compared with gemcitabine and cisplatin alone in patients with advanced pancreatic cancer: a randomised, multicentre, phase II trial. *Lancet Oncol.* **9**, 39–44 (2008).
30. Munter, M. *et al.* Final results of a phase II trial [PARC-Study ISRCTN56652283] for patients with primary inoperable locally advanced pancreatic cancer combining intensity modulated radiotherapy (IMRT) with cetuximab and gemcitabine [Abstract]. *J. Clin. Oncol.* **26**, 4613 (2008).
31. Burtness, B. A. *et al.* Phase II ECOG trial of irinotecan/docetaxel with or without cetuximab in metastatic pancreatic cancer: updated survival and CA19–19 results [Abstract]. *J. Clin. Oncol.* **26**, 4642 (2008).
32. Caplin, M. *et al.* Expression and processing of gastrin in pancreatic adenocarcinoma. *Br. J. Surg.* **87**, 1035–1040 (2000).
33. Chau, I. *et al.* Gastrazole (JB95008), a novel CCK2/gastrin receptor antagonist, in the treatment of advanced pancreatic cancer: results from two randomised controlled trials. *Br. J. Cancer* **94**, 1107–1115 (2006).
34. Kawasaki, D. *et al.* Effect of Z-360, a novel orally active CCK-2/gastrin receptor antagonist on tumor growth in human pancreatic adenocarcinoma cell lines *in vivo* and mode of action determinations *in vitro*. *Cancer Chemother. Pharmacol.* **61**, 883–892 (2008).
35. Meyer, T. *et al.* A phase IB/IIA, multicentre, randomised, double-blind placebo controlled study to evaluate the safety and pharmacokinetics of Z-360 in subjects with unresectable advanced pancreatic cancer in combination with gemcitabine [Abstract]. *J. Clin. Oncol.* **26**, 4636 (2008).
36. Shapiro, J. *et al.* G17DT + gemcitabine [Gem] versus placebo + Gem in untreated subjects with locally advanced, recurrent, or metastatic adenocarcinoma of the pancreas: results of a randomized, double-blind, multinational, multicenter study [Abstract]. *J. Clin. Oncol.* **23**, 4012 (2005).
37. Seo, Y., Baba, H., Fukuda, T., Takashima, M. & Sugimachi, K. High expression of vascular endothelial growth factor is associated with liver metastasis and a poor prognosis for patients with ductal pancreatic adenocarcinoma. *Cancer* **88**, 2239–2245 (2000).
38. Kindler, H. L. *et al.* A double-blind, placebo-controlled, randomized phase III trial of gemcitabine (G) plus bevacizumab (B) versus gemcitabine plus placebo (P) in patients (pts) with advanced pancreatic cancer (PC): a preliminary analysis of Cancer and Leukemia Group B (CALGB). *J. Clin. Oncol.* **25**, 4508–4509 (2007).
39. Vervenne, W. *et al.* A randomized, double-blind, placebo (P) controlled, multicenter phase III trial to evaluate the efficacy and safety of adding bevacizumab (B) to erlotinib (E) and gemcitabine (G) in patients (pts) with metastatic pancreatic cancer. *J. Clin. Oncol.* **26**, 4507–4509 (2008).
40. Wallace, J. A. *et al.* Sorafenib (S) plus gemcitabine (G) for advanced pancreatic cancer (PC): A phase II trial of the University of Chicago Phase II Consortium [Abstract]. *J. Clin. Oncol.* **25**, 4608 (2007).
41. Spano, J. P. *et al.* Efficacy of gemcitabine plus axitinib compared with gemcitabine alone in patients with advanced pancreatic cancer: an open-label randomised phase II study. *Lancet* **371**, 2101–2108 (2008).
42. Friess, H. *et al.* A randomized multi-center phase II trial of the angiogenesis inhibitor Cilengitide (EMD 121974) and gemcitabine compared with gemcitabine alone in advanced unresectable pancreatic cancer. *BMC Cancer* **6**, 285 (2006).
43. Evans, T. *et al.* Final results from cohort 1 of a phase II study of volociximab, an anti-α5β1 integrin antibody, in combination with gemcitabine (GEM) in patients (pts) with metastatic pancreatic cancer (MPC) [Abstract]. *J. Clin. Oncol.* **25**, 4549 (2007).
44. Mita, M. M. *et al.* Pharmacokinetics (PK) and pharmacodynamics (PD) of E7820—an oral sulfonamide with novel, α-2 integrin mediated antiangiogenic properties: results of a phase I study [Abstract]. *J. Clin. Oncol.* **23**, 3082 (2005).
45. Bramhall, S. R., Rosemurgy, A., Brown, P. D., Bowry, C. & Buckels, J. A. Marimastat as first-line therapy for patients with unresectable pancreatic cancer: a randomized trial. *J. Clin. Oncol.* **19**, 3447–3455 (2001).
46. Bramhall, S. R. *et al.* A double-blind placebo-controlled, randomised study comparing gemcitabine and marimastat with gemcitabine and placebo as first line therapy in patients with advanced pancreatic cancer. *Br. J. Cancer* **87**, 161–167 (2002).
47. Moore, M. J. *et al.* Comparison of gemcitabine versus the matrix metalloproteinase inhibitor BAY 12–9566 in patients with advanced or metastatic adenocarcinoma of the pancreas: a phase III trial of the National Cancer Institute of Canada Clinical Trials Group. *J. Clin. Oncol.* **21**, 3296–3302 (2003).
48. Ruggeri, B. A., Huang, L., Wood, M., Cheng, J. Q. & Testa, J. R. Amplification and overexpression of the *AKT2* oncogene in a subset of human pancreatic ductal adenocarcinomas. *Mol. Carcinog.* **21**, 81–86 (1998).
49. Schlieman, M. G., Fahy, B. N., Ramsamooj, R., Beckett, L. & Bold, R. J. Incidence, mechanism and prognostic value of activated Akt in pancreas cancer. *Br. J. Cancer* **89**, 2110–2115 (2003).
50. Asano, T. *et al.* The PI 3-kinase/Akt signaling pathway is activated due to aberrant *Pten* expression and targets transcription factors NF-κB and c-Myc in pancreatic cancer cells. *Oncogene* **23**, 8571–8580 (2004).
51. Abe, N. *et al.* Pancreatic duct cell carcinomas express high levels of high mobility group I(Y) proteins. *Cancer Res.* **60**, 3117–3122 (2000).
52. Liau, S. S. & Whang, E. HMGA1 is a molecular determinant of chemoresistance to gemcitabine in pancreatic adenocarcinoma. *Clin. Cancer Res.* **14**, 1470–1477 (2008).
53. Liau, S. S., Ashley, S. W. & Whang, E. E. Lentivirus-mediated RNA interference of HMGA1 promotes chemosensitivity to gemcitabine in pancreatic adenocarcinoma. *J. Gastrointest. Surg.* **10**, 1254–1262 (2006).
54. Trapasso, F. *et al.* Therapy of human pancreatic carcinoma based on suppression of HMGA1 protein synthesis in preclinical models. *Cancer Gene Ther.* **11**, 633–641 (2004).
55. Ito, D. *et al. In vivo* antitumor effect of the mTOR inhibitor CCI-779 and gemcitabine in xenograft models of human pancreatic cancer. *Int. J. Cancer* **118**, 2337–2343 (2006).
56. Wolpin, B. M. *et al.* Phase II study of RAD001 in previously treated patients with metastatic pancreatic cancer [Abstract]. *J. Clin. Oncol.* **26**, 4614 (2008).
57. Azzariti, A., Porcelli, L., Gatti, G., Nicolin, A. & Paradiso, A. Synergic antiproliferative and antiangiogenic effects of EGFR and mTOR inhibitors on pancreatic cancer cells. *Biochem. Pharmacol.* **75**, 1035–1044 (2008).
58. Tuncyurek, P. *et al.* Everolimus and mycophenolate mofetil sensitize human pancreatic cancer cells to gemcitabine *in vitro*: a novel adjunct to standard chemotherapy? *Eur. Surg. Res.* **39**, 380–387 (2007).
59. Rajan, A. *et al.* mTOR expression in pancreatic adenocarcinoma and its correlation with survival [Abstract]. *J. Clin. Oncol.* **26**, 22169 (2008).
60. Reuter, S., Eifes, S., Dicato, M., Aggarwal, B. B. & Diederich, M. Modulation of anti-apoptotic and survival pathways by curcumin as a strategy to induce apoptosis in cancer cells. *Biochem. Pharmacol.* **76**, 1340–1351 (2008).
61. Wang, Z. *et al.* Synergistic effects of multiple natural products in pancreatic cancer cells. *Life Sci.* **83**, 293–300 (2008).
62. Sun, M. *et al.* Curcumin (diferuloylmethane) alters the expression profiles of microRNAs in human pancreatic cancer cells. *Mol. Cancer Ther.* **7**, 464–473 (2008).
63. Dhillon, N. *et al.* Phase II trial of curcumin in patients with advanced pancreatic cancer. *Clin. Cancer Res.* **14**, 4491–4499 (2008).
64. Epelbaum, R., Vizel, B. & Bar-Sela, G. Phase II study of curcumin and gemcitabine in patients with advanced pancreatic cancer [Abstract]. *J. Clin. Oncol.* **26**, 15619 (2008).
65. Alberts, S. R. *et al.* PS-341 and gemcitabine in patients with metastatic pancreatic adenocarcinoma: a North Central Cancer Treatment Group (NCCTG) randomized phase II study. *Ann. Oncol.* **16**, 1654–1661 (2005).
66. Sloss, C. M. *et al.* Proteasome inhibition activates epidermal growth factor receptor (EGFR) and EGFR-independent mitogenic kinase signaling pathways in pancreatic cancer cells. *Clin. Cancer Res.* **14**, 5116–5123 (2008).
67. Tucker, O. N. *et al.* Cyclooxygenase-2 expression is up-regulated in human pancreatic cancer. *Cancer Res.* **59**, 987–990 (1999).
68. Ding, X. Z., Hennig, R. & Adrian, T. E. Lipoxygenase and cyclooxygenase metabolism: new insights in treatment and chemoprevention of pancreatic cancer. *Mol. Cancer* **2**, 10 (2003).
69. Wei, D. *et al.* Celecoxib inhibits vascular endothelial growth factor expression in and reduces angiogenesis and metastasis of human pancreatic cancer via suppression of Sp1 transcription factor activity. *Cancer Res.* **64**, 2030–2038 (2004).
70. Chuang, H. C., Kardosh, A., Gaffney, K. J., Petasis, N. A. & Schonthal, A. H. COX-2 inhibition is neither necessary nor sufficient for celecoxib to suppress tumor cell proliferation and focus formation *in vitro*. *Mol. Cancer* **7**, 38 (2008).
71. Xiong, H. Q. *et al.* A phase II trial of gemcitabine and celecoxib for metastatic pancreatic cancer [Abstract]. *J. Clin. Oncol.* **23**, 4174 (2005).
72. Ferrari, V. *et al.* Gemcitabine plus celecoxib (GECO) in advanced pancreatic cancer: a phase II trial. *Cancer Chemother. Pharmacol.* **57**, 185–190 (2006).
73. Dragovich, T. *et al.* Gemcitabine plus celecoxib in patients with advanced or metastatic pancreatic adenocarcinoma: results of a phase II trial. *Am. J. Clin. Oncol.* **31**, 157–162 (2008).
74. Kerr, S. *et al.* Phase II trial of gemcitabine and irinotecan plus celecoxib in advanced adenocarcinoma of the pancreas [Abstract]. *J. Clin. Oncol.* **23**, 4155 (2005).




© 2009 Macmillan Publishers Limited. All rights reserved

75. Goggins, M. *et al.* Genetic alterations of the transforming growth factor beta receptor genes in pancreatic and biliary adenocarcinomas. *Cancer Res.* **58**, 5329–5332 (1998).
76. Levy, L. & Hill, C. S. Smad4 dependency defines two classes of transforming growth factor β (TGF-β) target genes and distinguishes TGF-β-induced epithelial–mesenchymal transition from its antiproliferative and migratory responses. *Mol. Cell Biol.* **25**, 8108–8125 (2005).
77. Melisi, D. *et al.* LY2109761, a novel transforming growth factor beta receptor type I and type II dual inhibitor, as a therapeutic approach to suppressing pancreatic cancer metastasis. *Mol. Cancer Ther.* **7**, 829–840 (2008).
78. Medicherla, S. *et al.* Antitumor activity of TGF-beta inhibitor is dependent on the microenvironment. *Anticancer Res.* **27**, 4149–4157 (2007).
79. Hilbig, A. *et al.* Preliminary results of a phase I/II study in patients with pancreatic carcinoma, malignant melanoma, or colorectal carcinoma using systemic i.v. administration of AP 12009 [Abstract]. *J. Clin. Oncol.* **26**, 4621 (2008).
80. Furukawa, T., Duguid, W. P., Kobari, M., Matsuno, S. & Tsao, M. S. Hepatocyte growth factor and Met receptor expression in human pancreatic carcinogenesis. *Am. J. Pathol.* **147**, 889–895 (1995).
81. Tomioka, D. *et al.* Inhibition of growth, invasion, and metastasis of human pancreatic carcinoma cells by NK4 in an orthotopic mouse model. *Cancer Res.* **61**, 7518–7524 (2001).
82. Ogura, Y. *et al.* Peritumoral injection of adenovirus vector expressing NK4 combined with gemcitabine treatment suppresses growth and metastasis of human pancreatic cancer cells implanted orthotopically in nude mice and prolongs survival. *Cancer Gene Ther.* **13**, 520–529 (2006).
83. Jin, H. *et al.* MetMAb, the one-armed 5D5 anti-c-Met antibody, inhibits orthotopic pancreatic tumor growth and improves survival. *Cancer Res.* **68**, 4360–4368 (2008).
84. Garcia, A. *et al.* Phase 1 study of ARQ 197, a selective inhibitor of the c-Met RTK in patients with metastatic solid tumors reaches recommended phase 2 dose [Abstract]. *J. Clin. Oncol.* **25**, 3525 (2007).
85. Hakam, A., Fang, Q., Karl, R. & Coppola, D. Coexpression of IGF-1R and c-Src proteins in human pancreatic ductal adenocarcinoma. *Dig. Dis. Sci.* **48**, 1972–1978 (2003).
86. Adachi, Y. *et al.* Molecular targeting of IGF-I receptor for human pancreatic cancer [Abstract]. *J. Clin. Oncol.* **25**, 14051 (2007).
87. Piao, W. *et al.* Insulin-like growth factor-I receptor blockade by a specific tyrosine kinase inhibitor for human gastrointestinal carcinomas. *Mol. Cancer Ther.* **7**, 1483–1493 (2008).
88. Shen, Y. M., Yang, X. C., Yang, C. & Shen, J. K. Enhanced therapeutic effects for human pancreatic cancer by application of K-ras and IGF-IR antisense oligodeoxynucleotides. *World J. Gastroenterol.* **14**, 5176–5185 (2008).
89. Beltran, P. J. *et al.* Effect of AMG 479 on anti-tumor effects of gemcitabine and erlotinib against pancreatic carcinoma xenograft models. *J. Clin. Oncol.* **26**, 4617–4625 (2008).
90. Prewett, M. *et al.* IMC-A12 enhances the efficacy of cetuximab + gemcitabine therapy in human pancreatic carcinoma xenografts in *AACR Meeting Abstracts 2007* 652 (The American Association for Cancer Research, Philadelphia, 2007).
91. Furuyama, K. *et al.* Clinical significance of focal adhesion kinase in resectable pancreatic cancer. *World J. Surg.* **30**, 219–226 (2006).
92. Liu, W. *et al.* FAK and IGF-IR interact to provide survival signals in human pancreatic adenocarcinoma cells. *Carcinogenesis* **29**, 1096–1107 (2008).
93. Hatakeyama, S. *et al.* Anti-cancer activity of NVP-TAE226, a potent dual FAK/IGF-IR kinase inhibitor, against pancreatic carcinoma [Abstract]. *J. Clin. Oncol.* **24**, 13162 (2006).
94. Ischenko, I. *et al.* Effect of Src kinase inhibition on metastasis and tumor angiogenesis in human pancreatic cancer. *Angiogenesis* **10**, 167–182 (2007).
95. Baker, C. H. *et al.* Inhibition of PDGFR phosphorylation and Src and Akt activity by GN963 leads to therapy of human pancreatic cancer growing orthotopically in nude mice. *Int. J. Oncol.* **29**, 125–138 (2006).
96. Trevino, J. G. *et al.* Inhibition of SRC expression and activity inhibits tumor progression and metastasis of human pancreatic adenocarcinoma cells in an orthotopic nude mouse model. *Am. J. Pathol.* **168**, 962–972 (2006).
97. Thayer, S. P. *et al.* Hedgehog is an early and late mediator of pancreatic cancer tumorigenesis. *Nature* **425**, 851–856 (2003).
98. Kayed, H. *et al.* Indian hedgehog signaling pathway: expression and regulation in pancreatic cancer. *Int. J. Cancer* **110**, 668–676 (2004).
99. Berman, D. M. *et al.* Widespread requirement for Hedgehog ligand stimulation in growth of digestive tract tumours. *Nature* **425**, 846–851 (2003).
100. Shafaee, Z., Schmidt, H., Du, W., Posner, M. & Weichselbaum, R. Cyclopamine increases the cytotoxic effects of paclitaxel and radiation but not cisplatin and gemcitabine in Hedgehog expressing pancreatic cancer cells. *Cancer Chemother. Pharmacol.* **58**, 765–770 (2006).
101. Feldmann, G. *et al.* Blockade of hedgehog signaling inhibits pancreatic cancer invasion and metastases: a new paradigm for combination therapy in solid cancers. *Cancer Res.* **67**, 2187–2196 (2007).
102. Hu, W. G., Liu, T., Xiong, J. X. & Wang, C. Y. Blockade of sonic hedgehog signal pathway enhances antiproliferative effect of EGFR inhibitor in pancreatic cancer cells. *Acta Pharmacol. Sin.* **28**, 1224–1230 (2007).
103. Chang, D. Z. Synthetic miRNAs targeting the GLI-1 transcription factor inhibit division and induce apoptosis in pancreatic tumor cells in *AACR Meeting Abstracts 2007* 639b (The American Association for Cancer Research, Philadelphia, 2006).
104. Wang, Z. *et al.* Down-regulation of Notch-1 contributes to cell growth inhibition and apoptosis in pancreatic cancer cells. *Mol. Cancer Ther.* **5**, 483–493 (2006).
105. Wang, Z., Zhang, Y., Banerjee, S., Li, Y. & Sarkar, F. H. Notch-1 down-regulation by curcumin is associated with the inhibition of cell growth and the induction of apoptosis in pancreatic cancer cells. *Cancer* **106**, 2503–2513 (2006).
106. Dang, T., Vo, K., Washington, K. & Berlin, J. The role of Notch3 signaling pathway in pancreatic cancer [Abstract]. *J. Clin. Oncol.* **25**, 21049 (2007).
107. Doucas, H. *et al.* Expression of nuclear Notch3 in pancreatic adenocarcinomas is associated with adverse clinical features, and correlates with the expression of STAT3 and phosphorylated Akt. *J. Surg. Oncol.* **97**, 63–68 (2008).
108. Zeng, G. *et al.* Aberrant Wnt/beta-catenin signaling in pancreatic adenocarcinoma. *Neoplasia* **8**, 279–289 (2006).
109. Pasca di Magliano, M. *et al.* Common activation of canonical Wnt signaling in pancreatic adenocarcinoma. *PLoS ONE* **2**, e1155 (2007).
110. Nawroth, R. *et al.* Extracellular sulfatases, elements of the Wnt signaling pathway, positively regulate growth and tumorigenicity of human pancreatic cancer cells. *PLoS ONE* **2**, e392 (2007).
111. Romero, D., Iglesias, M., Vary, C. P. & Quintanilla, M. Functional blockade of Smad4 leads to a decrease in beta-catenin levels and signaling activity in human pancreatic carcinoma cells. *Carcinogenesis* **29**, 1070–1076 (2008).
112. Wang, Z. *et al.* Blockade of SDF-1/CXCR4 signalling inhibits pancreatic cancer progression *in vitro* via inactivation of canonical Wnt pathway. *Br. J. Cancer* **99**, 1695–1703 (2008).
113. Hermann, P. C. *et al.* Distinct populations of cancer stem cells determine tumor growth and metastatic activity in human pancreatic cancer. *Cell Stem Cell* **1**, 313–323 (2007).
114. Hiyama, E. *et al.* Telomerase activity is detected in pancreatic cancer but not in benign tumors. *Cancer Res.* **57**, 326–331 (1997).
115. Bernhardt, S. L. *et al.* Telomerase peptide vaccination of patients with non-resectable pancreatic cancer: a dose escalating phase I/II study. *Br. J. Cancer* **95**, 1474–1482 (2006).
116. Choudhury, A. *et al.* Treatment of advanced pancreatic cancer patients with a telomerase-peptide vaccine together with gemcitabine: a phase II clinical study in *AACR Meeting Abstracts 2007* 1863 (The American Association for Cancer Research, Philadelphia, 2007).
117. Calin, G. A. & Croce, C. M. MicroRNA signatures in human cancers. *Nat. Rev. Cancer* **6**, 857–866 (2006).
118. Tong, A. W. & Nemunaitis, J. Modulation of miRNA activity in human cancer: a new paradigm for cancer gene therapy? *Cancer Gene Ther.* **15**, 341–355 (2008).
119. Lee, E. J. *et al.* Expression profiling identifies microRNA signature in pancreatic cancer. *Int. J. Cancer* **120**, 1046–1054 (2007).
120. Lee, C. J., Dosch, J. & Simeone, D. M. Pancreatic cancer stem cells. *J. Clin. Oncol.* **26**, 2806–2812 (2008).
121. Olive, K. P. & Tuveson, D. A. The use of targeted mouse models for preclinical testing of novel cancer therapeutics. *Clin. Cancer Res.* **12**, 5277–5287 (2006).
122. Lev-Ari, S. *et al.* Curcumin synergistically potentiates the growth inhibitory and pro-apoptotic effects of celecoxib in pancreatic adenocarcinoma cells. *Biomed. Pharmacother.* **59 (Suppl. 2)**, S276–S280 (2005).
123. Kunnumakkara, A. B. *et al.* Curcumin potentiates antitumor activity of gemcitabine in an orthotopic model of pancreatic cancer through suppression of proliferation, angiogenesis, and inhibition of nuclear factor-κB-regulated gene products. *Cancer Res.* **67**, 3853–3861 (2007).
124. El-Rayes, B. F., Ali, S., Sarkar, F. H. & Philip, P. A. Cyclooxygenase-2-dependent and -independent effects of celecoxib in pancreatic cancer cell lines. *Mol. Cancer Ther.* **3**, 1421–1426 (2004).




© 2009 Macmillan Publishers Limited. All rights reserved

CORRECTION

## Pancreatic cancer: molecular pathogenesis and new therapeutic targets

Han H. Wong & Nicholas R. Lemoine

**Original article** Wong, H. H. & Lemoine, N. R. Pancreatic cancer: molecular pathogenesis and new therapeutic targets. *Nat. Rev. Gastroenterol. Hepatol.* **6**, 412–422 (2009).

In the July 2009 issue of *Nature Reviews Gastroenterology & Hepatology*, several errors were published in the Review article by Han H. Wong and Nicholas R. Lemoine. In Table 1, the targets Ras, Notch3 and SMAD4 should be displayed as *KRAS*, Notch 3, and *SMAD4*. On page 2, the 49th line of the right-hand column should read "…antisense inhibitors, such as ISIS 3521 and oblimersen…". In Figure 2, RAF should be displayed as Raf. On page 5, line 6 of the right-hand column, AKT2 should be displayed as *AKT2*. On page 7, the 4th line of the left-hand column should read '…KRas increases the therapeutic effect of IGF-I receptor antisense oligonucleotide.' In addition, the 10th line in the second paragraph of the right-hand column should read '…Ras, EGFR and TGF-α signaling…', and the 18th line should read "…γ-secretase inhibitor (L-685,458)…".

doi:10.1038/nrgastro.2009.123



© 2009 Macmillan Publishers Limited. All rights reserved

*Viruses* **2010**, *2*, 78-106; doi:10.3390/v2010078

OPEN ACCESS

*viruses*

**ISSN 1999-4915**

www.mdpi.com/journal/viruses

*Review*

# Oncolytic Viruses for Cancer Therapy: Overcoming the Obstacles

**Han Hsi Wong [1], Nicholas R. Lemoine [1,2] and Yaohe Wang [1,2,*]**

1 Centre for Molecular Oncology and Imaging, Institute of Cancer, Barts and The London School of Medicine and Dentistry, Queen Mary University of London, London EC1M 6BQ, UK; E-Mails: h.h.wong@qmul.ac.uk (H.H.W.); director@qmcr.qmul.ac.uk (N.R.L.)

2 Sino-British Research Centre for Molecular Oncology, Zhengzhou University, Zhengzhou 450052, China

* Author to whom correspondence should be addressed; E-Mail: yaohe.wang@qmul.ac.uk; Tel.: +44-2078823596, Fax: +44-2078823884.

*Received: 28 October 2009; in revised form: 2 January 2010 / Accepted: 6 January 2010 / Published: 11 January 2010*

---

**Abstract:** Targeted therapy of cancer using oncolytic viruses has generated much interest over the past few years in the light of the limited efficacy and side effects of standard cancer therapeutics for advanced disease. In 2006, the world witnessed the first government-approved oncolytic virus for the treatment of head and neck cancer. It has been known for many years that viruses have the ability to replicate in and lyse cancer cells. Although encouraging results have been demonstrated *in vitro* and in animal models, most oncolytic viruses have failed to impress in the clinical setting. The explanation is multifactorial, determined by the complex interactions between the tumor and its microenvironment, the virus, and the host immune response. This review focuses on discussion of the obstacles that oncolytic virotherapy faces and recent advances made to overcome them, with particular reference to adenoviruses.

**Keywords:** oncolytic virus; adenovirus; vaccinia virus; cancer gene; host immune response

---

## 1. Introduction

Cancer is a major cause of death globally. Although treatments for the disease have improved significantly, conventional chemotherapy or radiotherapy still have limited effects against many forms of cancer, not to mention a plethora of treatment-related side effects. This situation signifies a need for novel therapeutic strategies, and one such approach is the use of viruses. The ability of viruses to kill cancer cells has been recognized for more than a century [1]. They achieve this by a number of mechanisms, including direct lysis, apoptosis, expression of toxic proteins, autophagy and shut-down of protein synthesis, as well as the induction of anti-tumoral immunity. Although clinical trials of several naturally-occurring oncolytic viruses were started back in the 1950s, it was only in 1991 that a herpes simplex virus-1 (HSV-1) with deletion of its thymidine kinase *UL23* gene became the first genetically-engineered, replication-selective oncolytic virus to be tested in the laboratory [2]. In 2005, an adenovirus (Ad) with *E1B 55K* gene deletion (H101(Oncorine); Shanghai Sunway Biotech, Shanghai, China) was approved in China as the world's first oncolytic virus for head and neck cancer in combination with chemotherapy [3]. However, until now the widespread use of oncolytic virotherapy is still far from reality. Promising laboratory results have not been translated to improved clinical outcomes, and this appears to be determined by the complex interactions between the tumor and its microenvironment, the virus, and the host immunity. There are already a number of reviews on oncolytic viruses for cancer treatment but this article will focus on the obstacles facing oncolytic virotherapy, with particular reference to Ads, and the recent advances made to overcome these hurdles.

### *Mechanisms of tumor selectivity*

The term 'oncolytic viruses' applies to viruses that are able to replicate specifically in and destroy tumor cells, and this property is either inherent or genetically-engineered. Inherently tumor-selective viruses can specifically target cancer by exploiting the very same cellular aberrations that occur in these cells, such as surface attachment receptors, activated Ras and Akt, and the defective interferon (IFN) pathway (Figure 1). Some viruses have been engineered with specific gene deletion – these genes are crucial for the survival of viruses in normal cells but expendable in cancer cells (Figure 2). Deletion of the gene that encodes thymidine kinase, an enzyme needed for nucleic acid metabolism, results in dependence of viruses such as HSV and vaccinia virus on cellular thymidine kinase expression, which is high in proliferating cancer cells but not in normal cells. Vaccinia also produces the vaccinia growth factor (VGF) that binds to and activates the epidermal growth factor receptor (EGFR), creating an environment that supports its replication. It follows that deletion of genes encoding for both thymidine kinase and VGF leads to further selectivity of vaccinia virus in cancers with an activated EGFR-Ras pathway [4]. Another approach in conferring tumor selectivity is to restrict virus replication by its dependence on transcriptional activities that are constitutively activated in tumor cells. This can be achieved by the insertion of a tumor-specific promoter driving the expression of a critical gene [5-11]. Others viruses either possess naturally (e.g., Coxsackievirus A21 [12] and measles virus (MV) [13]) or have been designed to have specific tropism based on the expression of cell surface receptors unique to cancer cells [14-20].

**Figure 1.** Mechanisms of tumor selectivity of several oncolytic viruses. The interferon (IFN)/double-stranded RNA-activated protein kinase (PKR) pathway is a natural anti-viral defense system. IFNs produced by infected cells result in the upregulation of PKR. On binding to viral double-stranded RNA (dsRNA), PKR autophosphorylates, which in turn phosphorylates the α subunit of eIF-2. Phosphorylated eIF-2α sequesters eIF-2B, a guanine nucleotide exchange factor. Without eIF-2B, the GDP bound to eIF-2 cannot be exchanged for GTP. As a result eIF-2 is unable to bring the initiator transfer RNA (tRNA) to the 40S ribosomal subunit, and the synthesis of viral protein is inhibited. Inactivated IFN and activated Ras pathways are frequently found in cancer (the latter could inhibit PKR), and some naturally-found viruses can replicate selectively in cancer but not normal cells, including the Newcastle disease virus (NDV) [21], reovirus [22], vaccinia virus [23], and vesicular stomatitis virus (VSV) [24]. The herpes simplex virus (HSV) protein ICP34.5 interacts with cellular phosphatase 1α to dephosphorylate eIF-2α, leading to synthesis of proteins needed for virus replication. Deletion of gene that encodes for ICP34.5 (*RL1*) results in selective replication in tumors with a defective IFN/PKR pathway [25]. The influenza virus *NS1*-deleted mutant is also dependent on this defective pathway [26]. Adenoviruses normally produce virus-associated (VA) RNAs to inhibit PKR. As such, engineered *VAI*-deleted adenovirus (*dl*331) could replicate selectively in tumors with an activated Ras pathway [27]. Epstein-Barr virus (EBV) also expresses RNAs similar to VA RNAs and these can complement *dl*331, resulting in selectivity in EBV-associated tumors [28].

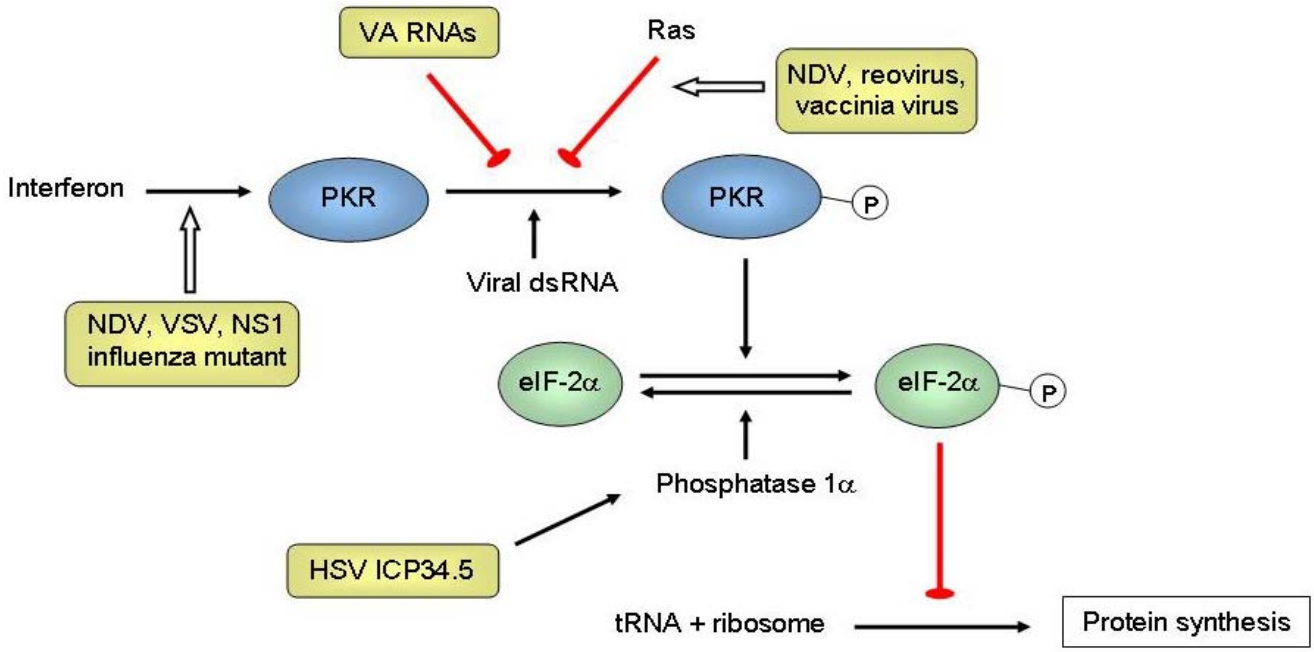

**Figure 2.** Engineered replication selectivity of oncolytic adenoviruses (Ads) by deletion of the *E1A*, *E1B 19K* or *E1B 55K* gene. Retinoblastoma protein (pRb) is normally hypophosphorylated and binds to transcription factors of the E2F family to regulate the G1-to-S checkpoint of the cell cycle. Upon stimulation by mitogenic signals, upregulation of cyclins enables cyclin-dependent kinases (CDKs) to phosphorylate pRb, releasing E2F that leads to the expression proteins needed for DNA synthesis and thus cell cycle progression. E2F upregulates $p14^{ARF}$, which inhibits Mdm2. Mdm2 normally results in p53 degradation. p53 is a transcription factor that is upregulated and activated by stress signals such as virus infection or DNA damage. It results in the expression of proteins that induce apoptosis (Bax), cell cycle arrest ($p21^{CIP1/WAF}$ via its inhibition of CDK2) or DNA repair. $p16^{INK4A}$ is a tumor suppressor that inactivates CDK4/6. The adenoviral E1A proteins bind to pRb to release E2F, so that viral DNA could be replicated. E1A also promotes the acetylation of pRb by p300/CBP, causing pRb to associate with Mdm2 to inhibit p53. Because cancer cells are often in the S phase, *E1A CR2*-deleted Ad5 mutant (*dl*922-947) could selectively replicate in and destroy replicating cancer cells but not normal resting cells [29]. E1B 19K binds to and inhibits Bax. The tumor selectivity of *E1B 19K*-deleted Ad2 (*dl*250) is due to multiple defects in the apoptotic pathways, where survival of the virus in normal cells would be limited owing to rapid apoptosis induction in the presence of tumor necrosis factor-α (TNF-α) [30]. E1B 55K interacts with the adenovirus E4 open reading frame 6 (E4orf6) protein to form an E3 ubiquitin ligase complex that targets p53 for degradation. It also induces the expression of cyclin E as well as simultaneously inhibits cellular mRNA export and promotes the export of late viral mRNAs. *E1B 55K*-deleted Ad could replicate in tumor selectively because of non-functioning p53 [31], cyclin E overexpression [32], and E1B 55K-independent late viral RNA export in cancer but not normal cells [33].

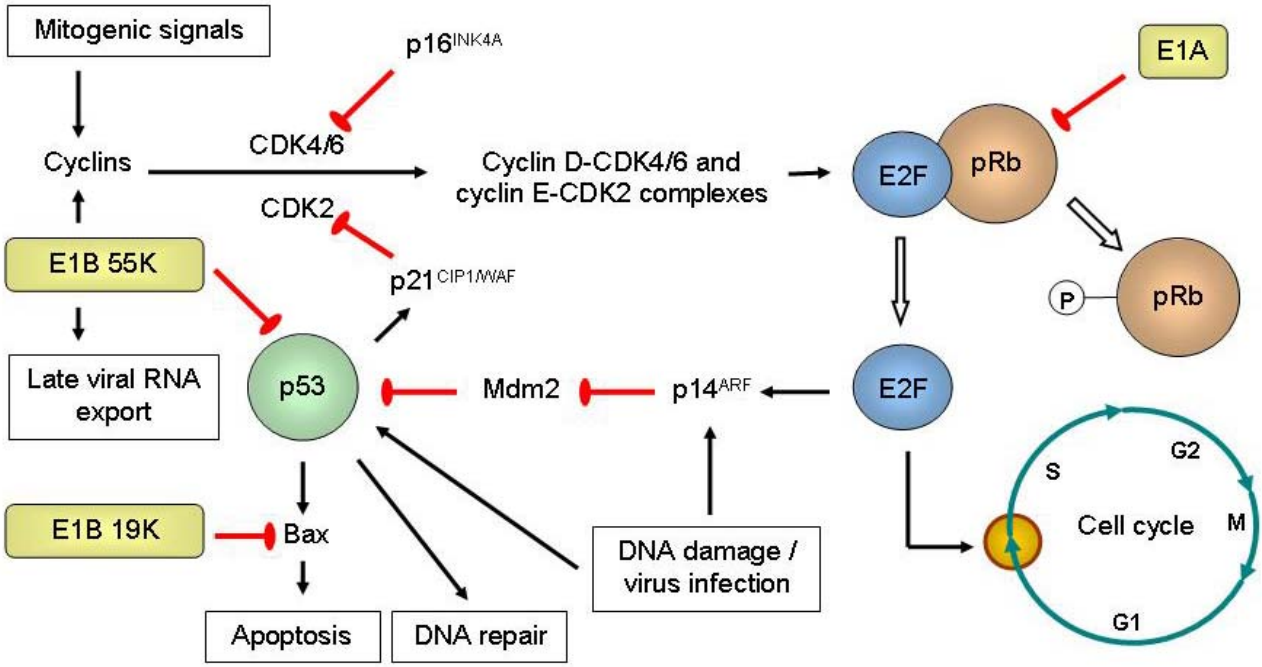

More recently, gene silencing by RNA interference technology has been utilized to confer tumor selectivity. MicroRNAs (miRNAs) or small interfering RNAs (siRNAs) regulate gene expression post-transcriptionally by translation block or cleavage of specific, complementary mRNA via the RNA-induced silencing complex (RISC). By inserting a complementary sequence next to a critical viral gene, it is possible to confine virus replication to tumor but not normal cells that express high levels of the corresponding miRNA. This has been demonstrated by several groups [34-38]. Gürlevik *et al.* [39] developed a recombinant Ad that encodes multiple RNA-interfering transcripts under the control of a p53-responsive promoter. The transcripts could effectively silence a set of critical viral genes. As p53 is a transcription factor often lost or mutated in human malignancy, this virus could therefore replicate in cancer but not normal cells where functional p53 would lead to an anti-viral RNA interference.

*Optimizing oncolytic viruses for improved anti-tumoral potency*

Gene-manipulated oncolytic viruses such as Ad, herpes virus and vaccinia virus are being developed as a new class of anti-tumoral agent [23,40,41]. Selective intratumoral replication of the virus may lead to improved efficacy over non-replicating agents due to the self-perpetuating nature of the treatment with virus multiplication, lysis of the infected tumor and spread to adjacent cells. One potential limitation of this approach, however, is that gene deletions resulting in tumor selectivity also frequently result in reduced oncolytic potency. For example, *dl*1520 (ONYX-015; Onyx Pharmaceuticals, California, USA) is an oncolytic Ad2/Ad5 hybrid with deletion of its *E1B 55K* and *E3B* genes. The E1B 55K protein is involved in p53 inhibition, viral mRNA transport and host cell protein synthesis shut-off [42] (Figure 2), whilst E3B proteins are important for immune avoidance (see below). This virus was the first engineered, replicating Ad to enter clinical trials for cancers including those of the head and neck [43-45] and pancreas [46,47]. Whilst the virus has shown good tumor selectivity and safety [48], durable objective responses with this virus as a single agent have been limited and this could be partly due to the loss of other essential functions of the *E1B 55K* and *E3B* genes. A recent finding by Thomas *et al*. [49] revealed that *dl*1520 was less efficient in lysing cells infected in the G1 phase of the cell cycle due to a reduced rate of late viral protein synthesis, and this appears to be a result of the adenoviral gene product encoded by open reading frame 1 of early region 4 (*E4orf1*). As such there is a need to increase the potency of these viruses by identifying mutations that result in tumor selectivity but not those that result in attenuated virus replication and oncolysis. Since the first generation of replication-selective Ads was tested in pre-clinical experiments and clinical trials, several advances have been made to improve potency by dissecting the functions of different genes of Ad.

The adenoviral *E1A* is the earliest gene to be transcribed after virus entry into the host cell [50]. E1A normally interacts with the retinoblastoma protein (pRb) (the latter is important in regulating the G1-to-S cell-cycle checkpoint), and this pushes quiescent cells into S phase to allow for virus replication (Figure 2). Therefore, *dl*922-947, the mutant Ad with specific deletion of the *E1A CR2* region (pRb binding site), was unable to replicate in quiescent normal cells but was able to do so in cancer cells with defective G1-to-S checkpoint. This virus has demonstrated superior anti-tumoral activity *in vivo* compared to *dl*1520 after intratumoral and intravenous injections [29], although it might also target proliferating non-malignant cells. In addition to its effect on virus release and

spread [51,52], adenoviral E1B 19K is a functional homolog of Bcl-2 and is able to bind to Bax [53-55] and also prevent Fas-mediated apoptosis [56]. Replication of the mutant Ad2 with *E1B 19K* deletion (*dl*250) was significantly reduced in normal cells secondary to rapid apoptosis induction in the presence of tumor necrosis factor-α (TNF-α), whilst the opposite occurred in cancer cells due to multiple defects in the apoptotic pathways (e.g., p53 mutation, Bcl-2 overexpression) [30] (Figure 2). Virus replication, spread and anti-tumoral potency was significantly better than *dl*1520 and wild-type Ad2. *E1B 19K*-deleted Ad5-infected cancer cells also expressed lower levels of EGFR and anti-apoptotic proteins [57].

Ads also produce the virus-associated (VA) RNAs. These are RNA polymerase III transcripts that, amongst other functions, are obligatory for efficient translation of viral and cellular mRNAs by blocking the double-stranded RNA-activated protein kinase (PKR) [58,59], a natural host anti-viral defense system (Figure 1). We have shown that *VAI*-deleted Ad5 (*dl*331) was able to selectively target Epstein-Barr virus (EBV)-associated tumors such as Burkitt's lymphoma and nasopharyngeal carcinoma [28]. This is because EBV expresses the RNAs EBER1 and EBER2, whereby EBER1 could complement *dl*331 to enable the synthesis of viral proteins. Interestingly, anti-tumoral efficacy *in vitro* and *in vivo* was superior to wild-type Ad5 and this might be the result of PKR-induced apoptosis, increased IFN-β production, and the adenoviral *E3B* gene deletion.

Gene products encoded by the adenoviral *E3* region could also affect its oncolytic potency. These include the *E3 11.6K* (or adenovirus death protein – ADP), which facilitates late cytolysis of infected cells and release of progeny viruses [60]. Ads that overexpress ADP showed better cell lysis and spread [61,62]. The effects of *E3B* and *E3 gp19K* genes on the potency of oncolytic adenovirus will be discussed later.

*Arming oncolytic viruses with therapeutic genes*

The discovery of the genetic basis of malignancy has in part promoted the development of cancer gene therapy, which involves the introduction of exogenous nucleic acid to restore, express or inhibit a particular gene of interest. Viruses are at present the most efficient gene delivery system. A well-known example is Gendicine (Shenzhen SiBiono GeneTech, Shenzhen, China), an Ad5 vector encoding the human *TP53* gene that was approved in 2004 by China's State Food and Drug Administration for the treatment of head and neck cancer [63]. Although developed for safety reasons, one major shortcoming of using non-replicating vectors such as Gendicine (by virtue of its *E1A* gene deletion) is that infectivity is limited to only one cycle. In contrast, oncolytic viruses can replicate and spread in cancer cells resulting in longer transgene expression. Together with tumor lysis this would lead to better therapeutic efficacy. Arming oncolytic viruses with anti-cancer genes has been a major focus in cancer virotherapy, and transgenes exploited include tumor suppressor, pro-apoptotic, anti-angiogenic, "suicide", and immunomodulatory genes.

Like Gendicine, oncolytic viruses could be armed with tumor suppressor or pro-apoptotic genes that are frequently lost in cancer. One example is by the use of $p16^{INK4A}$-armed oncolytic Ad, which has shown good inhibition of gastric tumor xenografts [64]. Wang *et al*. [65] developed an Ad in which the *E1A* gene is regulated by the human telomerase reverse transcriptase (hTERT) promoter and hypoxia response element, together with p53 under the strong cytomegalovirus (CMV) promoter. This virus

showed tumor selectivity with efficient p53 expression and oncolysis. Nonetheless, targeting a single gene is unlikely to have a major impact on survival, given that in cancer a large number of genetic alterations affect only a core set of signaling pathways and processes, as has been recently described for pancreatic cancer [66]. Hence there should be a move from targeting these genes individually to targeting cancer signaling pathways, such as arming oncolytic Ad with an engineered transgene that encodes transforming growth factor (TGF)-β receptor II fused with the human Fc $IgG_1$, as studied by Hu *et al*. [67]. Anti-tumoral effects were observed with a replication-selective (but not replication-deficient) virus encoding this gene, highlighting the importance of virus replication. Viruses that enhance the apoptotic pathways have also been studied. Jin *et al*. [68] and Chen *et al*. [69] utilized the chimeric Ad5/35 carrying the gene encoding the TNF-related apoptosis-inducing ligand (TRAIL) to promote receptor-independent infection (see below) and apoptosis of leukemic and gastric cancer cells, respectively. Zhang *et al*. [70] treated pancreatic cancer cells by replacing the gene for human somatostatin receptor 2 (lost in 90% of pancreatic cancers) and introducing the gene for TRAIL by means of an oncolytic Ad, with good results *in vivo*. A reciprocal approach is to ablate the function of oncogenes post-transcriptionally by arming oncolytic Ad with small hairpin RNA (shRNA). Recent work includes those targeting hTERT [71], Ki-67 [72], Survivin [73], and Apollon [74], all of which have shown efficient anti-tumoral effects *in vitro* and *in vivo*.

The tumor microenvironment plays a critical role in promoting malignant cell growth and progression, as well as restricting virus spread. One important issue is tumor angiogenesis. A recent finding by Ikeda *et al*. [75] suggested that the replication-selective Ad OBP-301, in which the *E1* genes are under the control of the hTERT promoter, could stimulate peripheral blood mononuclear cells (PBMCs) to produce IFN-γ that has anti-angiogenic properties, resulting in reduced tumor vascularity and slowed growth in immunocompetent mice. However, Kurozumi *et al*. [76] also showed that intratumoral treatment of rat glioma with oncolytic HSV could promote neovascularization of the residual tumor, and this was associated with a significant increase in the angiogenic factor CYR61. This could have an impact on subsequent tumor growth and the observation suggests that a combination of oncolytic virus with anti-angiogenic transgene might be needed; for this we refer the reader to our recent article for a more comprehensive review [77]. Recent work includes the use of the anti-angiogenic factors endostatin/angiostatin [78-80], interleukin-18 (IL-18) [81,82], canstatin [83], and trichostatin A [84], as well as arming viruses with genes that inhibit pro-angiogenic molecules such as IL-8 [85] and vascular endothelial growth factor (VEGF) [86,87]. Kang *et al*. [88] made use of a transcriptional repressor based on zinc-finger protein to target the VEGF promoter. An oncolytic Ad armed with this gene significantly reduced vessel density and tumor size of human glioblastoma xenografts in mice. The matrix metalloproteinases (MMPs) are a family of proteolytic enzymes that degrade the extracellular matrix and are essential for tumor spread and neovascularization. Oncolytic viruses armed with genes that encode MMP inhibitors have shown encouraging results in delaying tumor growth and angiogenesis [89,90].

Gene-directed prodrug activation therapy (or suicide gene therapy) involves the delivery of a gene that would lead to the expression of an enzyme, followed by the administration of a prodrug that is activated selectively by this enzyme. One example is the HSV thymidine kinase (HSV-TK)-ganciclovir method, whereby HSK-TV is able to monophosphorylate ganciclovir, which is subsequently converted by cellular kinases to the triphosphorylated forms, blocking DNA synthesis

and inducing cell death. Most publications have described the use of replication-deficient viruses with this approach, but recent studies that demonstrated its efficacy using replication-selective oncolytic Ads include treatment for prostate [91], gallbladder [92], and liver [93] cancers. Alternative combinations include nitroreductase with the prodrug CB1954 (converted into an alkylating agent) [94], and cytosine deaminase (CD) with 5-fluorocytosine, which is converted into the cytotoxic and radiosensitizing 5-fluorouracil [95,96]. An Ad5 with *E1B 55K* deletion, ADP overexpression and CD/TK fusion gene expression is currently in a phase III trial in combination with radiotherapy for patients with prostate cancer.

*The tumor environment and oncolytic viruses*

Viruses are naturally larger than other anti-cancer agents such as chemicals and antibodies (for example 90 nm and 300 nm for Ad and vaccinia virus, respectively). After intratumoral injection, effective virus spread could be impaired by the extracellular matrix, areas of fibrosis and necrosis, and surrounding normal cells in the tumor bed, although Kolodkin-Gal *et al*. [97] found that the extracellular components collagen and mucin could restrict HSV-1 infectivity in normal colon, but these molecules were expressed in lesser amounts in colonic carcinoma, facilitating its spread. Ganesh *et al*. [98] studied the co-administration of the enzyme hyaluronidase with oncolytic Ads during intratumoral injection. This degraded the major constituents of the extracellular matrix, hyaluronan, resulting in enhanced virus spread *in vivo*. Induction of cancer cell death with an apoptosis-inducing agent prior to injection of oncolytic HSV could also produce channels for effective virus spread [99]. Elevated interstitial hydrostatic pressure as a result of fibrosis and vessel abnormalities poses another physical barrier to successful virus delivery and this effect increases with tumor volume [100]. Injected viruses could escape back through the injection site or by drainage into the circulation, resulting in reduced efficacy and increased risk of systemic toxicities. Bazan-Peregrino *et al.* [101] examined the retention of Ad5 in MDA-231 and ZR75.1 human breast carcinoma xenografts after intratumoral injection. For MDA-231, occlusion of injection sites with surgical adhesives and the use of small injected volumes resulted in significantly higher virus retention within the tumors. ZR75.1, however, took up more Ad than MDA-231 when identically infected, suggesting a role of tumor type in virus retention. Recently, tumor-associated stromal cells have been shown to play a role in either enhancing or reducing the efficacy of oncolytic Ads, depending on the tumor type [102]. Hypoxia, a common feature in tumor tissues, has been found to reduce the replicative and oncolytic potential of Ads despite the unaltered expression of surface receptors [103,104]. In this regard there might be a role for the development of oncolytic viruses in which replication is not attenuated by hypoxia, such as vaccinia virus [105] or HSV [106,107].

For viruses that have reached the immediate vicinity of the tumor, cellular genetic changes could prevent successful virus entry into the cells. For cellular entry of most Ads (those in subgroups A, C, D, E and F – which include the commonly used Ad5), they must first bind to the Coxsackie and adenovirus receptor (CAR) on the surface membrane via the knob portions of their fibers, followed by internalization mediated by the viral penton proteins and cellular integrins. CAR is ubiquitously expressed in epithelial cells, but its expression is often downregulated in many cancer types due to activation of the Raf-MAPK pathway [108]. Recent work has shown that the molecule leucine-rich

repeat-containing protein 15 (LRRC15 or hLib), frequently overexpressed in tumor cells, could result in the redistribution of CAR away from cell surfaces, thus impeding Ad infection [109]. In contrast, most subgroup B Ads bind to CD46 [110], a receptor often upregulated in a number of tumor types, including breast, cervical, liver, lung, endometrial and hematological malignancies [111-113]. Several chimeric oncolytic Ad5 have been developed to contain the fiber tropism of subgroup B Ads and they all have shown encouraging results [68,69,114-117]. The use of intact subgroup B Ads as oncolytic agents is still under-explored but has great potential [118,119]. They have different tropism and infectivity compared to chimeric viruses [120], and are more beneficial in terms of a reduced propensity for neutralization by pre-existing antibodies (see below). Besides CD46, evidence suggests that the subgroup B Ad, Ad11, also utilizes another unidentified receptor [121,122], tentatively named 'receptor X' by Tuve *et al*. [123]. They also discovered that the other subgroup B Ads, Ad16, -21, -35 and -50 exclusively use CD46, whereas Ad3, -7 and -14 use 'receptor X' but not CD46. It is possible that Ad11 could infect a wider range of tumor cells and overcome receptor downregulation; the latter is a known problem with Ad35 and CD46 [124]. Strauss *et al*. [125] showed that Ads that utilize CAR or CD46 as primary attachment receptors failed to infect and lyse ovarian cancer cells of the epithelial phenotype, which are found in *in situ* tumors and tumor xenografts. These receptors are trapped in the tight junctions and therefore not accessible to the virus. However, Ads that use receptor X (Ad3, -7, -11 and -14) could induce epithelial-mesenchymal transition and result in efficient oncolysis.

Cellular signaling pathways can also affect virus infectivity. Recently our group [126] has shown that certain pancreatic cancer cell lines overexpress the carcinoembryonic antigen–related cell adhesion molecule 6 (CEACAM6), which antagonizes the Src signaling pathway, downregulates cancer cell cytoskeleton proteins, and blocks Ad trafficking to the nucleus. Knockdown of CEACAM6 by siRNA significantly enhanced the anti-tumoral potency of oncolytic Ad5. For virus that has successfully entered the cell, it needs to replicate for efficient cell lysis and virus spread. The protein $p21^{CIP1/WAF}$ normally inhibits cyclin-dependent kinase 2 (CDK2) (Figure 2) and blocks the progression of the cell cycle from G1 to S phase. Shiina *et al*. [127] showed that siRNA knockdown of $p21^{CIP1/WAF}$ increased Ad replication and oncolysis. It was suggested that this could be due to the inhibition of SET and proliferating cell nuclear antigen (PCNA) by $p21^{CIP1/WAF}$, whereby SET and PCNA normally increase viral DNA replication. In the case of vaccinia virus, recent work has suggested that cells with activated c-Jun NH2-terminal kinase (JNK) signaling cascade could activate PKR (Figure 1), thus reducing virus replication [128].

Cancer stem cells form part of the heterogenous tumor population. They not only contribute to neoplastic progression and metastasis, but also to resistance to chemotherapy and radiotherapy. Evidence has shown that oncolytic Ads are able to destroy these cells [129-131]. Zhang *et al*. [132] have recently demonstrated that a telomerase-specific oncolytic Ad armed with a gene that encodes the apoptotic TRAIL was able to preferentially target stem-like esophageal cancer cells and prolong the survival of mice bearing tumors composed of these cells. Whilst this is of interest, cancer stem cells only form a small subset of the tumor mass and the value of targeting them specifically will remain an issue to be resolved.

*Modification of the host immune response in favor of oncolytic viruses*

Most studies of oncolytic viruses have been done, by necessity, on human tumor xenografts in immunodeficient mice – far from reflective of the human condition. Unsurprisingly, data from these studies have not been predictive for clinical trial results. The effects of the host immune response on the efficacy of oncolytic viruses are complex. When stimulated, immune cells could result in virus clearance but might also induce specific and non-specific anti-tumoral activities. It appears that the innate immune response plays an important role in virus clearance, whereas T cell-mediated responses are largely responsible for the anti-tumoral effect [133-137].

For the treatment of metastatic or hematological malignancies, intravenous virus delivery could be hindered by neutralizing antibodies, complement activation, non-specific uptake by other tissues such as the liver and spleen, as well as poor virus escape from the vascular compartment (Figure 3). For Ad, adhesion to blood cells could also lead to therapeutic inhibition [138]. Numerous experiments have been done to modify the immune response in favor of virus replication and tumor lysis. One method is by using an immunosuppressive agent, such as cyclophosphamide, that has been shown to improve virus spread and anti-tumoral efficacy [139-145]. Kurozumi *et al*. [146] found that single doses of the angiostatic and anti-inflammatory cyclic peptide of arginine-glycine-aspartic (cRGD), given before an oncolytic HSV, resulted in reduced tumor vessel permeability, leukocyte infiltration and IFN-γ, leading to increased survival of rats with intracranial gliomas. Various data suggest that pre-existing antibodies decrease virus spread after intravenous delivery [147-149], but have a lesser effect on intratumoral injection [44,150,151]. Although antibodies could prevent possible toxicity [152], they could also reduce efficacy. Possible ways to circumvent this include plasmapheresis to deplete antibodies and the use of other viral strains with a lower prevalence of antibodies in the human population. One example is Ad11 [118,119], with a reported antibody prevalence of 10-31% compared to 45-90% for Ad5 [122,153-155]. These antibodies are mainly directed against the viral hexon proteins [156], suggesting that the use of Ad11 virion might be better than chimeric Ad5/11, where the fibers are derived from Ad11 but the rest, including hexon, belong to Ad5. A caveat to this is that for unknown reasons, Ad11 appears to induce more pro-inflammatory cytokines and chemokines than Ad5 or Ad5/11 in mice after systemic injection [120].

Instead of injecting naked virions, using cells as delivery vehicles could hide the viral antigen from antibodies and complements. This so-called "Trojan horse" strategy involved infecting the body's cells *in vitro* and administering these cells back systemically, which would then carry the oncolytic virus to the tumor environment. Cells that have been tested include mesenchymal stem cells [157-159], monocytes [160], outgrowth endothelial cells [160], tumor cells [161-163], T cells [164-166], and dendritic cells (DCs) [165]. Ong *et al*. [167] showed that MV-infected T cells could facilitate tumoral delivery in low, but not high antibody concentration. Power *et al*. [168] tested a number of carrier cells including solid tumor and leukemic cells, and demonstrated that the efficacy of oncolytic vesicular stomatitis virus (VSV) was significantly improved compared to naked virion injection. Interestingly, Zhu *et al*. [169] demonstrated that mice pre-immunized with HSV exhibited reduced growth of S-180 tumor after intratumoral treatment with HSV. PBMCs from seropositive mice showed greater cytotoxicity *in vitro* compared to naïve mice, with higher IFN-γ induction. It is not known if this also applies to intravenous virus delivery or to other oncolytic viral species. Whilst the cell carrier approach

has yielded promising data *in vivo*, numerous issues must be considered before clinical application, including the best cell type to use, ease of infection, tumor-targeting capabilities, protection of virus from the host immune response, virus delivery, and tumorigenicity. Recently Kangasniemi *et al*. [170] have demonstrated that silica gel-encapsulated Ads allowed for extended release of the viruses and slightly delayed the development of anti-Ad antibodies. This method has anti-tumoral activity, but comparison with other methods of administration was not performed.

After intravenous delivery the liver, part of the reticuloendothelial system, is the predominant site of Ad5 sequestration with significant hepatocyte transduction [171,172]. Ad5 is known to cause liver toxicity, and its use has raised some concerns after the death of Jesse Gelsinger in 1999 from Ad5-based gene therapy injected directly into the hepatic artery [173]. A landmark study by Waddington *et al*. [174] showed that liver transduction is mediated by interaction of the adenoviral hexon protein with the blood coagulation factor X. This provides a further rationale for the development of other Ad serotypes for oncolytic therapy, such as Ad11 and Ad35 as they bind weakly to factor X compared to Ad5 [118] or other Ad5 chimera. In CD46 transgenic mice, Ad11 persisted much longer in the circulation after intravenous delivery compared to Ad5 together with the absence of liver transduction [120,122]. As for Ad5, ways to reduce liver uptake include recent experiments performed by Barry *et al*. They studied the effect of Kupffer cell depletion (by pre-dosing mice with non-replicating Ad5) and warfarin treatment (to inhibit vitamin K-dependent coagulation factors) and found that this approach significantly increased the anti-tumoral effect of systemically delivered oncolytic Ad5 in nude mice [175]. Good results have also been demonstrated by coating Ad5 with high molecular weight polyethylene glycol [176] or by genetic modification of the hexon protein to ablate blood factor binding [177] for liver detargeting.

A plethora of immunostimulatory genes have been inserted into the genome of oncolytic viruses with the aim of stimulating effective anti-tumoral immune responses. Recent examples include the heat shock proteins [179,180], chemokine (C-C motif) ligand 5 (CCL5) [181], IFN [182], granulocyte macrophage colony-stimulating factor (GM-CSF) [183-185], IL-12 [186], IL-18 [81,82], and IL-24 [187,188]. Vaccinia virus normally expresses a number of type I IFN-inhibiting proteins to counteract the cellular IFN anti-viral response. Because cancer cells frequently have an inactivated IFN pathway, anti-IFN gene-deleted vaccinia could selectively replicate in these cells. Kirn *et al*. [189] utilized this mutant and inserted a gene that encodes IFN-β (which itself has anti-proliferative, anti-angiogenic, and immunomodulatory anti-tumoral effects), and demonstrated enhanced tumor selectivity and potency *in vivo*. Shashkova *et al*. [190] used a four-pronged approach by co-infecting cancer cells with a replicating oncolytic Ad with ADP overexpression and IFN-α expression, given together with a non-replicating virus encoding the gene for TRAIL, with impressive results. The currently used oncolytic MVs were derived from the attenuated Edmonston tag (Edmtag) strain. Significantly, they lack antagonizing activity against the host anti-viral IFN immune response, thus inhibiting virus spread. Recombinant MV encoding the measles phosphoprotein (*P*) gene product from wild-type MV, an IFN antagonist, has been found to exhibit reduced IFN sensitivity and better oncolytic potency *in vivo* [191]. A recombinant VSV vector which expresses a gene from human CMV has been found to have increased anti-tumoral activity *in vivo* [192]. The expressed protein inhibited the natural killer (NK) cell-activating ligand CD155, resulting in decreased accumulation of NK and NKT cells at the infected tumor site and elevated virus replication.

**Figure 3.** Obstacles to successful delivery of oncolytic viruses to tumor cells. After intravenous injection, viruses are neutralized by pre-existing antibodies and complement activation. Adenoviruses (Ads) also interact with blood cells. Recent work has revealed that Ad5 binds to erythrocytes via the Coxsackie and adenovirus receptor (CAR) and complement receptor 1 (CR1) in the absence and presence of anti-Ad5 antibodies, respectively [178]. Sequestration into other organs and the reticuloendothelial system is a particular problem, often with resulting toxicities. From the blood stream, viruses have to pass through a mixture of extracellular matrix, cells (including normal and immune cells) and high interstitial fluid pressure before reaching the tumor. They then have to attach to the cellular receptor (often trapped in tight junction), be internalized, translocate to the nucleus, replicate, produce structural and other proteins, lyse the cell and release their progenies – some of these steps could be inhibited by factors such as the natural host immune response, hypoxic environment, soluble factors, and genetic changes in the tumor cell.

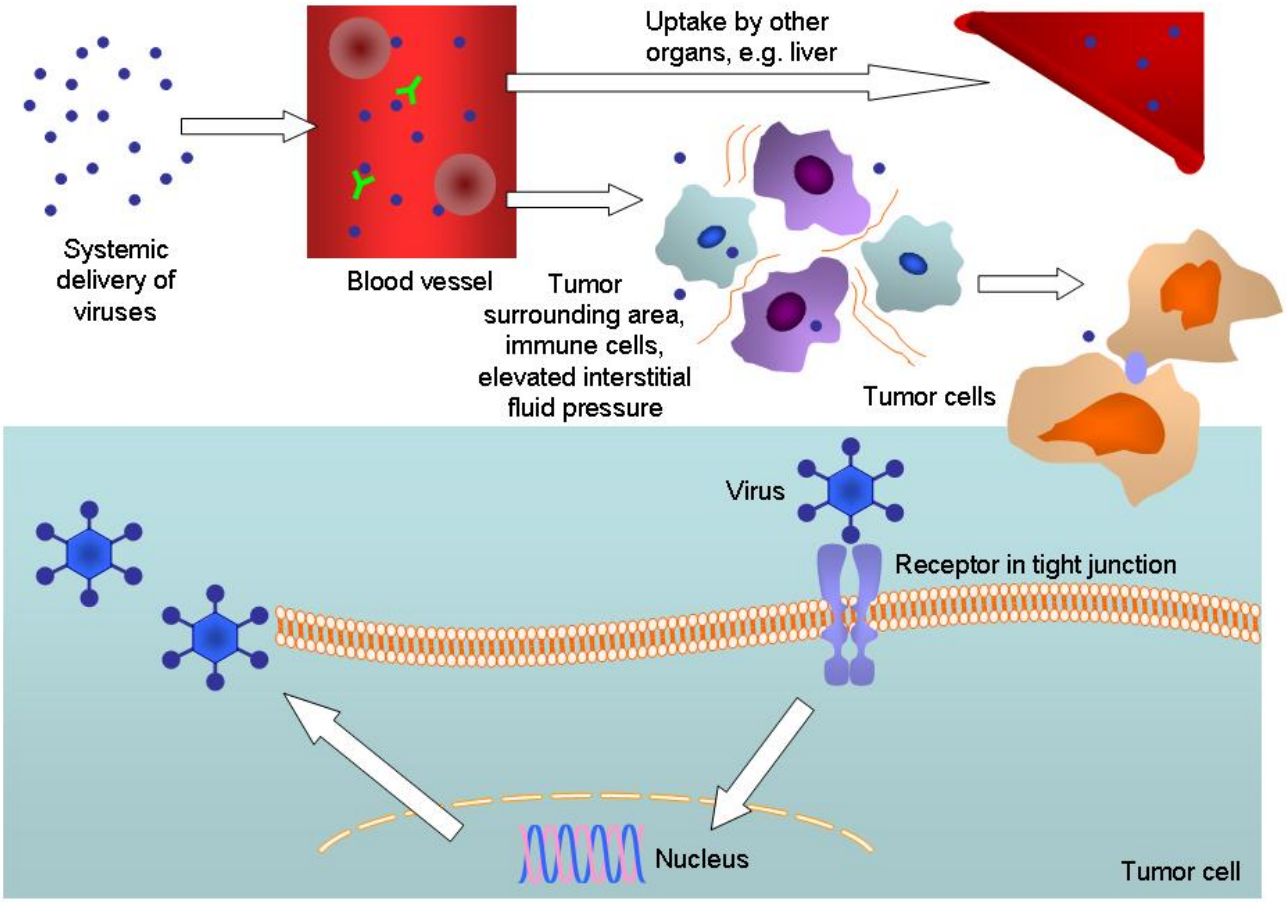


Antigen-specific activation and proliferation of lymphocytes are regulated by interaction of the peptide-antigen-major histocompatibility complex (MHC) with the T cell receptor, as well as both positive and negative signals from co-stimulatory molecules expressed on antigen-presenting cells (APCs). The most important of the APCs are the DCs. DCs are capable of capturing antigens secreted or shed by tumor cells and upon maturation, present the peptides to T cells. Endo *et al*. [193] showed that virus replication led to the production of uric acid in cancer cells, which stimulated DCs to

produce IFN-γ and IL-12. IFN-γ subsequently induced the expression of the proteosome activator PA28, which functions to generate tumor antigenic peptides required for MHC class I presentation, resulting in the induction of cytotoxic T lymphocytes (CTLs) against tumor cells. Lapteva *et al*. [194] and Ramakrishna *et al*. [195] demonstrated that increased DC migration and maturation by oncolytic Ad encoding β-defensin-2 or macrophage inflammatory protein 1α (MIP-1α) and Fms-like tyrosine kinase-3 ligand (Flt3L) significantly enhanced anti-tumoral immune responses. Chuang *et al*. [196] used another approach whereby tumor-bearing mice were first primed with DNA encoding a highly immunogenic foreign antigen ovalbumin (OVA), followed by intratumoral injection of vaccinia virus encoding the same antigen. The DNA vaccination served to generate OVA-specific CTLs against infected cancer cells, and the virus resulted in further oncolysis. A study by Diaz *et al*. [135] revealed that depletion of regulatory T cells reduced the efficacy of oncolytic VSV, due to the relief of anti-viral immune response suppression. Anti-tumoral immune activity could be improved by adoptive T cell transfer or incorporation of tumor-associated antigen into the virus. Huang *et al*. [197] utilized an oncolytic Ad armed with IL-12 and 4-1BB ligand, and demonstrated impressive results in mice bearing B16-F10 melanoma tumors. Amongst other functions, 4-1BB ligand (expressed on DCs) enhances T cell proliferation and IL-12 promotes their differentiation. The anti-tumoral effect was even greater when the virus was given together with DCs.

The *E3* region of the adenoviral genome is divided into *E3A* (encodes the 12.5K, 6.7K, gp19K and 11.6K proteins) and *E3B* (10.4K, 14.5K and 14.7K proteins) and is involved in immune response evasion and virus release from cells. Because it is dispensable, this region is frequently deleted in many adenoviral mutants to provide more space for therapeutic gene insertion, although recent work has suggested that transgene expression was higher if gene was inserted at regions other than *E3*, such as *L3* [198]. Deletion of the whole *E3B* region, however, could attenuate the virus oncolytic potency by increasing macrophage infiltration and expression of TNF and IFN-γ [51,133]. Potency could be restored by selective deletion of *E3 gp19K* whilst retaining other *E3* regions [133,199]. In addition to the inhibition of NK cell activation [200], gp19K is an endoplasmic reticulum membrane glycoprotein that inhibits the transport of MHC class I to the cell surface and delays its expression to avoid killing by CTLs [201,202]. CTL evasion is common in tumor cells and therefore the function of gp19k is redundant in these cells. Deletion of this gene, however, would ensure normal cells infected with this virus are eradicated, and in effect this confines virus replication to tumor cells.

## Conclusions

The field of oncolytic virotherapy is expanding and viruses continue to hold promise as effective treatments in combination with chemotherapy or other therapeutic modalities. As continuing work is being done to improve the currently available oncolytic viruses, novel viral species are also emerging and worth exploring, for example the porcine Seneca Valley virus [203], myxoma virus [204], Sindbis virus [205], and Semliki Forest virus [206]. Viruses have unique properties in comparison to small molecular drugs. They can replicate and spread in addition to carry anti-tumoral therapeutic genes. However, during the course of evolution the human body has developed ways to overcome infection and this has imposed a significant barrier towards achieving maximum therapeutic efficacy of oncolytic viruses. Recent advances in our understanding of tumor biology and virology have helped to

overcome some of these hurdles, and different groups have successfully targeted features that varied from virus delivery to altering the host immune response. It is hoped that this collective effort will finally pave way for the development of effective and safe viruses for cancer therapy.

**Acknowledgements**

The authors' work is supported by Cancer Research UK, Nature Sciences Foundation of China (30530800), the Medical Research Council, Digestive Cancer Campaign and the National Institute for Health Research (Experimental Cancer Medicine Centres).

**Competing interests**

The authors declare that they have no competing interests.

**References and Notes**

1. Kelly, E.; Russell, S.J. History of oncolytic viruses: genesis to genetic engineering. *Mol. Ther.* **2007**, *15*, 651-659.
2. Martuza, R.L.; Malick, A.; Markert, J.M.; Ruffner, K.L.; Coen, D.M. Experimental therapy of human glioma by means of a genetically engineered virus mutant. *Science* **1991**, *252*, 854-856.
3. Garber, K. China approves world's first oncolytic virus therapy for cancer treatment. *J. Natl. Cancer Inst.* **2006**, *98*, 298-300.
4. Thorne, S.H.; Hwang, T.H.; O'Gorman, W.E.; Bartlett, D.L.; Sei, S.; Kanji, F.; Brown, C.; Werier, J.; Cho, J.H.; Lee, D.E.; Wang, Y.; Bell, J.; Kirn, D.H. Rational strain selection and engineering creates a broad-spectrum, systemically effective oncolytic poxvirus, JX-963. *J. Clin. Invest.* **2007**, *117*, 3350-3358.
5. Huch, M.; Gros, A.; Jose, A.; Gonzalez, J.R.; Alemany, R.; Fillat, C. Urokinase-type plasminogen activator receptor transcriptionally controlled adenoviruses eradicate pancreatic tumors and liver metastasis in mouse models. *Neoplasia* **2009**, *11*, 518-528.
6. Pan, W.; Bodempudi, V.; Esfandyari, T.; Farassati, F. Utilizing ras signaling pathway to direct selective replication of herpes simplex virus-1. *PLoS One* **2009**, *4*, e6514.
7. Cafferata, E.G.; Maccio, D.R.; Lopez, M.V.; Viale, D.L.; Carbone, C.; Mazzolini, G.; Podhajcer, O.L. A novel A33 promoter-based conditionally replicative adenovirus suppresses tumor growth and eradicates hepatic metastases in human colon cancer models. *Clin. Cancer Res.* **2009**, *15*, 3037-3049.
8. Hsieh, J.L.; Lee, C.H.; Teo, M.L.; Lin, Y.J.; Huang, Y.S.; Wu, C.L.; Shiau, A.L. Transthyretin-driven oncolytic adenovirus suppresses tumor growth in orthotopic and ascites models of hepatocellular carcinoma. *Cancer Sci.* **2009**, *100*, 537-545.
9. Nakajima, O.; Matsunaga, A.; Ichimaru, D.; Urata, Y.; Fujiwara, T.; Kawakami, K. Telomerase-specific virotherapy in an animal model of human head and neck cancer. *Mol. Cancer Ther.* **2009**, *8*, 171-177.

10. Doloff, J.C.; Waxman, D.J.; Jounaidi, Y. Human telomerase reverse transcriptase promoter-driven oncolytic adenovirus with E1B-19 kDa and E1B-55 kDa gene deletions. *Hum. Gene Ther.* **2008**, *19*, 1383-1400.
11. Hsu, K.F.; Wu, C.L.; Huang, S.C.; Hsieh, J.L.; Huang, Y.S.; Chen, Y.F.; Shen, M.R.; Chung, W.J.; Chou, C.Y.; Shiau, A.L. Conditionally replicating E1B-deleted adenovirus driven by the squamous cell carcinoma antigen 2 promoter for uterine cervical cancer therapy. *Cancer Gene Ther.* **2008**, *15*, 526-534.
12. Shafren, D.R.; Dorahy, D.J.; Ingham, R.A.; Burns, G.F.; Barry, R.D. Coxsackievirus A21 binds to decay-accelerating factor but requires intercellular adhesion molecule 1 for cell entry. *J. Virol.* **1997**, *71*, 4736-4743.
13. Anderson, B.D.; Nakamura, T.; Russell, S.J.; Peng, K.W. High CD46 receptor density determines preferential killing of tumor cells by oncolytic measles virus. *Cancer Res.* **2004**, *64*, 4919-4926.
14. Nishimoto, T.; Yoshida, K.; Miura, Y.; Kobayashi, A.; Hara, H.; Ohnami, S.; Kurisu, K.; Yoshida, T.; Aoki, K. Oncolytic virus therapy for pancreatic cancer using the adenovirus library displaying random peptides on the fiber knob. *Gene Ther.* **2009**, *16*, 669-680.
15. Conner, J.; Braidwood, L.; Brown, S.M. A strategy for systemic delivery of the oncolytic herpes virus HSV1716: redirected tropism by antibody-binding sites incorporated on the virion surface as a glycoprotein D fusion protein. *Gene Ther.* **2008**, *15*, 1579-1592.
16. Coughlan, L.; Vallath, S.; Saha, A.; Flak, M.; McNeish, I.A.; Vassaux, G.; Marshall, J.F.; Hart, I.R.; Thomas, G.J. *In vivo* retargeting of adenovirus type 5 to alphavbeta6 integrin results in reduced hepatotoxicity and improved tumor uptake following systemic delivery. *J. Virol.* **2009**, *83*, 6416-6428.
17. Gomes, E.M.; Rodrigues, M.S.; Phadke, A.P.; Butcher, L.D.; Starling, C.; Chen, S.; Chang, D.; Hernandez-Alcoceba, R.; Newman, J.T.; Stone, M.J.; Tong, A.W. Antitumor activity of an oncolytic adenoviral-CD40 ligand (CD154) transgene construct in human breast cancer cells. *Clin. Cancer Res.* **2009**, *15*, 1317-1325.
18. Piao, Y.; Jiang, H.; Alemany, R.; Krasnykh, V.; Marini, F.C.; Xu, J.; Alonso, M.M.; Conrad, C.A.; Aldape, K.D.; Gomez-Manzano, C.; Fueyo, J. Oncolytic adenovirus retargeted to Delta-EGFR induces selective antiglioma activity. *Cancer Gene Ther.* **2009**, *16*, 256-265.
19. Morrison, J.; Briggs, S.S.; Green, N.; Fisher, K.; Subr, V.; Ulbrich, K.; Kehoe, S.; Seymour, L.W. Virotherapy of ovarian cancer with polymer-cloaked adenovirus retargeted to the epidermal growth factor receptor. *Mol. Ther.* **2008**, *16*, 244-251.
20. Allen, C.; Paraskevakou, G.; Iankov, I.; Giannini, C.; Schroeder, M.; Sarkaria, J.; Puri, R.K.; Russell, S.J.; Galanis, E. Interleukin-13 displaying retargeted oncolytic measles virus strains have significant activity against gliomas with improved specificity. *Mol. Ther.* **2008**, *16*, 1556-1564.
21. Lorence, R.M.; Katubig, B.B.; Reichard, K.W.; Reyes, H.M.; Phuangsab, A.; Sassetti, M.D.; Walter, R.J.; Peeples, M.E. Complete regression of human fibrosarcoma xenografts after local Newcastle disease virus therapy. *Cancer Res.* **1994**, *54*, 6017-6021.
22. Coffey, M.C.; Strong, J.E.; Forsyth, P.A.; Lee, P.W. Reovirus therapy of tumors with activated Ras pathway. *Science* **1998**, *282*, 1332-1334.
23. Kirn, D.H.; Thorne, S.H. Targeted and armed oncolytic poxviruses: a novel multi-mechanistic therapeutic class for cancer. *Nat. Rev. Cancer* **2009**, *9*, 64-71.

24. Stojdl, D.F.; Lichty, B.; Knowles, S.; Marius, R.; Atkins, H.; Sonenberg, N.; Bell, J.C. Exploiting tumor-specific defects in the interferon pathway with a previously unknown oncolytic virus. *Nat. Med.* **2000**, *6*, 821-825.
25. Whitley, R.J.; Kern, E.R.; Chatterjee, S.; Chou, J.; Roizman, B. Replication, establishment of latency, and induced reactivation of herpes simplex virus gamma 1 34.5 deletion mutants in rodent models. *J. Clin. Invest.* **1993**, *91*, 2837-2843.
26. Muster, T.; Rajtarova, J.; Sachet, M.; Unger, H.; Fleischhacker, R.; Romirer, I.; Grassauer, A.; Url, A.; Garcia-Sastre, A.; Wolff, K.; Pehamberger, H.; Bergmann, M. Interferon resistance promotes oncolysis by influenza virus NS1-deletion mutants. *Int. J. Cancer* **2004**, *110*, 15-21.
27. Cascallo, M.; Capella, G.; Mazo, A.; Alemany, R. Ras-dependent oncolysis with an adenovirus VAI mutant. *Cancer Res.* **2003**, *63*, 5544-5550.
28. Wang, Y.; Xue, S.A.; Hallden, G.; Francis, J.; Yuan, M.; Griffin, B.E.; Lemoine, N.R. Virus-associated RNA I-deleted adenovirus, a potential oncolytic agent targeting EBV-associated tumors. *Cancer Res.* **2005**, *65*, 1523-1531.
29. Heise, C.; Hermiston, T.; Johnson, L.; Brooks, G.; Sampson-Johannes, A.; Williams, A.; Hawkins, L.; Kirn, D. An adenovirus E1A mutant that demonstrates potent and selective systemic anti-tumoral efficacy. *Nat. Med.* **2000**, *6*, 1134-1139.
30. Liu, T.C.; Hallden, G.; Wang, Y.; Brooks, G.; Francis, J.; Lemoine, N.; Kirn, D. An E1B-19 kDa gene deletion mutant adenovirus demonstrates tumor necrosis factor-enhanced cancer selectivity and enhanced oncolytic potency. *Mol. Ther.* **2004**, *9*, 786-803.
31. Bischoff, J.R.; Kirn, D.H.; Williams, A.; Heise, C.; Horn, S.; Muna, M.; Ng, L.; Nye, J.A.; Sampson-Johannes, A.; Fattaey, A.; McCormick, F. An adenovirus mutant that replicates selectively in p53-deficient human tumor cells. *Science* **1996**, *274*, 373-376.
32. Zheng, X.; Rao, X.M.; Gomez-Gutierrez, J.G.; Hao, H.; McMasters, K.M.; Zhou, H.S. Adenovirus E1B55K region is required to enhance cyclin E expression for efficient viral DNA replication. *J. Virol.* **2008**, *82*, 3415-3427.
33. O'Shea, C.C.; Johnson, L.; Bagus, B.; Choi, S.; Nicholas, C.; Shen, A.; Boyle, L.; Pandey, K.; Soria, C.; Kunich, J.; Shen, Y.; Habets, G.; Ginzinger, D.; McCormick, F. Late viral RNA export, rather than p53 inactivation, determines ONYX-015 tumor selectivity. *Cancer Cell* **2004**, *6*, 611-623.
34. Ylosmaki, E.; Hakkarainen, T.; Hemminki, A.; Visakorpi, T.; Andino, R.; Saksela, K. Generation of a conditionally replicating adenovirus based on targeted destruction of E1A mRNA by a cell type-specific MicroRNA. *J. Virol.* **2008**, *82*, 11009-11015.
35. Cawood, R.; Chen, H.H.; Carroll, F.; Bazan-Peregrino, M.; van Rooijen, N.; Seymour, L.W. Use of tissue-specific microRNA to control pathology of wild-type adenovirus without attenuation of its ability to kill cancer cells. *PLoS Pathog.* **2009**, *5*, e1000440.
36. Lee, C.Y.; Rennie, P.S.; Jia, W.W. MicroRNA regulation of oncolytic herpes simplex virus-1 for selective killing of prostate cancer cells. *Clin. Cancer Res.* **2009**, *15*, 5126-5135.
37. Edge, R.E.; Falls, T.J.; Brown, C.W.; Lichty, B.D.; Atkins, H.; Bell, J.C. A let-7 MicroRNA-sensitive vesicular stomatitis virus demonstrates tumor-specific replication. *Mol. Ther.* **2008**, *16*, 1437-1443.

38. Kelly, E.J.; Hadac, E.M.; Greiner, S.; Russell, S.J. Engineering microRNA responsiveness to decrease virus pathogenicity. *Nat. Med.* **2008**, *14*, 1278-1283.
39. Gurlevik, E.; Woller, N.; Schache, P.; Malek, N.P.; Wirth, T.C.; Zender, L.; Manns, M.P.; Kubicka, S.; Kuhnel, F. p53-dependent antiviral RNA-interference facilitates tumor-selective viral replication. *Nucleic Acids Res.* **2009**, *37*, e84.
40. Cody, J.J.; Douglas, J.T. Armed replicating adenoviruses for cancer virotherapy. *Cancer Gene Ther.* **2009**, *16*, 473-488.
41. Benencia, F.; Coukos, G. Biological therapy with oncolytic herpesvirus. *Adv. Exp. Med. Biol.* **2008**, *622*, 221-233.
42. Blackford, A.N.; Grand, R.J. Adenovirus E1B 55-kilodalton protein: multiple roles in viral infection and cell transformation. *J. Virol.* **2009**, *83*, 4000-4012.
43. Ganly, I.; Kirn, D.; Eckhardt, G.; Rodriguez, G.I.; Soutar, D.S.; Otto, R.; Robertson, A.G.; Park, O.; Gulley, M.L.; Heise, C.; Von Hoff, D.D.; Kaye, S.B. A phase I study of Onyx-015, an E1B attenuated adenovirus, administered intratumorally to patients with recurrent head and neck cancer. *Clin. Cancer Res.* **2000**, *6*, 798-806.
44. Nemunaitis, J.; Ganly, I.; Khuri, F.; Arseneau, J.; Kuhn, J.; McCarty, T.; Landers, S.; Maples, P.; Romel, L.; Randlev, B.; Reid, T.; Kaye, S.; Kirn, D. Selective replication and oncolysis in p53 mutant tumors with ONYX-015, an E1B-55kD gene-deleted adenovirus, in patients with advanced head and neck cancer: a phase II trial. *Cancer Res.* **2000**, *60*, 6359-6366.
45. Nemunaitis, J.; Khuri, F.; Ganly, I.; Arseneau, J.; Posner, M.; Vokes, E.; Kuhn, J.; McCarty, T.; Landers, S.; Blackburn, A.; Romel, L.; Randlev, B.; Kaye, S.; Kirn, D. Phase II trial of intratumoral administration of ONYX-015, a replication-selective adenovirus, in patients with refractory head and neck cancer. *J. Clin. Oncol.* **2001**, *19*, 289-298.
46. Mulvihill, S.; Warren, R.; Venook, A.; Adler, A.; Randlev, B.; Heise, C.; Kirn, D. Safety and feasibility of injection with an E1B-55 kDa gene-deleted, replication-selective adenovirus (ONYX-015) into primary carcinomas of the pancreas: a phase I trial. *Gene Ther.* **2001**, *8*, 308-315.
47. Hecht, J.R.; Bedford, R.; Abbruzzese, J.L.; Lahoti, S.; Reid, T.R.; Soetikno, R.M.; Kirn, D.H.; Freeman, S.M. A phase I/II trial of intratumoral endoscopic ultrasound injection of ONYX-015 with intravenous gemcitabine in unresectable pancreatic carcinoma. *Clin. Cancer Res.* **2003**, *9*, 555-561.
48. Nemunaitis, J.; Cunningham, C.; Buchanan, A.; Blackburn, A.; Edelman, G.; Maples, P.; Netto, G.; Tong, A.; Randlev, B.; Olson, S.; Kirn, D. Intravenous infusion of a replication-selective adenovirus (ONYX-015) in cancer patients: safety, feasibility and biological activity. *Gene Ther.* **2001**, *8*, 746-759.
49. Thomas, M.A.; Broughton, R.S.; Goodrum, F.D.; Ornelles, D.A. E4orf1 limits the oncolytic potential of the E1B-55K deletion mutant adenovirus. *J. Virol.* **2009**, *83*, 2406-2416.
50. Frisch, S.M.; Mymryk, J.S. Adenovirus-5 E1A: paradox and paradigm. *Nat. Rev. Mol. Cell. Biol.* **2002**, *3*, 441-452.
51. Liu, T.C.; Wang, Y.; Hallden, G.; Brooks, G.; Francis, J.; Lemoine, N.R.; Kirn, D. Functional interactions of antiapoptotic proteins and tumor necrosis factor in the context of a replication-competent adenovirus. *Gene Ther.* **2005**, *12*, 1333-1346.

52. Subramanian, T.; Vijayalingam, S.; Chinnadurai, G. Genetic identification of adenovirus type 5 genes that influence viral spread. *J. Virol.* **2006**, *80*, 2000-2012.
53. Han, J.; Modha, D.; White, E. Interaction of E1B 19K with Bax is required to block Bax-induced loss of mitochondrial membrane potential and apoptosis. *Oncogene* **1998**, *17*, 2993-3005.
54. Han, J.; Sabbatini, P.; Perez, D.; Rao, L.; Modha, D.; White, E. The E1B 19K protein blocks apoptosis by interacting with and inhibiting the p53-inducible and death-promoting Bax protein. *Genes Dev.* **1996**, *10*, 461-477.
55. Sundararajan, R.; White, E. E1B 19K blocks Bax oligomerization and tumor necrosis factor alpha-mediated apoptosis. *J. Virol.* **2001**, *75*, 7506-7516.
56. Perez, D.; White, E. E1B 19K inhibits Fas-mediated apoptosis through FADD-dependent sequestration of FLICE. *J. Cell Biol.* **1998**, *141*, 1255-1266.
57. Vijayalingam, S.; Subramanian, T.; Ryerse, J.; Varvares, M.; Chinnadurai, G. Down-regulation of multiple cell survival proteins in head and neck cancer cells by an apoptogenic mutant of adenovirus type 5. *Virology* **2009**, *392*, 62-72.
58. Schneider, R.J.; Safer, B.; Munemitsu, S.M.; Samuel, C.E.; Shenk, T. Adenovirus VAI RNA prevents phosphorylation of the eukaryotic initiation factor 2 alpha subunit subsequent to infection. *Proc. Natl. Acad. Sci. USA* **1985**, *82*, 4321-4325.
59. Schneider, R.J.; Weinberger, C.; Shenk, T. Adenovirus VAI RNA facilitates the initiation of translation in virus-infected cells. *Cell* **1984**, *37*, 291-298.
60. Tollefson, A.E.; Ryerse, J.S.; Scaria, A.; Hermiston, T.W.; Wold, W.S. The E3-11.6-kDa adenovirus death protein (ADP) is required for efficient cell death: characterization of cells infected with adp mutants. *Virology* **1996**, *220*, 152-162.
61. Zou, A.; Atencio, I.; Huang, W.M.; Horn, M.; Ramachandra, M. Overexpression of adenovirus E3-11.6K protein induces cell killing by both caspase-dependent and caspase-independent mechanisms. *Virology* **2004**, *326*, 240-249.
62. Doronin, K.; Toth, K.; Kuppuswamy, M.; Krajcsi, P.; Tollefson, A.E.; Wold, W.S. Overexpression of the ADP (E3-11.6K) protein increases cell lysis and spread of adenovirus. *Virology* **2003**, *305*, 378-387.
63. Peng, Z. Current status of gendicine in China: recombinant human Ad-p53 agent for treatment of cancers. *Hum. Gene. Ther.* **2005**, *16*, 1016-1027.
64. Ma, J.; He, X.; Wang, W.; Huang, Y.; Chen, L.; Cong, W.; Gu, J.; Hu, H.; Shi, J.; Li, L.; Su, C. E2F promoter-regulated oncolytic adenovirus with p16 gene induces cell apoptosis and exerts antitumor effect on gastric cancer. *Dig. Dis. Sci.* **2009**, *54*, 1425-1431.
65. Wang, X.; Su, C.; Cao, H.; Li, K.; Chen, J.; Jiang, L.; Zhang, Q.; Wu, X.; Jia, X.; Liu, Y.; Wang, W.; Liu, X.; Wu, M.; Qian, Q. A novel triple-regulated oncolytic adenovirus carrying p53 gene exerts potent antitumor efficacy on common human solid cancers. *Mol. Cancer Ther.* **2008**, *7*, 1598-1603.
66. Jones, S.; Zhang, X.; Parsons, D.W.; Lin, J.C.; Leary, R.J.; Angenendt, P.; Mankoo, P.; Carter, H.; Kamiyama, H.; Jimeno, A.; Hong, S.M.; Fu, B.; Lin, M.T.; Calhoun, E.S.; Kamiyama, M.; Walter, K.; Nikolskaya, T.; Nikolsky, Y.; Hartigan, J.; Smith, D.R.; Hidalgo, M.; Leach, S.D.; Klein, A.P.; Jaffee, E.M.; Goggins, M.; Maitra, A.; Iacobuzio-Donahue, C.; Eshleman, J.R.; Kern, S.E.; Hruban, R.H.; Karchin, R.; Papadopoulos, N.; Parmigiani, G.; Vogelstein, B.; Velculescu,

V.E.; Kinzler, K.W. Core signaling pathways in human pancreatic cancers revealed by global genomic analyses. *Science* **2008**, *321*, 1801-1806.

67. Hu, Z.; Robbins, J.S.; Pister, A.; Zafar, M.B.; Zhang, Z.W.; Gupta, J.; Lee, K.J.; Neuman, K.; Yun, C.O.; Guise, T.; Seth, P. A modified hTERT promoter-directed oncolytic adenovirus replication with concurrent inhibition of TGFbeta signaling for breast cancer therapy. *Cancer Gene Ther.* **2009**, doi:10.1038/cgt.2009.72.
68. Jin, J.; Liu, H.; Yang, C.; Li, G.; Liu, X.; Qian, Q.; Qian, W. Effective gene-viral therapy of leukemia by a new fiber chimeric oncolytic adenovirus expressing TRAIL: *in vitro* and *in vivo* evaluation. *Mol. Cancer Ther.* **2009**, *8*, 1387.
69. Chen, L.; Chen, D.; Gong, M.; Na, M.; Li, L.; Wu, H.; Jiang, L.; Qian, Y.; Fang, G.; Xue, X. Concomitant use of Ad5/35 chimeric oncolytic adenovirus with TRAIL gene and taxol produces synergistic cytotoxicity in gastric cancer cells. *Cancer Lett.* **2009**, *284*, 141-148.
70. Zhang, Z.; Huang, Y.; Newman, K.; Gu, J.; Zhang, X.; Wu, H.; Zhao, M.; Xianyu, Z.; Liu, X. Reexpression of human somatostatin receptor gene 2 gene mediated by oncolytic adenovirus increases antitumor activity of tumor necrosis factor-related apoptosis-inducing ligand against pancreatic cancer. *Clin. Cancer Res.* **2009**, *15*, 5154-5160.
71. Zheng, J.N.; Pei, D.S.; Sun, F.H.; Zhang, B.F.; Liu, X.Y.; Gu, J.F.; Liu, Y.H.; Hu, X.L.; Mao, L.J.; Wen, R.M.; Liu, J.J.; Li, W. Inhibition of renal cancer cell growth by oncolytic adenovirus armed short hairpin RNA targeting hTERT gene. *Cancer Biol. Ther.* **2009**, *8*, 84-91.
72. Zheng, J.N.; Pei, D.S.; Mao, L.J.; Liu, X.Y.; Mei, D.D.; Zhang, B.F.; Shi, Z.; Wen, R.M.; Sun, X.Q. Inhibition of renal cancer cell growth *in vitro* and *in vivo* with oncolytic adenovirus armed short hairpin RNA targeting Ki-67 encoding mRNA. *Cancer Gene Ther.* **2009**, *16*, 20-32.
73. Shen, W.; Wang, C.Y.; Wang, X.H.; Fu, Z.X. Oncolytic adenovirus mediated Survivin knockdown by RNA interference suppresses human colorectal carcinoma growth *in vitro* and *in vivo*. *J. Exp. Clin. Cancer Res.* **2009**, *28*, 81.
74. Chu, L.; Gu, J.; Sun, L.; Qian, Q.; Qian, C.; Liu, X. Oncolytic adenovirus-mediated shRNA against Apollon inhibits tumor cell growth and enhances antitumor effect of 5-fluorouracil. *Gene Ther.* **2008**, *15*, 484-494.
75. Ikeda, Y.; Kojima, T.; Kuroda, S.; Endo, Y.; Sakai, R.; Hioki, M.; Kishimoto, H.; Uno, F.; Kagawa, S.; Watanabe, Y.; Hashimoto, Y.; Urata, Y.; Tanaka, N.; Fujiwara, T. A novel antiangiogenic effect for telomerase-specific virotherapy through host immune system. *J. Immunol.* **2009**, *182*, 1763-1769.
76. Kurozumi, K.; Hardcastle, J.; Thakur, R.; Shroll, J.; Nowicki, M.; Otsuki, A.; Chiocca, E.A.; Kaur, B. Oncolytic HSV-1 infection of tumors induces angiogenesis and upregulates CYR61. *Mol. Ther.* **2008**, *16*, 1382-1391.
77. Tysome, J.R.; Lemoine, N.R.; Wang, Y. Combination of anti-angiogenic therapy and virotherapy: arming the oncolytic viruses with anti-angiogenic genes. *Curr. Opin. Mol. Ther.* **2010**, in press.
78. Tysome, J.R.; Briat, A.; Alusi, G.; Cao, F.; Gao, D.; Yu, J.; Wang, P.; Yang, S.; Dong, Z.; Wang, S.; Deng, L.; Francis, J.; Timiryasova, T.; Fodor, I.; Lemoine, N.R.; Wang, Y. Lister strain of vaccinia virus armed with endostatin-angiostatin fusion gene as a novel therapeutic agent for human pancreatic cancer. *Gene Ther.* **2009**, *16*, 1223-1233.

79. Su, C.; Na, M.; Chen, J.; Wang, X.; Liu, Y.; Wang, W.; Zhang, Q.; Li, L.; Long, J.; Liu, X.; Wu, M.; Fan, X.; Qian, Q. Gene-viral cancer therapy using dual-regulated oncolytic adenovirus with antiangiogenesis gene for increased efficacy. *Mol. Cancer Res.* **2008**, *6*, 568-575.
80. Fang, L.; Pu, Y.Y.; Hu, X.C.; Sun, L.J.; Luo, H.M.; Pan, S.K.; Gu, J.Z.; Cao, X.R.; Su, C.Q. Antiangiogenesis gene armed tumor-targeting adenovirus yields multiple antitumor activities in human HCC xenografts in nude mice. *Hepatol. Res.* **2009**, doi: 10.1111/j.1872-034X.2009.00580.x.
81. Zheng, J.N.; Pei, D.S.; Mao, L.J.; Liu, X.Y.; Sun, F.H.; Zhang, B.F.; Liu, Y.Q.; Liu, J.J.; Li, W.; Han, D. Oncolytic adenovirus expressing interleukin-18 induces significant antitumor effects against melanoma in mice through inhibition of angiogenesis. *Cancer Gene Ther.* **2010**, *17*, 28-36.
82. Zheng, J.N.; Pei, D.S.; Sun, F.H.; Liu, X.Y.; Mao, L.J.; Zhang, B.F.; Wen, R.M.; Xu, W.; Shi, Z.; Liu, J.J.; Li, W. Potent antitumor efficacy of interleukin-18 delivered by conditionally replicative adenovirus vector in renal cell carcinoma-bearing nude mice via inhibition of angiogenesis. *Cancer Biol. Ther.* **2009**, *8*, 599-606.
83. He, X.P.; Su, C.Q.; Wang, X.H.; Pan, X.; Tu, Z.X.; Gong, Y.F.; Gao, J.; Liao, Z.; Jin, J.; Wu, H.Y.; Man, X.H.; Li, Z.S. E1B-55kD-deleted oncolytic adenovirus armed with canstatin gene yields an enhanced anti-tumor efficacy on pancreatic cancer. *Cancer Lett.* **2009**, *285*, 89-98.
84. Liu, T.C.; Castelo-Branco, P.; Rabkin, S.D.; Martuza, R.L. Trichostatin A and oncolytic HSV combination therapy shows enhanced antitumoral and antiangiogenic effects. *Mol. Ther.* **2008**, *16*, 1041-1047.
85. Yoo, J.Y.; Kim, J.H.; Kim, J.; Huang, J.H.; Zhang, S.N.; Kang, Y.A.; Kim, H.; Yun, C.O. Short hairpin RNA-expressing oncolytic adenovirus-mediated inhibition of IL-8: effects on antiangiogenesis and tumor growth inhibition. *Gene Ther.* **2008**, *15*, 635-651.
86. Frentzen, A.; Yu, Y.A.; Chen, N.; Zhang, Q.; Weibel, S.; Raab, V.; Szalay, A.A. Anti-VEGF single-chain antibody GLAF-1 encoded by oncolytic vaccinia virus significantly enhances antitumor therapy. *Proc. Natl. Acad. Sci. USA* **2009**, *106*, 12915-12920.
87. Guse, K.; Diaconu, I.; Rajecki, M.; Sloniecka, M.; Hakkarainen, T.; Ristimaki, A.; Kanerva, A.; Pesonen, S.; Hemminki, A. Ad5/3-9HIF-Delta24-VEGFR-1-Ig, an infectivity enhanced, dual-targeted and antiangiogenic oncolytic adenovirus for kidney cancer treatment. *Gene Ther.* **2009**, *16*, 1009-1020.
88. Kang, Y.A.; Shin, H.C.; Yoo, J.Y.; Kim, J.H.; Kim, J.S.; Yun, C.O. Novel cancer antiangiotherapy using the VEGF promoter-targeted artificial zinc-finger protein and oncolytic adenovirus. *Mol. Ther.* **2008**, *16*, 1033-1040.
89. McNally, L.R.; Rosenthal, E.L.; Zhang, W.; Buchsbaum, D.J. Therapy of head and neck squamous cell carcinoma with replicative adenovirus expressing tissue inhibitor of metalloproteinase-2 and chemoradiation. *Cancer Gene Ther.* **2009**, *16*, 246-255.
90. Mahller, Y.Y.; Vaikunth, S.S.; Ripberger, M.C.; Baird, W.H.; Saeki, Y.; Cancelas, J.A.; Crombleholme, T.M.; Cripe, T.P. Tissue inhibitor of metalloproteinase-3 via oncolytic herpesvirus inhibits tumor growth and vascular progenitors. *Cancer Res.* **2008**, *68*, 1170-1179.

91. Ahn, M.; Lee, S.J.; Li, X.; Jimenez, J.A.; Zhang, Y.P.; Bae, K.H.; Mohammadi, Y.; Kao, C.; Gardner, T.A. Enhanced combined tumor-specific oncolysis and suicide gene therapy for prostate cancer using M6 promoter. *Cancer Gene Ther.* **2009**, *16*, 73-82.
92. Fukuda, K.; Abei, M.; Ugai, H.; Kawashima, R.; Seo, E.; Wakayama, M.; Murata, T.; Endo, S.; Hamada, H.; Hyodo, I.; Yokoyama, K.K. E1A, E1B double-restricted replicative adenovirus at low dose greatly augments tumor-specific suicide gene therapy for gallbladder cancer. *Cancer Gene Ther.* **2009**, *16*, 126-136.
93. Zheng, F.Q.; Xu, Y.; Yang, R.J.; Wu, B.; Tan, X.H.; Qin, Y.D.; Zhang, Q.W. Combination effect of oncolytic adenovirus therapy and herpes simplex virus thymidine kinase/ganciclovir in hepatic carcinoma animal models. *Acta Pharmacol. Sin.* **2009**, *30*, 617-627.
94. Braidwood, L.; Dunn, P.D.; Hardy, S.; Evans, T.R.; Brown, S.M. Antitumor activity of a selectively replication competent herpes simplex virus (HSV) with enzyme prodrug therapy. *Anticancer Res.* **2009**, *29*, 2159-2166.
95. Chalikonda, S.; Kivlen, M.H.; O'Malley, M.E.; Eric Dong, X.D.; McCart, J.A.; Gorry, M.C.; Yin, X.Y.; Brown, C.K.; Zeh, H.J., 3rd; Guo, Z.S.; Bartlett, D.L. Oncolytic virotherapy for ovarian carcinomatosis using a replication-selective vaccinia virus armed with a yeast cytosine deaminase gene. *Cancer Gene Ther.* **2008**, *15*, 115-125.
96. Foloppe, J.; Kintz, J.; Futin, N.; Findeli, A.; Cordier, P.; Schlesinger, Y.; Hoffmann, C.; Tosch, C.; Balloul, J.M.; Erbs, P. Targeted delivery of a suicide gene to human colorectal tumors by a conditionally replicating vaccinia virus. *Gene Ther.* **2008**, *15*, 1361-1371.
97. Kolodkin-Gal, D.; Zamir, G.; Edden, Y.; Pikarsky, E.; Pikarsky, A.; Haim, H.; Haviv, Y.S.; Panet, A. Herpes simplex virus type 1 preferentially targets human colon carcinoma: role of extracellular matrix. *J. Virol.* **2008**, *82*, 999-1010.
98. Ganesh, S.; Gonzalez-Edick, M.; Gibbons, D.; Van Roey, M.; Jooss, K. Intratumoral coadministration of hyaluronidase enzyme and oncolytic adenoviruses enhances virus potency in metastatic tumor models. *Clin. Cancer Res.* **2008**, *14*, 3933-3941.
99. Nagano, S.; Perentes, J.Y.; Jain, R.K.; Boucher, Y. Cancer cell death enhances the penetration and efficacy of oncolytic herpes simplex virus in tumors. *Cancer Res.* **2008**, *68*, 3795-3802.
100. Heldin, C.H.; Rubin, K.; Pietras, K.; Ostman, A. High interstitial fluid pressure - an obstacle in cancer therapy. *Nat. Rev. Cancer* **2004**, *4*, 806-813.
101. Bazan-Peregrino, M.; Carlisle, R.C.; Purdie, L.; Seymour, L.W. Factors influencing retention of adenovirus within tumours following direct intratumoural injection. *Gene Ther.* **2008**, *15*, 688-694.
102. Lopez, M.V.; Viale, D.L.; Cafferata, E.G.; Bravo, A.I.; Carbone, C.; Gould, D.; Chernajovsky, Y.; Podhajcer, O.L. Tumor associated stromal cells play a critical role on the outcome of the oncolytic efficacy of conditionally replicative adenoviruses. *PLoS One* **2009**, *4*, e5119.
103. Shen, B.H.; Hermiston, T.W. Effect of hypoxia on Ad5 infection, transgene expression and replication. *Gene Ther.* **2005**, *12*, 902-910.
104. Shen, B.H.; Bauzon, M.; Hermiston, T.W. The effect of hypoxia on the uptake, replication and lytic potential of group B adenovirus type 3 (Ad3) and type 11p (Ad11p). *Gene Ther.* **2006**, *13*, 986-990.

105. Hiley, C.T.; Yuan, M.; Lemoine, N.R.; Wang, Y. Lister strain vaccinia virus, a potential therapeutic vector for hypoxic tumours. *Gene Ther.* **2009**, doi: 10.1038/gt.2009.132.
106. Aghi, M.K.; Liu, T.C.; Rabkin, S.; Martuza, R.L. Hypoxia enhances the replication of oncolytic herpes simplex virus. *Mol. Ther.* **2009**, *17*, 51-56.
107. Fasullo, M.; Burch, A.D.; Britton, A. Hypoxia enhances the replication of oncolytic herpes simplex virus in p53- breast cancer cells. *Cell Cycle* **2009**, *8*, 2194-2197.
108. Anders, M.; Christian, C.; McMahon, M.; McCormick, F.; Korn, W.M. Inhibition of the Raf/MEK/ERK pathway up-regulates expression of the coxsackievirus and adenovirus receptor in cancer cells. *Cancer Res.* **2003**, *63*, 2088-2095.
109. O'Prey, J.; Wilkinson, S.; Ryan, K.M. Tumor antigen LRRC15 impedes adenoviral infection: implications for virus-based cancer therapy. *J. Virol.* **2008**, *82*, 5933-5939.
110. Gaggar, A.; Shayakhmetov, D.M.; Lieber, A. CD46 is a cellular receptor for group B adenoviruses. *Nat. Med.* **2003**, *9*, 1408-1412.
111. Fishelson, Z.; Donin, N.; Zell, S.; Schultz, S.; Kirschfink, M. Obstacles to cancer immunotherapy: expression of membrane complement regulatory proteins (mCRPs) in tumors. *Mol. Immunol.* **2003**, *40*, 109-123.
112. Kinugasa, N.; Higashi, T.; Nouso, K.; Nakatsukasa, H.; Kobayashi, Y.; Ishizaki, M.; Toshikuni, N.; Yoshida, K.; Uematsu, S.; Tsuji, T. Expression of membrane cofactor protein (MCP, CD46) in human liver diseases. *Br. J. Cancer* **1999**, *80*, 1820-1825.
113. Murray, K.P.; Mathure, S.; Kaul, R.; Khan, S.; Carson, L.F.; Twiggs, L.B.; Martens, M.G.; Kaul, A. Expression of complement regulatory proteins-CD 35, CD 46, CD 55, and CD 59-in benign and malignant endometrial tissue. *Gynecol. Oncol.* **2000**, *76*, 176-182.
114. Nandi, S.; Ulasov, I.V.; Rolle, C.E.; Han, Y.; Lesniak, M.S. A chimeric adenovirus with an Ad 3 fiber knob modification augments glioma virotherapy. *J. Gene Med.* **2009**, *11*, 1005-1011.
115. Ganesh, S.; Gonzalez-Edick, M.; Gibbons, D.; Ge, Y.; VanRoey, M.; Robinson, M.; Jooss, K. Combination therapy with radiation or cisplatin enhances the potency of Ad5/35 chimeric oncolytic adenovirus in a preclinical model of head and neck cancer. *Cancer Gene Ther.* **2009**, *16*, 383-392.
116. Wang, G.; Li, G.; Liu, H.; Yang, C.; Yang, X.; Jin, J.; Liu, X.; Qian, Q.; Qian, W. E1B 55-kDa deleted, Ad5/F35 fiber chimeric adenovirus, a potential oncolytic agent for B-lymphocytic malignancies. *J. Gene Med.* **2009**, *11*, 477-485.
117. Zhu, Z.B.; Lu, B.; Park, M.; Makhija, S.K.; Numnum, T.M.; Kendrick, J.E.; Wang, M.; Tsuruta, Y.; Fisher, P.; Alvarez, R.D.; Zhou, F.; Siegal, G.P.; Wu, H.; Curiel, D.T. Development of an optimized conditionally replicative adenoviral agent for ovarian cancer. *Int. J. Oncol.* **2008**, *32*, 1179-1188.
118. Shashkova, E.V.; May, S.M.; Barry, M.A. Characterization of human adenovirus serotypes 5, 6, 11, and 35 as anticancer agents. *Virology* **2009**, *394*, 311-320.
119. Sandberg, L.; Papareddy, P.; Silver, J.; Bergh, A.; Mei, Y.F. Replication-competent Ad11p vector (RCAd11p) efficiently transduces and replicates in hormone-refractory metastatic prostate cancer cells. *Hum. Gene Ther.* **2009**, *20*, 361-373.
120. Stone, D.; Liu, Y.; Li, Z.Y.; Tuve, S.; Strauss, R.; Lieber, A. Comparison of adenoviruses from species B, C, E, and F after intravenous delivery. *Mol. Ther.* **2007**, *15*, 2146-2153.

121. Yu, L.; Shimozato, O.; Li, Q.; Kawamura, K.; Ma, G.; Namba, M.; Ogawa, T.; Kaiho, I.; Tagawa, M. Adenovirus type 5 substituted with type 11 or 35 fiber structure increases its infectivity to human cells enabling dual gene transfer in CD46-dependent and -independent manners. *Anticancer Res.* **2007**, *27*, 2311-2316.
122. Stone, D.; Ni, S.; Li, Z.Y.; Gaggar, A.; DiPaolo, N.; Feng, Q.; Sandig, V.; Lieber, A. Development and assessment of human adenovirus type 11 as a gene transfer vector. *J. Virol.* **2005**, *79*, 5090-5104.
123. Tuve, S.; Wang, H.; Ware, C.; Liu, Y.; Gaggar, A.; Bernt, K.; Shayakhmetov, D.; Li, Z.; Strauss, R.; Stone, D.; Lieber, A. A new group B adenovirus receptor is expressed at high levels on human stem and tumor cells. *J. Virol.* **2006**, *80*, 12109-12120.
124. Sakurai, F.; Akitomo, K.; Kawabata, K.; Hayakawa, T.; Mizuguchi, H. Downregulation of human CD46 by adenovirus serotype 35 vectors. *Gene Ther.* **2007**, *14*, 912-919.
125. Strauss, R.; Sova, P.; Liu, Y.; Li, Z.Y.; Tuve, S.; Pritchard, D.; Brinkkoetter, P.; Moller, T.; Wildner, O.; Pesonen, S.; Hemminki, A.; Urban, N.; Drescher, C.; Lieber, A. Epithelial phenotype confers resistance of ovarian cancer cells to oncolytic adenoviruses. *Cancer Res.* **2009**, *69*, 5115-5125.
126. Wang, Y.; Gangeswaran, R.; Zhao, X.; Wang, P.; Tysome, J.; Bhakta, V.; Yuan, M.; Chikkanna-Gowda, C.P.; Jiang, G.; Gao, D.; Cao, F.; Francis, J.; Yu, J.; Liu, K.; Yang, H.; Zhang, Y.; Zang, W.; Chelala, C.; Dong, Z.; Lemoine, N. CEACAM6 attenuates adenovirus infection by antagonizing viral trafficking in cancer cells. *J. Clin. Invest.* **2009**, *119*, 1604-1615.
127. Shiina, M.; Lacher, M.D.; Christian, C.; Korn, W.M. RNA interference-mediated knockdown of p21(WAF1) enhances anti-tumor cell activity of oncolytic adenoviruses. *Cancer Gene Ther.* **2009**, *16*, 810-819.
128. Hu, W.; Hofstetter, W.; Guo, W.; Li, H.; Pataer, A.; Peng, H.H.; Guo, Z.S.; Bartlett, D.L.; Lin, A.; Swisher, S.G.; Fang, B. JNK-deficiency enhanced oncolytic vaccinia virus replication and blocked activation of double-stranded RNA-dependent protein kinase. *Cancer Gene Ther.* **2008**, *15*, 616-624.
129. Jiang, H.; Gomez-Manzano, C.; Aoki, H.; Alonso, M.M.; Kondo, S.; McCormick, F.; Xu, J.; Kondo, Y.; Bekele, B.N.; Colman, H.; Lang, F.F.; Fueyo, J. Examination of the therapeutic potential of Delta-24-RGD in brain tumor stem cells: role of autophagic cell death. *J. Natl. Cancer Inst* **2007**, *99*, 1410-1414.
130. Eriksson, M.; Guse, K.; Bauerschmitz, G.; Virkkunen, P.; Tarkkanen, M.; Tanner, M.; Hakkarainen, T.; Kanerva, A.; Desmond, R.A.; Pesonen, S.; Hemminki, A. Oncolytic adenoviruses kill breast cancer initiating CD44+CD24-/low cells. *Mol. Ther.* **2007**, *15*, 2088-2093.
131. Mahller, Y.Y.; Williams, J.P.; Baird, W.H.; Mitton, B.; Grossheim, J.; Saeki, Y.; Cancelas, J.A.; Ratner, N.; Cripe, T.P. Neuroblastoma cell lines contain pluripotent tumor initiating cells that are susceptible to a targeted oncolytic virus. *PLoS One* **2009**, *4*, e4235.
132. Zhang, X.; Komaki, R.; Wang, L.; Fang, B.; Chang, J.Y. Treatment of radioresistant stem-like esophageal cancer cells by an apoptotic gene-armed, telomerase-specific oncolytic adenovirus. *Clin. Cancer Res.* **2008**, *14*, 2813-2823.

133. Wang, Y.; Hallden, G.; Hill, R.; Anand, A.; Liu, T.C.; Francis, J.; Brooks, G.; Lemoine, N.; Kirn, D. E3 gene manipulations affect oncolytic adenovirus activity in immunocompetent tumor models. *Nat. Biotechnol.* **2003**, *21*, 1328-1335.
134. Wakimoto, H.; Johnson, P.R.; Knipe, D.M.; Chiocca, E.A. Effects of innate immunity on herpes simplex virus and its ability to kill tumor cells. *Gene Ther.* **2003**, *10*, 983-990.
135. Diaz, R.M.; Galivo, F.; Kottke, T.; Wongthida, P.; Qiao, J.; Thompson, J.; Valdes, M.; Barber, G.; Vile, R.G. Oncolytic immunovirotherapy for melanoma using vesicular stomatitis virus. *Cancer Res.* **2007**, *67*, 2840-2848.
136. Worgall, S.; Wolff, G.; Falck-Pedersen, E.; Crystal, R.G. Innate immune mechanisms dominate elimination of adenoviral vectors following *in vivo* administration. *Hum. Gene Ther.* **1997**, *8*, 37-44.
137. Zamarin, D.; Martinez-Sobrido, L.; Kelly, K.; Mansour, M.; Sheng, G.; Vigil, A.; Garcia-Sastre, A.; Palese, P.; Fong, Y. Enhancement of oncolytic properties of recombinant newcastle disease virus through antagonism of cellular innate immune responses. *Mol. Ther.* **2009**, *17*, 697-706.
138. Lyons, M.; Onion, D.; Green, N.K.; Aslan, K.; Rajaratnam, R.; Bazan-Peregrino, M.; Phipps, S.; Hale, S.; Mautner, V.; Seymour, L.W.; Fisher, K.D. Adenovirus type 5 interactions with human blood cells may compromise systemic delivery. *Mol. Ther.* **2006**, *14*, 118-128.
139. Wakimoto, H.; Fulci, G.; Tyminski, E.; Chiocca, E.A. Altered expression of antiviral cytokine mRNAs associated with cyclophosphamide's enhancement of viral oncolysis. *Gene Ther.* **2004**, *11*, 214-223.
140. Fulci, G.; Breymann, L.; Gianni, D.; Kurozomi, K.; Rhee, S.S.; Yu, J.; Kaur, B.; Louis, D.N.; Weissleder, R.; Caligiuri, M.A.; Chiocca, E.A. Cyclophosphamide enhances glioma virotherapy by inhibiting innate immune responses. *Proc. Natl. Acad. Sci. USA* **2006**, *103*, 12873-12878.
141. Qiao, J.; Wang, H.; Kottke, T.; White, C.; Twigger, K.; Diaz, R.M.; Thompson, J.; Selby, P.; de Bono, J.; Melcher, A.; Pandha, H.; Coffey, M.; Vile, R.; Harrington, K. Cyclophosphamide facilitates antitumor efficacy against subcutaneous tumors following intravenous delivery of reovirus. *Clin. Cancer Res.* **2008**, *14*, 259-269.
142. Li, H.; Zeng, Z.; Fu, X.; Zhang, X. Coadministration of a herpes simplex virus-2 based oncolytic virus and cyclophosphamide produces a synergistic antitumor effect and enhances tumor-specific immune responses. *Cancer Res.* **2007**, *67*, 7850-7855.
143. Ungerechts, G.; Springfeld, C.; Frenzke, M.E.; Lampe, J.; Parker, W.B.; Sorscher, E.J.; Cattaneo, R. An immunocompetent murine model for oncolysis with an armed and targeted measles virus. *Mol. Ther.* **2007**, *15*, 1991-1997.
144. Hirasawa, K.; Nishikawa, S.G.; Norman, K.L.; Coffey, M.C.; Thompson, B.G.; Yoon, C.S.; Waisman, D.M.; Lee, P.W. Systemic reovirus therapy of metastatic cancer in immune-competent mice. *Cancer Res.* **2003**, *63*, 348-353.
145. Thomas, M.A.; Spencer, J.F.; Toth, K.; Sagartz, J.E.; Phillips, N.J.; Wold, W.S. Immunosuppression enhances oncolytic adenovirus replication and antitumor efficacy in the Syrian hamster model. *Mol. Ther.* **2008**, *16*, 1665-1673.
146. Kurozumi, K.; Hardcastle, J.; Thakur, R.; Yang, M.; Christoforidis, G.; Fulci, G.; Hochberg, F.H.; Weissleder, R.; Carson, W.; Chiocca, E.A.; Kaur, B. Effect of tumor microenvironment modulation on the efficacy of oncolytic virus therapy. *J. Natl. Cancer Inst.* **2007**, *99*, 1768-1781.

147. Ikeda, K.; Ichikawa, T.; Wakimoto, H.; Silver, J.S.; Deisboeck, T.S.; Finkelstein, D.; Harsh, G.R.t.; Louis, D.N.; Bartus, R.T.; Hochberg, F.H.; Chiocca, E.A. Oncolytic virus therapy of multiple tumors in the brain requires suppression of innate and elicited antiviral responses. *Nat. Med.* **1999**, *5*, 881-887.
148. Chen, Y.; Yu, D.C.; Charlton, D.; Henderson, D.R. Pre-existent adenovirus antibody inhibits systemic toxicity and antitumor activity of CN706 in the nude mouse LNCaP xenograft model: implications and proposals for human therapy. *Hum. Gene Ther.* **2000**, *11*, 1553-1567.
149. Tsai, V.; Johnson, D.E.; Rahman, A.; Wen, S.F.; LaFace, D.; Philopena, J.; Nery, J.; Zepeda, M.; Maneval, D.C.; Demers, G.W.; Ralston, R. Impact of human neutralizing antibodies on antitumor efficacy of an oncolytic adenovirus in a murine model. *Clin. Cancer Res.* **2004**, *10*, 7199-7206.
150. Herrlinger, U.; Kramm, C.M.; Aboody-Guterman, K.S.; Silver, J.S.; Ikeda, K.; Johnston, K.M.; Pechan, P.A.; Barth, R.F.; Finkelstein, D.; Chiocca, E.A.; Louis, D.N.; Breakefield, X.O. Pre-existing herpes simplex virus 1 (HSV-1) immunity decreases, but does not abolish, gene transfer to experimental brain tumors by a HSV-1 vector. *Gene Ther.* **1998**, *5*, 809-819.
151. Dhar, D.; Spencer, J.F.; Toth, K.; Wold, W.S. Effect of preexisting immunity on oncolytic adenovirus vector INGN 007 antitumor efficacy in immunocompetent and immunosuppressed Syrian hamsters. *J. Virol.* **2009**, *83*, 2130-2139.
152. Dhar, D.; Spencer, J.F.; Toth, K.; Wold, W.S. Pre-existing immunity and passive immunity to adenovirus 5 prevents toxicity caused by an oncolytic adenovirus vector in the Syrian hamster model. *Mol. Ther.* **2009**, *17*, 1724-1732.
153. Kostense, S.; Koudstaal, W.; Sprangers, M.; Weverling, G.J.; Penders, G.; Helmus, N.; Vogels, R.; Bakker, M.; Berkhout, B.; Havenga, M.; Goudsmit, J. Adenovirus types 5 and 35 seroprevalence in AIDS risk groups supports type 35 as a vaccine vector. *Aids* **2004**, *18*, 1213-1216.
154. Holterman, L.; Vogels, R.; van der Vlugt, R.; Sieuwerts, M.; Grimbergen, J.; Kaspers, J.; Geelen, E.; van der Helm, E.; Lemckert, A.; Gillissen, G.; Verhaagh, S.; Custers, J.; Zuijdgeest, D.; Berkhout, B.; Bakker, M.; Quax, P.; Goudsmit, J.; Havenga, M. Novel replication-incompetent vector derived from adenovirus type 11 (Ad11) for vaccination and gene therapy: low seroprevalence and non-cross-reactivity with Ad5. *J. Virol.* **2004**, *78*, 13207-13215.
155. Seshidhar Reddy, P.; Ganesh, S.; Limbach, M.P.; Brann, T.; Pinkstaff, A.; Kaloss, M.; Kaleko, M.; Connelly, S. Development of adenovirus serotype 35 as a gene transfer vector. *Virology* **2003**, *311*, 384-393.
156. Sumida, S.M.; Truitt, D.M.; Lemckert, A.A.; Vogels, R.; Custers, J.H.; Addo, M.M.; Lockman, S.; Peter, T.; Peyerl, F.W.; Kishko, M.G.; Jackson, S.S.; Gorgone, D.A.; Lifton, M.A.; Essex, M.; Walker, B.D.; Goudsmit, J.; Havenga, M.J.; Barouch, D.H. Neutralizing antibodies to adenovirus serotype 5 vaccine vectors are directed primarily against the adenovirus hexon protein. *J. Immunol.* **2005**, *174*, 7179-7185.
157. Komarova, S.; Kawakami, Y.; Stoff-Khalili, M.A.; Curiel, D.T.; Pereboeva, L. Mesenchymal progenitor cells as cellular vehicles for delivery of oncolytic adenoviruses. *Mol. Cancer Ther.* **2006**, *5*, 755-766.
158. Hakkarainen, T.; Sarkioja, M.; Lehenkari, P.; Miettinen, S.; Ylikomi, T.; Suuronen, R.; Desmond, R.A.; Kanerva, A.; Hemminki, A. Human mesenchymal stem cells lack tumor tropism but

enhance the antitumor activity of oncolytic adenoviruses in orthotopic lung and breast tumors. *Hum. Gene Ther.* **2007**, *18*, 627-641.

159. Sonabend, A.M.; Ulasov, I.V.; Tyler, M.A.; Rivera, A.A.; Mathis, J.M.; Lesniak, M.S. Mesenchymal stem cells effectively deliver an oncolytic adenovirus to intracranial glioma. *Stem Cells* **2008**, *26*, 831-841.
160. Iankov, I.D.; Blechacz, B.; Liu, C.; Schmeckpeper, J.D.; Tarara, J.E.; Federspiel, M.J.; Caplice, N.; Russell, S.J. Infected cell carriers: a new strategy for systemic delivery of oncolytic measles viruses in cancer virotherapy. *Mol. Ther.* **2007**, *15*, 114-122.
161. Munguia, A.; Ota, T.; Miest, T.; Russell, S.J. Cell carriers to deliver oncolytic viruses to sites of myeloma tumor growth. *Gene Ther.* **2008**, *15*, 797-806.
162. Coukos, G.; Makrigiannakis, A.; Kang, E.H.; Caparelli, D.; Benjamin, I.; Kaiser, L.R.; Rubin, S.C.; Albelda, S.M.; Molnar-Kimber, K.L. Use of carrier cells to deliver a replication-selective herpes simplex virus-1 mutant for the intraperitoneal therapy of epithelial ovarian cancer. *Clin. Cancer Res.* **1999**, *5*, 1523-1537.
163. Raykov, Z.; Balboni, G.; Aprahamian, M.; Rommelaere, J. Carrier cell-mediated delivery of oncolytic parvoviruses for targeting metastases. *Int. J. Cancer* **2004**, *109*, 742-749.
164. Qiao, J.; Kottke, T.; Willmon, C.; Galivo, F.; Wongthida, P.; Diaz, R.M.; Thompson, J.; Ryno, P.; Barber, G.N.; Chester, J.; Selby, P.; Harrington, K.; Melcher, A.; Vile, R.G. Purging metastases in lymphoid organs using a combination of antigen-nonspecific adoptive T cell therapy, oncolytic virotherapy and immunotherapy. *Nat. Med.* **2008**, *14*, 37-44.
165. Ilett, E.J.; Prestwich, R.J.; Kottke, T.; Errington, F.; Thompson, J.M.; Harrington, K.J.; Pandha, H.S.; Coffey, M.; Selby, P.J.; Vile, R.G.; Melcher, A.A. Dendritic cells and T cells deliver oncolytic reovirus for tumour killing despite pre-existing anti-viral immunity. *Gene Ther.* **2009**, *16*, 689-699.
166. Pfirschke, C.; Schirrmacher, V. Cross-infection of tumor cells by contact with T lymphocytes loaded with Newcastle disease virus. *Int. J. Oncol.* **2009**, *34*, 951-962.
167. Ong, H.T.; Hasegawa, K.; Dietz, A.B.; Russell, S.J.; Peng, K.W. Evaluation of T cells as carriers for systemic measles virotherapy in the presence of antiviral antibodies. *Gene Ther.* **2007**, *14*, 324-333.
168. Power, A.T.; Wang, J.; Falls, T.J.; Paterson, J.M.; Parato, K.A.; Lichty, B.D.; Stojdl, D.F.; Forsyth, P.A.; Atkins, H.; Bell, J.C. Carrier cell-based delivery of an oncolytic virus circumvents antiviral immunity. *Mol. Ther.* **2007**, *15*, 123-130.
169. Zhu, H.; Su, Y.; Zhou, S.; Xiao, W.; Ling, W.; Hu, B.; Liu, Y.; Qi, Y. Immune analysis on mtHSV mediated tumor therapy in HSV-1 seropositive mice. *Cancer Biol. Ther.* **2007**, *6*, 724-731.
170. Kangasniemi, L.; Koskinen, M.; Jokinen, M.; Toriseva, M.; Ala-Aho, R.; Kahari, V.M.; Jalonen, H.; Yla-Herttuala, S.; Moilanen, H.; Stenman, U.H.; Diaconu, I.; Kanerva, A.; Pesonen, S.; Hakkarainen, T.; Hemminki, A. Extended release of adenovirus from silica implants *in vitro* and *in vivo*. *Gene Ther.* **2009**, *16*, 103-110.
171. Huard, J.; Lochmuller, H.; Acsadi, G.; Jani, A.; Massie, B.; Karpati, G. The route of administration is a major determinant of the transduction efficiency of rat tissues by adenoviral recombinants. *Gene Ther.* **1995**, *2*, 107-115.

172. Alemany, R.; Suzuki, K.; Curiel, D.T. Blood clearance rates of adenovirus type 5 in mice. *J. Gen. Virol.* **2000**, *81*, 2605-2609.
173. Hollon, T. Researchers and regulators reflect on first gene therapy death. *Nat. Med.* **2000**, *6*, 6.
174. Waddington, S.N.; McVey, J.H.; Bhella, D.; Parker, A.L.; Barker, K.; Atoda, H.; Pink, R.; Buckley, S.M.; Greig, J.A.; Denby, L.; Custers, J.; Morita, T.; Francischetti, I.M.; Monteiro, R.Q.; Barouch, D.H.; van Rooijen, N.; Napoli, C.; Havenga, M.J.; Nicklin, S.A.; Baker, A.H. Adenovirus serotype 5 hexon mediates liver gene transfer. *Cell* **2008**, *132*, 397-409.
175. Shashkova, E.V.; Doronin, K.; Senac, J.S.; Barry, M.A. Macrophage depletion combined with anticoagulant therapy increases therapeutic window of systemic treatment with oncolytic adenovirus. *Cancer Res.* **2008**, *68*, 5896-5904.
176. Doronin, K.; Shashkova, E.V.; May, S.M.; Hofherr, S.E.; Barry, M.A. Chemical modification with high molecular weight polyethylene glycol reduces transduction of hepatocytes and increases efficacy of intravenously delivered oncolytic adenovirus. *Hum. Gene Ther.* **2009**, *20*, 975-988.
177. Shashkova, E.V.; May, S.M.; Doronin, K.; Barry, M.A. Expanded anticancer therapeutic window of hexon-modified oncolytic adenovirus. *Mol. Ther.* **2009**, *17*, 2121-2130.
178. Carlisle, R.C.; Di, Y.; Cerny, A.M.; Sonnen, A.F.; Sim, R.B.; Green, N.K.; Subr, V.; Ulbrich, K.; Gilbert, R.J.; Fisher, K.D.; Finberg, R.W.; Seymour, L.W. Human erythrocytes bind and inactivate type 5 adenovirus by presenting Coxsackie virus-adenovirus receptor and complement receptor 1. *Blood* **2009**, *113*, 1909-1918.
179. Li, J.L.; Liu, H.L.; Zhang, X.R.; Xu, J.P.; Hu, W.K.; Liang, M.; Chen, S.Y.; Hu, F.; Chu, D.T. A phase I trial of intratumoral administration of recombinant oncolytic adenovirus overexpressing HSP70 in advanced solid tumor patients. *Gene Ther.* **2009**, *16*, 376-382.
180. Ren, Z.; Ye, X.; Fang, C.; Lu, Q.; Zhao, Y.; Liu, F.; Liang, M.; Hu, F.; Chen, H.Z. Intratumor injection of oncolytic adenovirus expressing HSP70 prolonged survival in melanoma B16 bearing mice by enhanced immune response. *Cancer Biol. Ther.* **2008**, *7*, 191-195.
181. Lapteva, N.; Aldrich, M.; Weksberg, D.; Rollins, L.; Goltsova, T.; Chen, S.Y.; Huang, X.F. Targeting the intratumoral dendritic cells by the oncolytic adenoviral vaccine expressing RANTES elicits potent antitumor immunity. *J. Immunother.* **2009**, *32*, 145-156.
182. Willmon, C.L.; Saloura, V.; Fridlender, Z.G.; Wongthida, P.; Diaz, R.M.; Thompson, J.; Kottke, T.; Federspiel, M.; Barber, G.; Albelda, S.M.; Vile, R.G. Expression of IFN-beta enhances both efficacy and safety of oncolytic vesicular stomatitis virus for therapy of mesothelioma. *Cancer Res.* **2009**, *69*, 7713-7720.
183. Lei, N.; Shen, F.B.; Chang, J.H.; Wang, L.; Li, H.; Yang, C.; Li, J.; Yu, D.C. An oncolytic adenovirus expressing granulocyte macrophage colony-stimulating factor shows improved specificity and efficacy for treating human solid tumors. *Cancer Gene Ther.* **2009**, *16*, 33-43.
184. Lee, J.H.; Roh, M.S.; Lee, Y.K.; Kim, M.K.; Han, J.Y.; Park, B.H.; Trown, P.; Kirn, D.H.; Hwang, T.H. Oncolytic and immunostimulatory efficacy of a targeted oncolytic poxvirus expressing human GM-CSF following intravenous administration in a rabbit tumor model. *Cancer Gene Ther.* **2009**, doi: 10.1038/cgt.2009.50.
185. Chang, J.; Zhao, X.; Wu, X.; Guo, Y.; Guo, H.; Cao, J.; Lou, D.; Yu, D.; Li, J. A Phase I study of KH901, a conditionally replicating granulocyte-macrophage colony-stimulating factor: armed

oncolytic adenovirus for the treatment of head and neck cancers. *Cancer Biol. Ther.* **2009**, *8*, 676-682.

186. Bortolanza, S.; Bunuales, M.; Otano, I.; Gonzalez-Aseguinolaza, G.; Ortiz-de-Solorzano, C.; Perez, D.; Prieto, J.; Hernandez-Alcoceba, R. Treatment of pancreatic cancer with an oncolytic adenovirus expressing interleukin-12 in Syrian hamsters. *Mol. Ther.* **2009**, *17*, 614-622.
187. Zhang, K.J.; Wang, Y.G.; Cao, X.; Zhong, S.Y.; Wei, R.C.; Wu, Y.M.; Yue, X.T.; Li, G.C.; Liu, X.Y. Potent antitumor effect of interleukin-24 gene in the survivin promoter and retinoblastoma double-regulated oncolytic adenovirus. *Hum. Gene Ther.* **2009**, *20*, 818-830.
188. Luo, J.; Xia, Q.; Zhang, R.; Lv, C.; Zhang, W.; Wang, Y.; Cui, Q.; Liu, L.; Cai, R.; Qian, C. Treatment of cancer with a novel dual-targeted conditionally replicative adenovirus armed with mda-7/IL-24 gene. *Clin. Cancer Res.* **2008**, *14*, 2450-2457.
189. Kirn, D.H.; Wang, Y.; Le Boeuf, F.; Bell, J.; Thorne, S.H. Targeting of interferon-beta to produce a specific, multi-mechanistic oncolytic vaccinia virus. *PLoS Med.* **2007**, *4*, e353.
190. Shashkova, E.V.; Kuppuswamy, M.N.; Wold, W.S.; Doronin, K. Anticancer activity of oncolytic adenovirus vector armed with IFN-alpha and ADP is enhanced by pharmacologically controlled expression of TRAIL. *Cancer Gene Ther.* **2008**, *15*, 61-72.
191. Haralambieva, I.; Iankov, I.; Hasegawa, K.; Harvey, M.; Russell, S.J.; Peng, K.W. Engineering oncolytic measles virus to circumvent the intracellular innate immune response. *Mol. Ther.* **2007**, *15*, 588-597.
192. Altomonte, J.; Wu, L.; Meseck, M.; Chen, L.; Ebert, O.; Garcia-Sastre, A.; Fallon, J.; Mandeli, J.; Woo, S.L. Enhanced oncolytic potency of vesicular stomatitis virus through vector-mediated inhibition of NK and NKT cells. *Cancer Gene Ther.* **2009**, *16*, 266-278.
193. Endo, Y.; Sakai, R.; Ouchi, M.; Onimatsu, H.; Hioki, M.; Kagawa, S.; Uno, F.; Watanabe, Y.; Urata, Y.; Tanaka, N.; Fujiwara, T. Virus-mediated oncolysis induces danger signal and stimulates cytotoxic T-lymphocyte activity via proteasome activator upregulation. *Oncogene* **2008**, *27*, 2375-2381.
194. Lapteva, N.; Aldrich, M.; Rollins, L.; Ren, W.; Goltsova, T.; Chen, S.Y.; Huang, X.F. Attraction and activation of dendritic cells at the site of tumor elicits potent antitumor immunity. *Mol. Ther.* **2009**, *17*, 1626-1636.
195. Ramakrishna, E.; Woller, N.; Mundt, B.; Knocke, S.; Gurlevik, E.; Saborowski, M.; Malek, N.; Manns, M.P.; Wirth, T.; Kuhnel, F.; Kubicka, S. Antitumoral immune response by recruitment and expansion of dendritic cells in tumors infected with telomerase-dependent oncolytic viruses. *Cancer Res.* **2009**, *69*, 1448-1458.
196. Chuang, C.M.; Monie, A.; Wu, A.; Pai, S.I.; Hung, C.F. Combination of viral oncolysis and tumor-specific immunity to control established tumors. *Clin. Cancer Res.* **2009**, *15*, 4581-4588.
197. Huang, J.H.; Zhang, S.N.; Choi, K.J.; Choi, I.K.; Kim, J.H.; Lee, M.; Kim, H.; Yun, C.O. Therapeutic and tumor-specific immunity induced by combination of dendritic cells and oncolytic adenovirus expressing IL-12 and 4-1BBL. *Mol. Ther.* **2009**, doi:10.1038/mt.2009.205.
198. Robinson, M.; Ge, Y.; Ko, D.; Yendluri, S.; Laflamme, G.; Hawkins, L.; Jooss, K. Comparison of the E3 and L3 regions for arming oncolytic adenoviruses to achieve a high level of tumor-specific transgene expression. *Cancer Gene Ther.* **2008**, *15*, 9-17.

199. Bortolanza, S.; Bunuales, M.; Alzuguren, P.; Lamas, O.; Aldabe, R.; Prieto, J.; Hernandez-Alcoceba, R. Deletion of the E3-6.7K/gp19K region reduces the persistence of wild-type adenovirus in a permissive tumor model in Syrian hamsters. *Cancer Gene Ther.* **2009**, *16*, 703-712.
200. McSharry, B.P.; Burgert, H.G.; Owen, D.P.; Stanton, R.J.; Prod'homme, V.; Sester, M.; Koebernick, K.; Groh, V.; Spies, T.; Cox, S.; Little, A.M.; Wang, E.C.; Tomasec, P.; Wilkinson, G.W. Adenovirus E3/19K promotes evasion of NK cell recognition by intracellular sequestration of the NKG2D ligands major histocompatibility complex class I chain-related proteins A and B. *J. Virol.* **2008**, *82*, 4585-4594.
201. Bennett, E.M.; Bennink, J.R.; Yewdell, J.W.; Brodsky, F.M. Cutting edge: adenovirus E19 has two mechanisms for affecting class I MHC expression. *J. Immunol.* **1999**, *162*, 5049-5052.
202. Hermiston, T.W.; Tripp, R.A.; Sparer, T.; Gooding, L.R.; Wold, W.S. Deletion mutation analysis of the adenovirus type 2 E3-gp19K protein: identification of sequences within the endoplasmic reticulum lumenal domain that are required for class I antigen binding and protection from adenovirus-specific cytotoxic T lymphocytes. *J. Virol.* **1993**, *67*, 5289-5298.
203. Reddy, P.S.; Burroughs, K.D.; Hales, L.M.; Ganesh, S.; Jones, B.H.; Idamakanti, N.; Hay, C.; Li, S.S.; Skele, K.L.; Vasko, A.J.; Yang, J.; Watkins, D.N.; Rudin, C.M.; Hallenbeck, P.L. Seneca Valley virus, a systemically deliverable oncolytic picornavirus, and the treatment of neuroendocrine cancers. *J. Natl. Cancer Inst.* **2007**, *99*, 1623-1633.
204. Lun, X.; Yang, W.; Alain, T.; Shi, Z.Q.; Muzik, H.; Barrett, J.W.; McFadden, G.; Bell, J.; Hamilton, M.G.; Senger, D.L.; Forsyth, P.A. Myxoma virus is a novel oncolytic virus with significant antitumor activity against experimental human gliomas. *Cancer Res.* **2005**, *65*, 9982-9990.
205. Saito, K.; Uzawa, K.; Kasamatsu, A.; Shinozuka, K.; Sakuma, K.; Yamatoji, M.; Shiiba, M.; Shino, Y.; Shirasawa, H.; Tanzawa, H. Oncolytic activity of Sindbis virus in human oral squamous carcinoma cells. *Br. J. Cancer* **2009**, *101*, 684-690.
206. Vaha-Koskela, M.J.; Kallio, J.P.; Jansson, L.C.; Heikkila, J.E.; Zakhartchenko, V.A.; Kallajoki, M.A.; Kahari, V.M.; Hinkkanen, A.E. Oncolytic capacity of attenuated replicative semliki forest virus in human melanoma xenografts in severe combined immunodeficient mice. *Cancer Res.* **2006**, *66*, 7185-7194.

© 2010 by the authors; licensee Molecular Diversity Preservation International, Basel, Switzerland. This article is an Open Access article distributed under the terms and conditions of the Creative Commons Attribution license (http://creativecommons.org/licenses/by/3.0/).